1974

The Statistics Of Strong Winds For Engineering Applications

Colin John Baynes

Follow this and additional works at: https://ir.lib.uwo.ca/digitizedtheses

NOTICE

AVIS

The quality of this microfiche is heavily dependent upon the quality of the original thesis submitted for microfilming. Every effort has been made to ensure the highest quality of reproduction possible.

If pages are missing, contact the university which granted the degree.

Some pages may have indistinct print especially if the original pages were typed with a poor typewriter ribbon or if the university sent us a poor photocopy.

Previously copyrighted materials (journal articles, published tests, etc.) are not filmed.

Reproduction in full or in part of this film is governed by the Canadian Copyright Act, R.S.C. 1970, c. C-30. Please read the authorization forms which accompany this thesis.

La qualité de cette microfiche dépend grandement de la qualité de la thèse soumise au microfilmage. Nous avons tout fait pour assurer une qualité supérieure de reproduction.

S'il manque des pages, veuillez communiquer avec l'université qui a conféré le grade.

La qualité d'impression de certaines pages peut laisser à désirer, surtout si les pages originales ont été dactylographiées à l'aide d'un ruban usé ou si l'université nous a fait parvenir une photocopie de mauvaise qualité.

Les documents qui font déjà l'objet d'un droit d'auteur (articles de revue, examens publiés, etc.) ne sont pas microfilmés.

La reproduction, même partielle, de ce microfilm est soumise à la Loi canadienne sur le droit d'auteur, SRC 1970, c. C-30. Veuillez prendre connaissance des formules d'autorisation qui accompagnent cette thèse.

THIS DISSERTATION HAS BEEN MICROFILMED EXACTLY AS RECEIVED

LA THÈSE A ÉTÉ MICROFILMÉE TELLE QUE NOUS L'AVONS REÇUE

THE STATISTICS OF STRONG WINDS FOR

ENGINEERING APPLICATIONS

by

Colin John Baynes

Faculty of Engineering Science

Submitted in partial fulfillment

of the requirements for the degree of

Doctor of Philosophy

Faculty of Graduate Studies

The University of Western Ontario

London, Ontario

August, 1974

ABSTRACT

Several aspects of the statistical description of strong winds are investigated, together with their implications for certain engineering applications.

Wind speed distributions derived from the bivariate normal models of velocity are discussed, including the chi$_2$, Weibull and Rayleigh forms. The suitability of the Rayleigh model for most purposes is confirmed. Various extreme value distributions and their interrelation are reviewed. Functional relationships are developed between the Fisher-Tippett Type I parameters of extreme gusts and mean hourly winds; the deviation of some observational data from these curves is explained in part by the variation in terrain roughness around a given observing station. Comparative statistics of extreme winds around the world are compiled on the basis of the above considerations.

A recent deterministic approach to atmospheric boundary layer description is used to predict surface winds from upper level winds, but is found to be unsatisfactory in many practical situations. A simplified probabilistic model is proposed for predicting the distribution moments of surface wind speeds as functions solely of the terrain roughness and the standard vector deviation of gradient winds.

The methodology for synthesizing the wind climate at a given site is discussed, particularly the use of upper wind records. Errors in rawinsonde measurements are studied by power spectral methods. A synthesis of errors in observed climatic variances of gradient wind speeds was performed for representative conditions of wind strength and terrain roughness. Some gradient and geostrophic wind climates were obtained by objective isobar analysis from synoptic meteorological data. The

results compared favourably with direct rawinsonde measurements.

Three applications of this work are given: the optimum orientation of airport runways, the generation of electrical power from the wind and the prediction of extreme wave heights in relation to extreme wind speeds over the open ocean.

ACKNOWLEDGEMENTS

TABLE OF CONTENTS

CHAPTER 5 — SOME APPLICATIONS AND GENERAL CONCLUSIONS

* * *

APPENDIX I — EXTREME DISTRIBUTIONS OF MEAN WIND SPEEDS
AND GUSTS

APPENDIX II — A COMPARISON OF THEORETICAL AND OBSERVED DISTRIBUTIONS OF EXTREME GUSTS AND MEAN WIND SPEEDS

APPENDIX III — A SURVEY OF SOME EXTREME WIND STATISTICS

APPENDIX IV — UPPER AIR STATION DESCRIPTIONS   213

APPENDIX V — SELECTION OF NEUTRAL WIND PROFILES FROM UPPER AIR DATA

ix

LIST OF TABLES

LIST OF FIGURES

NOMENCLATURE[†]

a	exponential distribution parameter or power law index
A	mode of gust factor distribution
b	exponential distribution parameter
B	constant (defined in Equation 2.50)
c	Weibull parameter
c_g	geostrophic drag coefficient
C_D	drag coefficient
C_L	lift coefficient
D	balloon diameter
E	superimposed shearing stress
f	Coriolis parameter: $f = 2\,\omega\,\sin\lambda$
$_1F_1$	confluent hypergeometric function
g	acceleration due to gravity
h	depth of Ekman layer
H	wave height
I	Bessel function
J	Jacobian
k	Weibull parameter or von Karman's constant
K	eddy viscosity or ratio of surface to gradient wind speeds
l	length of instrument train
L	Monin-Obukhov length
L_i	Fourier coefficient
m	balloon mass or median value (with subscripted variable)

[†]Some notations are not included or are used in definitions other than those listed. To avoid ambiguity all notations are locally defined in the text.

m_a	apparent mass
m_o	mass of displaced air
M_i	Fourier coefficient
n	frequency
n_N	Nyquist or folding frequency
N	sample size
p	probability density or atmospheric pressure
P	probability distribution function
r	correlation coefficient (with subscripted variables)
R	return period or radius of curvature
Re	Reynolds number
Ro	Rossby number
$R(n)$	response or admittance function at frequency n
$\mathcal{R}$	gas constant
$S(n)$	spectral density at frequency n
t	reduced wind speed: $t = v/\sigma$
t'	transformed variable: $t' = t^2/\rho$
T	sensor response parameter (defined in Equation 4.4)
T_s	specific output
$\overline{T}$	mean temperature of thickness layer
T'	potential temperature
u_*	surface friction velocity
U	mode of Type I extreme value distribution
V	wind velocity
V_f	furling velocity
V_F	fastest-mile wind
V_g	geostrophic wind velocity
V_G	gradient wind velocity
V_i	cut-in velocity
V_o	surface wind velocity

V_p	rated wind velocity
$\overline{V}_r$	vector mean or resultant wind velocity
V_x, V_y	zonal and meridional wind velocity components
$\overline{w}$	mean balloon ascent rate
W	weighting function
y	normalized variable: $y = a(V-U)$
z	height above ground level
z_d	zero plane displacement
Z_G	gradient height
z_o	roughness length
z_u, z_v, z_w	Fourier amplitudes of sensor motion
a	angle of wind veering or sensor response parameter (defined in Equation 4.4)
$1/a$	dispersion of Type I extreme value distribution
β	scale parameter of Type II extreme value distribution
γ	shape parameter of Type II extreme value distribution or ratio of specific heats
Γ	gamma function
δ	angle of elevation to rawinsonde sensor
ϵ	random variable
ζ	transformation matrix (defined in Equation 4.49)
η_G	gust factor
η_R	ratio of R-year return gust to mean hourly wind speed
θ	wind direction
κ	surface drag coefficient
λ	angle of latitude or wind distribution parameter: $\lambda = \overline{V}_r/\sigma$
μ	equivalent degrees of freedom (defined in Equation 2.78)
ν	average cycling rate
ξ	variable defined in Equation 2.84
ρ	parameter defined in Equation 2.78
ρ_a	air density
σ	standard vector deviation

σ_a, σ_b standard deviations of uncorrelated wind velocity components

σ_x, σ_y standard deviations of wind velocity components

τ averaging period or shear stress

τ_o surface shear stress

ψ random variable

ω earth's rotational velocity

—   (overbar) mean quantity

′   (prime) perturbation quantity

CHAPTER 1

INTRODUCTION

1.1 Descriptions of the Winds from Early Times to 1800

This thesis is intended to contribute towards improved statistical description and prediction of strong winds with a specific emphasis on providing some useful tools for those who must design structures or human activities to accommodate the forces of nature. The necessary foundations for such work, the classification, measurement and physical explanation of the winds, have been laid down over the centuries, largely in response to the pragmatic requirements of farmers, sailors, merchants and, comparatively recently, engineers.

It was, perhaps, the philosphers of ancient Greece who first subjected meteorological phenomena to the revealing methods of scientific enquiry. An important landmark in these early attempts to rationalize the weather was the treatise "Meteorologica" by Aristotle (384-322 B.C.). In fact, this work formed the basis of the study of meteorology in Europe for nearly two thousand years.

The Greek concept of the winds relied essentially on a simple classification according to direction. Aristotle specified the winds blowing from the winter (south-west), equinoctial (west) and summer (northwest) sunsets and from the Great Bear (north), together with their respective opposing winds. There were an additional two winds originating from just west and east of north. This twelve-point wind-rose is depicted in Figure 1.1. The characteristics of the winds were described by Aristotle in terms of accompanying weather phenomena. There was also some physical explanation.
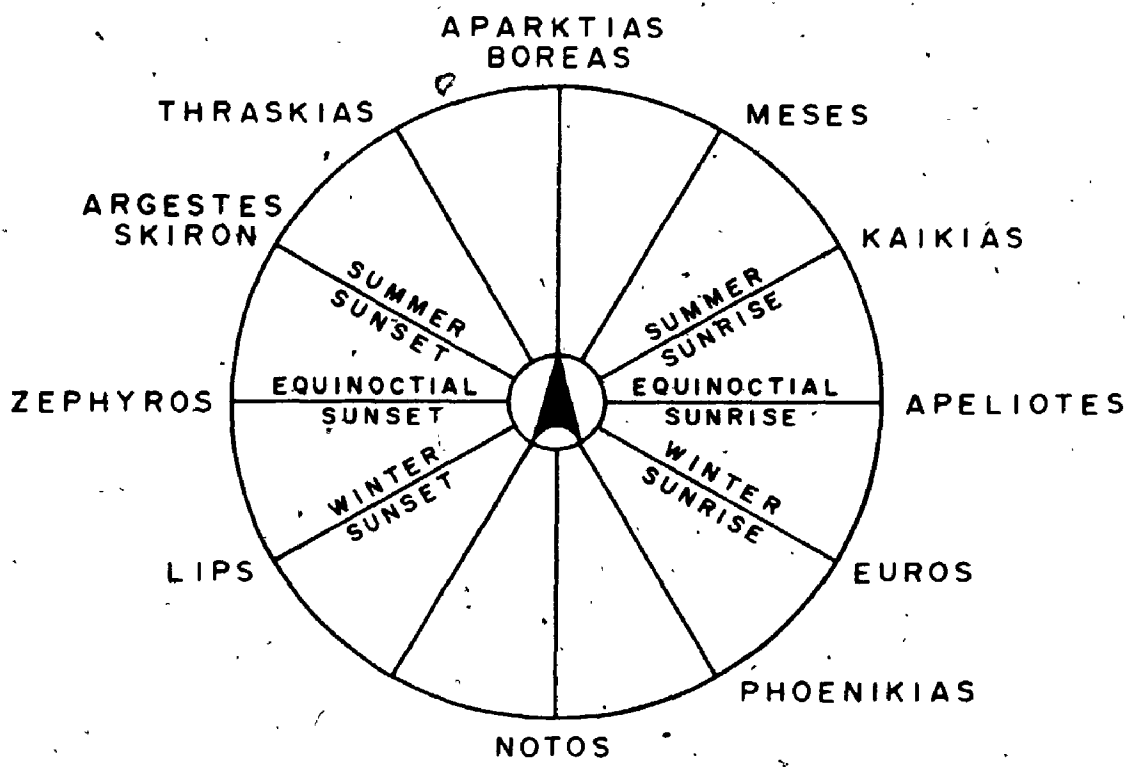
FIG I. THE GREEK WIND-ROSE OF ARISTOTLE

"As a general rule it is the winds from Aparktias, Thraskias and Argestes which continue after the other winds and make them cease, for that they are so frequent and that they blow so violently; it is because their point of origin is very near; also they give the clearest weather of all the winds; blowing from close by they have correspondingly more force and they suppress the other winds and dispersing the congested clouds they bring fine weather, at least when they are not at the same time very cold; then in effect there is not fine weather for if they are colder than they are strong they cause condensation before they have chased away the clouds." (Ross, 1913)

Aristotle's twelve-point wind-rose perhaps suggests a precision in the definition of directions and sectors which did not exist at that time; rather, the winds were simply known by their names. There is actually some evidence that the Greeks employed an eight-point wind-rose. The Tower of Winds (the Horologium of Andronikos Kyrrhestes) in Athens is an octagonal monument erected in the second century B.C. It's sides are oriented closely to the eight principal points of the modern compass. Each face bears the name of a wind and a sculptured figure representing its characteristics. The eight winds are: Boreas (north), Kaikias (northeast), Apeliotes (east), Euros (southeast), Notos (south), Lips (southwest), Zephyros (west) and Skiron (northwest).

Theophrastus (c. 373-286 B.C.), Aristotle's pupil, wrote two significant treatises on the weather, "On Winds" and "On the Signs of Rain, Winds, Storms and Fair Weather". He enlarged upon the work of his tutor and, in the second treatise, laid down a considerable body of weather-lore, to which very little of importance was added in the subsequent two thousand years. It was through weather-lore that the beginnings of the science of meteorology found practical application among sailors, farmers and others intimately concerned with the elements.

According to Theophrastus, winds could be predicted from the appearance of the sun and moon and from the behaviour of animals . . . and the human body:

"Also black spots on the sun or moon indicate rain, red spots wind.
Again, if, while a north wind blows, the horns of the crescent moon
stand out straight, westerly winds will generally succeed, and the
rest of the month will be stormy."

"A dog rolling on the ground is a sign of violent wind."

"If the feet swell, there will be a change to a south wind. This
also sometimes indicates a hurricane. So too does it, if a man has
a shooting pain in the right foot." (Hort, 1916)

Through Roman times and into the Middle Ages in Europe the understanding of meteorology remained essentially unchanged. Weather-lore and, to a certain extent, astrology constituted man's guide to the vagaries of the weather. The invention of printing in the fifteenth century greatly increased the availability of astrological pre-dictions through the publication of almanacs, but perhaps the most significant development was the growing practice of keeping a diary of the weather. The increasing volume of data, however, imperfect, would ultimately lead to the modern science of meteorology. One of the earliest known diaries was kept by the Rev. William Merle. He recorded daily weather observations for seven years, from 1337 to 1344, at Oxford and Driby, Lincolnshire.

It was probably not until the seventeenth century that the first anemometers enabled reasonably consistent description of the winds. The invention of the pen-dulum anemometer is generally attributed to Robert Hooke, although Leonardo da Vinci (1452-1519) had earlier constructed a similar instrument "to measure how great a distance one covers with the current of the wind" (Hart, 1963). The anemometer consisted of a light plate suspended by a rod. The plate was faced into the wind and, as it was deflected, the rod moved across a graduated scale. Various modifications of this design, and other instruments which measured the wind force exerted on a given area, appeared through the eighteenth century. Meanwhile, the predecessor of the modern pressure-tube anemometer appeared, attributed to Pierre Daniel Huet. Details of his invention were first published in Paris in 1722. He described a tin funnel "like the cowl of a monk" connected to a U-tube filled with mercury. A vane kept the funnel turned into the wind.

Whilst the determination of wind pressure was now possible, the direct measurement of wind velocity was a problem never satisfactorily resolved until Robinson introduced the cup anemometer in 1846. In the meantime, wind velocity was often observed with the aid of floating objects such as clouds and feathers.

'By 1800 scientists were well on the way to the modern understanding of the winds and general atmospheric circulation. Considerable activity followed Torricelli's invention of the barometer or "weather glass" in 1643. The expansion of overseas trade heightened the interest of sailors and merchants in the behaviour of ocean winds. In 1697 William Dampier published "A voyage round the World", based on his buccaneering exploits and containing an excellent account of the winds. Edmund Halley, regarded as the father of dynamical meteorology, also published an account of the trade-winds and monsoons at about this time. However, the man who first explained the trade-winds in terms of the rotational effect of the earth was a London lawyer, George Hadley. His explanation was presented before the Royal Society in 1735. The mathematical formulation was to be derived by Coriolis one hundred years later.

Throughout the eighteenth century meteorological data, as contained in the diaries and logs of numerous individuals, grew rapidly in both scope and volume. In North America such leading citizens as George Washington, Benjamin Franklin and Thomas Jefferson made regular observations. Moreover, the practice of maintaining and comparing simultaneous weather records at two or more locations was beginning to provide clues to the structure and movement of weather systems.

1.2 Some Classifications of Wind Force

It is interesting to note that one of the first civil engineers, John Smeaton, was himself very much concerned with the force of the wind, and particularly the power generated by windmills. In a remarkable paper before the Royal Society in 1759 he proposed a classification of the winds "according to their common appellations" (reproduced in Table 1.1). It was originally communicated to him by a Mr. Rouse "from a considerable number of facts and experiments". There were eleven "appellations" of force, ranging from "hardly perceptible" to "an hurricane that tears

VELOCITY OF THE WIND		PERPENDICULAR FORCE ON ONE FOOT AREA IN POUNDS AVOIRDUPOIS	COMMON APPELLATIONS OF THE FORCE OF WINDS
Miles in one hour	*Feet in one second*		
1	1.47	.005	Hardly perceptible
2	2.93	.020	Just perceptible
3	4.40	.044	
4	5.87	.079	Gentle pleasant wind
5	7.33	.123	
10	14.67	.492	Pleasant brisk gale
15	22.00	1.107	
20	29.34	1.968	Very brisk
25	36.67	3.075	
30	44.01	4.429	High winds
35	51.34	6.027	
40	58.68	7.873	Very high
45	66.01	9.963	
50	73.35	12.300	A storm or tempest
60	88.02	17.715	A great storm
80	117.36	31.490	An hurricane
100	146.70	49.200	An hurricane that tears up trees, carries buildings before it, etc.

TABLE 1.1 THE VELOCITY AND FORCE OF WIND ACCORDING TO THEIR COMMON APPELLATIONS (after Smeaton, 1759)

up trees, carries buildings before it, etc.".

There were other wind scales in use by the weather observers of the time. In 1723 James Jurin, Secretary of the Royal Society, encouraged observers to send their records to the Society and recommended certain measuring instruments and procedures. For the wind he prescribed a scale of five divisions from 0 (a perfect calm), 1 (the lightest breeze), through 2 and 3 to 4 (the most violent wind). This system was in use for over a hundred years before it was overtaken by the more precise Beaufort Scale.

Admiral Sir Francis Beaufort kept a meticulous meteorological log throughout his distinguished career with the Royal Navy, both afloat and later on land. He used the first versions of his wind scale and weather notation in his private log of 1806. There were initially fourteen classes of wind strength including calm. This was later reduced to thirteen by combining the faint air and light air categories into a new Force 1. Since his scale was intended for everyday application at sea, it was naturally defined in terms easily recognized by the sailor, that is, the speed or sail carried by a ship of that period. Eventually the scale and weather notation were officially adopted by the Royal Navy. The wind categories, as specified in the Admiralty Memorandum of 1838, are given in Table 1.2.

The Beaufort Scale of wind force has undergone several modifications since its introduction. In its present form it also provides a reasonable guide for the land-based observer by associating the thirteen Beaufort numbers with the movement of common objects and ranges of wind velocity (see Table 1.3).

1.3 More Recent Developments in General Wind Description

In 1820 Heinrich Brandes published a description of the weather over Europe in the year 1783. He had collected data from a number of sources and prepared daily synoptic charts of the deviations of atmospheric pressure from the normal. Super-imposed on the patterns of isobars were arrows denoting the direction of the wind. From these and other prototypes of the now familiar "weather map" meteorologists

0	denotes	Calm	
1		Light Air ·	just sufficient to give . . .	Steerage way

2	Light Breeze	with which a well-executioned man-of-war, under all sail, and clean hull, would go in smooth water from . . .	1 to 2 knots
3	Gentle Breeze		3 to 4 knots
4	Moderate Breeze		5 to 6 knots

5	Fresh Breeze		Royals, etc.
6	Strong Breeze	in which the same ship could just carry, close hauled . . .	Single-reefs and top-gallant sails
7	Moderate Gale		Double-reefs, jib, etc.
8	Fresh Gale		Triple-reefs, courses, etc.
9	Strong Gale		Close-reefs and courses

10	Whole Gale	with which she could only bear . . .	Close-reefed main top-sail and reefed fore-sail
11	Storm	with which she would be reduced to . . .	Storm staysails
12	Hurricane	to which she could show	No canvas

TABLE 1.2 THE BEAUFORT WIND SCALE AS SPECIFIED BY ADMIRALTY MEMORANDUM, 1838 (from Garbett, 1926)

BEAUFORT NO.	DESCRIPTION	INDICATIONS	VELOCITY 20 FT. ABOVE LEVEL GROUND	
			m/sec	mph
0	Calm	Smoke rises vertically	under .6	under 1
1	Light air	Wind direction shown by smoke drift but not by vanes	0.6— 1.7	1— 3
2	Slight breeze	Wind felt on face; leaves rustle; ordinary vane moved by wind	1.8— 3.3	4— 7
3	Gentle breeze	Leaves and twigs in constant motion; wind extends light flag	3.4— 5.2	8—11
4	Moderate breeze	Dust, loose paper and small branches are moved	5.3— 7.4	12—16
5	Fresh breeze	Small trees in leaf begin to sway	7.5— 9.8	17—22
6	Strong breeze	Large branches in motion; whistling in telegraph wires	9.9—12.4	23—27
7	Moderate gale	Whole trees in motion	12.5—15.2	28—34
8	Fresh gale	Twigs broken off trees; progress generally impeded	15.3—18.2	35—41
9	Strong gale	Slight structural damage occurs; chimney pots removed	18.3—21.5	42—48
10	Whole gale	Trees uprooted; consider-able structural damage	21.6—25.4	49—56
11	Storm	Very rarely experienced; widespread damage	25.5—29.0	57—67
12	Hurricane		over 29.	over 67

TABLE 1.3 THE BEAUFORT WIND SCALE WITH INDICATIONS AND VELOCITY EQUIVALENTS

were soon to describe the occurrence and progress of storms in relation to centres of low pressure, thus foreshadowing the regular prediction of winds by isobaric analysis, a concept which will be taken up in Chapter 4 of this thesis. Meanwhile, detailed descriptions of the trade-winds and tropical storms had already been contributed by Dampier and his successors. By 1840 Heinrich Dove, in his "Law of Storms", was able to conclude that the general circulation consisted of equatorial and polar currents conflicting to produce the migratory weather systems of the temperate zones.

Throughout the nineteenth century the concept of the extratropical storm was constantly discussed and modified. In the light of present knowledge, perhaps one of the more significant models was proposed by Jinman in 1861 and recently rescued from obscurity by Ludlam (1966). Jinman's cyclone is reproduced in Figure 1.2 alongside the present-day representation of a typical storm centre over eastern Canada.

The requirements of marine navigation remained uppermost in the heyday of the sailing ship. By about 1850 extensive charts of ocean winds were generally available. Prominent among the draftsmen of ocean climate was the American naval officer Matthew Maury. He collected a wealth of meteorological information from ships' logs and compiled charts of, among other things, the winds and the most favourable sailing routes.

The necessary precursors of the modern understanding of the winds were the improved instruments and recording techniques. These were largely initiated in the last century.

Robinson designed his cup anemometer in 1846 and described it in a paper before the Royal Irish Academy in 1850. In its original form it consisted of four hemispherical cups mounted at the ends of cross-arms and free to rotate in the horizontal plane. A revolution counter was connected. The instrument was widely adopted but later redesigned with only three cups. This configuration, with the addition of beading around the lips of the cups, was proposed in Canada by Patterson (1926). The three-cup anemometer is still in widespread operational use, particularly in the United States and Canada.
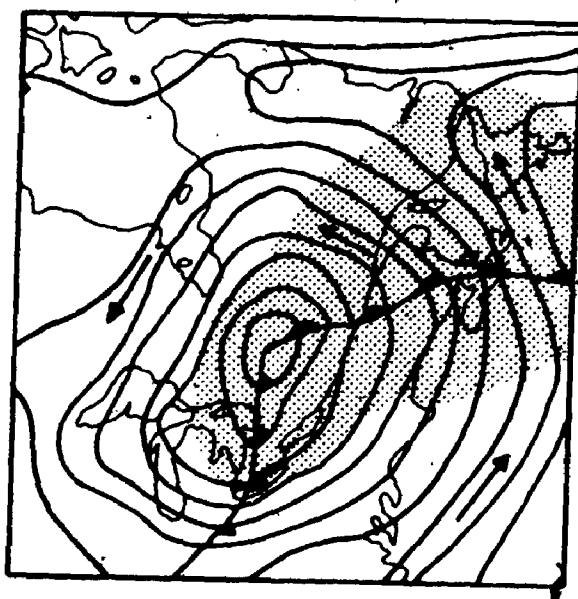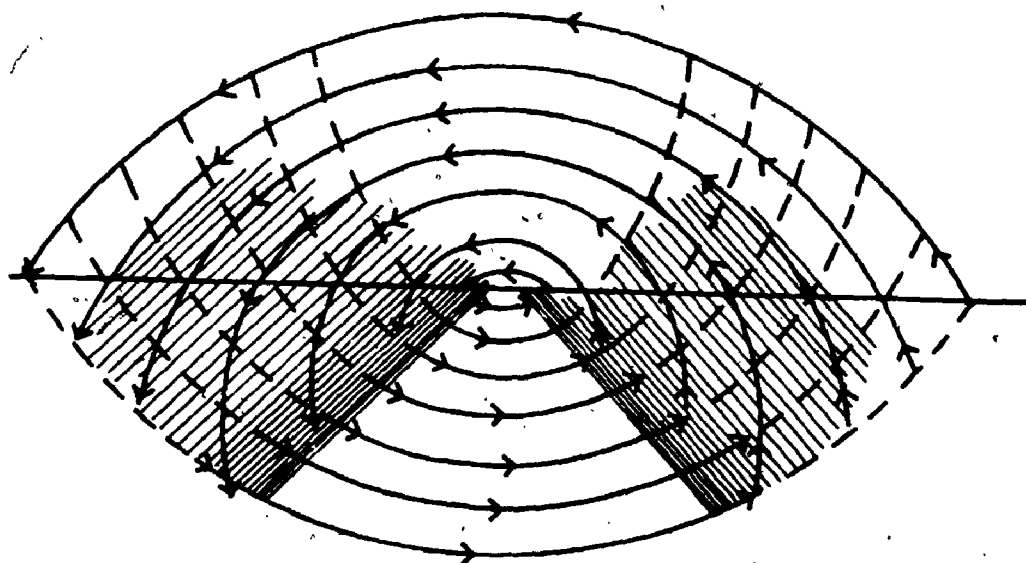
FIG. 1.2   COMPARISON OF JINMAN'S CYCLONE MODEL OF
1861 (FROM LUDLAM, 1966) AND A TYPICAL
STORM CENTRE OVER EASTERN CANADA

The Dines pressure-tube anemometer went into general use in the United Kingdom. It was designed to sense the dynamic pressure of the wind and, by means of a manometer and calibrated scale, directly indicate wind velocity. Both the Robinson and Dines instruments were soon adapted to provide continous records.

A third basic type of anemometer worked on the principle of the windmill. Numerous designs based on this idea were produced over the years, including a light six-bladed version favoured by the French engineer Gustave Eiffel and which he used to measure wind velocities at the top of his celebrated tower in Paris (Eiffel, 1900). However, not until after World War II did Friez (U.S.A.) and Sanuki (Japan) develop instruments of this type sufficiently compact and robust for regular service. In view of the later discussion in Chapter 3, it is interesting to note in passing that Eiffel's experiments at about 300 meters above ground level provided some of the first observational evidence of the vertical variation of the wind field.

Despite some recent standardization of wind measurement and recording procedures by the various meteorological agencies, the diversity of anemometer types and averaging periods of mean winds causes some difficulties in many engineering applications of wind statistics. Specific aspects of this problem will be discussed in Chapter 2 of this thesis.

The electric telegraph, which made its public debut in 1845, linking Washington, D.C. and Baltimore, Maryland, provided the technological means for widespread simultaneous weather reporting and central analysis. This, in turn, enabled prompt return of important information, such as storm warnings. The necessary administrative structures were also being formed at this time.

In the United States the Smithsonian Institute organized the first network of simultaneous observing stations linked by telegraph. From its small beginnings in 1849 it grew to over 600 stations just before the Civil War. In 1870 Congress established a national weather service under the Army Signals Corps. It was specifically charged

with predicting storms on the Great Lakes and the eastern seaboard. This reflected the current concern over the considerable loss of ships and lives due to unforeseen weather conditions. In 1868 alone, storms on the Great Lakes sank or damaged 1,164 vessels and claimed 321 lives. The weather service expanded rapidly to meet the requirements of trade, agriculture and later aviation. As well as tackling the immediate task of storm forecasting, the service soon began compiling local climatologies and issuing regular weekly bulletins on climate and crops. A hurricane first appeared on a weather map in 1874, and in 1898 a hurricane warning network was established.

A development of particular interest in the context of the present study is the measurement of upper level winds by tracking ascending balloons (see Chapter 4). In 1909 the U.S. Weather Bureau began releasing pilot balloons on a regular basis. Initially, these were tracked by theodolite, but in 1937 upper air soundings were begun using the radiosonde (invented by Moltchanoff in the Soviet Union around 1927). Improved methods of tracking by radio and radar were introduced during World War II.

Whilst these and other milestones were being passed in the United States, parallel developments were taking place in national meteorological services around the world. International co-operation was also encouraged such that, by 1885, the American and British services were jointly involved in storm forecasting for the Atlantic Ocean. As early as 1910, the U.S. Weather Bureau was routinely collecting simultaneous weather observations for almost the entire northern hemisphere.

1.4 Wind Records in Canada

The "Magnetical Observatory" was established in Toronto in 1839. Wind measurements began there in 1841 using the pendulum anemometer, so that wind strengths were initially recorded in pounds. Directions and velocities (in miles per hour) were first recorded in 1848. Elsewhere, observations were contributed by amateur meteorologists and scientists, notably Dr. Charles Smallwood of Montreal, who established an observatory at St. Martin's in what was then Canada East.

Two Canadian scientific journals of the nineteenth century published regular meteoro-
logical summaries. The "Canadian Journal" carried monthly and annual climatological
data for the Toronto observatory. Among the parameters of the wind climate noted
were the resultant wind vector, the mean velocity and the maximum velocity. As an
example, the wind summary for the year 1867 is reproduced in Table 1.4. Tabulations
of data for St. Martin's (on the St. Lawrence River northeast of Montreal) appeared in
the "Canadian Naturalist" and, in the same journal, Smallwood published descriptions
of the climate recorded at his observatory:

> "The greatest velocity recorded here exceeds somewhat 60 miles
> per hour linear, — there seems a disposition for a change both in
> the direction and velocity, at 3 p.m. and at 3 a.m., which
> corresponds precisely with the diurnal barometric fluctuations.
> The whole amount of miles linear of wind during the past year
> (1856) was 53061.63 miles, which being resolved into the four
> cardinal points, gave, N. 6969.80 miles; S. 5298.89 miles; -
> E. 10776.40 miles, and W. 30016.56 miles. The maximum
> velocity during the past year was 44.40 miles per hour."
> (Smallwood, 1857)

The somewhat cumbersome representation of annual mean velocities reflects the direct
registration of miles of wind obtained from a self-recording cup anemometer.

The observatory at Toronto formed the nucleus of Canada's meteorological service
when, in 1871, the government approved the expenditure of $5,000 for further obser-
vations. Like its counterpart in the United States, the service's task was to issue
storm warnings. Nevertheless, climatological data was soon being assembled and issued
in the "Monthly Weather Review". An interesting feature of this publication was the
inclusion of wind-roses to describe the wind climate at each observing station
(Figure 1.3), forerunners of today's more complex roses and frequency distributions
(see Figure 1.4 and applications in later chapters).

Detailed statistics were also given in the annual reports of the service and, from
1916, in the "Monthly Record". At a time when observations were usually taken three
times per day, statistics relating to these times were tabulated separately. Normally, the

	1867	RESULT OF 19 YRS.	EXTREMES	
Resultant direction	N60°W	N61°W		
Resultant velocity in miles	2.05	1.89		
Mean velocity, without regard to direction	7.00	6.89	8.55/1860	5.10/1853
Month of greatest mean velocity	Dec.	Mar.	Mar. 1860	Jan. 1848
Greatest monthly mean velocity	10.32	8.83	12.41	5.82
Month of least mean velocity	Jun.	Jul.	Aug. 1852	Sept. 1860
Least monthly mean velocity	4.13	4.95	3.30	5.79
Day of greatest mean velocity	May 1		Mar. 19/59	Dec. 2/59
Greatest daily mean velocity	20.99	23.05	31.16	15.30
Day of least mean velocity	Aug. 7			
Least daily mean velocity	0.23			
Hour of greatest absolute velocity	Dec. 6 7–8 pm		Dec. 27/61 9–10 am	Mar. 14/53 11–noon
Greatest velocity	36.8	40.02	46.0	25.6

TABLE 1.4 SUMMARY OF WIND OBSERVATIONS AT TORONTO FOR 1867
(from the Canadian Journal, 1868 — wind velocities in m.p.h.)
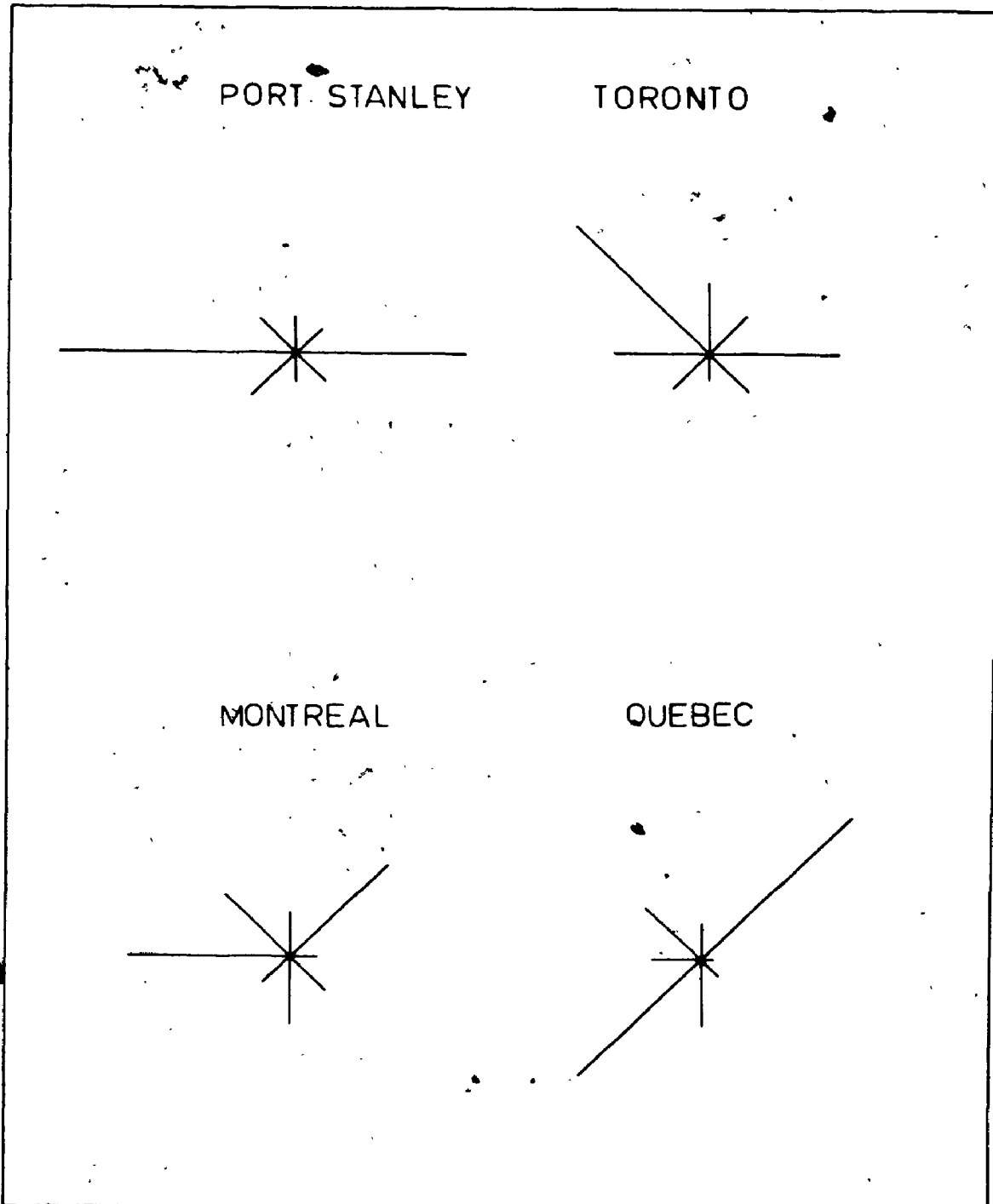
FIG. 1.3   DIAGRAMS SHOWING THE NUMBER OF HOURS IN
THE MONTH DURING WHICH THE WIND BLEW
FROM EACH DIRECTION; ONE INCH REPRESENTING
200 HOURS (FROM THE MONTHLY WEATHER
REVIEW, MARCH 1882)

HOURLY WIND DATA

KEY

MEAN WIND 4.92 M/S

1-3 4-8 9-13 >14 M/S

5.81

5.32

6.53

3.7% CALM

6.22

5.05

5.18

5.99

b. WIND ROSE

5   10   15   20 M/S

10^2

10^3

10^4

FREQUENCY PER .45° SECTOR

c. HOURLY FREQUENCY DISTRIBUTION

FIG. 1.4   FREQUENCY DISTRIBUTION OF WINDS
AT LONDON, ONTARIO (JANUARY 1957-66)

step is in the realm of statistical inference. The evidence of the data, and other theoretical and empirical factors, might well suggest a behavioural model expressed in probabilistic terms, such as a certain probability distribution function. The model can then be employed, with a certain level of statistical confidence, to predict a given meteorological event. This general area will be the concern of Chapter 2.

The traditional statistical measures applied to the winds are, as indicated in the previous section, the mean speed and the resultant, or vector mean. It is now common practice to classify the observations into finite intervals of speed and direction to produce a frequency distribution. Frequencies are usually normalized by the total number of observations. Other measures of central tendency can then be estimated, particularly the modal, or most likely, values of speed and direction (the "prevailing" wind).

A statistic commonly employed by climatologists is "persistence", defined as the ratio of the magnitude of the resultant wind to the mean wind speed. It implies the relative strength of winds from the prevailing direction. Variability can be measured by the standard deviation, and higher moments of the data (skewness and kurtosis) can indicate the general shape of the frequency distribution. The variability of wind vectors is measured by the standard vector deviation.

The modern wind-rose is a diagrammatic representation of the bivariate frequency distribution of speed and direction. This notation can also indicate the incidence of calms and the mean wind speeds associated with each direction (see Figure 1.4b). An alternative treatment is to plot frequency against direction and the mid-point of the wind speed interval, and then construct contours of frequency. Although this form has a certain illustrative value, it erroneously suggests that a finite frequency can be assigned to a specific wind vector. To avoid this objection, it is possible to rearrange the frequency distribution to give the frequencies of wind speeds less than or equal to given values (the cumulative frequency distribution) and, conversely, the frequencies of exceedance. The latter can also be plotted on a plane of wind vectors to give a two-dimensional representation of the familiar "probability mountain".

resultant wind vector was given, together with the mean and maximum velocities for the month or year.

Due to the steady increase in the number of Canadian weather stations and the frequency of observations, the scope of available wind records is now considerable. In March 1973, for example, the "Monthly Record" summarized hourly wind data from 248 stations. It listed not only the traditional quantities (means and maxima), but also the occurrence frequencies of wind speeds and directions, and the maximum gust speeds. More detailed information for a number of stations is available in the "Annual Meteorological Summaries", which include historical records of the monthly and annual maximum winds. In addition, the "Hourly Data Summaries" contain mean monthly frequency distributions.

Apart from these sources of surface wind data, there are a number of published climatologies covering various regions of Canada. Most of these have been listed by Thomas (1961).

The Canadian radiosonde network began operation in 1941, preceeded by a limited programme of pilot balloon ascents. The "Monthly Bulletin" of upper air data first appeared in 1959. It provides those interested in wind climate aloft with the processed results from twice-daily radiosonde flights at over thirty stations, data which will be used extensively in the present study. Wind speed and direction are recorded for the surface and certain standard pressure surfaces above 1000 millibars. As a further aid to the understanding of upper winds, but closer to the ground, a quarterly bulletin is now available giving regular observations taken on towers of various heights. There are some seventeen locations, generally in urban surroundings.

1.5 The Application of Statistics to Wind Climate

The collection of a substantial volume of data is but the first step towards successful prediction of wind climate. Suitable statistical tools must then be used to summarize the data and provide some quantitiative notion of passed events. The third

These methods of depicting a bivariate frequency distribution are illustrated in Figure 1.4. The same hourly wind records for London, Ontario in the month of January have been used throughout. The original data tabulation is shown in Figure 1.4a.

Perhaps the first probabilistic model to be applied to meteorological elements was the simple law of errors, or normal distribution. The (cumulative) probability distribution function, and its derivative the density function, are defined completely by the mean and standard deviation. It has often been applied to atmospheric pressure and temperature, suggesting that the various physical factors contributing to their occurrence are, at least effectively, independent. However, this may not always hold true and other considerations, such as a known skewness in the frequency distribution, might indicate an alternative model. Such is the case with rainfall and wind speed.

The choice of a theoretical distribution to describe the winds is still, to a large extent, a matter of personal preference. However, there are a number of pointers to a group of closely related exponential functions. For example, it has been shown (Brooks, Durst and Carruthers, 1946, and others) that upper winds can be well represented by the bivariate normal distribution. In a particular restriction of the general form, closely followed by many data samples, the density function is circular and centred at the origin of the axes. It turns out that the corresponding distribution of wind speeds, derived by integrating the bivariate function over all directions, is Rayleigh, a particular case of the chi distribution (see Figure 1.5). It is defined by a single parameter equivalent to the standard vector deviation of the original bivariate form.

The general concepts outlined above are now firmly established among engineers and others concerned with future meteorological events. Unfortunately, it is often insufficient to simply prescribe a distribution of the entire population of winds (the parent distribution). Many areas of application are concerned with the occurrence of extreme values, a branch of statistics for which a good body of theory is now available.

CUMULATIVE DISTRIBUTION

PARENT PROBABILITY
FUNCTIONS-RAYLEIGH

DENSITY FUNCTION

WIND SPEED

PROBABILITY

CUMULATIVE
DISTRIBUTION

DENSITY
FUNCTION

EXTREME PROBABILITY
FUNCTIONS

WIND SPEED

PROBABILITY

PROBABILITY

N

BIVARIATE NORMAL DENSITY
FUNCTION
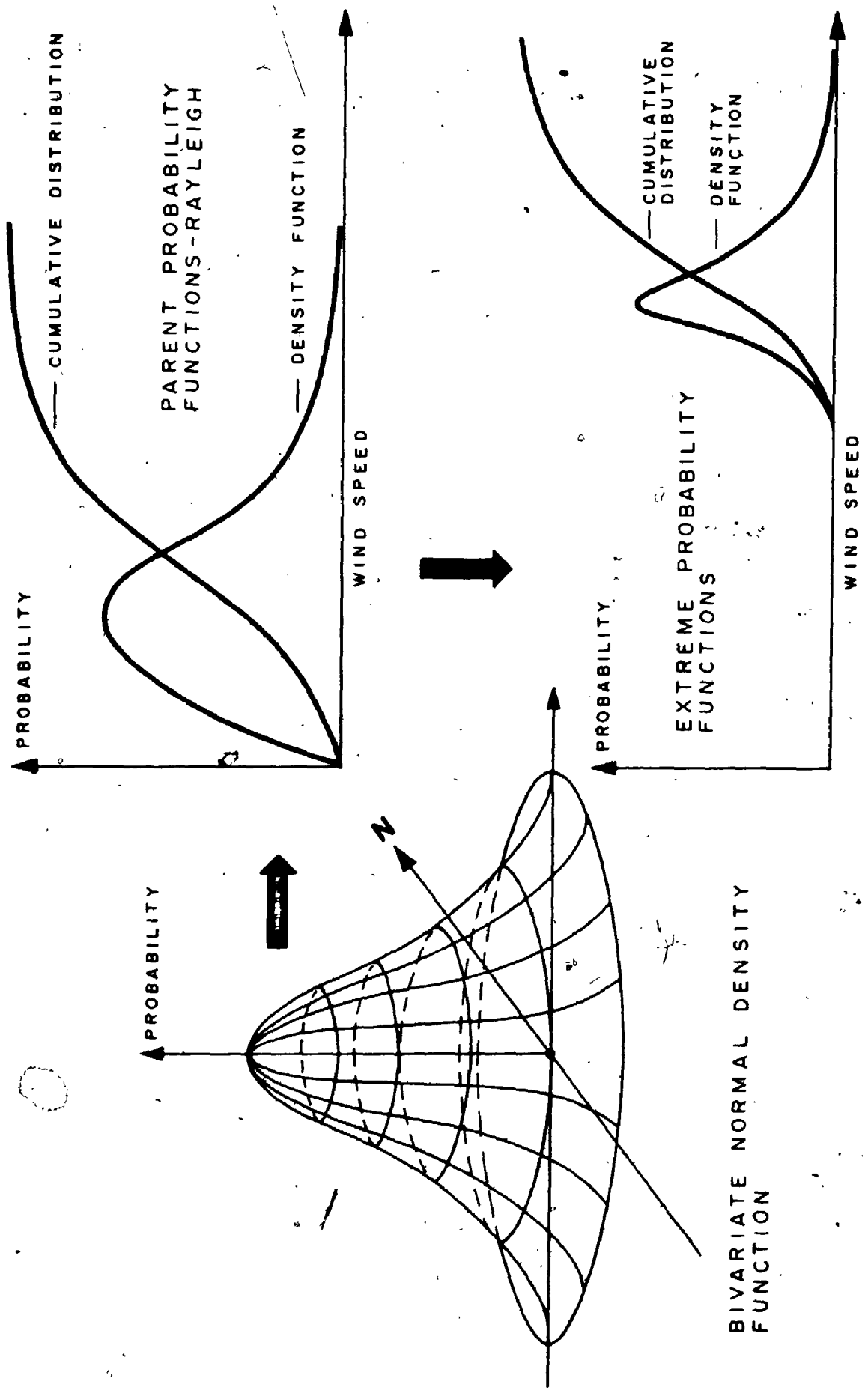
FIG. 1.5   RELATIONSHIP BETWEEN PARENT DISTRIBUTIONS OF WIND VECTORS
AND WIND SPEEDS AND THE DISTRIBUTION OF EXTREME VALUES

The modern theory of the statistics of extremes originated around 1920. Initially, investigations centred on the extremes of samples taken from the normal distribution and their relation to sample size. A significant contribution was made by Fisher and Tippett (1928), who derived the three asymptotic distributions of extreme values. They pointed out that the same results are obtained from a group of parent distributions. Later, von Mises was to define the conditions under which the asymptotic forms were valid. The three distributions may be interpreted physically as describing the largest or smallest value of an unlimited variable (Type I), the largest value of a variable with a lower limit (Type II) and the largest or smallest value limited in the range of interest (Type III). It should be noted that both the first and second types are completely defined by two parameters which express the scale and shape of the distribution. The general relationship between the extreme and parent probability functions is illustrated in Figure 1.5.

In 1932 a significant discussion contributed by S.P. Wing appeared in the proceedings of the American Society of Civil Engineers on the subject of wind loads on steel buildings (Wing, 1932). This was one of the earliest proposals to introduce the statistics of extreme winds into engineering design. Another pioneer in the application of extreme value theory, E.J. Gumbel, devised a widely-adopted method for fitting extreme data to the first asymptotic distribution (see Gumbel, 1954). He is largely responsible for the considerable practical acceptance which the theory has gained over the past fifteen years or so, including applications to wind climate.

Since, in meteorology, there exists a natural periodicity of one year, the analysis of strong winds has concentrated on the annual maxima. Thus Shellard (1960) applied the Type I extreme distribution to the recorded yearly maxima in the United Kingdom and developed maps of the surface wind speed likely to be exceeded, on average, once in 50 years (the 2% quantile or 50-year return wind). Thom (1968) undertook similar work for the United States, but preferred to use the Type II distribution.

In extreme wind analysis and other investigations of wind climate, difficulties frequently arise due to non-independence of samples, averaging times of observations and instrument response. These and other factors may impair the homogeneity of

climatic data and the validity of statistical models. To understand and perhaps avoid such pitfalls, the theory of stochastic processes may be brought to bear on the problem.

Wind speed can be regarded as a continuous random function which consists of a number of harmonic components of various strengths, represented by the power spectrum (shown schematically in Figure 1.6). The function can only be described in statistical terms and, if the statistics are constant throughout a given record, the process is said to be stationary. Stationarity is an important assumption facilitating fairly straightforward analysis. Wind can be considered in this way be separating the fluctuations according to their characteristic time scales and regarding each as a "locally stationary" process. They divide roughly into "gusts" in the micrometeorological range, with periods less than about 20 minutes, and the remaining low frequency or mean wind components. The latter derive from diurnal influences and the passage of individual storms (the mesometeorological range), and seasonal fluctuations. Thus, a series of hourly surface wind or twelve-hourly upper wind measurements will constitute a roughly stationary record of the larger scale climatic process. A knowledge of the microscale components is also important to explain, for example, the statistical differences between hourly records of maximum gusts, and ten-minute mean wind speeds (see Chapter 2).

The theory of stochastic processes is not new to the communications and control engineers, who have used such concepts since the 1930's, but it is a relatively recent departure in the study of winds. Much of the initial work centred on the high frequency fluctuations, or atmospheric turbulence, and particularly the implications for structural design against wind action (see, for example, Davenport, 1968). The theory has also been used to derive improved distributions of extreme values and other statistics of wind climate, such as the durations of storms. These developments draw heavily on earlier work, notably by Rice (1954) and Cartwright and Longuet-Higgins (1956), concerning the crossing rate of certain levels of a random function.

1.6   Engineering Uses of Wind Statistics

The interaction of the natural wind and man-made structures is at least of passing concern to many engineers and planners. It may add an unwelcome dimension

MICROMETEOROLOGICAL
RANGE
(TURBULENCE)

MESOMETEOROLOGICAL
RANGE

STRONG
WIND

PERIOD: 1 YEAR   4 DAYS 12 HOURS 1 HOUR   1 MINUTE   1 SECOND
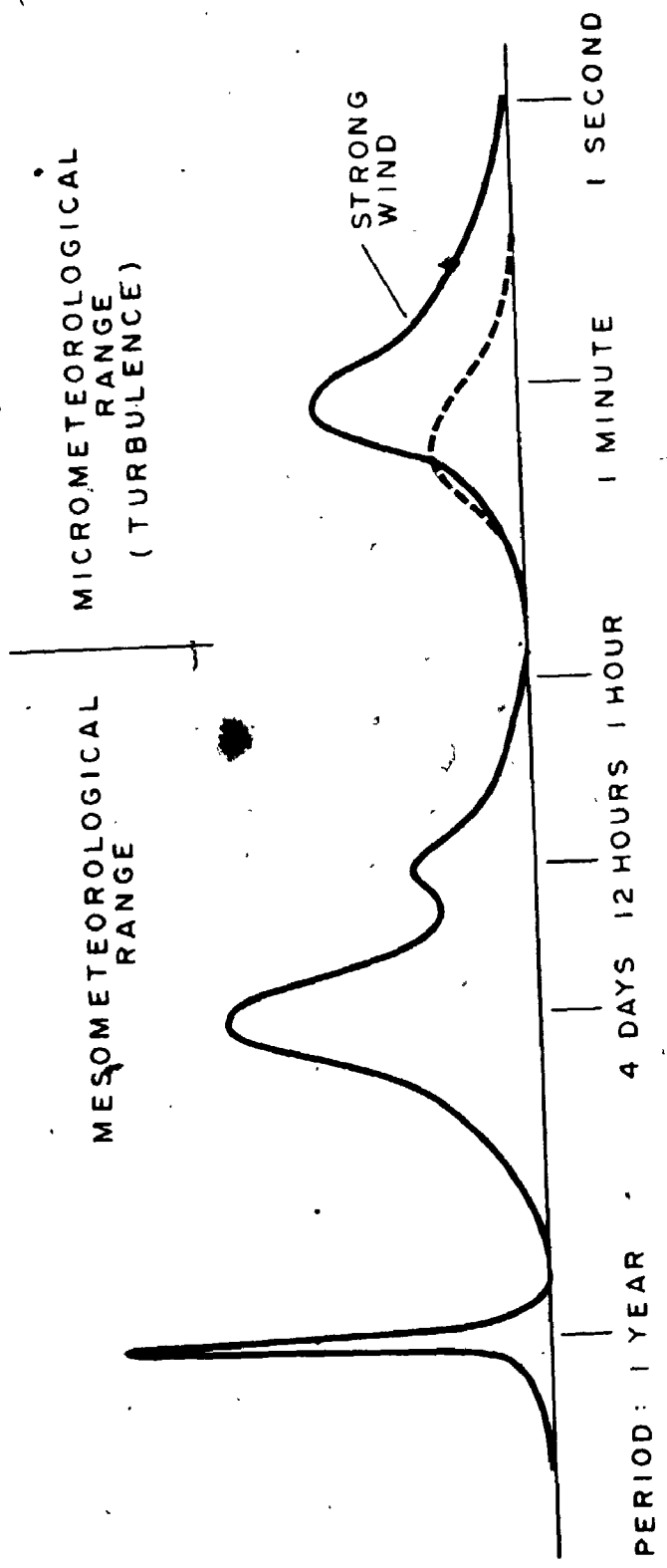
FIG. 1.6   SCHEMATIC OF WIND SPECTRUM

to a structural design problem, such as a tall building, or it may be the *raison d'etre* for the entire project, such as power generation from the wind. In either case a good understanding of future climatic events is required. As outlined in the previous discussion, this is best expressed in statistical terms. Depending on the design philosophy, the required information may range from a specific wind condition to a detailed probability distribution.

Many countries have now established codes of practice containing procedures for dealing with wind loads on structures. Design wind speeds in different locations are often recommended, based on a certain return period of years. These may be either maximum gust speeds, as in the British Code of Practice (British Standards Institution 1972), or maximum mean hourly speeds to be used in conjunction with recommended gust factors, as in the Canadian National Building Code (National Research Council, 1970). However, for unconventional structures a special investigation may be necessary, perhaps involving a meteorological study of the site and wind tunnel tests to determine the static and dynamic behaviour under wind action. The results, such as peak responses, might well be expressed in probabilisitc terms, an essential ingredient being a reliable model of the bivariate distribution of mean winds (see Davenport, 1971, for a discussion of the general approach). Similar methods can be employed to describe the microclimate in the vicinity of tall buildings from the point of view of pedestrian comfort.

Good statistical models of wind climate are also applicable in studies of the distribution of air pollutions over wide areas. Some numerical methods (for example, Bowne, 1969) divide the region into grid squares and use plume and puff idealizations to find the proportion of source concentrations carried into squares downwind. The overall picture is obtained by summing the effects of all sources under given weather conditions. By incorporating probability distributions of the meteorological elements, including wind, this method can be extended to yield statistical descriptions of pollution "climate" over the area.

The operation of short take-off and landing (STOL) aircraft into small areas close to city centres is likely to become a common feature of air transportation in the next

few years. Wind climate will be an important factor in the siting and orientation of landing strips for at least two reasons.

Firstly, concerning siting, it is desirable to position the STOL-port such that it is most often upwind of the built-up city centre, thus minimizing general levels of atmospheric turbulence near the ground. The aircraft types in question, having low wing loadings, experience handling difficulties in highly turbulent conditions. Clearly, optimum siting will involve a close examination of prevailing wind statistics.

Secondly, the runway should be aligned such that the proportion of time the facility is unusable due to high crosswinds is minimized. A bivariate wind distribution model will be useful here, from which the probabilities of exceeding a specified crosswind component can be calculated for any given alignment. Similar techniques will apply to conventional airports and can be extended to encompass cases of two or more runways (a recent approach has been given by Falls and Brown, 1972).

Strong winds over oceans and coastal regions, especially those affected by cyclones or hurricanes, can create particular difficulties for the engineer. Statistical models of hurricanes are still far from finalised, but there is some evidence that the probability distributions of extreme wind speeds in tropical storms are distinctly different (for example, Thom, 1970). It is also possible to formulate the statistics of extreme wave heights from the wind climate over oceans, this being of considerable importance in the design of harbour defenses and other marine structures (Thom, 1973).

The last application to be mentioned in this brief survey is that of power generation from the natural wind. This possibility has recently enjoyed a revival as part of the public debate on the rising cost and diminishing availability of fossil fuels. In theory, the power generated by a windmill device or aerovane is proportional to the cube of the wind speed. However, there are inevitable losses which might cut the output of the generator to below 50% of the energy of the incidence airflow. In general, the proportion of theoretical power available will be a function of wind speed, there being also a minimum wind speed at which generation begins and a maximum operational speed. These machine properties can be combined with the probability distribution of winds to predict the total energy likely to be delivered in any one year period. Other

critical statistics would be the proportion of time the wind dips below the maximum generating speed or exceeds the maximum, and the distribution of idle periods. Although these considerations are not new (see Tagg, 1957), renewed investigations may be in order in the light of current trends and recent advances in the statistical description of winds.

The questions of airport runway alignment, ocean wave heights and wind power will be discussed in greater detail towards the conclusion of this thesis.

1.7 The Present Study

This study will be principally concerned with various statistical models of mean wind climate, the emphasis being placed on strong winds at ground level and gradient height, at the top of the atmospheric boundary layer. The purpose is to examine these models and their interrelation, introducing some improved approaches likely to be of practical interest.

Chapter 2 will discuss bivariate distributions of wind vectors and corresponding distributions of speeds, extreme value theory applied to wind climate, and the relationship between gust and mean wind statistics. Some of the results will then be used in a comparative survey of extreme wind statistics for a number of countries around the world.

The connection between surface and gradient winds will be investigated in Chapter 3 with the aid of some physical, as well as statistical, models.

The general problem of establishing wind climate will be treated in Chapter 4. The suitability of surface wind records and upper air data will be discussed from the standpoint of various terrain influences and statistical errors. In addition, climates of winds calculated from synoptic records of atmospheric pressure will be derived and compared with those obtained by conventional methods.

Finally, the outcome of this work will be discussed in the context of some specific engineering applications.

CHAPTER 2

STATISTICAL PROPERTIES OF WINDS AND THEIR EXTREME VALUES

2.1 General

The practical requirement for good statistical models of wind climate, and particularly extreme events, has already been outlined. Some specific distribution types have evolved, from both theoretical and empirical considerations, as being representative in most situations. These include the bivariate normal distributions (at upper levels) and the Weibull and Rayleigh distributions of wind speed regardless of direction. Of the extreme value forms, the first and second asymptotic types are most commonly encountered.

In view of the fundamental importance of selecting an appropriate distribution, and the frequent necessity of comparing statistics derived from different models, it is pertinent to re-examine the relationships between the bivariate and univariate forms and the various extreme distributions, and then to explore the significance of averaging time, as between mean winds and peak gusts.

2.2 The Bivariate Normal Distribution

The general bivariate normal distribution of wind vectors has the following probability density function:

$$p(V_x,V_y) = \frac{(1 - r_{xy}^2)^{-1/2}}{2\pi\sigma_x\sigma_y} \ exp[\frac{-1}{2(1 - r_{xy}^2)}$$

$$(\frac{(V_x - \bar{V}_x)^2}{\sigma_x^2} - \frac{2r_{xy}(V_x - \bar{V}_x)(V_y - \bar{V}_y)}{\sigma_x\sigma_y} + \frac{(V_y - \bar{V}_y)^2}{\sigma_y^2})] \qquad (2.1)$$

in which V_x and V_y are the zonal and meridional velocity components respectively,

$\quad\bar{V}_x$ and $\bar{V}_y$ are the component means,

$\quad\sigma_x$ and σ_y are the component standard deviations

and $\quad r_{xy}$ is the correlation coefficient between the components.

The vector mean, or resultant, is given by

$$\bar{V}_r = (\bar{V}_x^2 + \bar{V}_y^2)^{1/2} \qquad\qquad (2.2)$$

Following the usual meteorological convention, x and y will be defined as posi-. tive for winds blowing from the west and south respectively. The bivariate surface, when projected onto the x-y plane, can be represented as a series of elliptical contours of certain probability levels centred on the vector mean (Figure 2.1a). The ellipse drawn through the component standard deviations will enclose approximately 39% of the distribution and is used to illustrate the special cases of the distribution in the remainder of Figure 2.1.

Winds aloft have been found to be distributed closely in accordance with the bivariate normal function (Brooks, Durst and Carruthers, 1946, and others). Furthermore, the restrictions of zero x-y correlation and equal component standard deviations apply at most locations and altitudes. This is the offset circular case. Crutcher and Halligan (1967) note that noncircular distributions are found where the overall wind climate is composed of distinctly different regimes, such as along the boundary between prevailing westerlies and easterly trade winds, over mountainous regions, above coastlines and, at higher altitudes, in regions of preferred jetstream formation and just above monsoon circulations. From an examination of over one thousand seasonal upper wind distributions, they report that, although noncircularity is at least twice as

a) GENERAL DISTRIBUTION
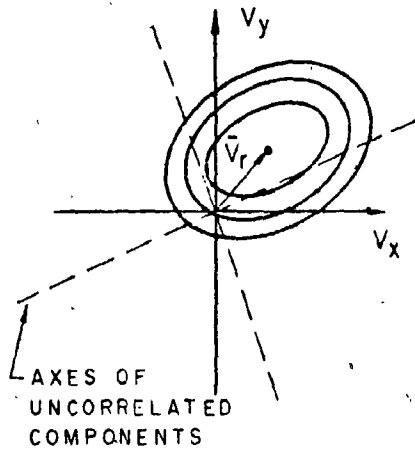
$$p\ (V_x, V_y) = \frac{(1-r_{xy}^2)^{-1/2}}{2\pi\sigma_x\sigma_y}\ \exp\left[\frac{-1}{2(1-r_{xy}^2)}\right.$$

$$\left(\frac{(V_x-\bar{V}_x)^2}{\sigma_x^2} - \frac{2r_{xy}(V_x-\bar{V}_x)(V_y-\bar{V}_y)}{\sigma_x\sigma_y} + \right.$$

$$\left.\left.\frac{(V_y-\bar{V}_y)^2}{\sigma_y^2}\right)\right]$$

$$\bar{V}_r = (\bar{V}_x^2 + \bar{V}_y^2)^{1/2}$$

AXES OF
UNCORRELATED
COMPONENTS

b) UNCORRELATED ELLIPTICAL
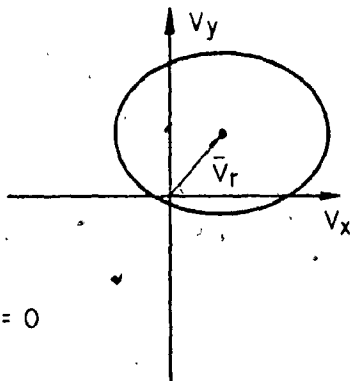
$r_{xy} = 0$

c) CENTRAL ELLIPTICAL
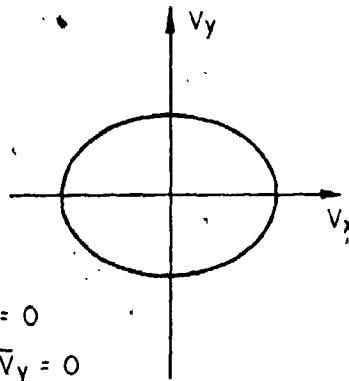
$r_{xy} = 0$
$\bar{V}_x = \bar{V}_y = 0$

d) NON-CENTRAL CIRCULAR
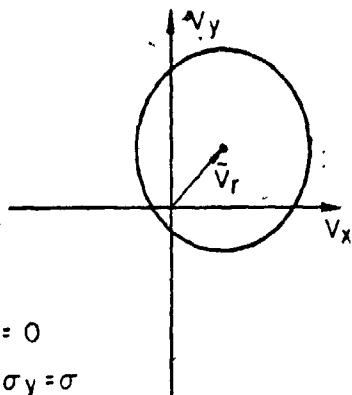
$r_{xy} = 0$
$\sigma_x = \sigma_y = \sigma$

e) CENTRAL CIRCULAR
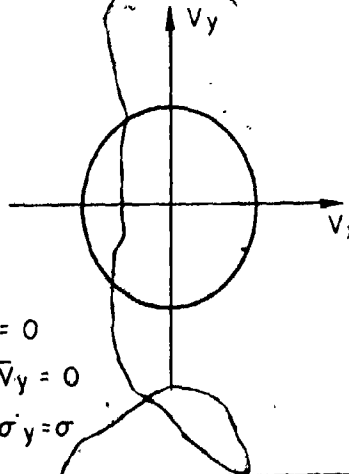
$r_{xy} = 0$
$\bar{V}_x = \bar{V}_y = 0$
$\sigma_x = \sigma_y = \sigma$

FIG. 2.1   BIVARIATE NORMAL DISTRIBUTIONS
OF WIND VELOCITIES

frequent over continents than over oceans, the proportion of elliptical to circular distributions over the Northern Hemisphere is about one to six (in this case a distribution was considered elliptical if the ratio of the larger component standard deviation to the smaller was 1.2 or more).

The offset circular density function is:

$$p(V_x, V_y) = \frac{1}{2\pi\sigma^2} \, exp[\frac{-((V_x - \bar{V}_x)^2 + (V_y - \bar{V}_y)^2)}{2\sigma^2}] \qquad (2.3)$$

where

$$\sigma = \sigma_x = \sigma_y \qquad (2.4)$$

Conveniently, the sole defining parameters are the standard vector deviation, σ, and the magnitude and direction of the vector mean. These quantities are suitable for mapping and this has been done for most of the world and at various altitudes, usually at standard pressure surfaces above 850 millibars. Examples are to be found in Brooks et al (1950), Henry (1957) and Crutcher and Halligan (1967). However, of more immediate interest to the earth-bound engineer is the wind climate at gradient height, at what can be regarded as the top of the atmospheric boundary layer. As shall be described in a later chapter, this can be related to the surface climate. In a previous study the writer (Baynes, 1971) established a preliminary climate of gradient winds over Canada, also based on the circular model. As indicated above, the circular distribution is best followed when only one distinct wind regime predominates, so the analysis is usually applied to seasonal or monthly accumulations of data.

2.3 Wind Speed Distributions Derived from the Bivariate Normal Model

Given a bivariate distribution of winds, it is useful to obtain directly the corresponding distribution of wind speeds, regardless of direction. Unfortunately, in only one special case is the solution obtainable in closed form, but Weill (1954) has given a general expression for the density function of speed, V,

where the components, V_x and V_y, are completely uncorrelated. It can be written as follows:

$$p(V) = A_0 V \exp(-A_1 V^2) \cdot [I_0(A_2 V^2) I_0(A_3 V)$$

$$+ 2 \sum_{j=1}^{\infty} I_j(A_2 V^2) I_{2j}(A_3 V) \cos 2j\psi] , \quad V \geqslant 0 \tag{2.5}$$

where

$$A_0 = \frac{1}{\sigma_x \sigma_y} \exp[-\frac{1}{2}(\frac{\overline{V}_x^2}{\sigma_x^2} + \frac{\overline{V}_y^2}{\sigma_y^2})];$$

$$A_1 = \frac{\sigma_x^2 + \sigma_y^2}{4\sigma_x^2 \sigma_y^2} ; \quad A_2 = \frac{\sigma_x^2 - \sigma_y^2}{4\sigma_x^2 \sigma_y^2}$$

$$A_3 = [(\frac{\overline{V}_x}{\sigma_x^2})^2 + (\frac{\overline{V}_y}{\sigma_y^2})^2]^{1/2}$$

and $\tan \psi = \frac{\overline{V}_y \sigma_x^2}{\overline{V}_x \sigma_y^2}$ \hfill (2.6)

I denotes a Bessel function of the first kind.

If the components are correlated, as when the major and minor axes of the elliptical distribution are oriented other than in the x-y directions, it is necessary to transform them to uncorrelated variables. In fact the transformation consists of a simple rotation of the axes so as to be parallel with the axes of the ellipse (see Figure 2.1a). This results in a redefinition of the parameters listed above (Yadavalli, 1967):

$$A_0 = \frac{1}{\sigma_a \sigma_b} \, expl - \frac{1}{2}(\frac{\overline{V}_x^2}{\sigma_a^2} + \frac{\overline{V}_y^2}{\sigma_b^2})l;$$

$$A_1 = \frac{\sigma_x^2 + \sigma_y^2}{4(1 - r_{xy}^2) \, \sigma_x^2 \sigma_y^2};$$

$$A_2 = \frac{[(\sigma_x^2 - \sigma_y^2)^2 + 4r_{xy}\sigma_x^2\sigma_y^2]^{1/2}}{(1 - r_{xy}^2)\sigma_x^2\sigma_y^2};$$

$$A_3 = [(\frac{\overline{V}_x}{\sigma_a^2})^2 + (\frac{\overline{V}_y}{\sigma_b^2})^2]^{1/2};$$

$$tan\psi = \frac{\overline{V}_y \sigma_a^2}{\overline{V}_x \sigma_b^2} \qquad\qquad (2.7)$$

where σ_a^2 and σ_b^2 are the uncorrelated component variances, given by the positive and negative roots respectively from:

$$\frac{1}{2} [\sigma_x^2 + \sigma_y^2 \pm ((\sigma_x^2 + \sigma_y^2)^2 - 4\sigma_x^2\sigma_y^2(1 - r_{xy}^2))]^{1/2} \qquad\qquad (2.8)$$

The wind speed distributions associated with each of the restrictions illustrated in Figure 2.1 can be deduced straightforwardly from these general expressions. The circular cases, of particular significance here, will now be examined in detail.

2.4 Wind Speeds from Bivariate Circular Models

For the offset circular distribution Equation 2.5 reduces to:

$$p(V) = \frac{V}{\sigma^2} \, expl - \frac{(V^2 + \overline{V}_r^2)}{2\sigma^2} lI_0 (\frac{\overline{V}_r V}{\sigma^2}), \quad V \geqslant 0 \qquad\qquad (2.9)$$

in which $\overline{V}_r$ is taken as the magnitude of the vector mean. This is known as the non-central chi_2 distribution and can be rewritten in terms of the non-dimensional quantities t and λ as follows:

$$p(t) = t \, expl - \frac{(t^2 + \lambda^2)}{2} l \, I_0(\lambda t), \quad t > 0 \qquad\qquad (2.10)$$

where

$$t = \frac{V}{\sigma}; \lambda = \frac{\bar{V}_r}{\sigma} \qquad (2.11)$$

The cumulative probability function is then given by:

$$P(t) = exp\left(-\frac{\lambda^2}{2}\right) \int_0^t t \, exp\left(-\frac{t^2}{2}\right) I_0(\lambda t) dt \qquad (2.12)$$

Following Smith (1971), the Bessel function can be expanded as

$$I_0(\lambda t) = \sum_{j=0}^{\infty} \frac{(-1)^j (\lambda t)^{2j}}{2^{2j} j! \, \Gamma(j+1)} \qquad (2.13)$$

and then, integrating term by term, a series solution is obtained:

$$P(t) = exp\left(-\frac{\lambda^2}{2}\right)[(1 - exp(-\frac{t^2}{2}))$$

$$+ \frac{1}{(1!)^2}\left(\frac{\lambda}{2}\right)^2 [2(1 - exp(-\frac{t^2}{2})) - t^2 \, exp\left(-\frac{t^2}{2}\right)]$$

$$+ \frac{1}{(2!)^2}\left(\frac{\lambda}{4}\right)^4 [4[2(1 - exp(-\frac{t^2}{2}))$$

$$- t^2 \, exp(-\frac{t^2}{2})] - t^4 \, exp\left(-\frac{t^2}{2}\right)] + \ldots] \qquad (2.14)$$

According to Smith this converges satisfactorily for λ less than about 3.5. Fortunately, the distribution can be characterized fairly readily by its various moments, an expression for which has been derived by Park (1961). The first two moments are:

$$m_1 = \left(\frac{\pi}{2}\right)^{1/2} exp\left(-\frac{\lambda^2}{2}\right) {}_1F_1\left(1\frac{1}{2}; 1; \frac{\lambda^2}{2}\right) \qquad (2.15)$$

and $m_2 = 2 \, exp\left(-\frac{\lambda^2}{2}\right) {}_1F_1\left(2; 1; \frac{\lambda^2}{2}\right) \qquad (2.16)$

where $_1F_1$ denotes the confluent hypergeometric function. The above examples can be easily transformed to fall within the range of parameters commonly listed in mathematical tables (for example, Abramowitz and Stegun, 1964). The behaviour of the mean and standard deviation of t as a function of λ has thus been developed and plotted in Figure 2.2.

As the non-dimensional variable λ approaches zero, the bivariate circular form becomes central with respect to the x-y axes and the wind speed distribution is Rayleigh:

$$P(V) = 1 - exp(-\frac{V^2}{2\sigma^2}) \qquad (2.17)$$

with a mean value of $(\pi/2)^{1/2}\sigma$ and standard deviation 0.656σ $(t = 1.253$ and $\sigma_t = 0.656)$. Investigations of the monthly gradient wind climate over Canada (Baynes 1971) have revealed that λ seldom exceeds 0.5 so that, considering Figure 2.2 the Rayleigh model might be a reasonable choice. However, the standard vector deviations may be large, of the order of 10 m/sec, and this would result in under-estimates of the mean and variance of V and perhaps unacceptably low extreme value statistics.

As an attempt to overcome the practical shortcomings of the Rayleigh model, an alternative and somewhat empirical approach is to allow the function a second variable parameter, such that

$$P(V) = 1 - exp(-(\frac{V}{c})^k) \qquad (2.18)$$

This is known as the Weibull distribution and has often been used successfully to describe actual wind speed occurrences at ground level as well as higher elevations. By way of illustration, Figure 2.3 shows distributions of mean hourly surface winds at Toronto International Airport in the decade 1957-66. Rewriting Equation 2.18 in terms of t, and redefining c,
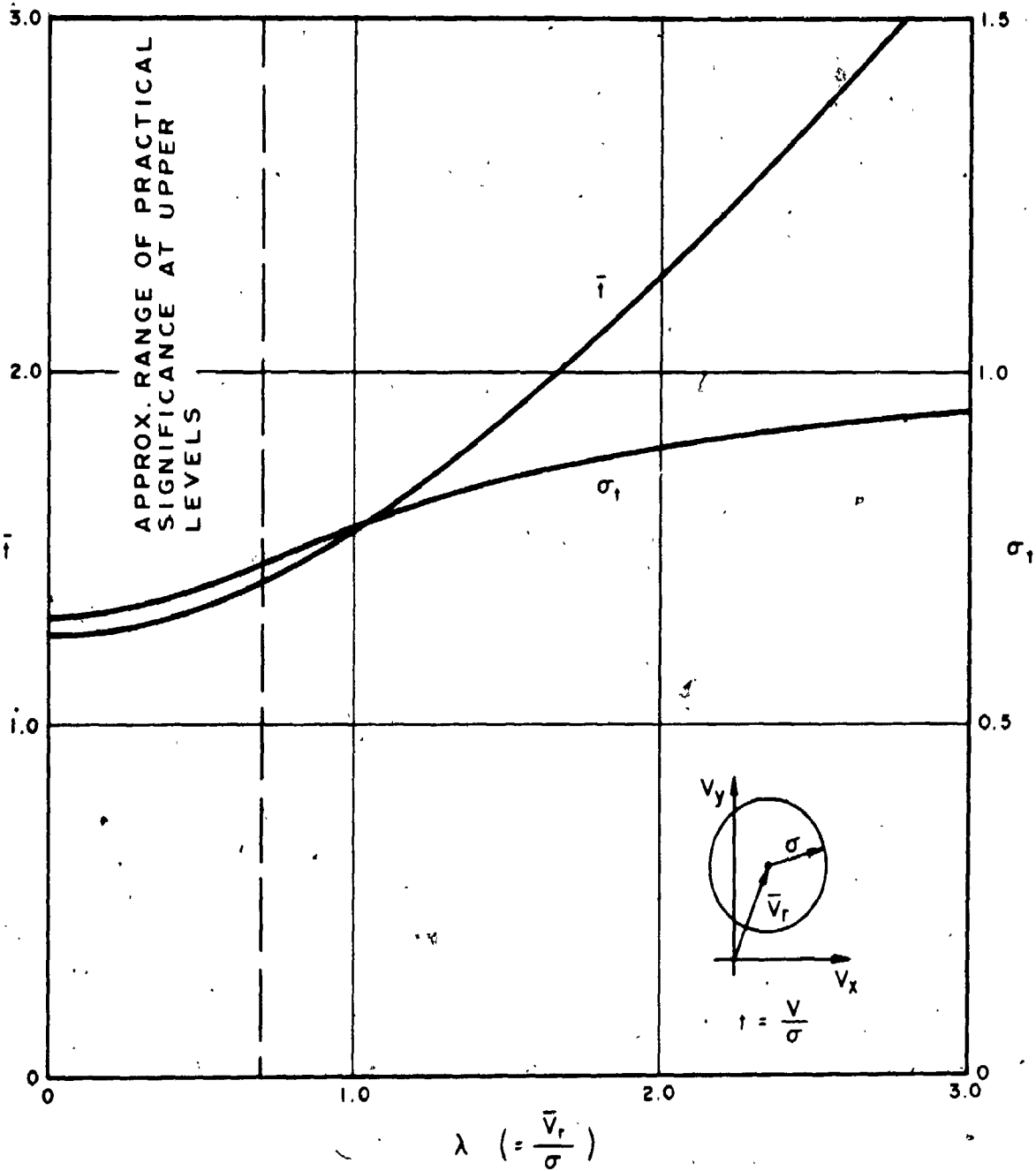
FIG. 2.2 MEAN AND STANDARD DEVIATION OF REDUCED
WIND SPEED $\dagger$ FOR NON-CENTRAL CIRCULAR
VELOCITY DISTRIBUTIONS
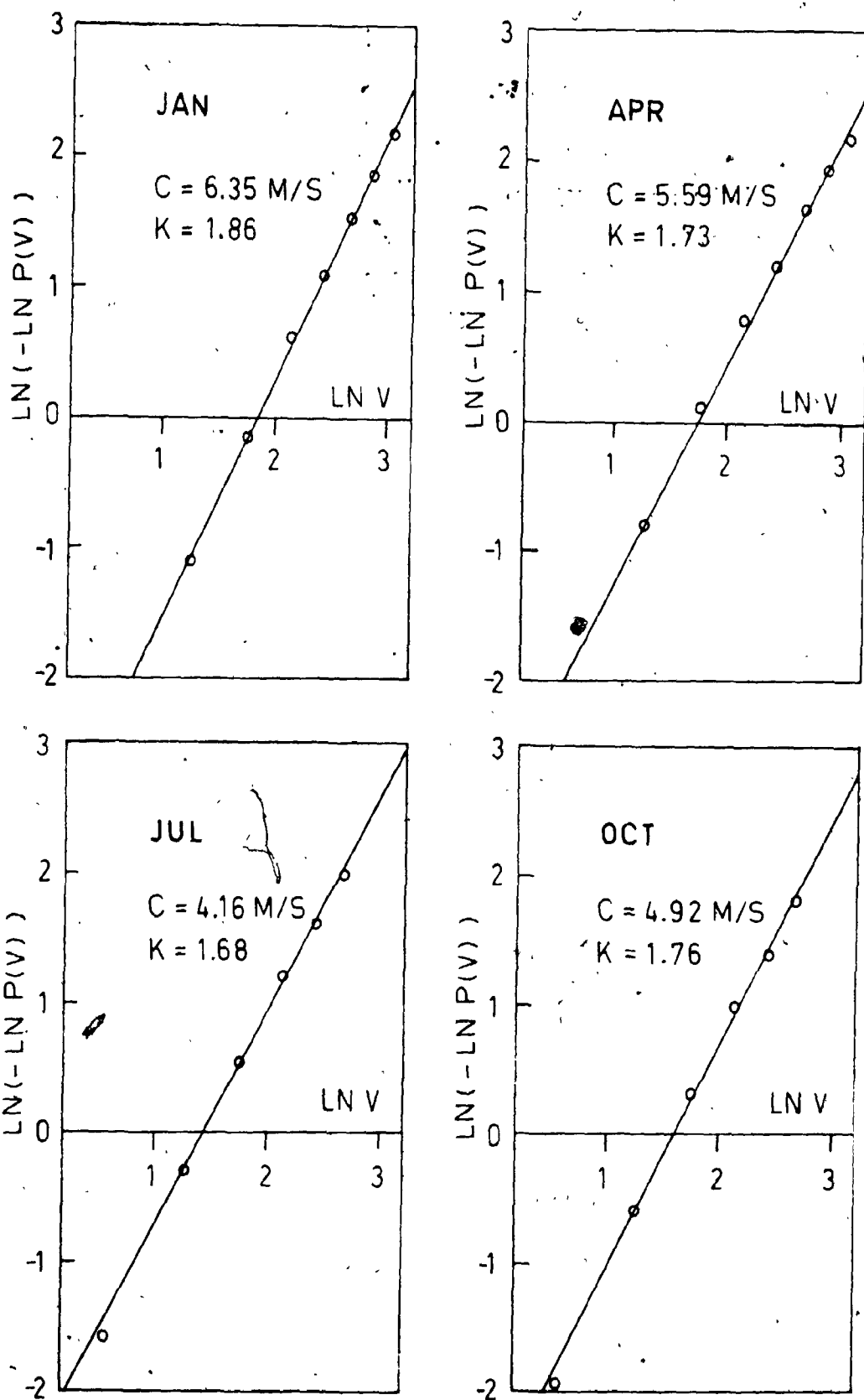
FIG 2.3 WEIBULL DISTRIBUTIONS OF HOURLY MEAN WIND
SPEEDS AT TORONTO INTL. AIRPORT
(1957-66)

$$P(t) = 1 - exp(-(\tfrac{t}{c})^k)$$
(2.19)

with the mean value

$$\bar{t} = c\, \Gamma(1 + \tfrac{1}{k})$$
(2.20)

and standard deviation

$$\sigma_t = c[\Gamma(1 + \tfrac{2}{k}) - \Gamma^2(1 + \tfrac{1}{k})]^{1/2}$$
(2.21)

In the Rayleigh form, $k = 2$ and $c = \sqrt{2}$.

The convenient Weibull distribution can be used with upper wind data by some scheme of curve fitting to the wind speed frequencies. In the absence of such detailed statistics a direct relationship can be established between the Weibull parameters and the defining parameters of the offset circular distribution, $\bar{V}_r$ and σ. One approach is to match the first and second moments of the non-central chi_2 and Weibull functions.

Firstly, the relationship of k to λ is derived by equating the coefficients of variation:

$$v_t(\lambda) = \frac{\sigma_t(\lambda)}{\bar{t}(\lambda)} = [\frac{\Gamma(1 + 2/k)}{\Gamma^2(1+1/k)} - 1]^{1/2}$$
(2.22)

Then the behaviour of C is found by equating the means:

$$\bar{t}(\lambda) = c\, \Gamma(1 + \tfrac{1}{k})$$
(2.23)

Both $\sigma_t(\lambda)$ and $\bar{t}(\lambda)$ are taken from Figure 2.2. The final relationships are shown in Figure 2.4, indicating that, within the range of λ usually encountered, k can be taken as 2.0. This is again the Rayleigh distribution, but with the value of c greater than $\sqrt{2}$ and increasing quite rapidly with λ.
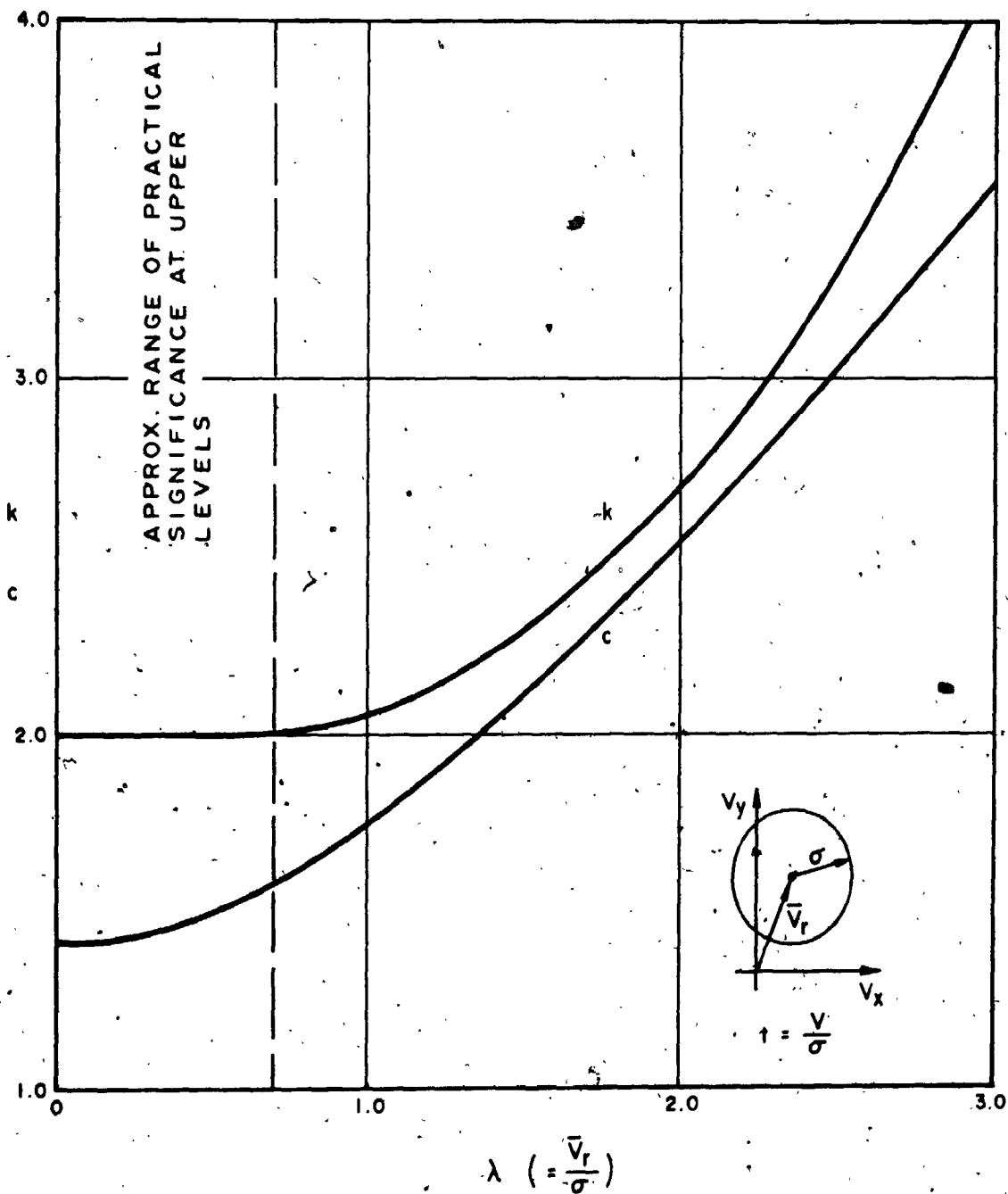
FIG. 2.4 PARAMETERS OF THE WEIBULL DISTRIBUTION OF WIND SPEED FOR NON-CENTRAL CIRCULAR VELOCITY DISTRIBUTIONS

2.5 Other Bivariate Distributions

Brief mention will be made here of some other bivariate models which have been employed in the analysis of wind climate, particularly near ground level where the influences of terrain roughness and general topography often produce a more complex distribution.

Taking the special case of the bivariate normal model in which it is both central and circular, the probability density function can be expressed in polar coordinates as:

$$p(V,\theta) = \frac{V}{2\pi\sigma^2} \, exp[-\tfrac{1}{2}(\tfrac{V}{\sigma})^2] \tag{2.24}$$

where θ is the wind direction. An empirical extension of this, which could allow for the directional properties of the terrain, is:

$$p(V,\theta) = V \, exp[-(a(\theta)V^2 + b(\theta)V + C)] \tag{2.25}$$

where C is a constant and $a(\theta)$ and $b(\theta)$ can be represented as infinite harmonic series. Their exact forms are determined by fitting to observational data. This approach has been used in an investigation of winds in Toronto by Davenport, Hogan and Isyumov (1969).

Recently, the Weibull curve has been used to describe separately the probability of wind speeds blowing from within a given sector (for example, Davenport and Jandali, 1973). Thus the aggregate bivariate distribution can be written as:

$$P(V,\theta) = a(\theta)(1 - exp[-(\tfrac{V}{c(\theta)})^{k(\theta)}]) \tag{2.26}$$

The functions $a(\theta)$, $c(\theta)$ and $k(\theta)$ can again be expressed as finite harmonic series in accordance with the available data, with the necessary condition that:

$$\int_0^{2\pi} a(\theta)d\theta = 1 \qquad (2.27)$$

In that the latter model has a singularity at the origin, it may not be applicable at low wind speeds. Nevertheless, both methods discussed here provide a reasonable means of extrapolating to very high winds from any required direction.

2.6 The Statistical Theory of Extreme Wind Speeds

Turning to the statistical properties of extreme winds regardless of direction, it is well to consider first the basic approaches to the problem. Four of these will be identified, as follows:

a) exact solutions;

b) approximations to exact solutions at low probability levels;

c) asymptotic forms; and

d) forms derived from a continuous stochastic process.

Fundamentally, for a random sample of N independent observations of wind speed, which are themselves identically distributed, the cumulative distribution function of the maxima is given by:

$$P(V) = F^N(V) \qquad (2.28)$$

where $F(V)$ refers to the parent distribution. Since wind speed is continous, as opposed to discrete valued, the probability density function is:

$$p(V) = N F^{N-1}(V) \cdot f(V) \qquad (2.29)$$

$f(V)$ being the density function corresponding to $F(V)$. Thus, if $f(V)$ and $F(V)$ are known, the exact distribution of extremes in N samples can also be determined.

Unfortunately, calculation of the various moments of the distribution would usually require some cumbersome numerical integration and, in any event, the rather complex function would not lend itself to easy application.

In some cases a considerable simplification can be made at low probability levels, that is towards the right-hand tail of the extreme distribution. As an example, consider a Weibull parent distribution (Equation 2.18), then

$$P(V) = [1 - exp(-(\frac{V}{c})^k)]^N \tag{2.30}$$

Expanding the logarithm of the left-hand side of (2.30) and ignoring terms of second order and above.

$$ln(P(V)) = -N \cdot exp(-(\frac{V}{c})^k) \tag{2.31}$$

Now, the return period, R, can be introduced in place of $P(V)$. It is the average number of observations between occurrences of values exceeding V, defined by:

$$R = \frac{1}{1 - P(V)} \tag{2.32}$$

so that, for R greater than about 5,

$$ln(P(V)) = -\frac{1}{R} \tag{2.33}$$

It follows from Equation 2.31 that

$$V = c(ln\ NR)^{1/k} \tag{2.34}$$

If annual maximum wind speeds are considered, R will be expressed in years and N should be the number of independent observations in one year, as distinct from the total number recorded. It is often taken as the average number of "cycles" of wind in a year, based on an examination of the power spectra for the process. The average cycling rate is given by:

$$\dot{v} = \left[\frac{\int_0^\infty n^2 S(n)dn}{\int_0^\infty S(n)dn}\right]^{1/2} \tag{2.35}$$

where $S(n)$ is the spectral density at frequency n. For hourly mean winds, $\dot{v}$ is typically about 0.1 cycles per hour (Davenport, 1968), so that $N \sim 876$ and

$$V \sim c(8.6 + \ln R)^{1/k} \tag{2.36}$$

Without the simplification outlined above, an extreme distribution can often be derived from a knowledge of the parent distribution and the assumption of large N. The question is, how soon is such an asymptotic solution approached as N increases. Gumbel (1954) has studied this by introducing two parameters, the expected largest value in N observations, U_N, and a_N defined by:

$$a_N = N f(U_N) \tag{2.37}$$

It can then be shown that

$$\frac{d U_N}{d(\ln N)} = \frac{1}{a_N} \tag{2.38}$$

from which it is apparent that the parameter $1/a_N$ represents the rate of increase of the expected largest value with respect to the logarithm of sample size. In the case of a Weibull parent distribution, it turns out that:

$$U_N = c(\ln N)^{1/k} \tag{2.39}$$

Also

$$\frac{1}{a_N} = \frac{c}{k}(\ln N)^{1/k - 1} \tag{2.40}$$

These relationships are plotted in Figure 2.5 for $c = \sqrt{2}$ and $k = 2$, the Rayleigh form. It will be noted that in the case shown U_N increases more slowly than $\ln N$, whereas if k were less than 1 the increase would be more rapid than $\ln N$.
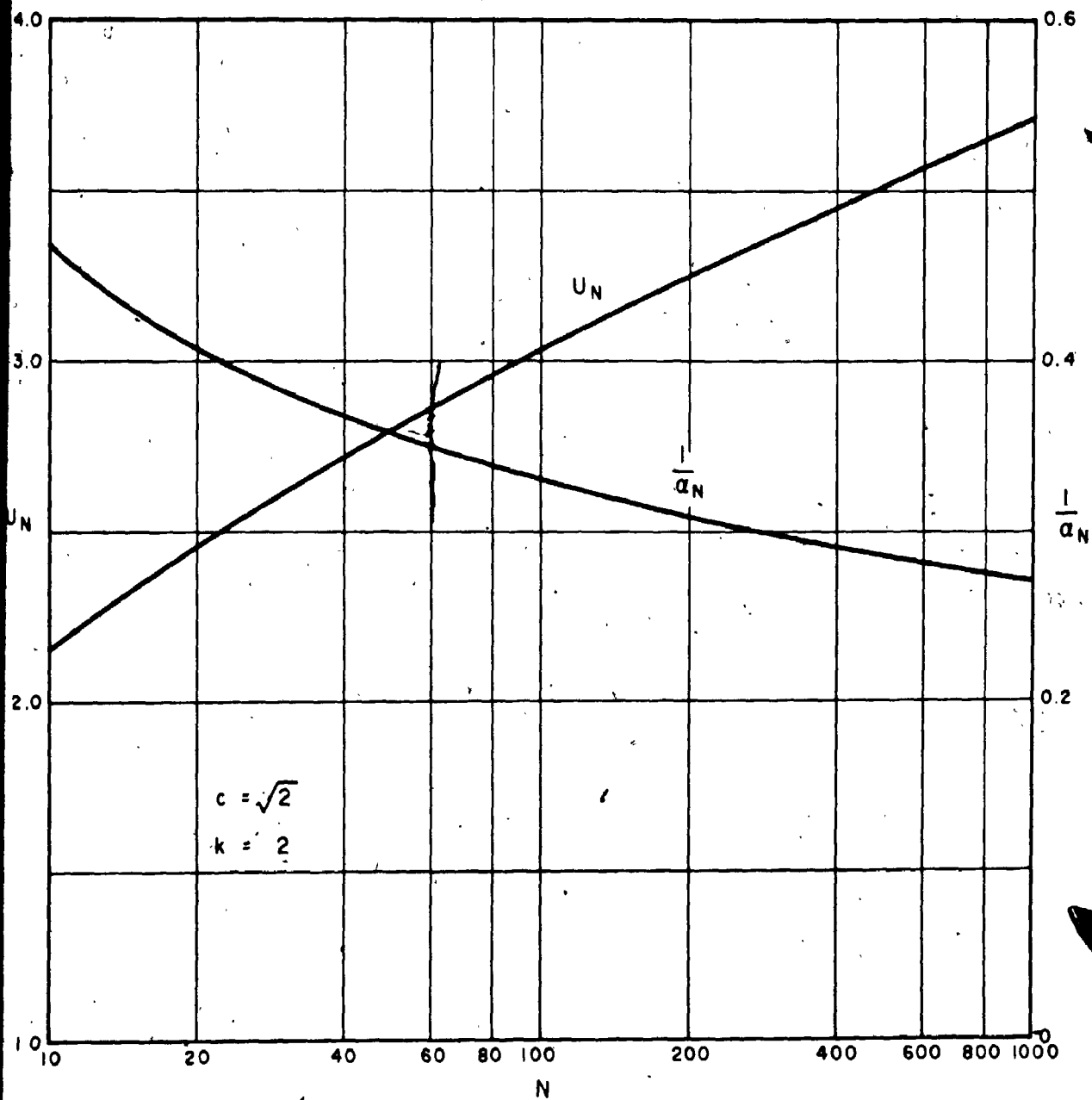
FIG. 2.5 ASYMPTOTIC PARAMETERS FOR THE RAYLEIGH DISTRIBUTION

Extreme value theory, which will not be detailed here, can now be invoked to obtain the distribution of the maxima, provided that values of the variate are sufficiently large. The first asymptote, the Fisher-Tippett Type I or Gumbel distribution, is derived from a parent of the general exponential type, for example, the normal, lognormal, chi-squared and Weibull distributions. The Type I has the form:

$$P(V) = exp(-exp(-y)), \ -\infty < y < \infty \tag{2.41}$$

in which

$$y = a_N(V - U_N) \tag{2.42}$$

The parameters U_N and a_N now take on new meaning as measures of the scale and shape of the extreme distribution. In fact, U_N is the modal value and a_N the inverse of the dispersion.

Parent distributions of the Cauchy type, that is,

$$\underset{L \to \infty}{Lim} (1 - F(V)) \ V^k = A \tag{2.43}$$

For $A > 0$ and $k > 0$, give rise to the second asymptote:

$$P(V) = exp(-(\frac{V}{\beta_N})^{-\gamma}) \tag{2.44}$$

This is the Fisher-Tippett Type II or Frechet distribution, in which β_N increases with N but γ is independent of N. For applications involving wind speed it has the theoretical advantage that, like the distribution of the parent, it is left-bounded at zero. However, since observations often conform to the Weibull, the Type I may be preferred as the corresponding asymptotic distribution of extremes.

A third class of initial distributions, limited in the tail of interest, has extreme distributions of the Type III:

$$P(V) = exp[-(\frac{w-V}{w-C_N})^k], \quad -\infty < V \leqslant w \qquad (2.45)$$

The corresponding distribution of smallest values is:

$$P(V)_o = 1 - exp[-(\frac{V-w_1}{C_1-w_1})^k], \quad V \geqslant w_1 < C_1 \qquad (2.46)$$

For the particular case of $w_1 = 0$, the lower limit, Equation 2.46 reduces to the Weibull form, although it should be noted that this does not constitute any theoretical foundation for its use as a parent distribution of wind speeds.

The final approach to the statistics of extreme winds considers the wind as a continous process (see Davenport and Baynes, 1972). The basic elements of this method are as follows. The "crossings" of a high value of the variate, V, in a given period, T, are treated as rare independent events following the Poisson distribution. An expression can be found for the crossing rate in terms of the probability density function of the original process, its average cycling rate, ν (Equation 2.35), and its standard deviation, σ. It is assumed that the process is stationary and independent of its derivative with respect to time, and that the derivative is normally distributed. Thus, the probability of there being no crossings at level V in time T is given by:

$$P(V) = exp(-C\, p(V)\, T) \qquad (2.47)$$

where the constant C is defined by:

$$C = \sqrt{2\pi}\sigma.\nu \qquad (2.48)$$

The formulation then proceeds on the basis of a suitable probability model of wind speed for each month or season of the year. If the Weibull distribution is chosen, it can be shown that, for the whole year, the extreme value distribution becomes:

$$P(V) = exp[-B\sum_{i=1}^{m} (\frac{V}{c_i})^{k_i-1} exp(-(\frac{V}{c_i})^{k_i})] \qquad (2.49)$$

where

$$B \simeq \sqrt{2\pi} \, v \, T \times 0.93, \quad 1.5 < k_i < 2.2 \tag{2.50}$$

If the summation in (2.49) refers to the twelve months, then $T \sim 720$ hours and c_i and k_i are the Weibull parameters for each month.

Returning momentarily to the first asymptotic distribution, it is readily shown that, for very large values of the variate, it approaches the simple exponential form:

$$P(V) = 1 - a \exp(-bV) \tag{2.51}$$

This has been employed in some studies of extreme winds and is mentioned here for the sake of completeness.

Essentially, the parameters of a required distribution of extremes can be determined either from the parameters of a known parent distribution (as in Equations 2.39 and 2.40) or from a suitable fit of the general form of the extreme distribution, to observed maxima. There is a distinct practical advantage in taking the former approach; the parent distribution can be established from a shorter period of record utilizing all the available data, whereas any valid analysis of annual maxima would require many years of observations. Gomes and Vickery (1974) have recently compared the extreme wind speed distributions for Sydney Australia derived from 18 annual maxima and just 5 years of hourly data fitted to Weibull curves. A close similarity was found (within .77 m/s up to the 100-year return period) and further analysis showed the distributions derived from the individual 1 year records to fall within the 80% confidence band centred on the 5 year result.

The process of curve fitting to observed largest values is facilitated by certain relationships existing between the extreme parameters and the moments of the maxima over N years. For the Fisher-Tippett Type I, it can be shown (Gumbel, 1954) that:

$$\frac{1}{a_N} = \frac{\sigma}{\sigma_N} \tag{2.52}$$

and

$$U_N = \bar{V} - \frac{\bar{y}_N}{a_N} \tag{2.53}$$

where $\bar{V}$ and σ here are the sample mean and standard deviation of the observed maxima, and σ_N and $\bar{y}_N$ are the expected values of the normalized standard deviation and mean for a sample size of N. These have been computed and plotted by Gumbel and are shown in Figure 2.6. The normalized variable y was previously defined in Equation 2.42. For large N the above relationships become:

$$\frac{1}{a} = \frac{\sqrt{6}}{\pi} \times \sigma \tag{2.54}$$

$$U = \bar{V} - \frac{0.5772}{a} \tag{2.55}$$

Gumbel has shown how these are obtained from least squares fitting of the Type I to the observational data, in which the maxima are ranked in ascending order and plotted as:

$$P(V) = \frac{m}{N+1} \tag{2.56}$$

m being the rank (1 to N) of an observation of V. In this case, if the reduced probability, $-ln(-ln\ P(V))$, is plotted against V, the curve to be fitted is a straight line with intercept U_N and slope $1/a_N$.

It will be noted that, should a Type II distribution be required, the above approach can be applied by using a logarithmic transformation of the original variate. It is apparent from a comparison of Equations 2.41 and 2.44 that $ln\ V$ will be distributed according to the Type I.
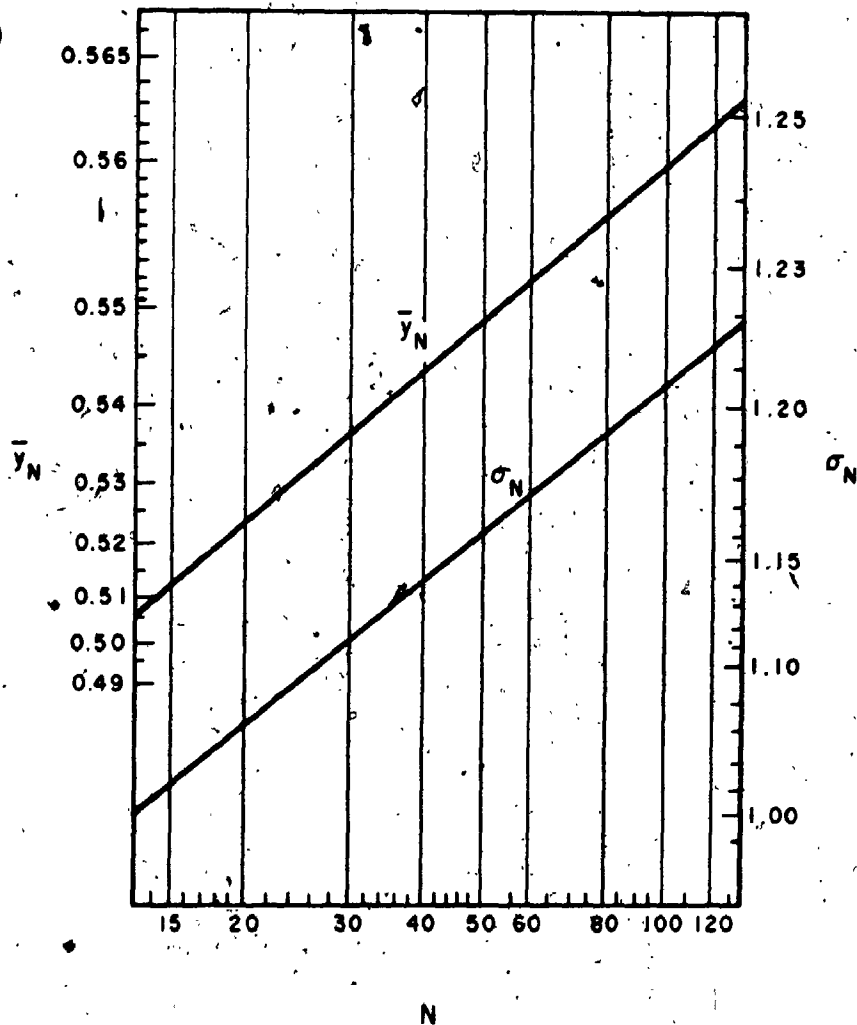
FIG. 2.6. EXPECTED NORMALIZED MEANS AND STANDARD
DEVIATIONS OF EXTREME VALUES FOR
DIFFERENT SAMPLE SIZES (AFTER GUMBEL, 1954)

Alternative methods are available for establishing the extreme distribution from observed maxima, although they appear to offer little practical advantage over Gumbel's method (notable examples are those of Jenkinson, 1955 and Gringorten, 1963).

2.7 The Interrelation of Extreme Wind Speed Distributions

It has been seen that the first two asymptotic forms of the distribution of extremes are generally suitable for describing maximum wind speeds. They are, rewritten without subscripts N:

$$P(V) = exp[-exp(-a(V-U))] \tag{2.57}$$

and $$P(V) = exp(-(\frac{V}{\beta})^{\gamma}) \tag{2.58}$$

For the purposes of comparison of wind statistics based on these two distributions, they can be matched at any required probability level. If the correspondence occurs at wind speed V' with cumulative probability $P(V')$, the parameters of the distributions are related by:

$$\gamma(\ln V' - \ln \beta) + a(V' - U) = 0 \tag{2.59}$$

and, setting the rates of change of the reduced probabilities with V equal,

$$a = \frac{d[\gamma(\ln V - \ln\beta)]}{dV}\Big|_{V = V'} \tag{2.60}$$

or $$a = \frac{\gamma}{V} \tag{2.61}$$

Where the distributions are matched at their modes, it follows that

$$U = \beta \text{ and } a = \frac{\gamma}{\beta} \tag{2.62}$$

Figure 2.7 shows that if this method is used to transform a Type II distribution to a Type I, estimates of high wind speed quantiles from the second model will be generally low.

As an alternative, since the quantity $ln\,V$ is distributed as V in the Type I model, the means and standard deviations for large samples can be written:

$$\bar{V} = U + \frac{0.5772}{a} \; ; \; \sigma_V = \frac{\pi}{a\sqrt{6}} \tag{2.63}$$

and $\overline{lnV} = ln\beta + \frac{0.5772}{\gamma} \; ; \; \sigma_{lnV} = \frac{\pi}{\gamma\sqrt{6}} \tag{2.64}$

It is then possible to relate the various parameters by assuming that, towards the modes of the distributions, the extreme values of V and $ln\,V$ are normally distributed. This may be realized by first writing the Type I density function in the form

$$p(V) = a\,exp(y - exp\,y) \tag{2.65}$$

Then, expanding $exp\,y$ and neglecting terms in y^3 and above,

$$p(V) = \frac{a}{e}\,exp(-\frac{y^2}{2}) \tag{2.66}$$

which is of the form of the normal distribution. The following standard relationships then apply (see, for example, Benjamin and Cornell, 1970):

$$\overline{lnV} = ln\,\bar{V} - \frac{1}{2}\,\sigma_{lnV}^2 \tag{2.67}$$

$$\sigma_{lnV}^2 = ln\,\frac{\sigma_V^2}{\bar{V}^2} + 1 \tag{2.68}$$

Substituting for $\bar{V}$, σ_V, $\overline{lnV}$ and σ_{lnV} from Equations 2.63 and 2.64,

$$ln\beta + \frac{0.5772}{\gamma} = ln(U + \frac{0.5772}{a}) - \frac{\pi^2}{12\gamma^2} \tag{2.69}$$
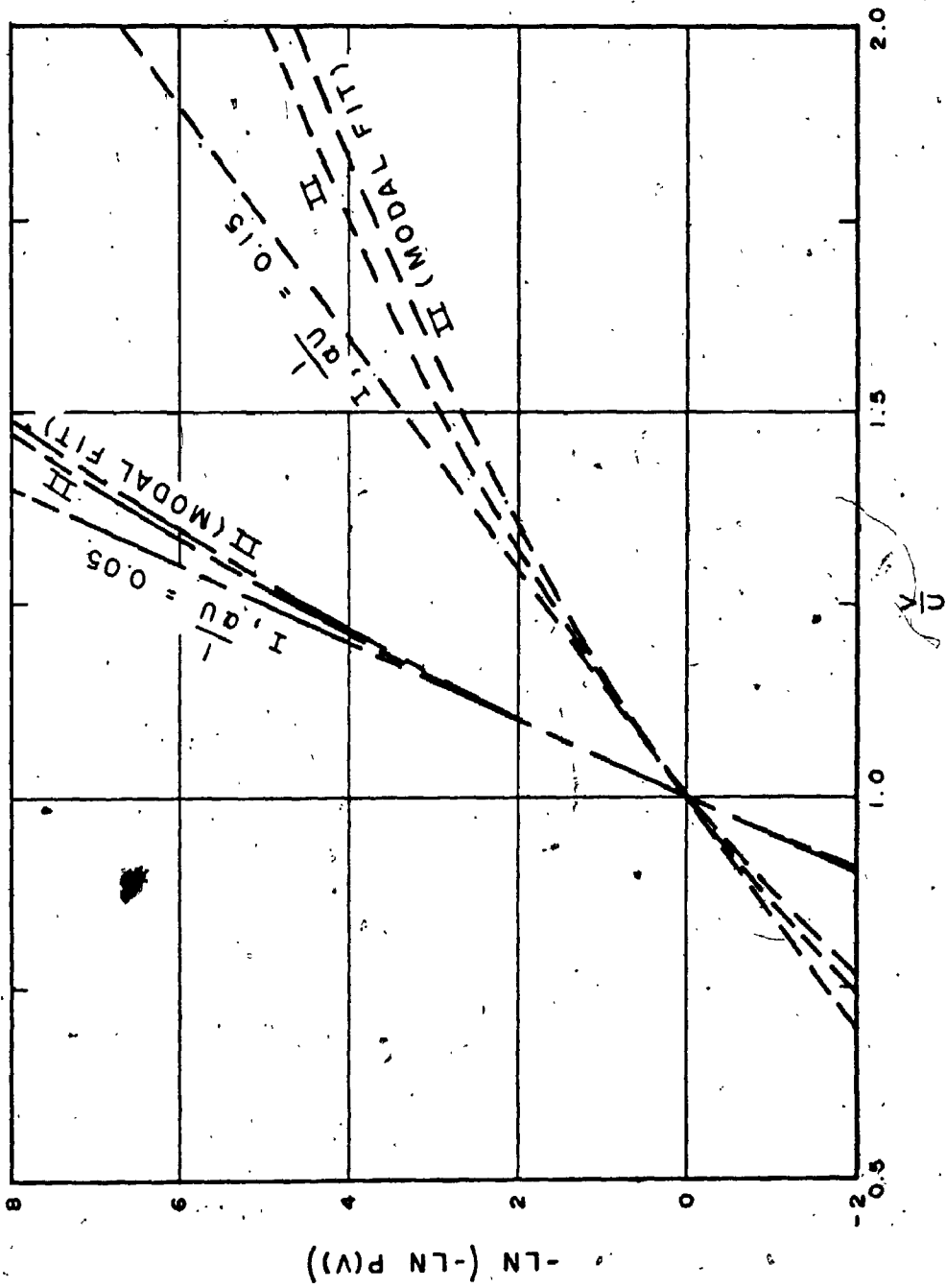
FIG. 2.7 FISHER-TIPPETT TYPE I, TYPE II DISTRIBUTIONS FITTED TO TYPE I AT COMMON MODES AND USING EQUATIONS 2.71, 2.72

$$\frac{\pi^2}{6\gamma^2} = ln(\frac{\pi^2}{6a^2 \ (U + \frac{0.5772}{a})} + 1) \tag{2.70}$$

Now, it is found in practice that the value of $1/aU$ is usually less than about 0.2. Therefore, to a first approximation, ignoring terms in $(1/aU)^2$ and above, it can be shown that (2.69) and (2.70) reduce to:

$$aU = \gamma - 0.5772 \tag{2.71}$$

and $lnU = ln\beta - \dfrac{0.5772^2}{\gamma(\gamma - 0.5772)}$ (2.72)

Figure 2.7 clearly indicates that, for representative Type I parameters, the latter method of matching a Type II distribution results in a closer correspondence for all probability levels, but again a transformation from the Type II to the Type I will give subsequently low predictions of wind speed. In making the transformation in this direction, therefore, it may be preferable to simply match probabilities at two points in the range of interest using Equation 2.59.

The simple exponential distribution, derived from the first asymptotic form at very large values of the variate (Equation 2.51), is linked to the original Type I through the identities:

$$a = exp(aU); \ b = a \tag{2.73}$$

The more complex distribution obtained from a consideration of wind as a continous stochastic process (Equation 2.49) can also be related to the more manageable Type I by matching at a common mode. In this case the Type I will provide, from the design point of view, a conservative approximation. The parameters will be given by the solution to:

$$\sum_{i=1}^{m} (\frac{V}{c_i})^{k_i-1} exp(-(\frac{V}{c_i})^{k_i}) = \frac{1}{B} \tag{2.74}$$

and, requiring equal slopes of the reduced probability curves,

$$a = \frac{d(ln\Sigma)}{dV}\Big|_{V=U} \qquad (2.75)$$

(denoting the left-hand side of (2.74) by Σ) Figure 2.8 illustrates the general relationship between the two distributions derived in this way.

The distributions discussed above, all used in the analysis of maximum wind speeds, are summarized in Table 2.1, along with their respective relationships to the Fisher-Tippett Type I.

2.8 Maxima from the Non-central Chi$_2$ Model

It has been seen that the non-central circular case of the bivariate normal distribution of upper level winds leads to a non-central *chi$_2$* model of wind speeds. Consequently, it is of some interest to examine briefly the distribution of maximum speeds derived from this. The parent distribution has already been related to the more manageable Weibull form by requiring common first and second moments (Section 2.4), but it is expected that a substitution on this basis would result in low predicted values of the maxima. Furthermore, an alternative approach might yield the comparatively high values (greater than about 0.1) of the Type I parameter grouping $1/aU$ suggested by the observations at some locations but generally unattainable through the usual asymptotic treatment of a Weibull parent.

In order to render the extreme value problem tractable in this case, an approximation to the non-central *chi$_2$* model has been employed which, according to Patnaik (1949), provides a close correspondence in the tails of the distribution. This is the simple *chi^2* distribution, given by

$$f(t') = \frac{t'^{\frac{\mu}{2}-1} \exp(-\frac{t'}{2})}{2^{\mu/2}\ \Gamma(\frac{\mu}{2})} \qquad (2.76)$$

in which

$$t' = \frac{t^2}{\rho} \qquad (2.77)$$
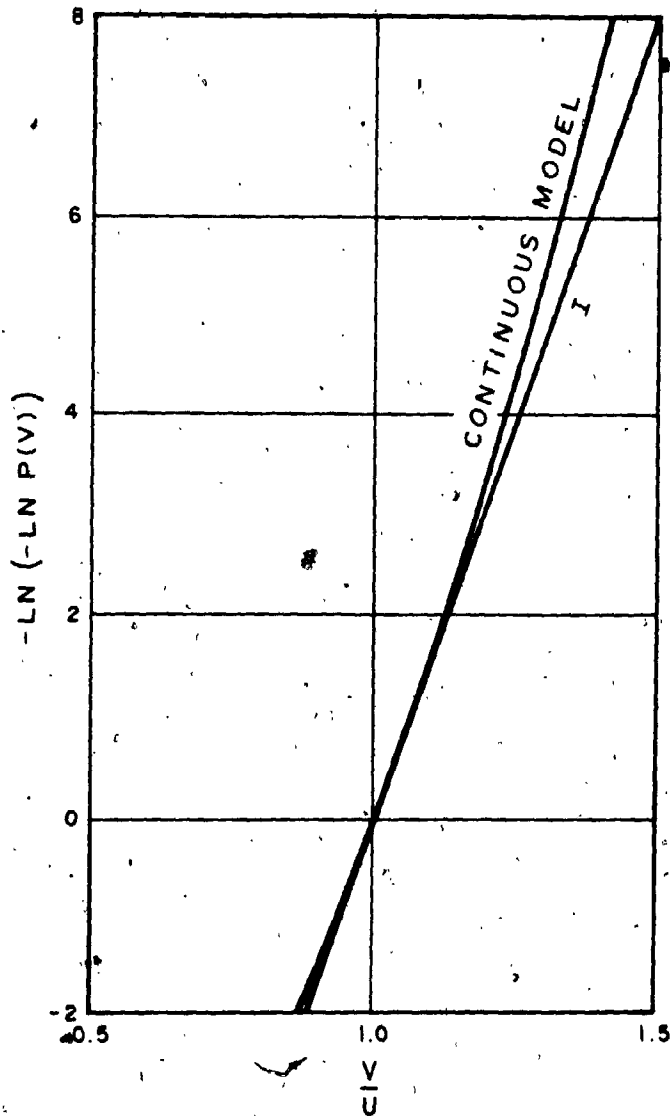
FIG. 2.8 RELATIONSHIP OF EXTREME DISTRIBUTION
DERIVED FROM CONTINUOUS MODEL TO
FITTED FISHER-TIPPETT TYPE I

DISTRIBUTION	RELATIONSHIP TO TYPE I
Fisher-Tippett Type I $P(V) = exp[-exp(-a(V-U))]$	
Fisher-Tippett Type II $P(V) = exp(-(\frac{V}{\beta})^{\gamma})$	$U = \beta; \ a = \frac{\gamma}{\beta}$ or $aU = \gamma - 0.5772$ $ln \ U = ln\beta - \frac{0.5772^2}{\gamma(\gamma-.5772)}$
Exponential $P(V) = 1 - a \ exp(-bV)$	$aU = ln \ a$ $a = b$
Continuous Model $P(V) = exp -B \cdot$ $\sum_{i=1}^{m} (\frac{V}{c_i})^{k_i-1} exp(-(\frac{V}{c_i})^{k_i})$	U _given by_ $\sum_{i=1}^{m} (\frac{V}{c_i})^{k_i-1} exp(-(\frac{V}{c_i})^{k_i}) = \frac{1}{B}$ $a = \frac{d(ln\Sigma)}{dV}\Big|_{V=U}$

TABLE 2.1 DISTRIBUTIONS OF EXTREME WIND SPEEDS AND
THEIR RELATIONSHIPS TO THE TYPE I FORM

and, in this application,

$$\rho = \frac{2 + 2\lambda^2}{2 + \lambda^2}; \mu = \frac{(2 + \lambda^2)^2}{2 + 2\lambda^2} \qquad (2.78)$$

μ is the equivalent number of degrees of freedom in (2.76).

Following asymptotic extreme value theory, the modes and dispersions have been calculated for a range of values of λ, by again assuming 876 independent observations per annum. The results are presented in Figure 2.9. Up to about $\lambda = 1$ there is no significant departure from the parameters which would be obtained from the corresponding Rayleigh parent as indicated by Figure 2.4. Although higher ratios of the vector mean to standard vector deviation would give large values of $1/aU$, this would represent exceptional circumstances at the elevations of interest here.

2.9 The Influence of Averaging Time on Wind Records

The previous section dealt with the means by which extreme wind statistics based on different probability models can be compared and, if desired, transformed to comply with a standard distribution type. Another inconsistency which often arises in the study of wind climate is caused by the various averaging periods over which the wind speed is measured. It is not uncommon, for example, to be presented with "hourly mean" winds recorded over a full hour or ten minutes, as well as peak "gust" speeds relating to periods of about 2 to 5 seconds, depending on the response characteristics of the anemometer. In addition, the standard wind speed measurement in the United States is the "fastest mile" of wind, being the highest mean velocity of any mile run of wind passing the anemometer in the record interval, usually an hour.

The physical link between these quantities will be the degree of gustiness at a given time and location. This will be affected by the general character, or roughness, of the upwind terrain, the presence of convective activity as indicated by atmospheric stability, the height of the anemometer above ground level and the turbulent wake of
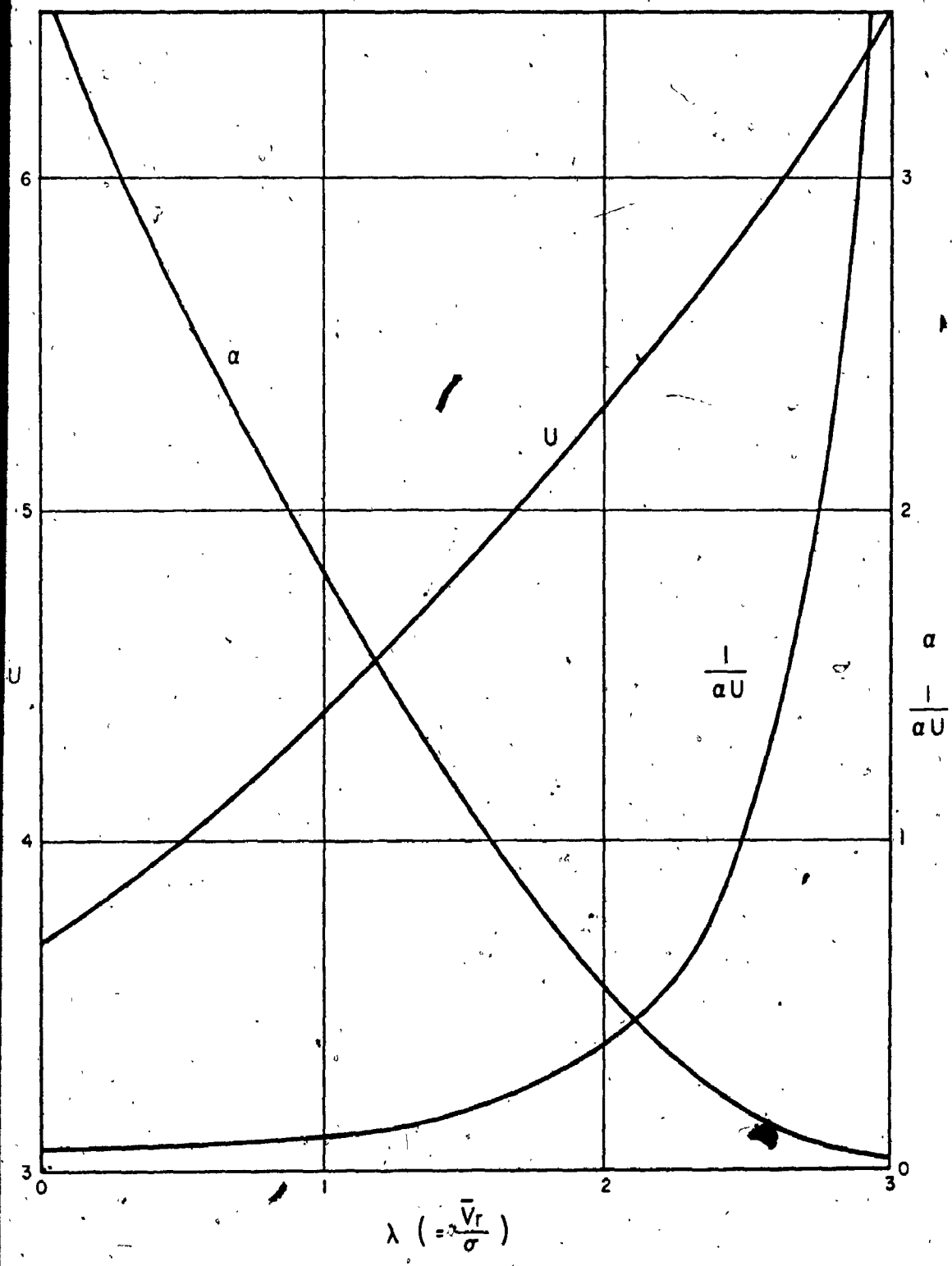
FIG. 2.9   EXTREME DISTRIBUTION PARAMETERS FOR THE
NON-CENTRAL CHI_2 MODEL

any nearby building or other obstruction. In this discussion it will be assumed that mechanically, rather than thermally induced atmospheric turbulence will predominate, as in conditions of high mean winds and roughly neutral stability. Furthermore, it will be taken that the anemometer is well sited, away from local influences and at about the standard height of 10 metres.

Durst (1960) has investigated the gust factor, the ratio of the peak gust speed to the mean hourly speed, using measurements made at Cardington, England. His results apply to a range of mean hourly speeds with the anemometer positioned 15 metres above open level grassland. This work has been extended by Deacon (1965) by utilizing additional data obtained at Sale, Australia and Shellard's (1958) figures for maximum annual mean winds and gusts at some 30 locations in the United Kingdom. The effect of terrain roughness is included, using three descriptive categories. The dependence of mean gust factor on averaging period, as indicated by Deacon, is shown in Figure 2.10 (Deacon used a ratio based on the 2-second gust but, for the purpose of this study, a gust factor based on a one-hour averaging period is shown. Definitions of the roughness categories are also given in the figure).

When considering the fastest mile of wind the averaging period is itself a function of wind speed, according to:

$$\tau = K \cdot \frac{1}{V_F} \tag{2.79}$$

where V_F is the speed of the fastest mile and K is a constant depending on the units employed (if τ is expressed in seconds and V_F in miles per hour, then $K = 3600$; if V_F is in metres per second, then $K = 1607$). Then, if a mean gust factor, η_G, relating the τ-second gust to the mean hourly can be assigned, the ratio of the fastest mile to the mean hourly is given by

$$\eta_F = \eta_G(\tau) = \eta_G(V_F) \tag{2.80}$$

DEFINITION OF TERRAIN ROUGHNESS CATEGORIES

A — OPEN COUNTRY WITH FEW TREES;
SHORT OR NO VEGETATION

B — TERRAIN WITH FAIRLY NUMEROUS
HEDGES AND SCATTERED TREES,
WIND BREAKS, BUILDINGS ETC.

C — MORE NUMEROUS TREES AND/OR
BUILDINGS, E.G. OUTSKIRTS OF
LARGE CITY

FIG. 2.10 MEAN GUST FACTORS FOR
DIFFERENT AVERAGING
PERIODS AND TERRAIN
ROUGHNESSES (FROM
DEACON, 1965)
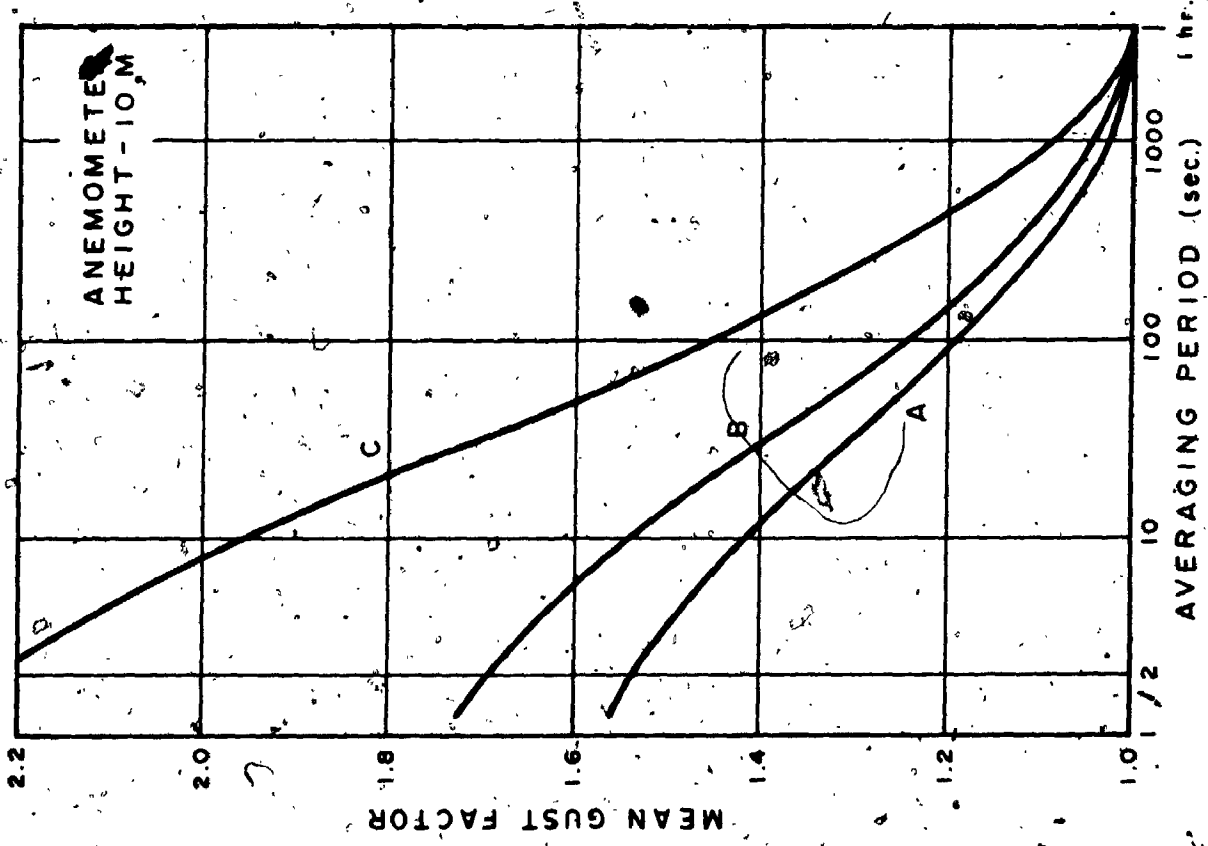
Hollister (1969), using estimates of η_G by Durst and others for various averaging times, has fitted the following curve:

$$\eta_F = 1.73 - 0.115 \ln \left(\frac{K}{V_F}\right) \qquad (2.81)$$

It is recommended that this equation be used specifically with the U.S. Weather Bureau records normally taken at airport locations in relatively smooth terrain. The influence of rougher terrain can be judged by using the gust factor relationships shown in Figure 2.10 for roughness categories B and C. The results are plotted in Figure 2.11, together with Hollister's empirical curve.

2.10 Distributions of Gusts and Gust Factors

Up to now the discussion has been confined to the mean gust factor, that is the ratio of the peak gust wind to the mean wind which is expected to exist for any hourly record. Turning to the statistical distribution of the gust factor, some initial indication of the deviation of values can be gained from Durst's (1960) analysis of observations over relatively smooth terrain.

Durst calculated the standard deviations of gusts for various averaging times and mean wind speed conditions. For example, the standard deviation of 5-second gusts expressed as a ratio of the one-hour mean, is 0.159 for moderate winds. The figure is slightly less for light winds and greater for strong winds, although the total range of values is only about 5%. It is reasonable to conclude, considering the typical mean gust factor for this type of terrain, that both the distributions of gusts and maximum gusts are quite peaked and little influenced by wind speed. This is further supported by some statistics given by Deacon (1965).

Davenport (1964) has proposed a theoretical distribution of gust factors, based on the distribution of the largest value of a stationary random function. First, the normalized gust factors, η, are characterized as a normally distributed random function. The

$$\eta_F = 1.73 - 0.115 \ln\left(\frac{K}{V_F}\right) \text{ (HOLLISTER, 1969)}$$

ROUGHNESS CAT. C

ROUGHNESS CAT. B

MPH (K = 3600)

M/S (K = 1607)
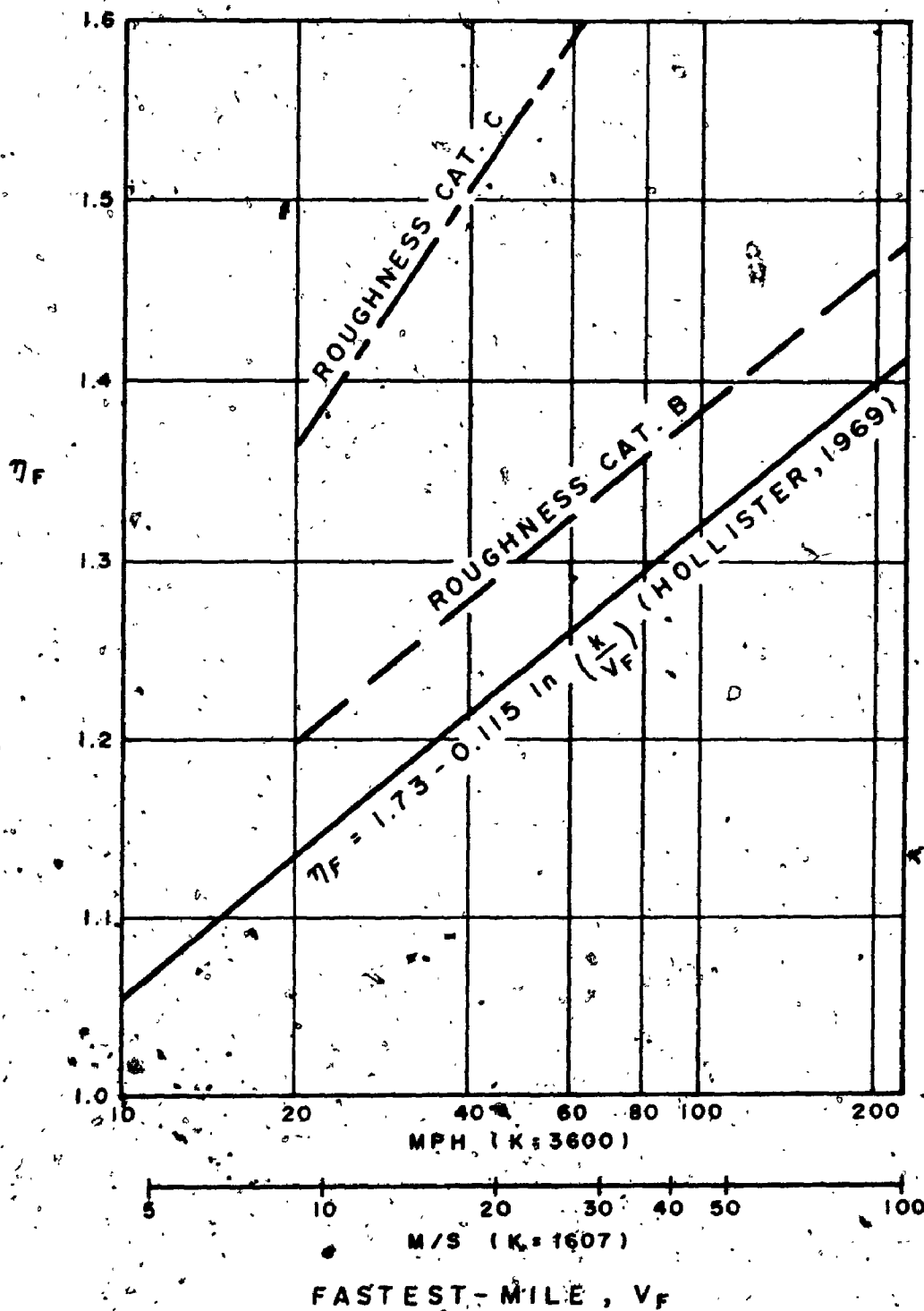
FASTEST-MILE , V_F

FIG. 2.11 RATIO OF FASTEST-MILE TO MEAN HOURLY
WINDS OVER SMOOTH TERRAIN WITH
ESTIMATES FOR ROUGHER TERRAIN
CATEGORIES

cumulative probability of the maxima of the same function, $Q(\eta)$, can then be obtained following Cartwright and Longuet-Higgins (1956). From this, the probability of the largest maximum or peak gust factor in N maxima can be derived as:

$$p(\eta)d\eta = N(1 - Q(\eta))^{N-1} q(\eta)d\eta \qquad (2.82)$$

This is, in words, the probability that one maximum has a value in the range of η to $\eta + d\eta$ and the remainder are smaller. It can then be shown that, for large N and invoking Rice's (1954) expression for the number of maxima in time τ, $p(\eta)$ can usually be represented by

$$p(\eta) = \eta \zeta \exp(-\zeta) \qquad (2.83)$$

where ζ is defined by

$$\zeta = \nu_a \tau \exp(-\frac{\eta^2}{2}) \qquad (2.84)$$

ν_a is taken as the average cycling rate of the fluctuating process, η. This will be, in practical terms, the cycling rate of the horizontal component of atmospheric turbulence as seen by the anemometer. In most cases τ will refer to a period of one hour. The distributions of the original function and the peak gust factors for different values of $\nu_a\tau$ are illustrated in Figure 2.12. The very peaked distributions of the maxima are clearly shown.

Davenport has compared his theoretical model with some data collected by Shellard (1963) in strong winds. In this instance the anemometer was a cup generator type, for which the frequency response curve, or admittance function, was known. This, combined with a chosen spectrum of atmospheric turbulence, determined the spectrum seen by the anemometer. The mean square fluctuation (the area under the spectrum) and the second moment of the final spectrum were then required in the calculation of the average cycling rate, ν_a (see Equation 2.35). Some deviation of the
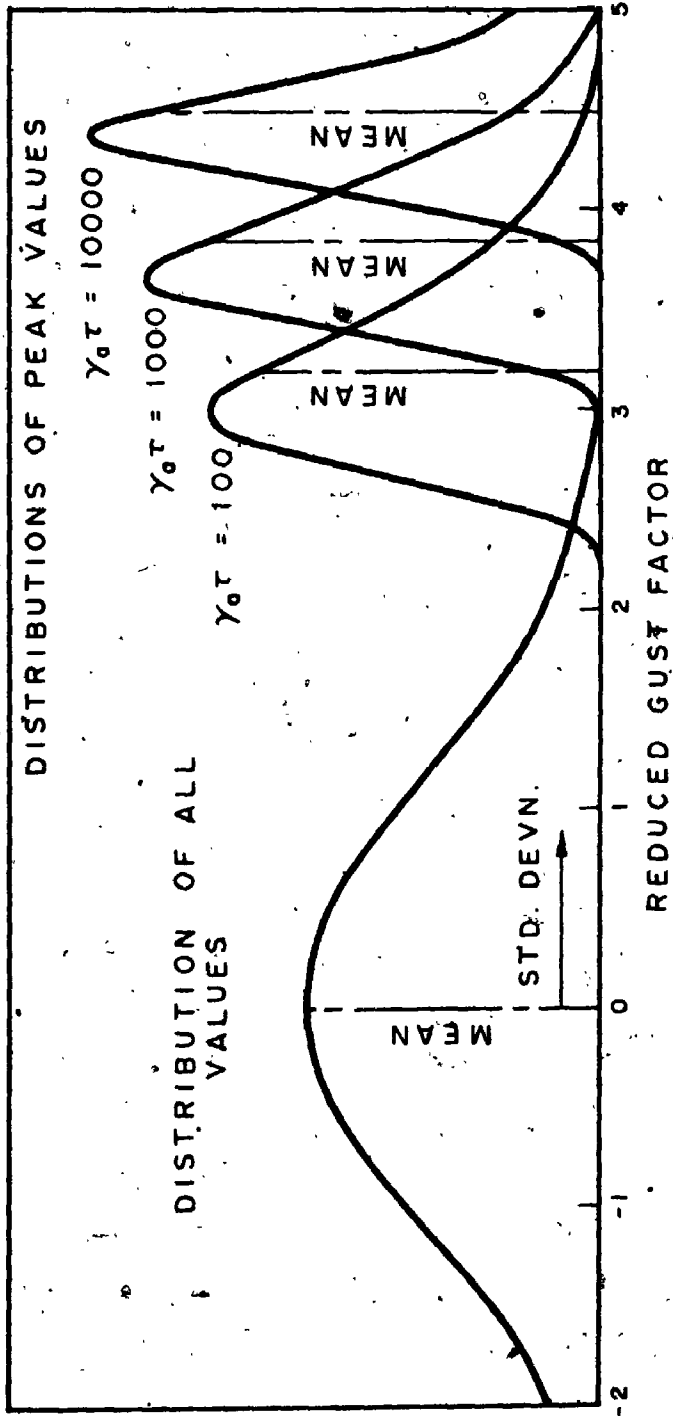
FIG. 2.12 DISTRIBUTIONS OF GUST FACTORS AND PEAK GUST FACTORS FOR DIFFERENT VALUES OF $\gamma_a\tau$ (FROM DAVENPORT, 1964)

theory from Shellard's data was noted, particularly insofar as the model seemed to suppress the highest values of peak gust factor. This possibly arose from non-uniform terrain roughness, in the sense that the wind blowing from different directions over diverse terrain types would have different turbulent structures. Gust factor might also have been influenced by mean wind speed and atmospheric stability; in the spectrum used a constant wind speed and more or less neutral stability was assumed. Nevertheless, the theory compared quite favourably with the data and, if used with a slightly high mean gust factor, provides a useful distribution which to some extent overcomes the difficulties just mentioned.

The purpose of introducing such a theoretical model of peak gust factors here is to obtain a general form for the distribution of peak gust speeds, given a distribution of mean hourlies. This can now be achieved provided that the mean wind and peak gust factor can be considered independent, in which case

$$p(V_G) = p(\eta) \cdot p(V_M) \qquad (2.85)$$

where suffices M and G have been added to denote mean and gust velocities respectively. If $p(V_M)$ is of the Weibull form with the parameter k greater than unity, the probability density function can be described by:

$$p(V_G) = \frac{k}{c}(1 + \frac{0.5772}{A^2})(\frac{V_G}{cA})^{k-1} \exp(-(\frac{V_G}{cA})^k) \qquad (2.86)$$

in which A is the mode of the distribution of gust factors. The derivation of (2.86) is included in Appendix I.

2.11 Extreme Mean Wind and Gust Statistics

From a continuous model of the annual record of mean winds it can be shown that the distribution of the maxima is given by:

$$P(V_M) = exp[-B_M \left(\frac{V_M}{c}\right)^{k-1} exp(-\left(\frac{V_M}{c}\right)^k)] \qquad (2.87)$$

where

$$B_M = \sqrt{2\pi} \, \nu_M T \times \frac{k}{c} \sigma_M \qquad (2.88)$$

and ν_M is the average cycling rate of the process (typically 0.1 cycles per hour),

T is the period of the record (one year)

σ_M is the standard deviation of mean winds, V_M,

k,c are the parameters of the parent Weibull distribution.

Matching this form to the Fisher-Tippett Type I distribution at the mode, the corresponding parameters of the Type I are given by:

$$\left(\frac{U_M}{c}\right)^{k-1} exp(-\left(\frac{U_M}{c}\right)^k) = \frac{1}{B_M} \qquad (2.89)$$

and $\frac{1}{a_M} = [\frac{(1-k)}{U_M} + \frac{k}{c} \cdot \left(\frac{U_M}{c}\right)^{k-1}]^{-1}$ $\qquad (2.90)$

If a similar argument is followed for the extreme distribution of peak gusts using the parent density function given in (2.86), it is found that

$$P(V_G) = exp[-B_G \left(\frac{V_G}{cA}\right)^{k-1} exp(-\left(\frac{V_G}{cA}\right)^k)] \qquad (2.91)$$

where the quantities with suffix G have the same meaning for gusts as similar quantities in Equation 2.87. Another Type I curve can now be defined as:

$$\left(\frac{U_G}{cA}\right)^{k-1} exp(-\left(\frac{U_G}{cA}\right)^k) = \frac{1}{B_G} \qquad (2.92)$$

and $\frac{1}{a_G} = [\frac{(1-k)}{U_G} + \frac{k}{cA} \left(\frac{U_G}{cA}\right)^{k-1}]^{-1}$ $\qquad (2.93)$

The detailed derivation and explanation of Equations 2.87 to 2.93 have been relegated to Appendix I.

The implications of these equations can be studied in terms of the relationship between extreme mean hourlies and gusts with given return periods. This will obviously depend on the character of the parent distribution of mean winds and the assumed mean gust factor. A convenient expression for the first variable is the ratio $1/a_M U_M$, since this is a recognisable quantity quoted in the literature and is found to be effectively dependent on the single Weibull parameter k. It subsequently turns out that the gust factors appropriate to high return periods are themselves virtually independent of the parameter c. It follows from the definition of return period, R, for $R > 5$, that the ratio of the R-year return gust to the mean hourly wind is:

$$\eta_R = \frac{V_G}{V_M}(R) = \frac{\frac{1}{a_G} \ln R + U_G}{\frac{1}{a_M} \ln R + U_M} \qquad (2.94)$$

Therefore

$$\eta_R = \frac{\frac{a_M}{a_G} \cdot \frac{1}{a_M U_M} \ln R + \frac{U_G}{U_M}}{\frac{1}{a_M U_M} \ln R + 1} \qquad (2.95)$$

Values of η_R have been computed for return periods of 10, 100 and 1000 years and a range of $1/a_M U_M$ from 0 to about 1.25, corresponding to k values greater than 1.0. This has been done twice, assuming one-hour and 10-minute averaging times for the mean hourlies, and with mean peak gust factors of 1.5, 1.6 and 1.7. These figures determine the parameter A in the above expressions (see Appendix I) and represent terrain roughnesses in categories A and B as previously defined, the normal environment for regularly recording meteorological stations. The plots of η_R against $1/a_M U_M$ and k are given in Figures 2.13 and 2.14. It will be noted that, as k tends to infinity, η_R approaches the simple ratio of the modes, or most likely values of the extreme gust and mean wind speed.

Strictly, the curves apply only to gusts recorded by the particular anemometer for which the response to a typical power spectrum of turbulence was found by Davenport (1964). From this the cycling rate ν_a is given by:

$$\nu_a = 0.0065 \, \bar{V} \ Hz \qquad (2.96)$$
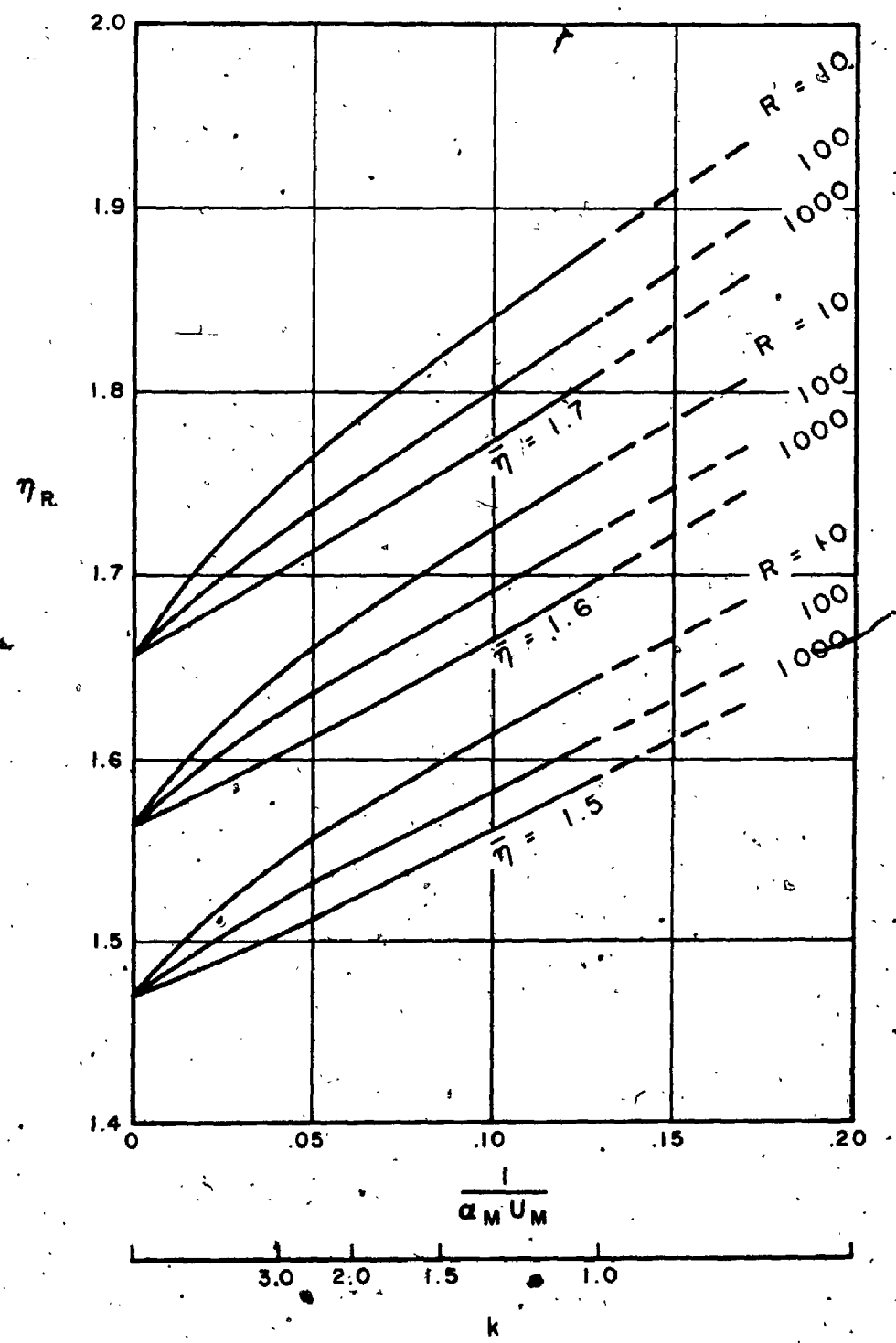
FIG. 2.13 PEAK GUST FACTORS FOR 10,100 AND 1000 YEAR RETURN WINDS (AVERAGING PERIOD OF MEAN HOURLIES - 10 MIN.)
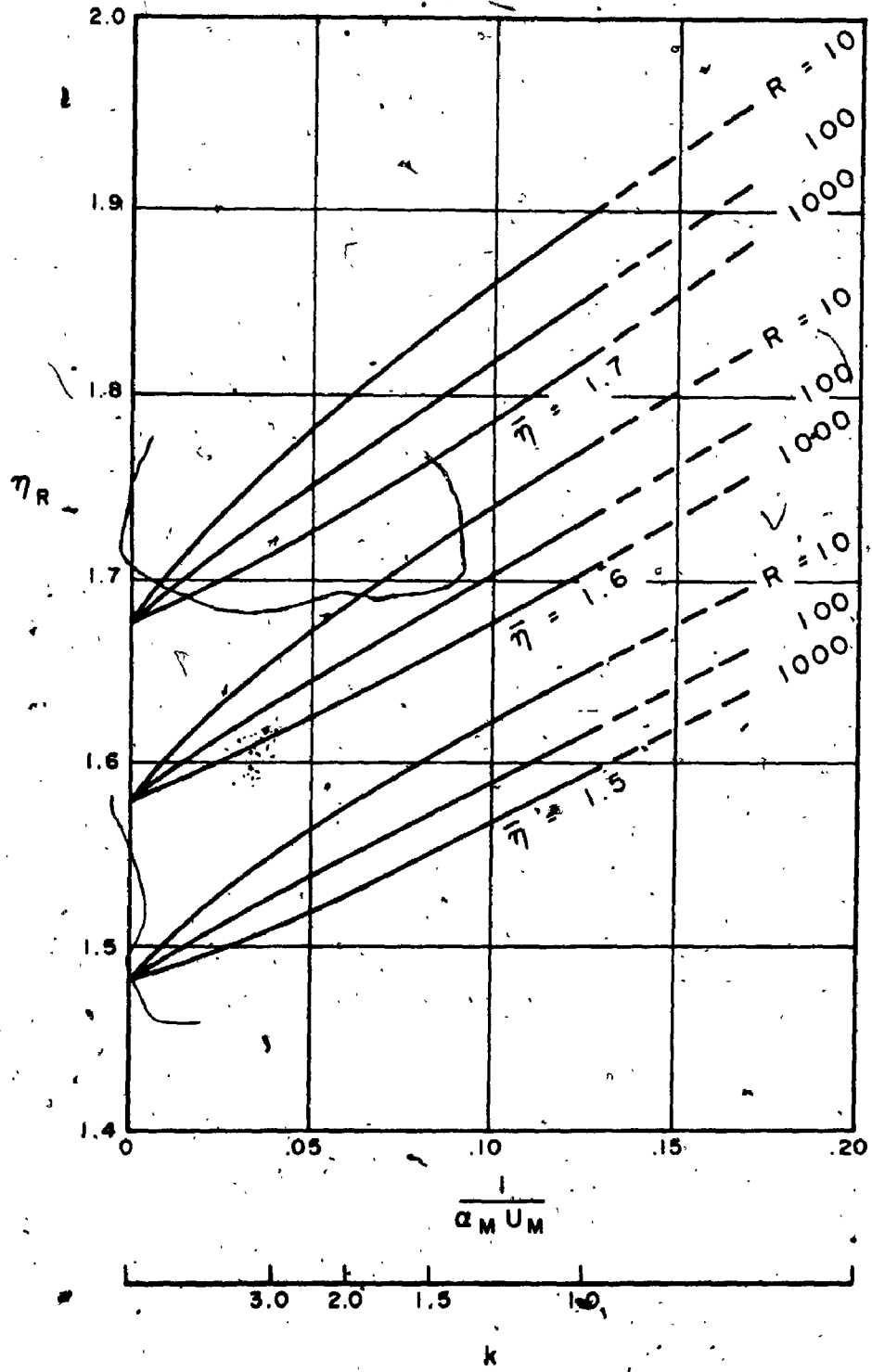
FIG. 2.14   PEAK GUST FACTORS FOR 10, 100 AND 1000
YEAR RETURN WINDS (AVERAGING PERIOD
OF MEAN HOURLIES - 1 HOUR)

The mean wind speed, $\overline{V}$, is taken here as the mean of the prescribed Weibull distribution, given by:

$$\overline{V} = c \cdot \Gamma(1 + \frac{1}{k})$$

(2.97)

Even with these assumptions, the results will hold for most situations and gust anemometer types since the theory is not sensitive to v_a.

In Figures 2.15 and 2.16 are shown the corresponding functions of U_G/U_M and a_M/a_G versus $1/a_M U_M$, again for mean hourlies with averaging periods of 10 minutes and one hour. It is noticeable that the ratio of modes is consistently higher than the mean gust factor for values of k normally encountered in wind records, whereas the ratio of dispersions is lower. However, both increase as k approaches unity. In practice a large degree of scatter is encountered in these relationships but, as detailed in Appendix II, the general trend of the curves is in accordance with records of peak gusts and mean winds for a number of stations in Europe.

It is apparent that the theory in its present form represents a considerable simplification and cannot account for deviations brought about by such meteorological conditions as thunderstorm activity and other gustiness of thermal, rather than mechanical, origins. Other possible causes are statistical departures from the Weibull distribution of mean winds; this being a particular problem in areas susceptible to cyclones or strong local winds. Finally, there are the weaknesses of the probability model of peak gust factors outlined earlier, as well as the inevitable uncertainty over a suitable choice of mean gust factor in a given situation.

2.12 The Effect of Non-uniform Terrain Roughness

It has been noted that certain effects of terrain may cause a departure from the theoretical statistical distribution of gust factors, and hence a divergence from the relationships derived above. Specifically, if the terrain roughness surrounding a given observing station is non-uniform with respect to wind direction and the greatest roughness
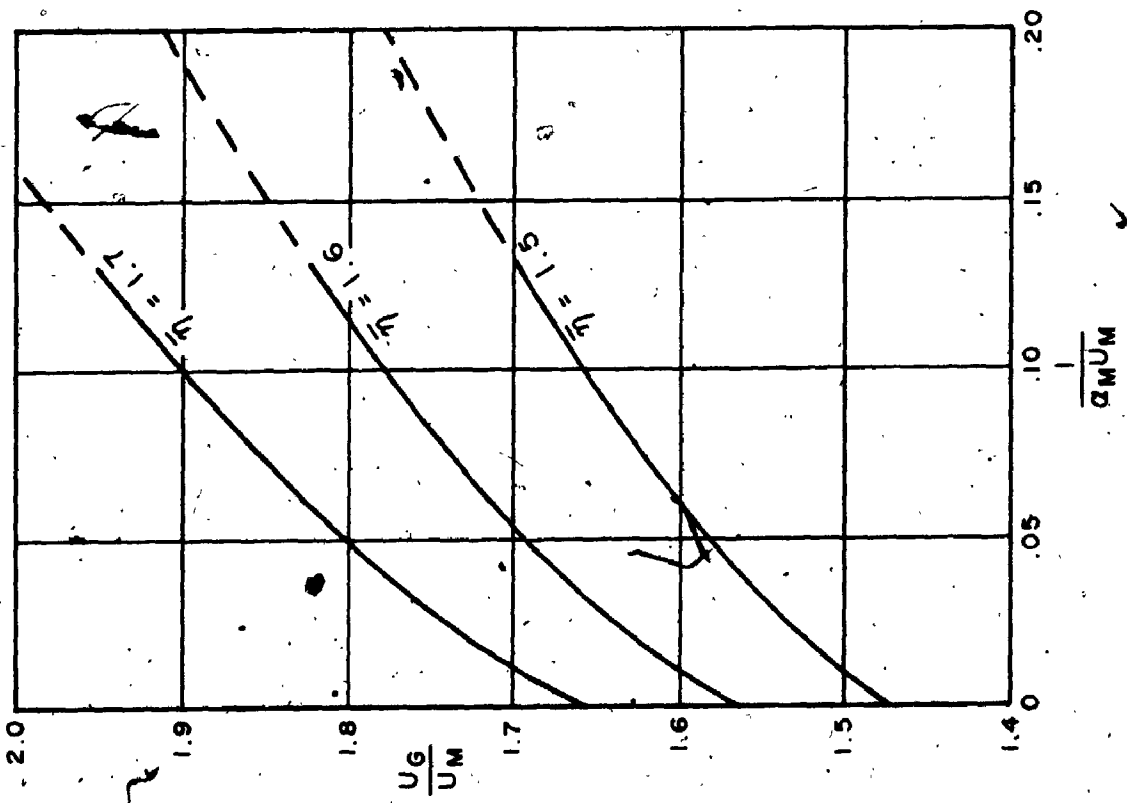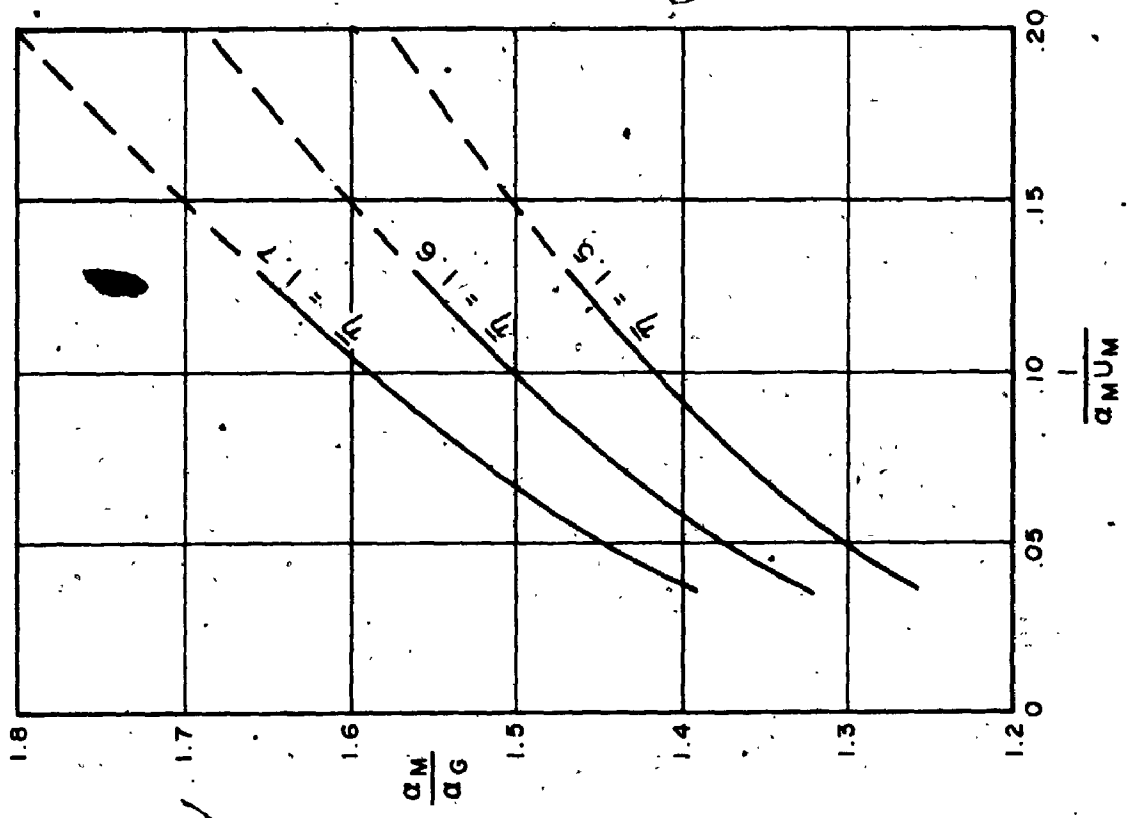
FIG. 2.15 RELATIONSHIPS OF MEAN WIND AND GUST MODES AND DISPERSIONS (AVERAGING PERIOD OF MEAN HOURLIES – 10 MINUTES)
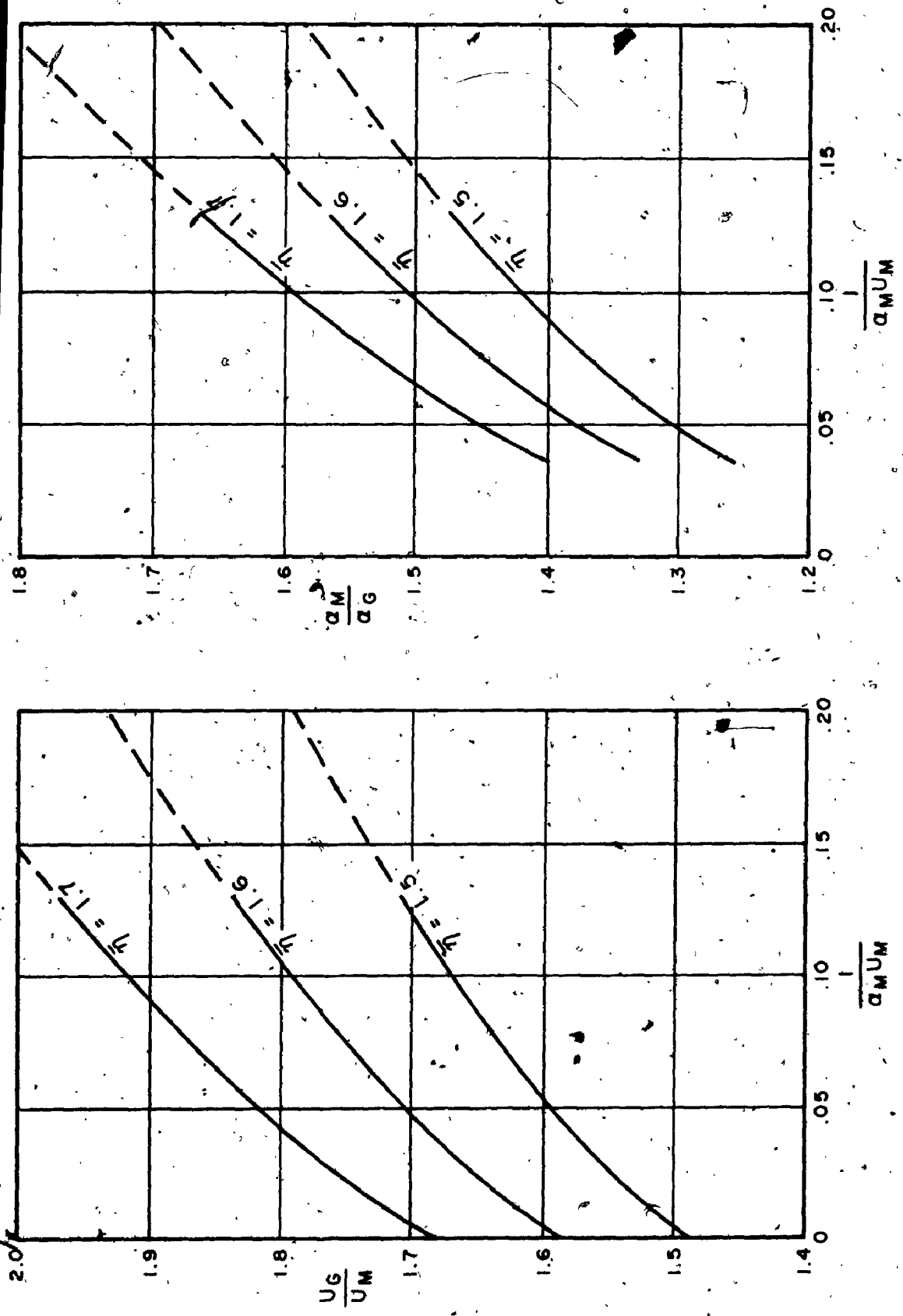
FIG. 2.16   RELATIONSHIPS OF MEAN WIND AND GUST MODES AND DISPERSIONS
(AVERAGING PERIODS OF MEAN HOURLIES — 1 HOUR)

corresponds with the prevailing direction of strong winds, then a considerable divergence from the theory can reasonably be expected. A preliminary investigation has been made to estimate the magnitude of this effect by numerical simulation of typical conditions of pronounced terrain roughness variation and strongly directional mean wind climate.

Monte Carlo methods, in conjunction with present-day digital computer facilities, provide an effective means of estimating the statistical outcome of a multivariate process where analytical approaches are intractable. In this case, only three variables are involved but the third, the gust factor, is distributed in such a way as to make a simulation procedure preferable. The three are:

a) The meridional (N-S) wind component, normally distributed with a prescribed mean and standard deviation (equivalent to the vector mean and standard deviation of a non-central circular normal distribution).

b) The zonal (E-W) wind component, also normally distributed with the same standard deviation and a mean value of zero.

c) The gust factor, the normalized form of which has the probability density given by Equation 2.83. It is exponential in ξ. For any given wind direction the actual gust factor will be determined by the mean factor defined for the terrain upwind in that direction.

In the relatively simple simulations described here, two mean wind climates are considered with ratios of the vector mean to standard deviation of 1.0 and 0.5. The mean gust factor, as a function of azimuth θ, is defined by

$$\bar{\eta} = 1.6 + 0.4 \cos(\theta - \phi) \qquad (2.98)$$

where ϕ is taken as 0°, 45°, 90°, 135° and 180° in five simulations. These parameters, together with a block diagram of the simulation procedure, are illustrated in Figure 2.17.

$$p(V_x)$$

$$\frac{1}{\sqrt{2\pi}\,\sigma} \int_{-\infty}^{V_x} \exp\left[\frac{-V_x^2}{2\sigma^2}\right] dV_x$$

SELECT
r

RANDOM NUMBER GENERATOR
$p(r)$

$$\frac{\overline{V_r}}{\sigma} = 1, 0.5.$$

$$p(V_y)$$

$$\frac{1}{\sqrt{2\pi}\,\sigma} \int_{-\infty}^{V_y} \exp\left[\frac{-(V_y-\overline{V_r})^2}{2\sigma^2}\right] dV_y$$

SELECT
r

DETERMINE
V_M, θ

V_x
V_y

θ

DETERMINE
$\overline{\eta}$

$$\overline{\eta} = 1.6 + 4\cos(\theta - \phi)$$
$$\phi = 0°, 45°, 90°, 135°, 180°$$

$$p(\xi)$$

$$1 - \exp[-\xi]$$

SELECT
r

DEFINE:
MEAN WIND SPEED
AVERAGING TIME OF MEAN WINDS
AVERAGE CYCLING RATE OF GUSTS

$\overline{\eta}$ ξ

DETERMINE
$V_G = \eta V_M$ V_M
η

DETERMINE
η

REPEAT

V_G
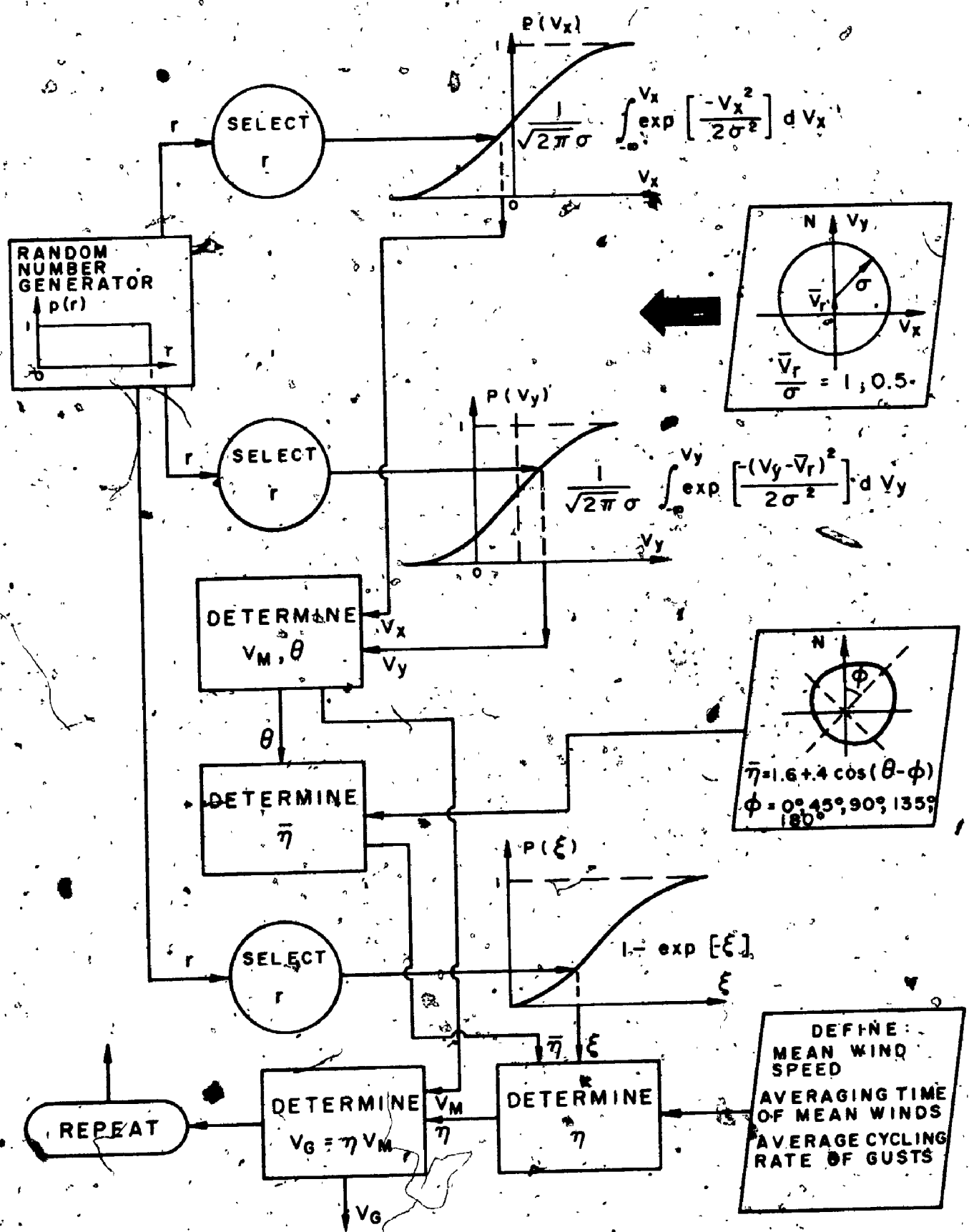
FIG. 2.17   SIMULATION OF GUSTS FROM MEAN WINDS

1.0

2.8 2.5

3.2 2.2

2.0

1.1

1.8

1.25 1.4 1.6

RESOLUTION TEST CHART
OF STANDARDS-1963-A

ARC-374
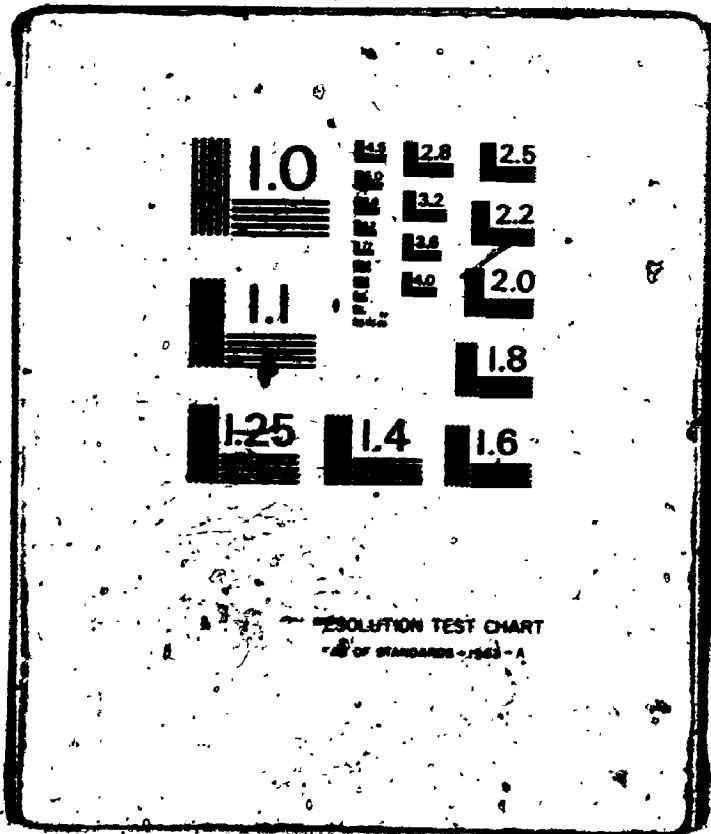
The necessary transformations to obtain the required variables from the uniformly distributed random function generated by the computer are straightforward and will not be detailed here (reference may be made to Hamming, 1962).

The statistical distributions of both the mean wind speeds and the simulated gust speeds were characterized by the Weibull form, and the parameters of the corresponding extreme distributions found from the continuous model of the annual wind records (Equations 2.89 and 2.90). In this way the quantities U_G/U_M and a_M/a_G were computed and expressed as a ratio of the same quantities obtained for uniform terrain conditions. These are shown in Figure 2.18, plotted against the angle ϕ.

It is shown that the theoretical relationship of gust to mean hourly modes can be as much as 50% in error. This occurs in a typically severe case where $\overline{V}_r/\sigma$ for the mean wind climate is unity and the mean gust factor is 25% above the average in the direction of the resultant mean wind. In these circumstances the relationship between the dispersions can be about 70% in error.

2.13 Conclusions

The principal features of this chapter have been as follows:

a)   A conclusion reached by earlier investigators, that the non-central circular case of the bivariate normal distribution of velocities provides an adequate description of upper level wind vectors was confirmed. From an examination of the scalar wind speed distributions derived from the bivariate models it was found that the Rayleigh form is likely to be as good as the Weibull form over the range of λ usually encountered. However, the defining parameter should be generally greater than that derived simply from the central circular velocity distribution.

b)   The statistics of extreme values applicable to wind climate were reviewed and relationships between the various extreme distributions suggested. It was noted that
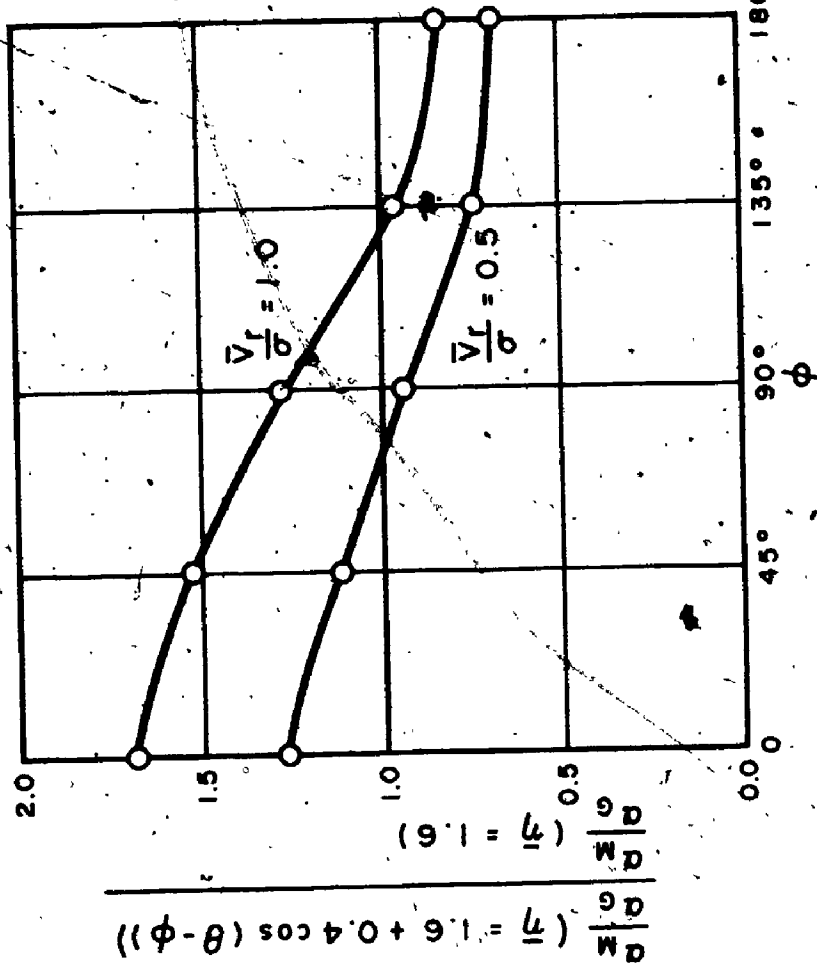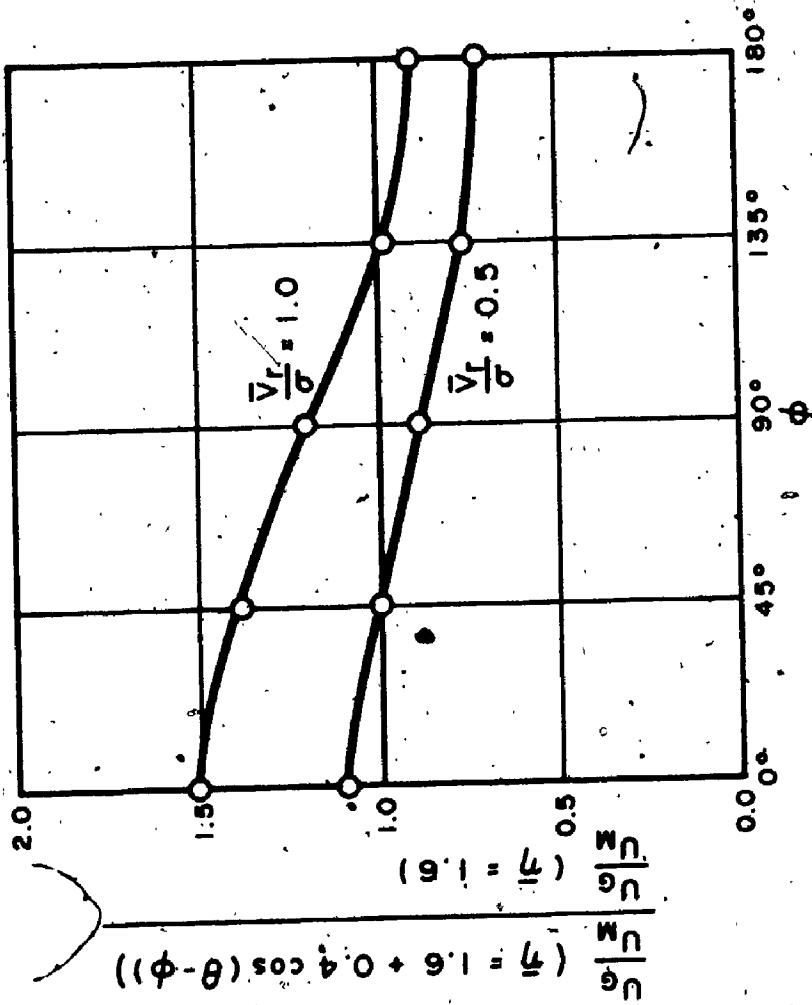
FIG. 2.18   EFFECT OF NON-UNIFORM TERRAIN ROUGHNESS ON THE RATIOS $\dfrac{U_G}{U_M}$ AND $\dfrac{a_M}{a_G}$

values of the ratio of dispersion to mode, given by the parameter grouping $1/aU$, are often significantly greater than those suggested by extreme value theory applied to a parent Weibull distribution. However, apart from the influence of singularities (such as thunderstorms) on the wind record, a large offset of the original bivariate velocity distribution would go some way to reconcile this discrepancy.

c) The influence of averaging time on maximum wind statistics was considered, specifically the differences between observed mean hourlies and peak gusts. Based on Davenport's (1964) theoretical distribution of gust factors, functions were developed for the relationships between the Fisher-Tippett Type I parameters of extreme gusts and mean winds. Higher gust winds are predicted by this approach, compared with the simple application of a mean gust factor to a given maximum mean hourly wind speed. The additional effects of thunderstorm gusts were not determined here.

d) Some European data on extreme wind speeds indicated considerable scatter about these derived relationships. A short numerical simulation showed that significant deviations might be caused by variations in terrain roughness around the observing station.

An immediate application of b) and c) is in the comparison of design wind speeds based on different averaging times and probability models. A survey of extreme wind information in various parts of the world is given in Appendix III.

CHAPTER 3

THE RELATIONSHIP OF SURFACE TO GRADIENT WINDS

3.1 Some Useful Wind Profiles

It has long been established that the mean wind usually increases with height above ground level until the freestream conditions are reached at the top of the atmospheric boundary layer, above the frictional influence of the earth's surface. This is often accompanied by a distinct turning of the wind vector. In the northern hemisphere there is a clockwise rotation, or veering, away from the direction of decreasing atmospheric pressure. Although these phenomena are readily observed, their precise behaviour in any given situation is quite difficult to predict, as is the exact thickness of the boundary layer (for convenience, the layer thickness has been taken as the "gradient height", at which the freestream velocity is first attained, although other definitions are frequently encountered in the meteorological literature).

In order to simplify the problem, it is common to consider only steady flow over homogeneous terrain. Since neutrally stratified atmospheres are usually associated with windy conditions during the passage of a centre of low pressure, this further restriction is particularly relevant here. It has the advantage of permitting more straightforward models of the mean wind profile.

The atmospheric boundary layer can be visualized as being composed of an inner and outer sublayer. In the inner sublayer, or surface layer, it can be shown by one of a number of approaches that the wind velocity as a function of height above ground level, z, is given by the logarithmic law

$$\frac{V}{u_*} = \frac{u}{u_*} = \frac{1}{k} \ln \left(\frac{z}{z_0}\right) \qquad\qquad (3.1)$$

where z_0 is the roughness length and k is von Karman's constant (~ 0.4). It should be noted that there is no veering of the wind vector in the surface layer, there being only one velocity component along the x-axis of the adopted coordinate system shown in Figure 3.1. The surface friction velocity, u_*, is defined by

$$\tau_0 = \rho u_*^2 \qquad\qquad (3.2)$$

wherein τ_0 is the surface shear stress and ρ is the fluid density. The depth of the layer over which the logarithmic law applies has been estimated as about 10% of the total boundary layer thickness, or approximately 100 m under typical conditions (see Tennekes, 1973a, for a contemporary discussion of the logarithmic profile).

It has been suggested that the introduction of a zero-plane displacement, z_d, improves the applicability of the model, especially where large and frequent obstructions are features of the underlying terrain, as in urban centres or dense forests. Essentially, the origin of z is shifted such that

$$\frac{V}{u_*} = \frac{1}{k} \ln \left(\frac{z - z_d}{z_0}\right) \qquad\qquad (3.3)$$

In a recent paper, Simiu (1973) has applied this formula to the prediction of wind speeds over London, England. He concludes that the designer can use this form "up to heights of the order of a few hundred metres". (Wind profiles over the city were estimated from observations at suburban locations. The connection between the logarithmic models in and out of the city relied on the reasonable assumption of a common gradient wind and a relationship between this and the friction velocity for a certain terrain roughness. Simiu utilized an expression derived by Csanady (1967) and others, which is also applied and discussed later in this chapter.)

The roughness parameters, z_d and z_0, have been investigated by a number of writers. Values of z_0 for different surface types have been summarized by Davenport (1963) and are indicated in Figure 3.2; estimates of z_d in cities can be made from the
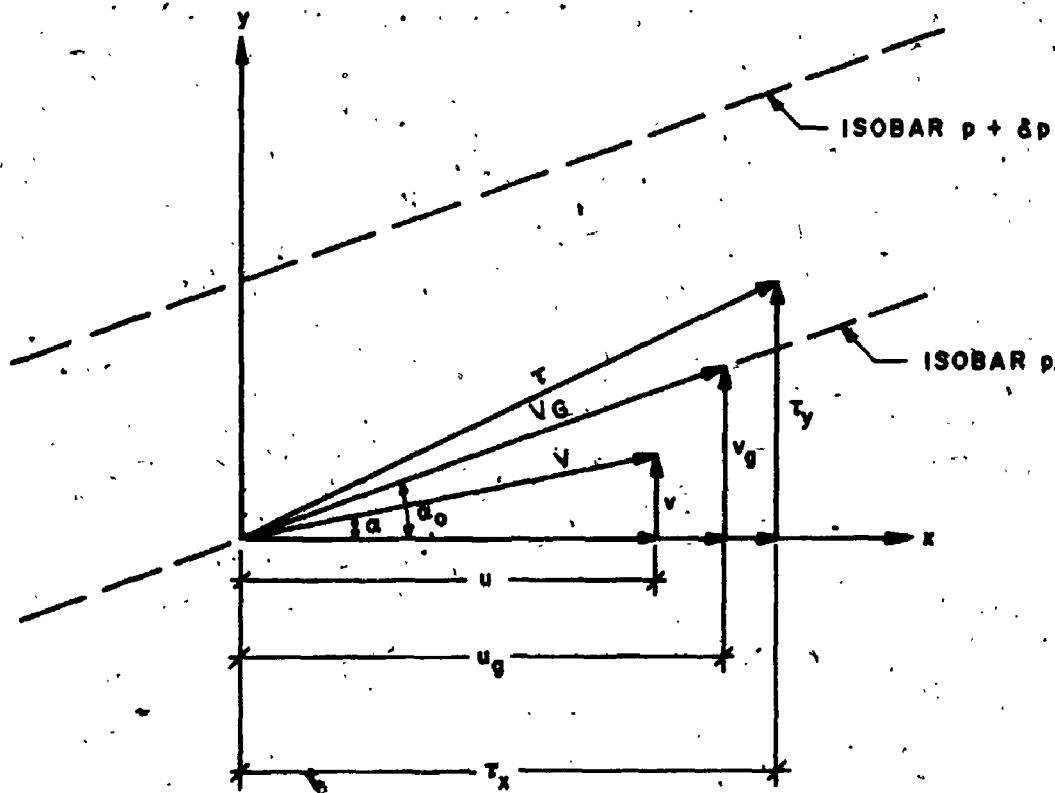
FIG 3.1 CO-ORDINATE SYSTEM FOR THE
ATMOSPHERIC BOUNDARY LAYER
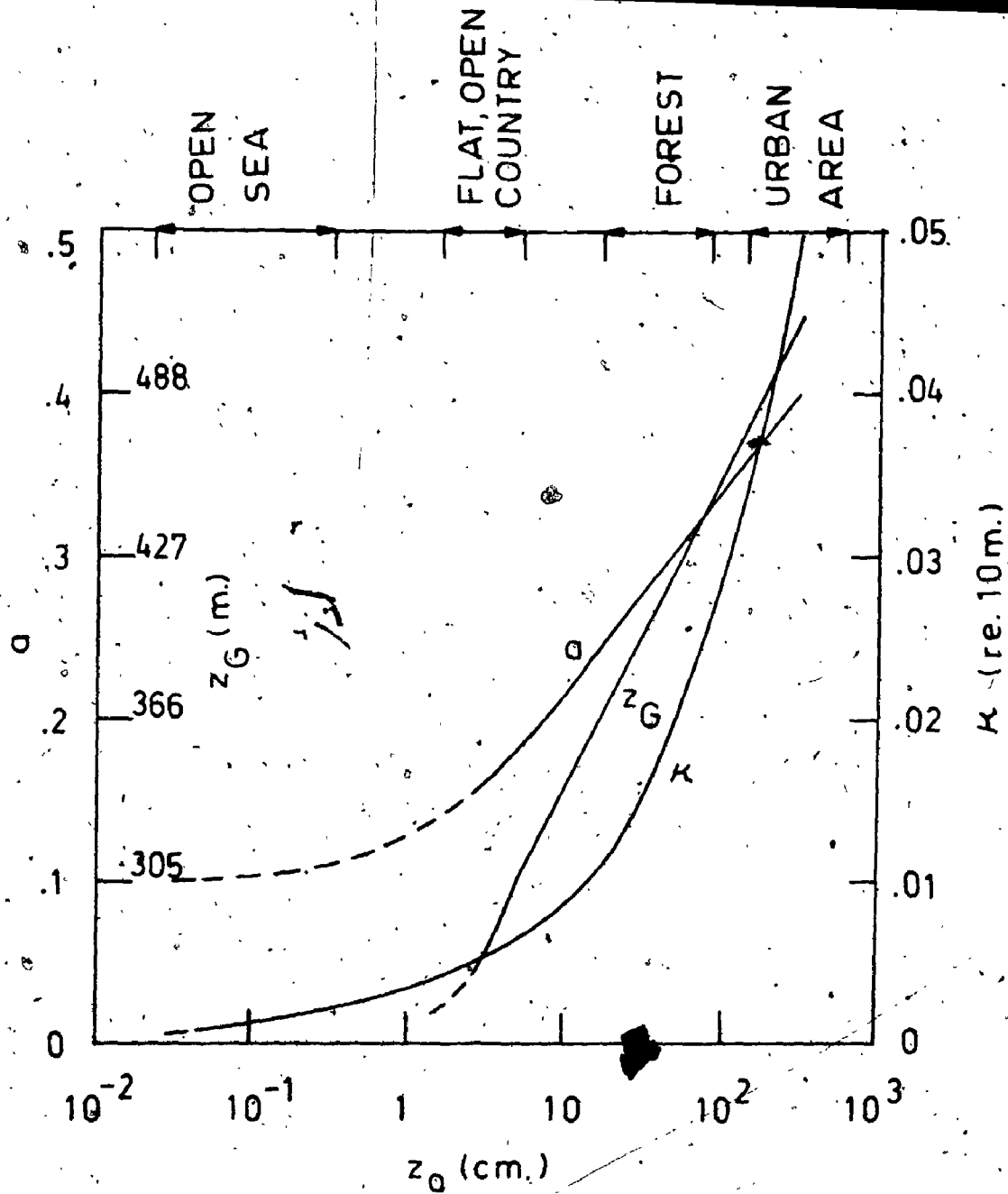
FIG 3.2   POWER LAW PARAMETERS FOR VARIOUS
TERRAINS (from DAVENPORT, 1963)

following formula provided by Helliwell (1971):

$$z_d = .1 \int \frac{z_0}{k}$$ (3.4)

where l is taken as the general level of the roof-tops. In the case of dense crops or trees, to a good approximation z_d can be assumed equal to the cover height (Plate, 1971).

When the boundary layer becomes either stably or unstably stratified the physical foundations for the logarithmic law no longer apply and other models must be found. One such is the log-linear model, generally applicable in conditions of slight instability (forced convection) or stability. It has the form

$$\frac{V}{u_*} = \frac{1}{k}(\ln \frac{z}{z_0} + \frac{\beta z}{L})$$ (3.5)

in which β is an empirical constant and L is a scaling length defined by Monin and Obukhov and expressing the vertical heat flux (the value of β has been the subject of some controversy, estimates ranging from 0.6 to 7). The validity of the log-linear law has been discussed more fully in Lumley and Panofsky (1964) and by Plate (1971), who has also suggested that in general stable stratifications the ordinary logarithmic law is suitable for $z/L < 0.01$.

Turning to the mean wind profile in the outer sublayer, an empirical but practical model in wide use and suitable for neutral, strong wind situations is the power-law

$$\frac{V_1}{V_2} = (\frac{z_1}{z_2})^a$$ (3.6)

which relates the mean wind velocities at any two heights, z_1 and z_2. A reference level is normally introduced, either the standard anemometer height of 10 m or the gradient height, z_G, so that

$$\frac{V}{V_{10}} = (\frac{z}{10})^a \quad \text{or} \quad \frac{V}{V_G} = (\frac{z}{z_G})^a$$ (3.7)

These have been used to describe the mean wind profile throughout the boundary layer, including the surface layer.

Davenport (1960) has studied a large body of wind data in order to determine values of the index a for various types of terrain. They range from approximately 0.16 for flat, open country through 0.28 in woodland to 0.4 in urban areas. He also estimated gradient heights, although these are harder to define and reliable data at these levels is relatively scarce. In a subsequent paper, Davenport (1963) summarized the dependence of a and z_G on terrain roughness in a diagram shown here as Figure 3.2 (also given is the surface drag coefficient, κ, defined by $u_*^2 = \kappa V_{10}^2$).

As noted by Harris (1971), in built-up centres a is difficult to establish due to the localised influences of individual roughness elements (buildings), and so a high-index indicated by anemometers at street level and on top of buildings may not be appropriate in the upper regions of the boundary layer. It may again be preferable, as with the logarithmic model, to adopt a zero-plane displacement with a flatter power-law profile.

So far, mean wind veering in the atmospheric boundary layer has been disregarded. However, it is a phenomenon having important implications, for example, in the horizontal dispersion of a plume (Csanady, 1972). In the classical Ekman theory the eddy viscosity, K, is assumed constant and the equations of motion solved to yield the two velocity components

$$u = V_G\left(1 - \cos\frac{z}{h}\cdot\exp\left(-\frac{z}{h}\right)\right) \qquad (3.8)$$

and

$$v = V_G \sin\frac{z}{h}\exp\left(-\frac{z}{h}\right) \qquad (3.9)$$

in which h is the depth of the Ekman layer, defined by $h = \sqrt{2K/f}$ (f is the Coriolis parameter).

This gives at least a qualitative indication of the asymptotic approach to the geostrophic wind, which is a fundamental feature of this and other spiral models. Unfortunately, the theory considerably overestimates the angle between the surface and geostrophic winds, typically less than half the predicted 45°. In fact K cannot be regarded as constant, and several later models have been proposed to allow for this. For example, Blackadar (1962) described the eddy viscosity as being some function of height and Lettau (1962) proposed an indirect relationship by assuming a height dependence of the angle between the shear stress, τ, and the vector difference of V and V_G (see Figure 3.1). Although these and other spirals can be fairly representative of the real atmosphere, they are formulated in numerical terms and are of limited practical value.

3.2 A Recent Approach to Boundary Layer Description

Considerations will again be restricted to steady, neutrally stratified boundary layers over homogeneous terrain, referring to the coordinate system shown in Figure 3.1. Firstly, in the inner sublayer the equations of motion can be non-dimensionalized by the velocity scale u_* and the length scale z_0, so that

$$\frac{u}{u_*} = f_x \left(\frac{z}{z_0}\right); \quad \frac{v}{u_*} = f_y \left(\frac{z}{z_0}\right) \tag{3.10}$$

In the outer regions of the boundary layer, however, it has been shown (Blackadar and Tennekes, 1968, and Csanady, 1967) that a scaling length h, defining the top of the layer, must be substituted, where

$$h \propto \frac{u_*}{f} \tag{3.11}$$

Velocity-defect laws are then required, of the general form

$$\frac{u - u_g}{u_*} = g_x \left(\frac{zf}{u_*}\right); \quad \frac{v - v_g}{u_*} = g_y \left(\frac{zf}{u_*}\right) \tag{3.12}$$

These satisfy the required boundary conditions, approaching zero at $z = h$, and are independent of the geostrophic velocity. Both (3.10) and (3.12) depend solely on a Rossby number defined by u_*/fz_0.

Given that v is zero at the wall, or ground level, and so f_y in Equation 3.10 is asymptotically zero, it remains to reconcile both (3.10) and (3.12). This has been done by requiring that they hold simultaneously in a "matched region" with a logarithmic velocity distribution, a process which yields (Blackadar and Tennekes, 1968).

$$\frac{u_g}{u_*} = -\frac{1}{k}(ln(\frac{u_*}{fz_0}) + A) \qquad (3.13)$$

and

$$\frac{v_g}{u_*} = -\frac{B}{k} \qquad (3.14)$$

(3.13) and (3.14) can be combined to give a relationship between the geostrophic drag coefficient $c_g (= u_*/V_G)$ and the surface Rossby number, Ro, and an expression for the angle between the surface and geostrophic wind vectors, a_0.

Thus, with

$$Ro = \frac{V_G}{fz_0}, \qquad (3.15)$$

$$ln \, Ro = k(\frac{1}{c_g^2} - (\frac{B}{k})^2)^{1/2} + 1.15 \, log_{10} \frac{1}{c_g^2} - A \qquad (3.16)$$

$$sin \, a_0 = -\frac{B}{k} c_g \qquad (3.17)$$

The above equations were also developed by Csanady (1967) and their derivation has been explained in greater detail by Plate (1971) and Tennekes (1973b). Csanady

went on to attempt to establish values of the universal constants A and B. Fitting Equation 3.17 to observations by Lettau and associates at Leipzig and Scilly, he estimated B/k as 10.7 $(B = 4.28$ with $k = 0.4)$ and then satisfied (3.16) with $A = 1.52$ for one particular spiral observed at Scilly. Since then Deacon (1973) has surveyed the parameters for neutral boundary layers using the more reliable data in several publications and calculated the means of A and B as 1.9 and 4.7 respectively.

At this point brief mention will be made of an alternative relationship between the Rossby number and the geostrophic drag coefficient. This was first proposed by Taylor (1962) and later extended by Davenport (1963) to give

$$c_g = 0.16 \, Ro^{-0.09} \qquad (3.18)$$

The numerical constants are based partly on theoretical considerations and some observational data. The two curves (3.16) and (3.18) are compared in Figure 3.3.

Some recent work by Swinbank (1970), also discussed in Plate (1971), has apparently yielded a useful model relating the pressure gradient (and hence the geostrophic wind), wind structure and shear stress throughout the Ekman layer. From the basic equations of motion and assuming that τ is parallel to V at all elevations, it can be shown that

$$\frac{d\tau}{dz} = -f \, V_G \, sin(a - a_0) \qquad (3.19)$$

To proceed further with the solution, Swinbank expanded τ in a Taylor series about $z = h$ and obtained the equations

$$sin(a - a_0) = \frac{da}{dz} \Big|_h (z-h) \qquad (3.20)$$

and

$$c_g = .16 \, Ro^{-.09}$$

$$\ln Ro = k \left[\frac{1}{c_g^2} - \left(\frac{B}{k} \right)^2 \right]^{\frac{1}{2}} + 1.15 \cdot \log_{10} \frac{1}{c_g^2} - A$$

$$B = 4.7$$
$$A = 1.9$$

$$Ro = \frac{V_G}{f z_o}$$
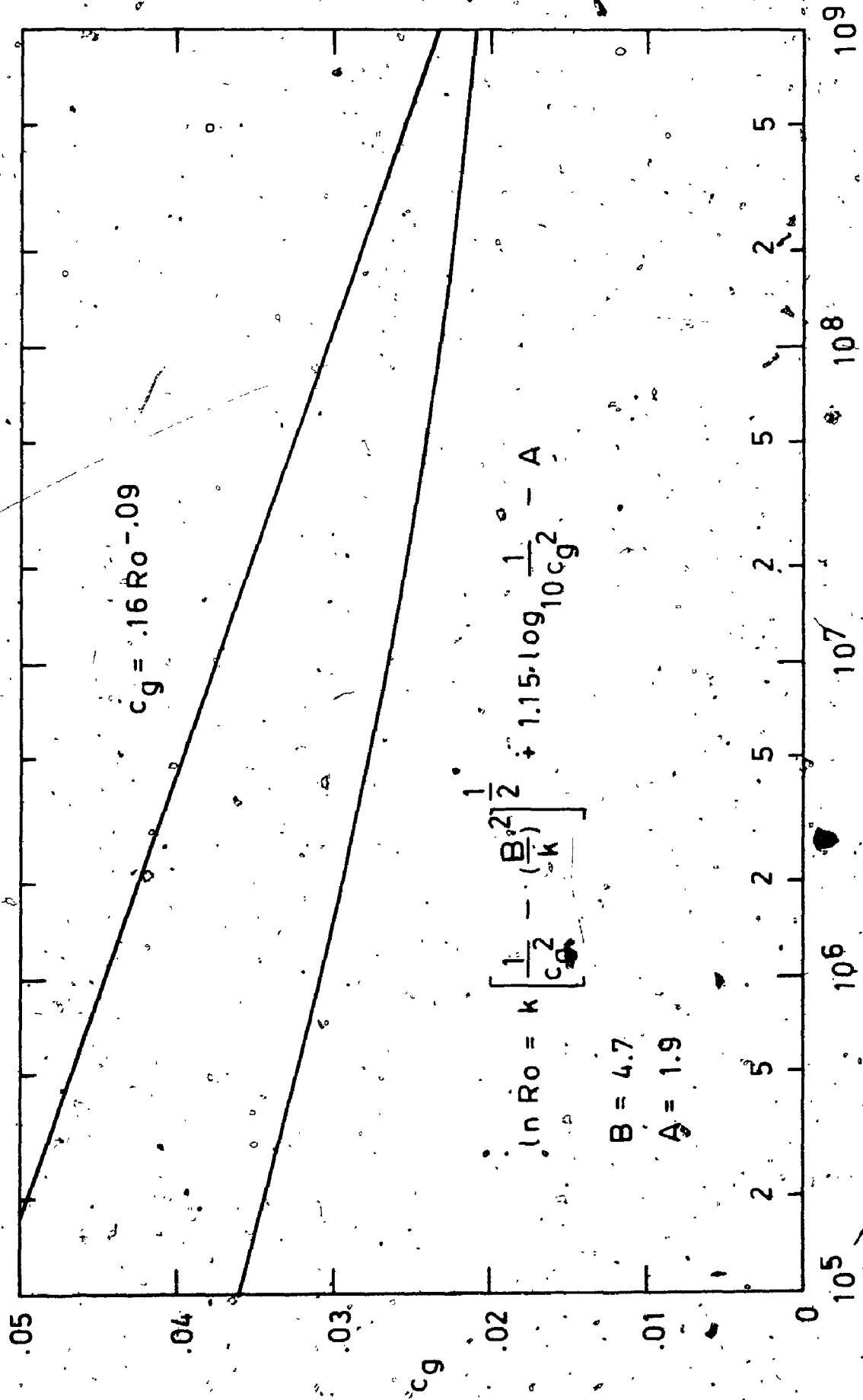
FIG. 3.3 GEOSTROPHIC DRAG COEFF. - ROSSBY NO. RELATIONSHIPS

$$\tau = -\frac{fV_G}{2} \frac{da}{dz}\Big|_h (h-z)^2 \qquad (3.21)$$

These equations are supported by data from the Leipzig profile for most of the boundary layer depth. It must also be noted that Swinbank's theory apparently applies to any thermal stratification.

The final step is to determine the quantities $\frac{da}{dz}\Big|_h$ and h. This can be done by setting $z = 0$ and applying Equation 3.17, so that

$$\sin a_0 = \frac{da}{dz}\Big|_h h = -\frac{B}{k} \cdot \frac{u_*}{V_G} \qquad (3.22)$$

By requiring that $\tau/u_*^2 = 1$ at $z = 0$, it can then be shown that

$$h = 2\frac{k}{B} \cdot \frac{u_*}{f} \qquad (3.23)$$

and

$$\frac{da}{dz}\Big|_h = -\left(\frac{B}{k}\right)^2 \cdot \frac{f}{2V_G} \qquad (3.24)$$

Thus, the constant of proportionality between h and u_*/f, defining the depth of the Ekman layer (see Equation 3.11), is approximately 0.2.

3.3 Deterministic Predictions of Surface Winds from Observations at Gradient Height

To assess the usefulness of the theory just described, an investigation was carried out to predict mean surface wind vectors from gradient velocities and compare them with the surface observations. Only atmospheric boundary layers of near neutral stability were considered. Furthermore, barotropic conditions were assumed (no thermal wind component).

In many practical situations the necessary two of three defining parameters (u_*, z_0 and V_G) will not be directly available. One approach is to set h, the Ekman layer thickness, at a generally acceptable gradient height and assume V_G is the wind velocity observed at that level. If an estimate of the quantity $\frac{da}{dz}|_h$ is also available, the angle a_0 can be found without relying on an assumed value of the constant B (Equations 3.24 and 3.22). B can then be "variable" according to the situation, thus giving the boundary layer model of Equations 3.16 and 3.17 an additional, if somewhat empirical, degree of freedom.

A suitable level for which a large body of upper air data has been compiled is 500 m, although this may be a low estimate of h. Since $\sin a_0$ in (3.22) is linearly dependent on both $\frac{da}{dz}|_h$ and h this may result in low values of a_0, but offset by an expected increase in the detectable rotation rate of the wind vector at the lower elevation. Now, the independent variable in (3.16) is $1/c_g^2$, which depends on the measureable quantities as

$$\frac{1}{c_g^2} = \frac{-2 \, V_G}{fh^2 \frac{da}{dz}|_h} \tag{3.25}$$

so that the impact of putting $h \sim 500 \, m$ may again be offset by the expected tendency to increase $\frac{da}{dz}|_h$ and reduce the assumed value of V_G. If the surface Rossby number can be estimated in this way, by invoking either of Equations 3.16 and 3.18, the surface wind speed (at the standard anemometer height of 10 m) can be found by using the resulting estimate of the roughness length in the logarithmic law for the inner sublayer. The surface friction velocity, u_*, will be that obtained from the definition of c_g ($u_* = c_g V_G$).

In North America, useful sources of upper wind (and surface) data are the Winds Aloft Summaries prepared for an extensive network of U.S. radiosonde stations. The writer has prepared similar summaries for ten Canadian stations in the course of earlier research (Baynes, 1971). These include wind frequency distributions and other statistics for each month of the year and elevations in the range of interest here (surface,

300 m and 500 m).

In applying the above theory to this data, it should be remembered that the fundamental velocity profile functions in (3.10) and (3.12) depend on the scaling lengths z_0 and u_*/f. The selection of data should therefore reflect as far as possible distinct characteristics of terrain roughness and wind speed distribution. A convenient approach is to consider separately winds blowing from within prescribed direction intervals; 45^0 sectors are suggested. If, as in this study, it is required to predict the surface wind from the mean gradient wind vector, then the vector mean will be close to the simple mean wind speed within the sector. This statistic is given in the regular upper wind summaries (however, the rotation of the mean wind vector cannot be found from such summaries, in which case a value of the constant B must be assumed).

In this investigation the data was selected from ten years of upper air records at three locations in Canada; Moosonee, Sable Island and the Pas. Details of each station, including descriptions of the surrounding terrain, are given in Appendix IV. Since records of the individual radiosonde balloon ascents were readily available, they were separately screened to extract only those occasions when the boundary layer was virtually neutrally stratified. Other acceptance criteria were applied and finally the vector means were calculated at the surface, 300 m and 500 m levels, and for eight subsamples of profiles with observed surface wind directions within the prescribed 45^0 intervals (see Appendix V).

Predictions of the surface vector mean winds, together with their observed values, are summarized in Tables 3.1 – 3.3. Corresponding estimates of the parameters u_*, c_g, Ro and z_0 are also given.

3.4 Departures from the Deterministic Model

It is evident from the tables of results, and from Figure 3.4 which shows the predicted against the observed angles a_0, that negative values occur in some areas. In these instances the mean vector backs rather than veers with increasing height, a situation

Surface Wind Exposure	PREDICTED					1*			2*			OBSERVED		
	a_o (°)	$\sin a_o$	B/k	u_* (m/s)	c_g	Ro	z_o (m)	V_o (m/s)	Ro	z_o (m)	V_o (m/s)	a_o (°)	$\sin a_o$	V_o (m/s)
N	−1.0	−0.02	−2.4	0.07	.007	7.6×10^{26}	1.2×10^{-22}	9.09	1.6×10^{15}	5.5×10^{-11}	4.47	−1.3	−0.02	5.97
NE	−21.4	−0.36	−8.5	0.24	.043	3.9×10^{4}	1.6	1.10	2.3×10^{6}	2.2×10^{-2}	3.71	−18.6	−0.32	5.42
E	−7.5	−0.13	−4.5	0.13	.029	7.0×10^{6}	5.6×10^{-3}	2.41	1.8×10^{8}	2.1×10^{-4}	3.46	−7.1	−0.12	5.73
SE	16.8	0.29	10.2	0.29	.028	5.8×10^{6}	1.5×10^{-2}	4.70	2.3×10^{8}	3.9×10^{-4}	7.36	26.8	0.45	6.26
S	14.7	0.25	9.7	0.28	.026	2.3×10^{7}	4.1×10^{-3}	5.40	5.6×10^{8}	1.7×10^{-4}	7.61	18.3	0.32	5.76
SW	13.1	0.23	9.9	0.28	.023	2.3×10^{8}	4.8×10^{-4}	6.98	2.4×10^{9}	4.6×10^{-5}	8.62	23.8	0.40	6.22
W	9.2	0.16	8.2	0.23	.019	7.3×10^{9}	1.4×10^{-5}	7.83	1.5×10^{10}	7.2×10^{-6}	8.24	12.6	0.22	6.35
NW	2.0	0.03	3.7	0.10	.009	7.3×10^{19}	1.3×10^{-15}	9.53	4.8×10^{13}	2.0×10^{-9}	5.82	0.8	0.01	6.35

*1. Derived from $\ln(Ro) = k\sqrt{\frac{1}{c_g^2} - \left(\frac{B}{k}\right)^2} + 1.15 \log_{10} \frac{1}{c_g^2} - 1.52$

*2 Derived from $c_g = 0.16\, Ra^{-0.09}$

TABLE 3.1 PREDICTED AND OBSERVED SURFACE MEAN WIND VECTORS, MOOSONEE, ONTARIO

Surface Wind Exposure	PREDICTED					1*			2*			OBSERVED		
	α_o (°)	sin α_o	B/k	u_* (m/s)	c_g	Ro	z_o (m)	V_o (m/s)	Ro	z_o (m)	V_o (m/s)	α_o (°)	sin α_o	V_o (m/s)
N	−0.1	0	−0.7	0.02	.002	1.7×10^{38}	6.2×10^{-34}	3.32	2.0×10^{22}	5.3×10^{-18}	1.77	0.6	0.01	8.39
NE	1.1	0.02	2.9	0.07	.007	2.4×10^{27}	4.6×10^{-23}	9.96	2.0×10^{15}	5.5×10^{-11}	4.81	0.1	0	8.58
E	3.6	0.06	5.1	0.13	.012	1.6×10^{15}	6.3×10^{-11}	8.32	2.2×10^{12}	4.7×10^{-8}	6.18	1.8	0.03	7.46
SE	25.8	0.44	13.4	0.34	.033	4.2×10^{5}	2.4×10^{-1}	3.14	4.8×10^{7}	2.2×10^{-3}	7.13	19.7	0.34	7.53
S	17.6	0.30	11.2	0.28	.027	1.1×10^{7}	9.7×10^{-3}	4.89	3.7×10^{8}	2.7×10^{-4}	7.40	18.9	0.32	7.27
SW	6.1	0.11	7.1	0.18	.015	5.2×10^{12}	2.3×10^{-8}	8.98	2.7×10^{11}	4.4×10^{-7}	7.65	9.0	0.16	7.49
W	0.4	0.01	1.8	0.05	.003	1.7×10^{38}	7.5×10^{-34}	8.92	2.8×10^{18}	4.6×10^{-14}	3.75	3.3	0.06	9.00
NW	−2.0	−0.04	−4.0	0.10	.009	1.5×10^{21}	7.8×10^{-17}	10.06	1.0×10^{14}	1.1×10^{-9}	5.85	−1.1	−0.02	8.99

*1 Derived from $ln(Ro) = k \sqrt{\dfrac{1}{c_g^2} - \left(\dfrac{B}{k}\right)^2} + 1.15 \log_{10} \dfrac{1}{c_g^2} - 1.52$

*2 Derived from $c_g = 0.16 \, Ro^{-0.09}$

TABLE 3.2 PREDICTED AND OBSERVED SURFACE MEAN WIND VECTORS,
SABLE ISLAND, NOVA SCOTIA

Surface Wind Exposure	PREDICTED					1*			2*			OBSERVED		
	α_0 (°)	$\sin \alpha_0$	B/k	u_* (m/s)	c_g	Ro	z_0 (m)	V_0 (m/s)	Ro	z_0 (m)	V_0 (m/s)	α_0 (°)	$\sin \alpha_0$	V_0 (m/s)
N	−1.8	−0.03	−3.1	0.09	.010	1.9×10^{18}	3.9×10^{-14}	7.59	1.8×10^{13}	4.1×10^{-9}	4.94	−5.9	−0.10	7.54
NE	−0.7	−0.01	−1.8	0.05	.007	1.0×10^{26}	6.3×10^{-22}	6.98	1.1×10^{45}	5.8×10^{-11}	3.53	−1.6	−0.03	6.87
E	10.8	0.19	6.6	0.20	.028	7.9×10^{6}	7.4×10^{-3}	3.57	2.2×10^{8}	2.6×10^{-4}	5.22	11.0	0.19	6.55
SE	16.1	0.28	8.6	0.26	.032	9.8×10^{5}	6.7×10^{-2}	3.20	5.2×10^{7}	1.3×10^{-3}	5.73	13.6	0.24	7.86
S	10.7	0.19	6.9	0.21	.027	1.9×10^{7}	3.4×10^{-3}	4.13	4.2×10^{8}	1.5×10^{-4}	5.72	2.9	0.05	7.21
SW	9.9	0.17	7.3	0.22	.024	1.7×10^{8}	4.6×10^{-4}	5.45	1.7×10^{9}	4.4×10^{-5}	6.72	14.8	0.26	7.36
W	7.9	0.14	6.6	0.20	.021	1.8×10^{9}	4.3×10^{-5}	6.07	6.8×10^{9}	1.2×10^{-5}	6.71	9.7	0.17	7.73
NW	4.6	0.08	5.3	0.16	.015	3.7×10^{12}	2.4×10^{-8}	7.78	2.3×10^{11}	3.7×10^{-7}	6.70	3.7	0.07	8.42

*1 Derived from $\ln(Ro) = k \sqrt{\dfrac{1}{c_g^2} - \left(\dfrac{B}{k}\right)^2} + 1.15 \log_{10} \dfrac{1}{c_g^2} - 1.52$

*2 Derived from $c_g = 0.16 \, Ro^{-0.09}$

TABLE 3.3 PREDICTED AND OBSERVED SURFACE MEAN WIND VECTORS.
THE PAS, MANITOBA
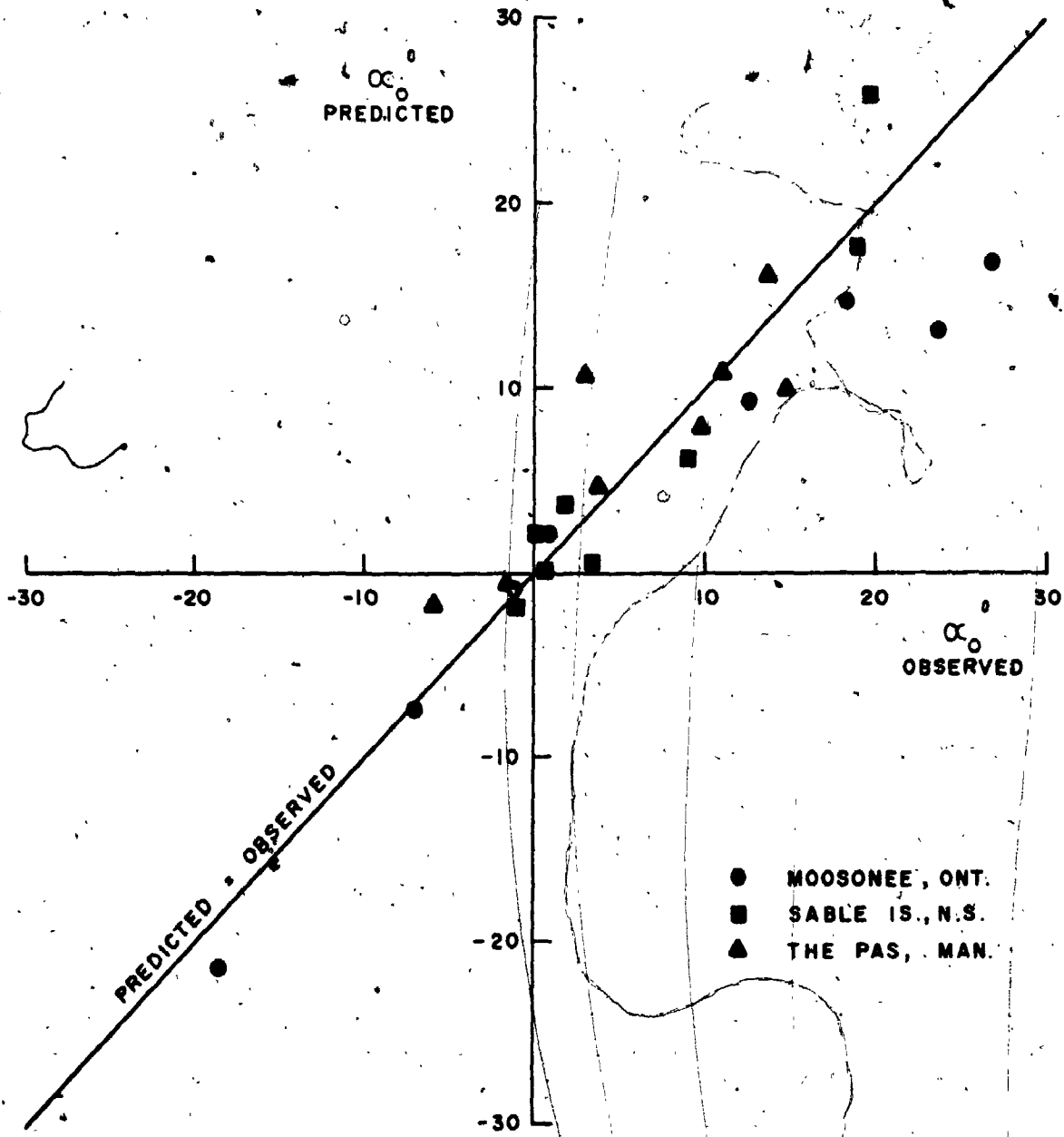
FIG 3.4 PREDICTED AND OBSERVED MEAN VEERING BETWEEN 500M AND SURFACE

which is not allowed for in the Ekman spiral, except for very small direction changes close to the asymptotic solution of geostrophic balance.

There are a number of possible reasons for this departure from the model, for example, the effects of thermal or topographic features peculiar to the location. As far as this writer is aware these factors have not been incorporated in a deterministic boundary layer description. In general terms, however, a superimposed shear flow might be included in the equations of motion and the theory reworked. This has been done in Appendix VI, to give

$$sin\ a_O = (\frac{da}{dz}|_h - \frac{E'(h)}{fV_G})h - (\frac{E(0)}{fV_G}$$ (3.26)

$$= (\frac{da}{dz}|_h)h = -\frac{B_e}{k}\frac{u_*}{V_G}$$ (3.27)

where subscript e denotes equivalent quantities for the modified wind spiral. B_e can be written as a function of B and the superimposed shearing stress term $E(0)$ as

$$\frac{B_e}{k} = \frac{E(0)}{2u_*f} \pm [(\frac{E(0)}{2u_*f})^2 + (\frac{B}{k})^2]^{1/2}$$ (3.28)

Although B cannot be other than a positive quantity it can then be argued that, for certain superimposed shear flows, small negative values of the equivalent constant, and thus slight backing of the wind with height, can be predicted for some practical situations.

Figures 3.4 and 3.5 are scatter diagrams of the predicted and observed angles a_O and surface winds V_O. Twenty-five per cent of the points in Figure 3.4 indicate wind backing with increasing height, only two of these six being beyond the restriction of reasonably small negative a_O. There is a high level of agreement between the predicted and observed angles, but much less for the surface wind speeds when either of the relationships between Ro and c_g were used. The percentage discrepencies in surface
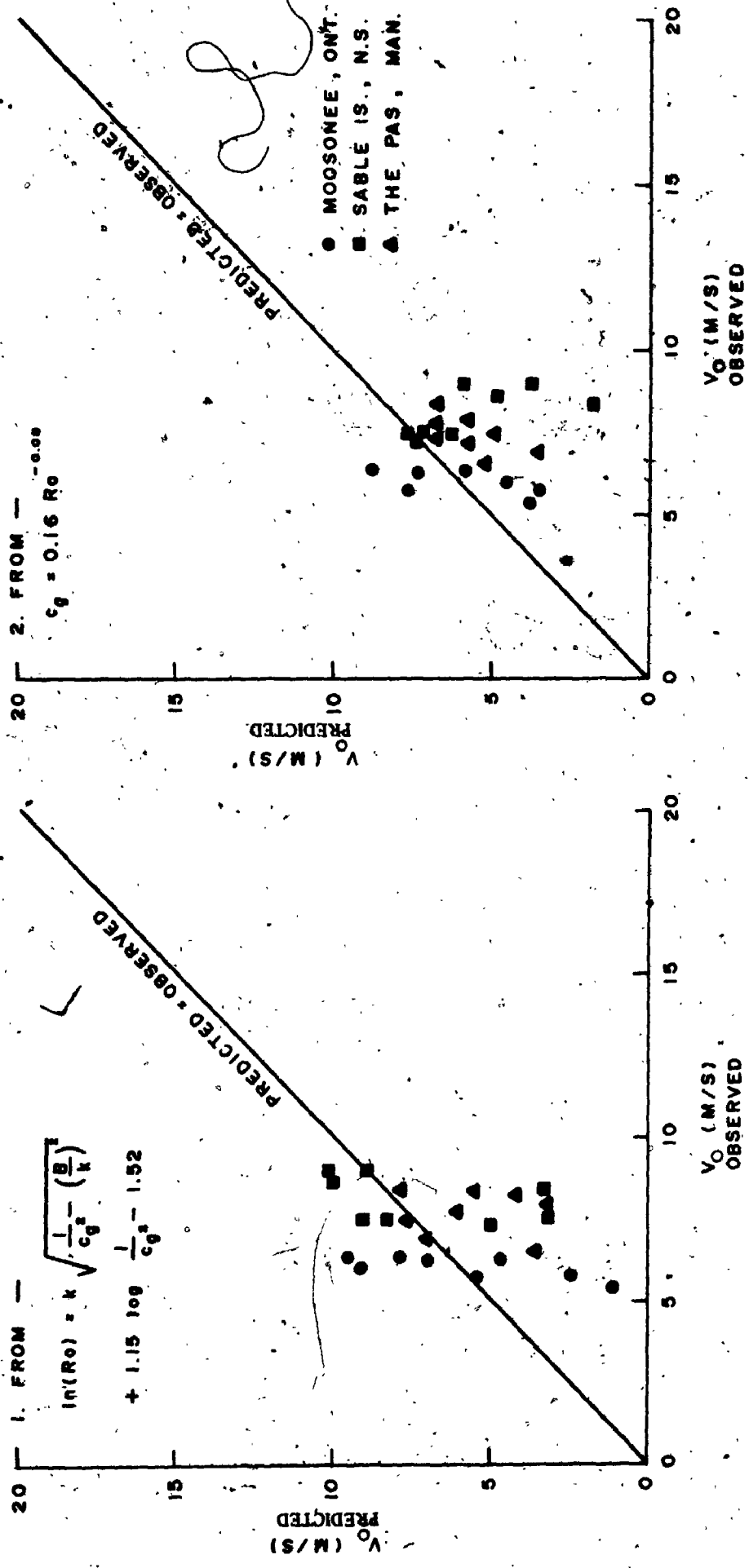
FIG 3.5 PREDICTED AND OBSERVED MEAN WIND SPEEDS AT 10M

winds can be related to the geostrophic drag coefficient as shown in Figure 3.6. Best agreement is apparently obtained for c_g between about 0.01 and 0.02, although the function $c_g = 0.16 \, Ro^{-0.09}$ yielded considerably better predictions than the alternative equation above 0.02. This may be partly explained by the empirical derivation of the power law, which was fitted to data in the range $c_g = 0.02$ to 0.05 (Davenport, 1963). It is interesting to note that, for the four cases here with c_g between 0.01 and 0.02, the mean estimate of B is 2.57, significantly lower than the hitherto accepted value.

In this study, no attempt was made to isolate the thermal wind, or geostrophic veering, where it existed. A statistical study of wind veering in the atmospheric boundary layer has been carried out by Mendenhall (1967) using radiosonde data from six locations. The thermal wind was computed and separated from each observation so that the mean deviation from the Ekman spiral due to this phenomenon could be obtained; the layer chosen was between the surface and 900 mb ((about 1000 m). Veering associated with departures from neutral conditions was also isolated. The results can be summarized for the "ideal" conditions of no thermal wind and a lapse rate of $6.5^o \, C/Km$ (U.S. Standard Atmosphere). Mendenhall's correction table is given here as Table 3.4, from which it is apparent that the contribution due to geostrophic veering is relatively small for the land-based, moderate latitude site at Shreveport. The more significant deviations, occuring during the summer days and winter nights, are also small when taken together over a one year period. Thus, there appears to be some support for the prediction of the mean wind direction at ground level from winds aloft using the model of a neutral barotropic atmosphere.

Since the microclimates of the areas in which the three upper air stations are situated have not been studied, it is only possible to discuss the influence of topography in general qualitative terms. At Moosonee the station is adjacent to the Moose River, which empties into James Bay only 10 miles to the northeast. The channeling effect of the river valley, although relatively shallow, and the convective phenomena associated with the nearby coastline may well be reflected in the surface wind climate. Therefore, model
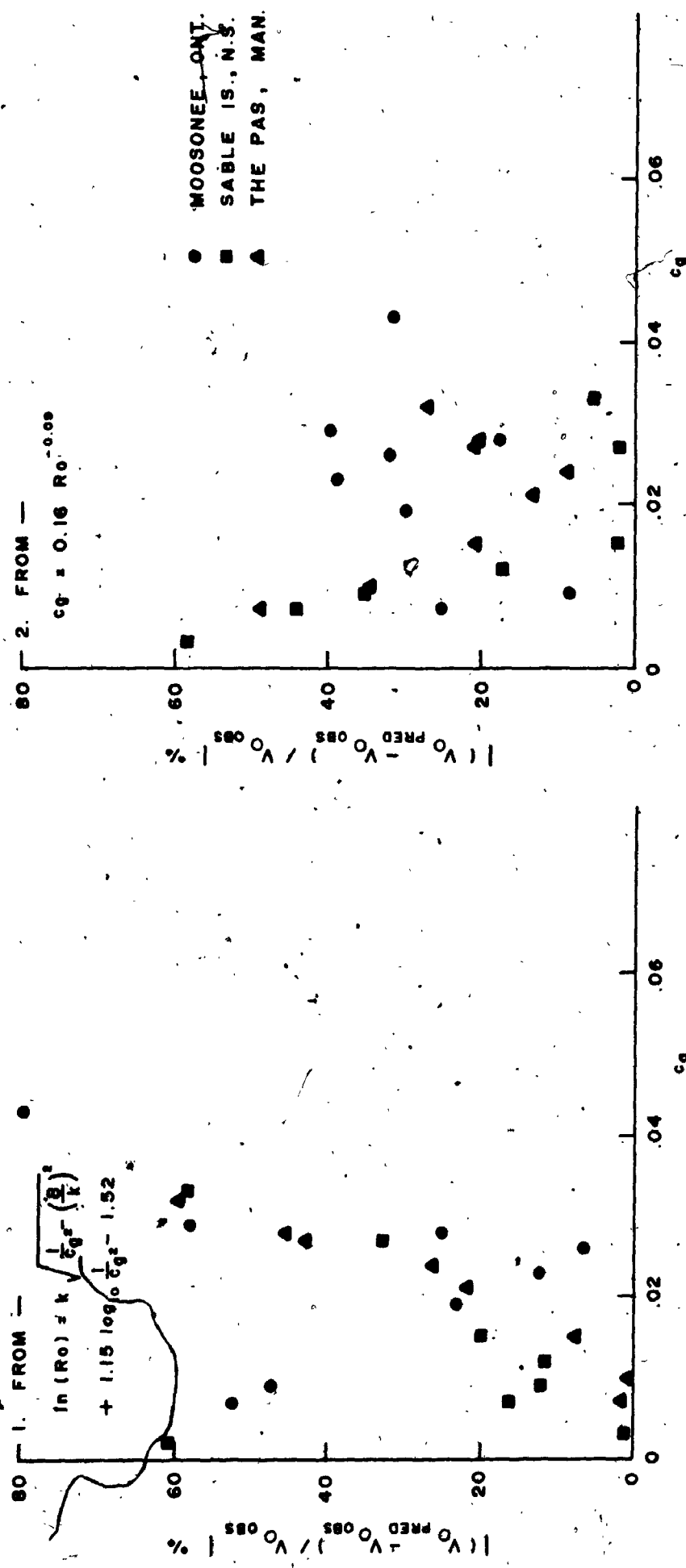
FIG 3.6   PREDICTED MEAN WIND SPEEDS AT 10M AND GEOSTROPHIC
DRAG COEFFICIENT RELATIONSHIPS

STATION	MEDIAN OBSERVED VEERING (deg)	CORRECTION			CORRECTED VEERING (deg)
		GEOSTR. VEERING	LAPSE RATE	TOTAL	
SHREVEPORT					
— summer day	6	+4	+9	+13	19
— summer night	28	+1	−10	−9	19
— winter day	18	−6	+7	+1	19
— winter night	38	−1	−18	−19	19
JOHNSTON IS.	4	+6	+2	+8	12
SHIP N	2	+8	+1	+9	11
SHIPS I and J	8	−1	+2	+1	9
SWAN IS.	22	−1	0	−1	21

TABLE 3.4 CORRECTION TABLE TO OBTAIN FRICTIONAL VEERING FOR STANDARD CONDITIONS OF ZERO GEOSTROPHIC VEERING AND 6.5°C/Km LAPSE RATE IN THE SURFACE TO 900 mb LAYER (Mendenhall (1967))

predictions for winds particularly in the north to east quadrant should be regarded with some caution; the results given in Table 3.1 would seem to bear this out.

Whilst at Sable Island the surroundings are quite uniform, consisting of low sand dunes and ocean, the station at The Pas is situated on a slight rise, roughly at the centre of a large airport clearing, with a lake to the immediate north. In the east to south quadrant the observed surface mean winds are well in excess of the values suggested by the theory. The general accelerating effect of rising terrain may be in evidence here.

3.5 A Model for Standard Deviations of Surface and Gradient Winds

Pershina (1968) has used rawinsonde data from several aerological stations in the U.S.S.R. to show that the monthly mean wind speeds and standard deviations in the atmospheric boundary layer can be related by simple expressions of the form

$$\sigma_z = b_1 \bar{V}_z + b_0 \qquad\qquad (3.29)$$

where $\bar{V}_z$ and σ_z are the mean and standard deviation at elevation z. b_1 varies with height and b_0 adopts one of two values, depending on whether the data is collected by anemometer or the rawinsonde. Above about 1 Km, b_1 is also a constant.

Now, it has been suggested that if winds blowing from within certain 45° sectors at the surface are treated separately, this is a convenient means of reflecting distinct upwind terrain conditions and wind speed distributions. Under these circumstances the vector mean of the subsample approximates to the simple mean. This is also true of the standard deviations, so it is possible to invoke Pershina's findings to postulate a similar relationship between standard vector deviations and vector means at the surface and gradient height. The separation of climatic characteristics is achieved by grouping the data according to surface wind direction, rather than month of the year as in the Russian study.

Again, data was drawn from the radiosonde records for Moosonee, Sable Island and The Pas to give the surface, 300 m and 500 m winds under neutrally stratified conditions (Appendix V). The standard vector deviations were computed and used with the observed vector means of the preceding investigation (Section 3.3) in a linear regression analysis by the method of least squares. The resulting functions, of the form of Equation 3.29, are shown in Figure 3.7. For surface observations it was found that

$$\sigma_O \sim 0.7 \, \overline{V}_O - 2.6 \qquad\qquad (3.30)$$

and, in the region of gradient height,

$$\sigma_G \sim 0.3 \, \overline{V}_G + 2.7 \qquad\qquad (3.31)$$

The value of b_O was approximately the same for both the 300 m and 500 m levels.

3.6 Probabilistic Approaches to the Surface/Gradient Wind Problem

The boundary layer descriptions discussed hitherto provide some deterministic estimates of the surface wind velocity, given certain gradient wind conditions and terrain characteristics. In this study these have been applied to some specific mean wind vectors corresponding to 45° sectors of wind direction. In addition, a strictly empirical connection has been proposed between the mean wind vector and its standard deviation at either the surface or gradient height. These two ingredients themselves provide the basis of a simplified probabilistic model of wind climate at the two levels of interest.

Within a sufficiently large azimuth interval, such as 45°, the distribution of wind vectors can often be adequately represented by a bivariate normal distribution of the circular type and centred on the vector mean (see Section 2.2). Writing the probability density function in polar coordinates

$$p(V,\theta') = \frac{1}{2\pi\sigma^2} \exp\left(\frac{-(V^2 + \overline{V}^2 - 2V\overline{V}\cos(\theta'-\phi))}{2\sigma^2}\right) \qquad (3.32)$$

1) 500M

$$\sigma_{500} = .28\,\bar{V}_{500} + 2.73$$

σ_{500} (M/S)

$\bar{V}_{500}$ (M/S)

2) 300M

$$\sigma_{300} = .18\,\bar{V}_{300} + 2.80$$

σ_{300} (M/S)

$\bar{V}_{300}$ (M/S)
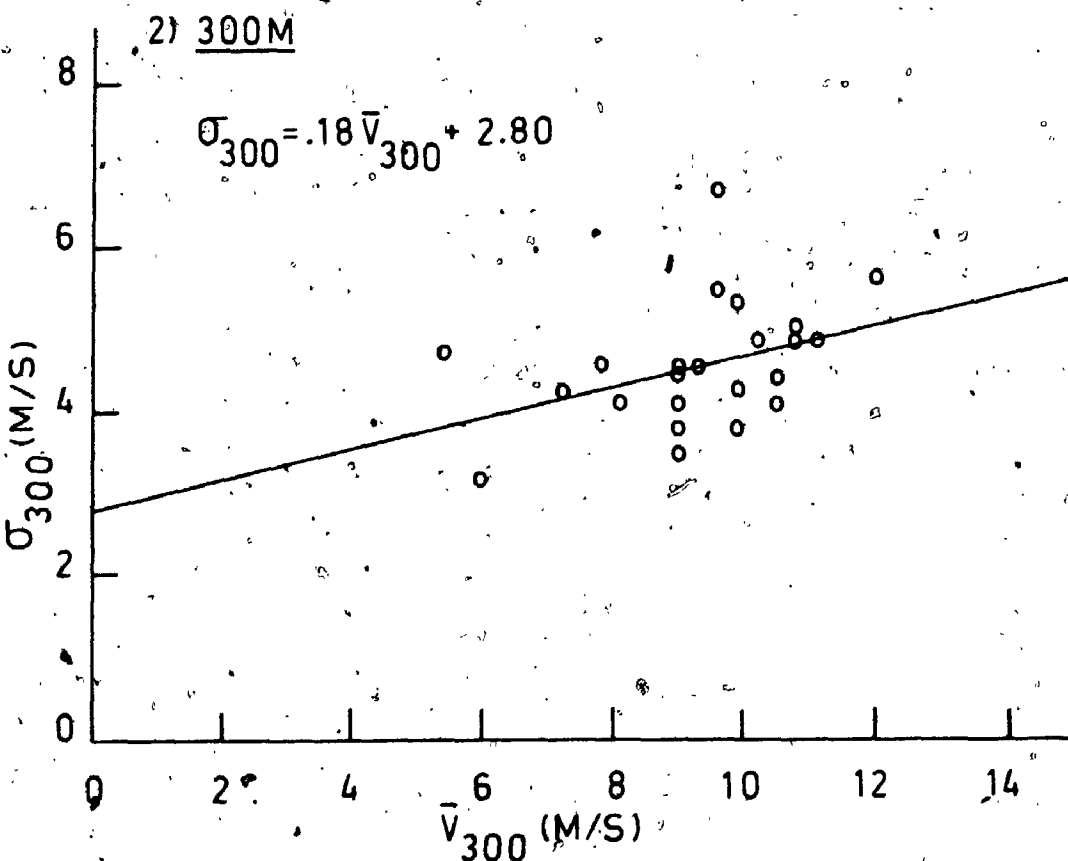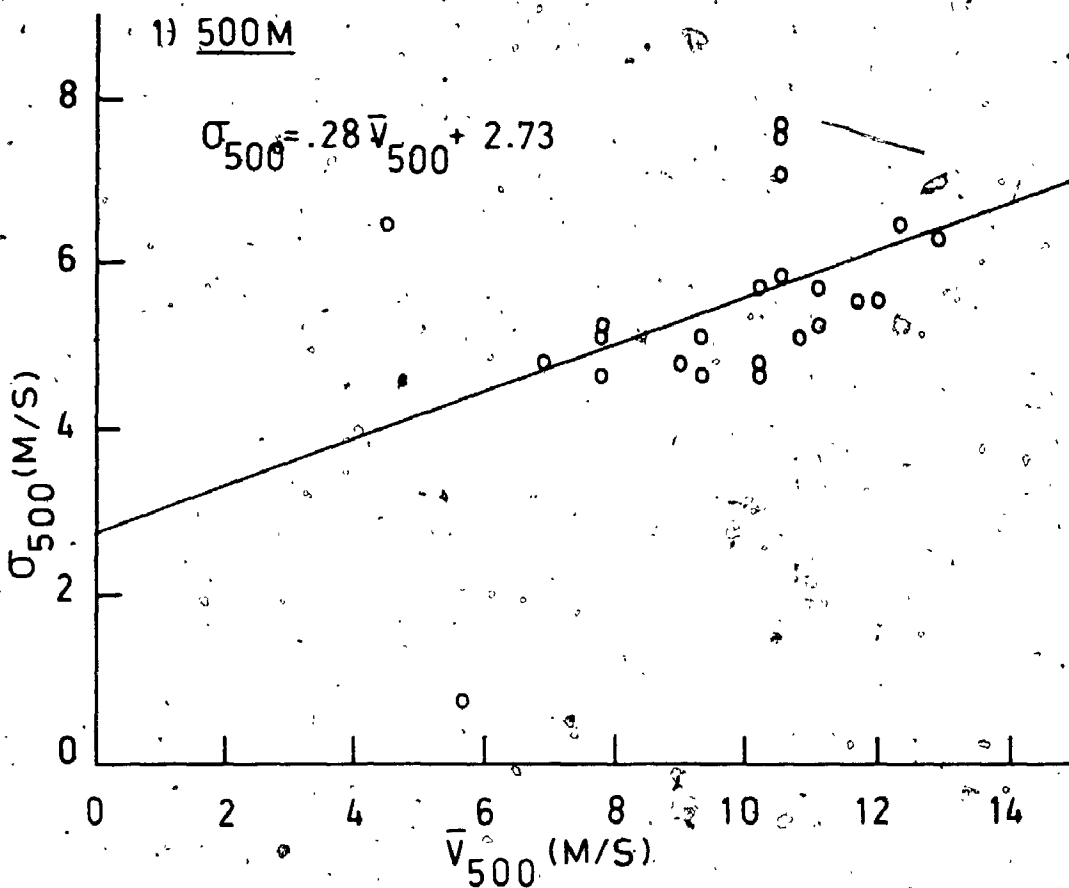
FIG 3.7 STANDARD VECTOR DEVIATION AND VECTOR MEAN RELATIONSHIPS

3) Surface

$$\sigma_0 = .73\,\bar{V}_0 - 2.57$$
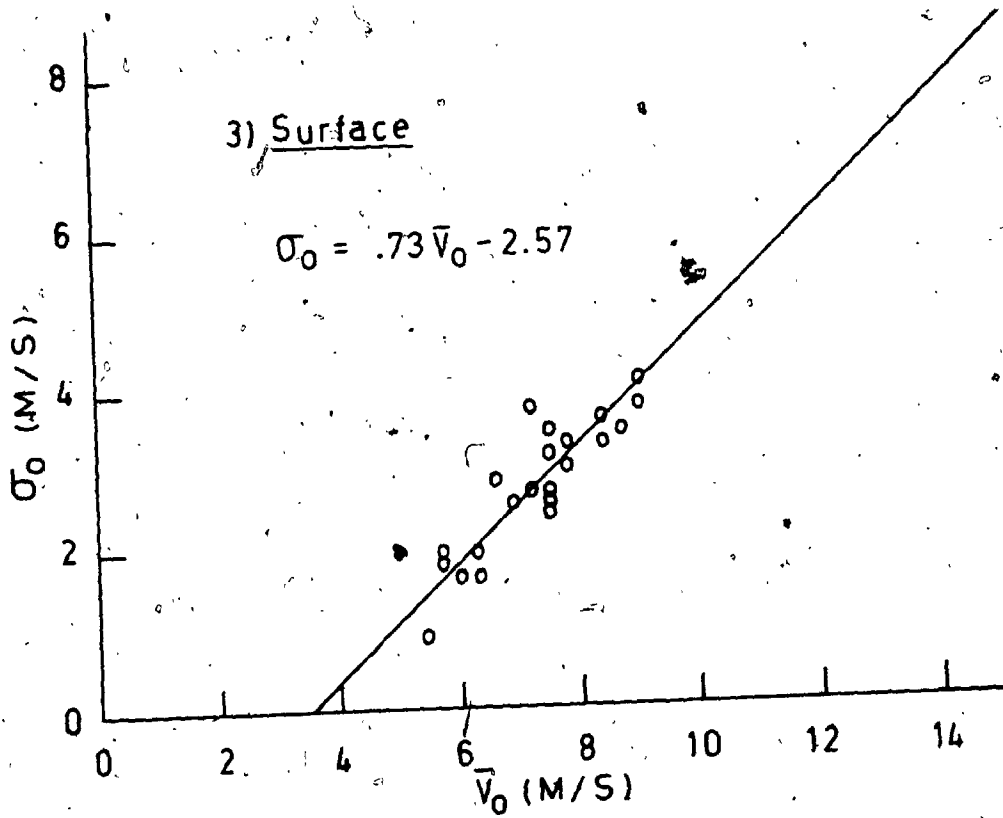
FIG. 3.7 (contd)

where $\bar{V}$ is the vector mean wind with direction ϕ and σ is the standard deviation of vectors. This is illustrated in Figure 3.8. For small angles $(\theta'-\phi)$ it follows that the frequency of wind speeds within the sector can be approximated by the normal distribution:

$$p(V) = \frac{1}{\sqrt{2\pi}\sigma} \exp(\frac{-(V - \bar{V})^2}{2\sigma^2}) \qquad (3.33)$$

Hence, for the entire azimuth range, the probability density per sector is

$$p(V,\theta) = \frac{1}{\sqrt{2\pi}\sigma(\theta)} \exp(\frac{-(V - \bar{V}(\theta))^2}{2\sigma^2(\theta)}) \qquad (3.34)$$

The necessary parameters for the surface wind distribution can then be estimated from the above-mentioned boundary layer models, of the general form

$$\bar{V}_0(\theta) = f(\bar{V}_G(\theta)); \quad \sigma_0(\theta) = g(\bar{V}_0(\theta)) \qquad (3.35)$$

These may be extended to continuous functions by a suitable harmonic series representation.

Unfortunately, near ground level the normal distribution may be inadequate to describe the local wind climate and other forms may be preferred. Two such distributions have been employed by Davenport, Hogan and Isyumov (1969) and Davenport and Jandali (1973) and are discussed in Chapter 2 (Equations 2.25 and 2.26). In the first of these the gradient wind climate over Toronto was determined from surface records in and around the city. The relationship of gradient to surface winds was given in general terms by

$$V_0(\theta) = K(\theta) V_G(\theta) \qquad (3.36)$$

so that, for any given wind direction
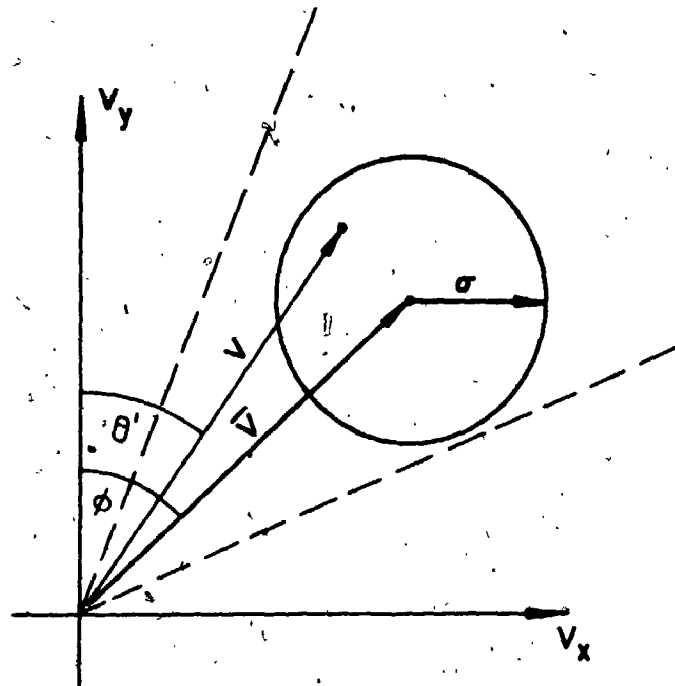
FIG 3.8 BIVARIATE NORMAL DISTRIBUTION
WITHIN WIND DIRECTION INTERVAL

$$p_O(V_O, \theta) = \frac{1}{K(\theta)} \, p_G\!\left(\frac{V_O}{K}, \theta\right) \qquad\qquad (3.37)$$

The factor K was found, in this case, from a topographic wind tunnel model.

In this and other specific studies reasonably good predictions of wind regimes have been made, but it appears from the literature that no attempt has yet been made to formulate generalized probabilistic relationships between climates aloft and at surface level. This link is required in the many practical situations where adequate meteorological records are not available. A first step in this direction is proposed below.

3.7 A Basic Statistical Model

In a broad sense, it is possible to think of the surface wind speed as dependent on the wind direction at the time, thus incorporating the influence of the upstream terrain, and the gradient wind speed. In addition, the more uncertain effects of local topography and convective activity can be included in some variable, which will be considered random. This can be written

$$V_O = \epsilon \, K(\theta_G) V_G \qquad\qquad (3.38)$$

It will also be assumed that the surface wind direction is given by

$$\theta_O = \psi + (\theta_G - a_O(\theta_G)) \qquad\qquad (3.39)$$

ϵ and ψ are random variables independent of V_G and θ_G, the wind speed and direction at gradient height. The transformation from the gradient probability distribution to the surface distribution can then be found as follows.

Now

$$p_G(V_G, \theta_G) = J \, p_O(V_O, \theta_O) \qquad\qquad (3.40)$$
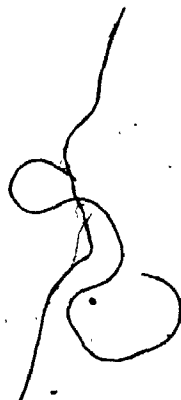
where J is the Jacobian given by

$$J = \frac{\partial(\mathcal{V}_O, \theta_O)}{\partial(V_G, \theta_G)} = \begin{vmatrix} \dfrac{\partial V_O}{\partial V_G} & \dfrac{\partial V_O}{\partial \theta_G} \\[2ex] \dfrac{\partial \theta_O}{\partial V_G} & \dfrac{\partial \theta_O}{\partial \theta_G} \end{vmatrix} \tag{3.41}$$

Therefore, writing $\dfrac{da_O}{d\theta_G}$ as a_O'

$$J = \begin{vmatrix} \epsilon K & \epsilon V_G K' \\[2ex] 0 & (1 - a_O') \end{vmatrix} = \epsilon K(1 - a_O') \tag{3.42}$$

and

$$p_O(V_O, \theta_O) = \frac{p_G(V_G, \theta_G)}{\epsilon K(1 - a_O')} \tag{3.43}$$

Given the nature of ϵ, this is not an immediately useful equation. However, from the expression for V_O in (3.38), an indication of the climate of surface winds can be gained in the form of the statistical moments. The expected value of V_O is given by

$$E(V_O) = \int V_O \, p(V_O) dV_O \tag{3.44}$$

which, assuming independence of ϵ, K and V_G, becomes

$$E(V_O) = \iiint \epsilon K V_G p(\epsilon) p(K) p(V_G) \, d\epsilon dK dV_G \tag{3.45}$$

This eventually reduces to (Appendix VII)

$$E(V_O) = \sqrt{\frac{\pi}{2}} \, \bar{K} \, \sigma_G \, m_\epsilon \, \exp(\tfrac{1}{2} \sigma_{\ln\epsilon}^2) \tag{3.46}$$

with the following conditions and definitions:

a)   The gradient wind distribution can be represented by the central, circular bivariate

normal model. The density function $p(V_G)$ is then Rayleigh. It was pointed out earlier (Section 2.4) that this is not an unreasonable simplification to apply to upper winds.

b) K is described by a harmonic series of the form

$$K = \bar{K} + \sum_{i=1}^{\infty} L_i \cos i\theta_G + \sum_{i=1}^{\infty} M_i \sin i\theta_G \qquad (3.47)$$

c) ϵ is log-normally distributed, where $\sigma_{ln\epsilon}$ is the standard deviation of $ln\epsilon$ and m_ϵ is the median value. Some support for this assumption can be found in data collected for the World Trade Center wind study by Davenport (unpublished). In this case geostrophic wind speeds were compared with mean hourlies recorded at 108 m (355 ft.) above ground level (see Fig. 3.9).

It can be similarly shown that the second moment of the distribution of V_0 is

$$E(V_0^2) = 2(\bar{K}^2 + \frac{1}{2} \sum_{i=1}^{\infty} (L_i^2 + M_i^2)) \cdot \sigma_G^2 \, m_\epsilon^2 \, exp(2\,\sigma_{ln\epsilon}^2) \qquad (3.48)$$

so that, to summarize,

$$\bar{V}_0 = \sqrt{\frac{\pi}{2}} \, \bar{K} \, \sigma_G \, m_\epsilon \, exp(\frac{1}{2}\,\sigma_{ln\epsilon}^2) \qquad (3.49)$$

and

$$\sigma_0^2 = \sigma_G^2 \, m_\epsilon^2 \, exp(\sigma_{ln\epsilon}^2) \cdot [(2\bar{K}^2 + \sum_{i=1}^{\infty} (L_i^2 + M_i^2)) \, exp(\sigma_{ln\epsilon}^2) - \frac{\pi}{2} \bar{K}^2] \qquad (3.50)$$

Since, as shall be shown, the parameters of the distribution of ϵ can be regarded as essentially universal, (3.49) and (3.50) are functions solely of the standard deviation of gradient wind vectors, σ_G, and the average ratio of surface to gradient velocities, K. The latter can be estimated from an examination of terrain roughness in conjunction with one of the deterministic profile models, such as the power law. Because σ_G is characteristic of the wind climate over a wide area, this can be found from suitable maps of upper winds. The above equations therefore appear to offer a convenient
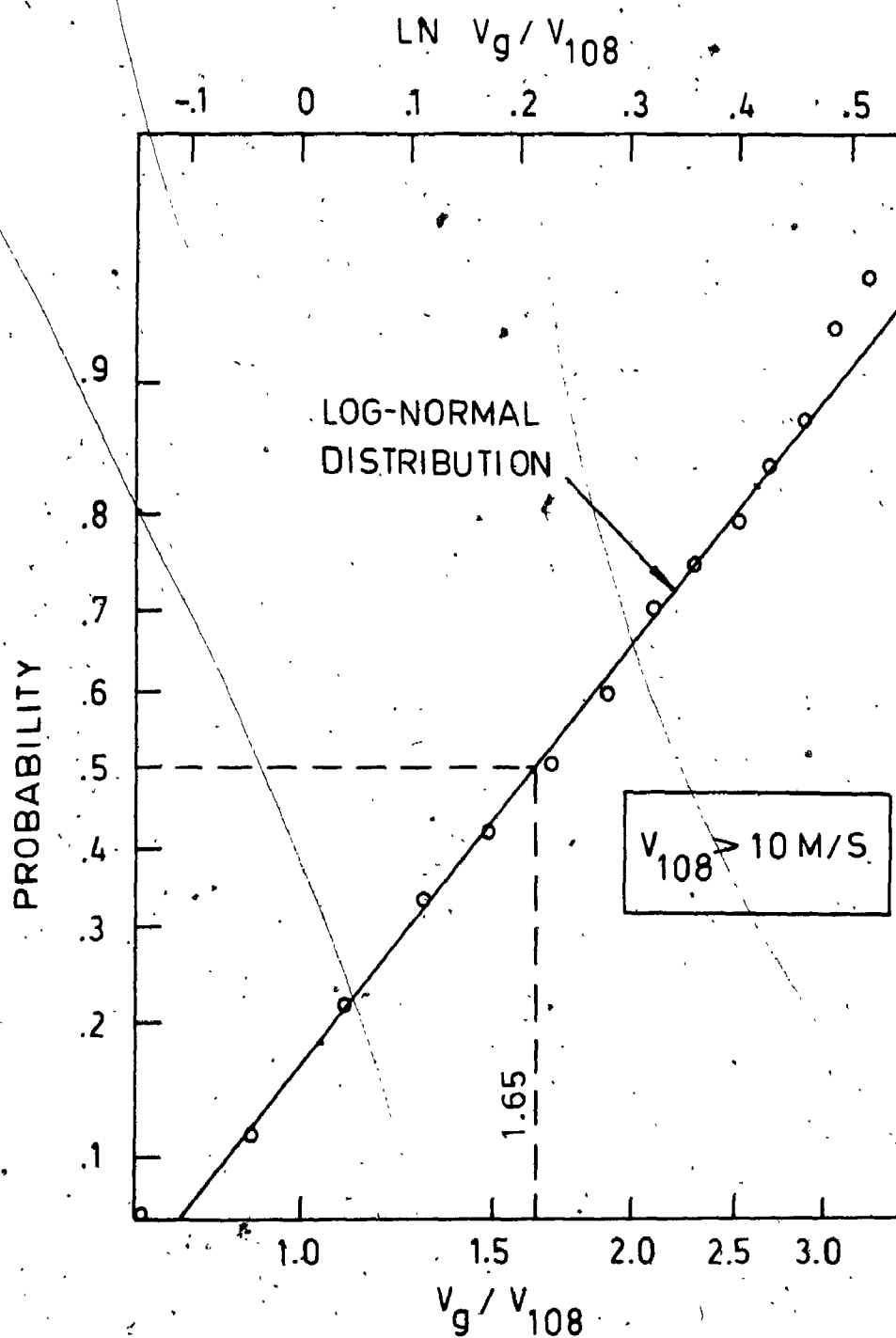
FIG 3.9 DISTRIBUTION OF RATIOS OF GEOSTROPHIC
TO HOURLY WIND SPEED AT 108M (355 FT)
AT BROOKHAVEN, N.Y. (after DAVENPORT)

means of obtaining the surface wind speed climate directly from a single and commonly quoted statistic of gradient winds. If desired, the Weibull distribution corresponding to the estimated mean and standard deviation can be found straightforwardly, and extreme value theory invoked to determine the maximum annual wind probabilities. Such a procedure will be applied in Chapter 5 in determining extreme wind speeds over the open ocean, and it will be shown how this method for estimating the annual mean wind speed can be used to assess the potential for wind energy conversion at a given site.

3.8 Parameters of the Statistical Model

The statistical parameters of the random function ϵ have been investigated using the radiosonde data for Moosonee, Sable Island and The Pas in neutrally stratified atmospheres (detailed in Appendix V).

It follows from Equation 3.38 that

$$ln\epsilon = ln\left(\frac{V_0}{V_G}\right) - lnK \tag{3.51}$$

and if ϵ follows the log-normal distribution, then it remains to fit normal probability curves to observations of the quantity $ln(V_0/V_G)$. Using the method of maximum likelihood, it is readily found that this process reduces to finding $ln\ K$ and $\sigma_{ln\epsilon}$ from n records as

$$ln\ K = \frac{1}{n}\sum_{i=1}^{n} ln\left(\frac{V_0}{V_G}\right)_i \tag{3.52}$$

and

$$\sigma_{ln\epsilon}^2 = \frac{1}{n}\sum_{i=1}^{n}\left(ln\left(\frac{V_0}{V_G}\right)_i - ln\ K\right)^2 \tag{3.53}$$

The unbiased estimate of $\sigma_{ln\epsilon}$ for small samples was obtained by putting

$$\hat{\sigma}_{ln\epsilon}^2 = \frac{n}{n-1}\sigma_{ln\epsilon} \tag{3.54}$$

It should be noted that, because the mean value of $ln\epsilon$ must be zero, $m_\epsilon = 1$.

The computations were carried out for the three locations and for prescribed intervals of gradient wind speed and direction. These were:

a) Twelve $30°$ azimuth intervals for all wind speeds.

b) Wind speed intervals of $2m/s$ for all directions.

c) Wind speed intervals of $2m/s$ for winds blowing from within specified quadrants. These were chosen such that, as far as possible, the prevailing gradient wind direction was included, variations of the parameters within the interval were relatively slight and the upstream fetch was essentially uniform. The purpose was to isolate any effects due to wind speed alone, at the same time retaining a fairly large sample.

Results of the analysis are shown in Figures 3.10 – 3.12. With the exception of Moosonee, where abnormally high deviations of the surface to gradient wind ratio seem to be associated with strong winds out of the north to east quadrant, the standard deviation $\sigma_{ln\epsilon}$ appears remarkably independent of location, upstream fetch and wind speed, usually ranging between values of 0.2 and 0.3. Certainly, in terms of predicting the surface climate from Equations 3.49 and 3.50, such a range will be of little consequence because both $\bar{V}_0$ and σ_0 vary with the term $exp(\sigma_{ln\epsilon}^2)$.

Some verification for the magnitude of $\sigma_{ln\epsilon}$ obtained here can be found in the World Trade Center wind study already mentioned, and in which the ratios of geostrophic wind speed to hourly wind speed at 108 m were analysed for 108 m winds greater than $10m/s$ (22 mph.) at Brookhaven, N.Y. The equivalent parameter was found to be 0.21. More recently, McNamara (1974) has fitted power law profiles to observations of neutral atmospheric boundary layers at Cedar Hill, Texas, estimating a standard deviation in the power law index a of about 0.058 for V_G above $13m/s$ (30 mph.). In this case, gradient height was taken as 433 m (1420 ft.). The
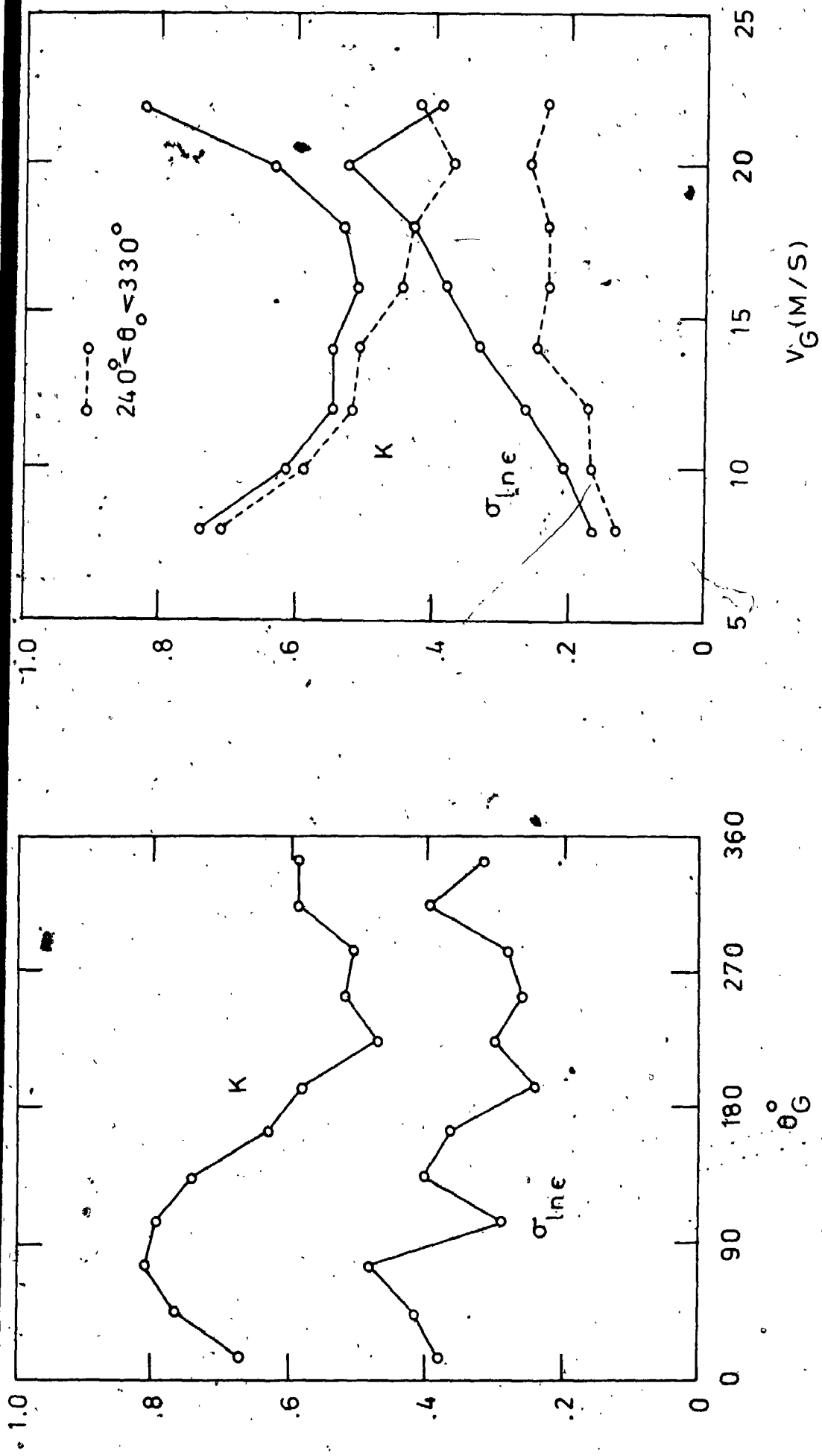
FIG. 3.10 PARAMETERS σ_{lne} AND K VERSUS GRADIENT WIND SPEED AND DIRECTION AT MOOSONEE
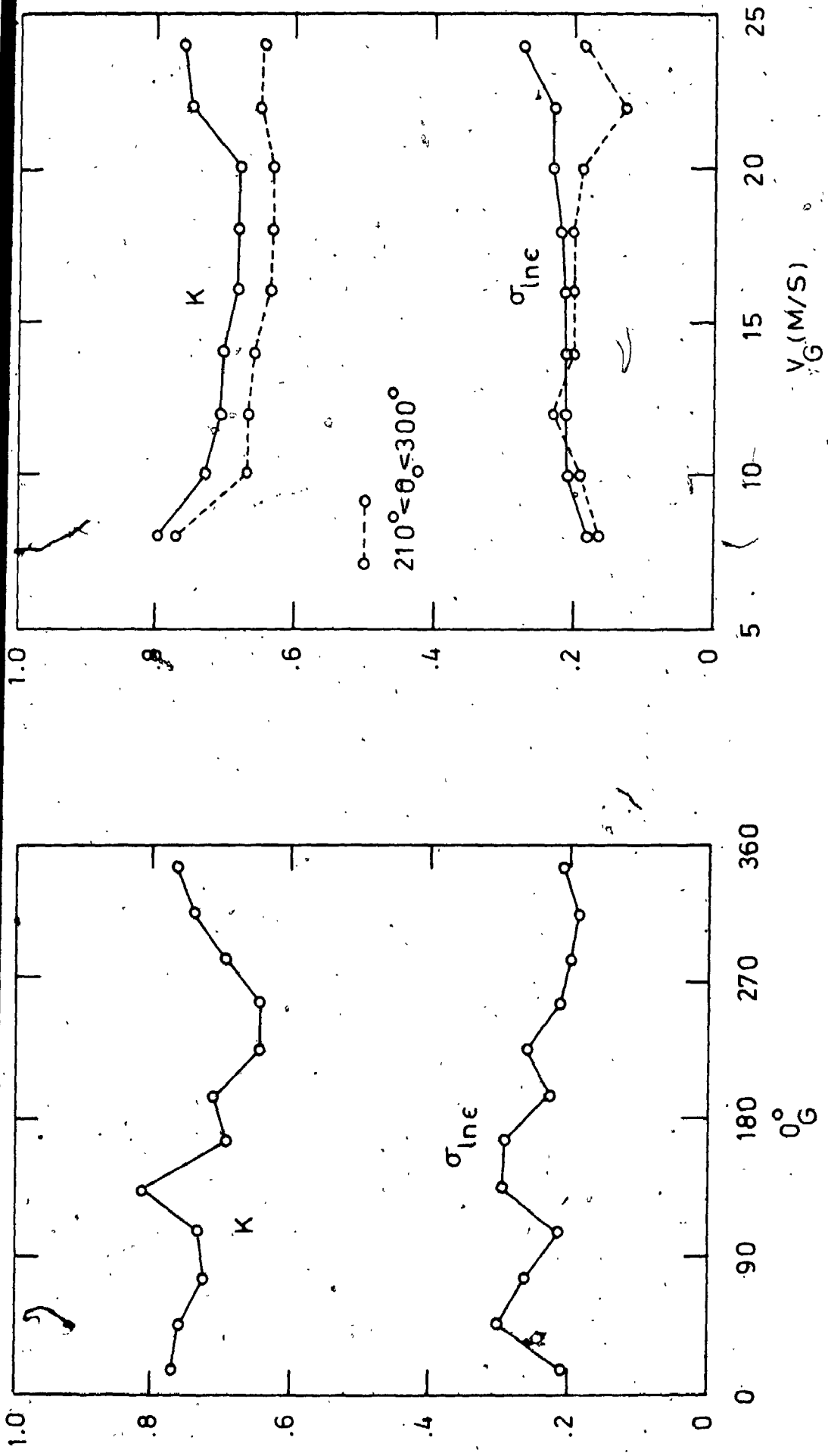
FIG. 3.11 PARAMETERS $\sigma_{ln\epsilon}$ AND K VERSUS GRADIENT WIND SPEED AND DIRECTION AT SABLE IS.
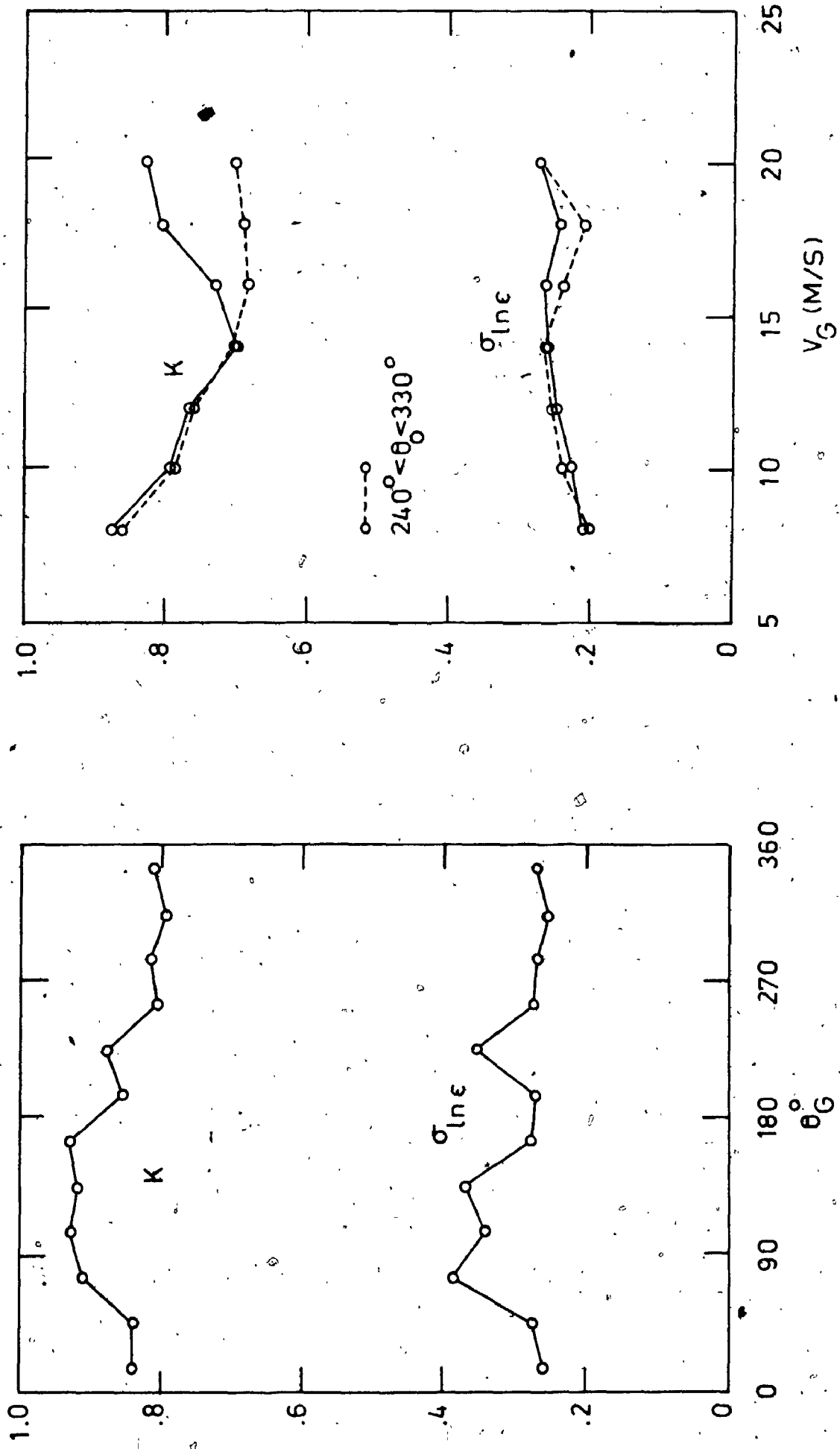
FIG. 3.12 PARAMETERS $\sigma_{ln\epsilon}$ AND K VERSUS GRADIENT WIND SPEED AND DIRECTION AT THE PAS

surface velocity at 10 m, by the power law, is given by

$$\frac{V_o}{V_G} = (\frac{10}{433})^a \qquad (3.55)$$

and

$$ln(\frac{V_o}{V_G}) = -3.77\,a \qquad (3.56)$$

Hence, the corresponding $\sigma_{ln\epsilon}$ is approximately 0.22.

An analysis of 900 mb and surface winds at two land-based and two ocean stations by Findlater et al (1966) also provides an opportunity to examine the results of the present study in the light of comparable statistics obtained elsewhere. Findlater and his associates collected radiosonde measurements at the 900 mb level at Crawley, England and Shanwell, Scotland and compared them with simultaneous surface observations at London Heathrow Airport and Leuchars respectively. The data was grouped according to time of day, season, atmospheric lapse rate, and 900 mb wind speed and direction. The ocean observations were similarly grouped and the average ratio $\bar{V}_o/V_{900}$, or K, was computed in each case. The components of this ratio along and normal to the upper wind vector were also found, together with their respective standard deviations. The components will be denoted p and q. The variance of V_o/V_{900}, or ϵ, is then given by

$$\sigma_\epsilon^2 = \sigma_p^2 + \sigma_q^2 \qquad (3.57)$$

and the transformation to find $\sigma_{ln\epsilon}$ is

$$exp(\sigma_{ln\epsilon}^2) = \frac{\sigma_\epsilon^2}{K^2} + 1 \qquad (3.58)$$

Tables 3.5 and 3.6 have been prepared in this way from the values of σ_p, σ_q and $\overline{V_o}/V_{900}$ published by Findlater et al. Estimates of $\sigma_{ln\epsilon}$ are indicated for various conditions of wind speed in roughly neutral stratifications, and for six stability classes when the 900 mb wind is 15–19 m/s (30–39 knots). The stability classes are defined in terms of specific lapse rates in Table 3.6; class 1 represents conditions of greatest instability and class 3 includes the dry adiabatic or neutral case.

Referring to Table 3.5, it is apparent that the values of $\sigma_{ln\epsilon}$ associated with the range of wind speeds considered at the three Canadian stations are predominantly between 0.2 and 0.3. It will be noted that the winds in Findlater's lowest speed category, which give rise to higher values, would have been excluded from the Canadian data. Table 3.6 shows that peak values of $\sigma_{ln\epsilon}$ generally occur in neutral or slightly stable conditions over the ocean. Over land, the same pattern is discernible but less pronounced, particularly at Leuchars.

Although only a small portion of Findlater's extensive data has been examined here, the results lend support to the findings of this investigation under the relevant conditions of neutral stability and gradient winds from about 10 to 25 m/s. Additional evidence is provided about the behaviour of the parameter $\sigma_{ln\epsilon}$ in stable and unstable atmospheric boundary layers.

In the course of computing $\sigma_{ln\epsilon}$, the mean ratios of V_o to V_G were obtained, and these are also plotted in Figures 3.10 – 3.12. Values of K are higher than would be expected at Moosonee and the Pas, in the bush country of the Canadian Shield; when considering only the selected quadrants of gradient wind azimuth (for example, $240^\circ - 330^\circ$ at Moosonee) these are closer to the predictions of the power law wind profile for this kind of terrain $(K \approx 0.4)$. Where the effects of wind speed have been isolated, the expected decrease in K with increasing V_G is in fact observed.

STATION	900 mb WIND SPEED					ALL SPEEDS
	10–19 kt 5– 9m/s	20–29 kt 10–14m/s	30–39 kt 15–19m/s	40–49 kt 20–24m/s	>50 kt >25m/s	
Ocean Stn. I	0.36	0.25	0.24	0.22	0.17	0.30
Ocean Stn. J	0.40	0.27	0.22	0.21	0.21	0.32
Heathrow (day-time)	0.47	0.30	0.25	0.18	0.14	0.38
Leuchars (day-time)	0.62	0.45	0.29	0.31	0.21	0.51

TABLE 3.5   VALUES OF $\sigma_{\ln\epsilon}$ FROM DATA OF FINDLATER ET AL (1966), LAPSE CLASS 3 ONLY (NEUTRAL STABILITY)

STATIONS	LAPSE CLASS						ALL CLASSES
	1 >5.5 °F/1000ft >10 °C/Km	2 4.0–5.4 7.3–9.9	3 2.5–3.9 4.5–7.2	4 1.0–2.4 1.8–4.4	5 –0.5–0.9 –0.9–1.7	6 <–0.6 <–1.0	
Ocean Stn. I	0.16	0.18	0.24	0.20	0.20	0.12	0.20
Ocean Stn. J	0.18	0.20	0.22	0.24	0.21	0.14	0.22
Heathrow (day-time)	0.12	0.22	0.25	0.27	0.23	0.34	0.27
Leuchars (day-time)	0.23	0.29	0.29	0.41	0.30	0.66	0.32

TABLE 3.6   VALUES OF $\sigma_{\ln\epsilon}$ FROM DATA OF FINDLATER ET AL (1966), 900 MB WIND SPEEDS 15–19 M/S ONLY

3.9 Applying the Statistical Model

The principal obstacle in extending and applying the general relationship between the surface and gradient probability distributions (Equation 3.43) is the uncertainty surrounding the nature of the function ψ and the average veering of the wind between the two levels.

Summarizing the evidence of the Canadian data used in the preceding investigation, the coefficient of variation of the veering was large, generally around 3.0, and there was no apparent consistency in the standard deviation and hence the distribution of ψ. The mean values fluctuated wildly at the land-based stations and were between 0° and 5° at Sable Island for most exposures and wind speeds. Other observational data in the literature is sparse, particularly as regards ψ and the dependence of a_o on terrain roughness. However, Findlater et al (1966) and Mendenhall (1967) both suggest a_o is about 20° for locations in relatively smooth terrain and 10° over the ocean. This applies to neutral, barotropic atmospheres.

The deterministic approach to wind spiralling in the boundary layer has already been discussed and, as a result of the theory developed by Csanady (1967) and others, it was proposed that

$$sin\ a_O\ =\ -\frac{B}{k}c_g \tag{3.59}$$

Since c_g is some function of the Rossby number V_G/fz_0, the average wind veering can be estimated from this expression, given the upstream terrain roughness and an average gradient wind condition. This would appear to offer the best approach to a problem involving the generalized probability model.

Turning to the application of the specific model for surface winds in Equations 3.49 and 3.50, this relies ultimately on the choice of the Fourier coefficients $\overline{K}$, L_i and M_i. It has been seen that $\sigma_{ln\epsilon}$ usually takes values between 0.2 and 0.3, so that

with $m_\epsilon = 1$ and $\sigma_{ln\epsilon} = 0.25$,

$$\bar{V}_O = 1.29 \, \bar{K} \, \sigma_G \qquad\qquad (3.60)$$

and

$$\sigma_O^2 = 1.06 \, \sigma_G^2 (0.55 \, \bar{K}^2 + 1.06 \sum_{i=1}^{\infty} (L_i^2 + M_i^2)) \qquad (3.61)$$

In most cases L_i and M_i will be small compared with $\bar{K}$, and

$$\sigma_O = 0.76 \, \bar{K} \, \sigma_G (1 + \frac{0.96 \sum_{i=1}^{\infty} (L_i^2 + M_i^2)}{\bar{K}^2}) \qquad (3.62)$$

Furthermore, if the terrain is reasonably uniform around the site in question

$$\sigma_O = 0.76 \, \bar{K} \, \sigma_G = 0.59 \, \bar{V}_O \qquad\qquad (3.63)$$

Figure 3.13 shows the dependency of K on terrain type and the corresponding surface roughness length. This is based on the power-law profile, using the parameters suggested by Davenport (1963) and given in Figure 3.2. The above equations can now be applied, for example, to the wind climate at the three Canadian stations previously considered.

Detailed descriptions of the stations' surroundings have been compiled in Appendix IV. On the basis of the available information, the terrain at Moosonee can be regarded as quite uniform, even considering the proximity of the Moose River to the east of the site. At Sable Island the exposure is almost entirely across the open ocean. Therefore, suitable choices of $\bar{K}$ would be 0.4 and 0.7 respectively, with $L_i = M_i = 0$. The presence of a sizeable lake to the north of the station at The Pas suggests that a significant Fourier coefficient should be included; here $\bar{K}$ is taken as 0.5 with L_1 or M_1 equal to 0.2. Estimates were made of the overall annual climates of surface wind speeds using the standard vector deviations of gradient (500 m) winds computed from radiosonde data by the writer (Baynes, 1971). The
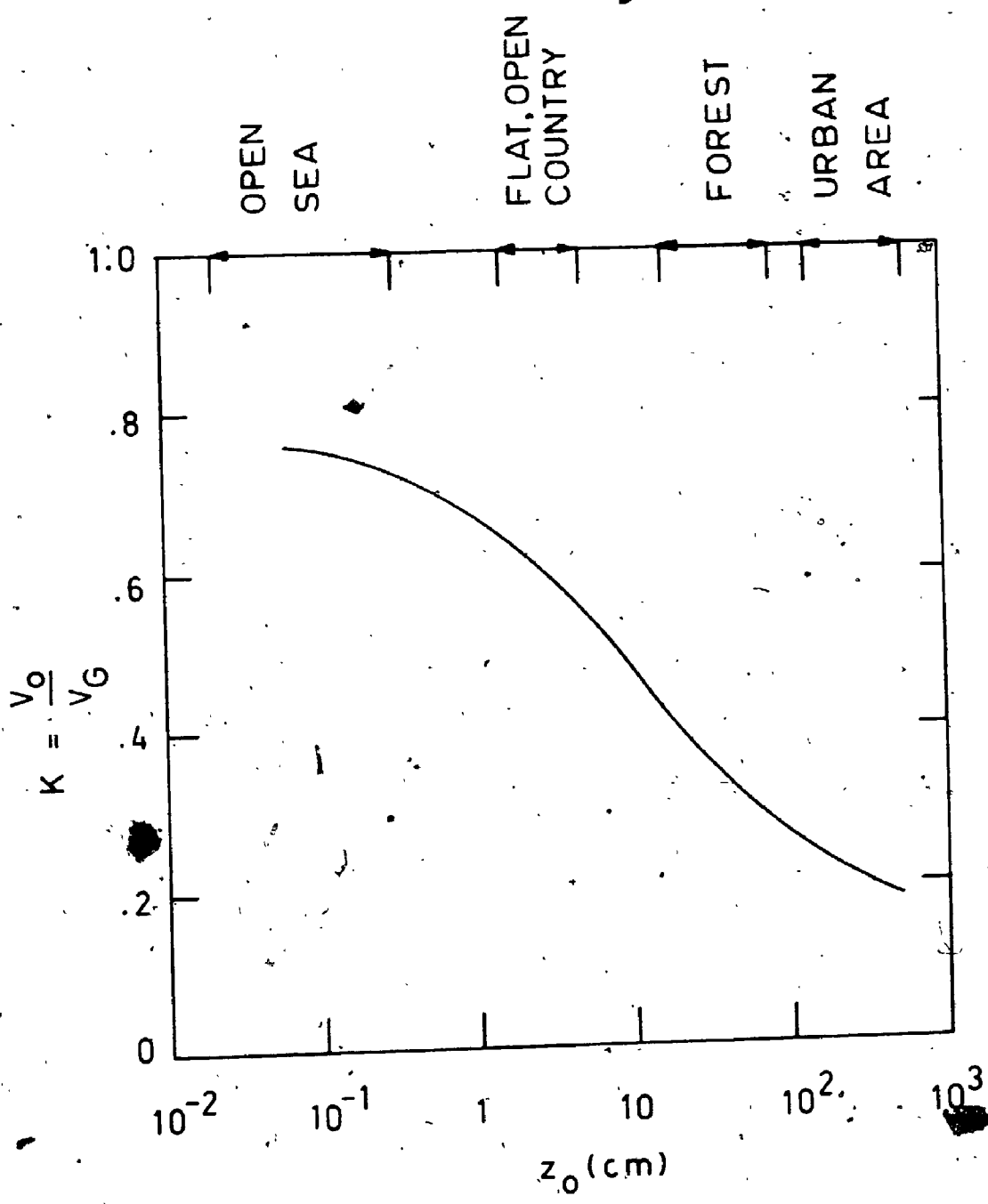
FIG 3.13 PARAMETER K FOR VARIOUS TERRAINS

resulting statistics are given in Table 3.7 alongside the observed values.

For these examples, the statistical model for surface wind climate is remarkably good, if somewhat conservative; the idealizations adopted in the theoretical development would not be closely followed by the annual climate. However, strong topographic effects are still likely to upset the predictions and these must be accounted for in individual cases. It must also be emphasised that the parameter $\sigma_{ln\epsilon}$, which has been considered a universal constant, obtains only when upper winds have been measured by a radiosonde system. It is expected that a portion of the variation in the ratios of surface to gradient winds is derived from the response characteristics of the instrument. This point is investigated in Chapter 4.

3.10 Conclusions

This chapter has been concerned with the problem of estimating the climate of mean surface winds from a knowledge of the conditions prevailing at or near gradient height. This can be approached either deterministically, in which certain boundary layer profiles or spirals are applied to typical climatic situations, or statistically, in which a probabilistic relationship is employed encompassing all or a selected sub-sample of events. Both of these have been discussed, mainly in the context of neutral, barotropic atmospheres, as follows:

a) The traditional methods available through the log law and power law profiles were reviewed, including typical profile parameters for various terrains and the use of a zero-plane displacement in particularly built-up areas.

b) A recent deterministic model was considered relating Rossby number and the wind veering angle to the surface drag coefficient. Using selected rawinsonde observations at three Canadian locations, the mean surface wind vectors within prescribed direction intervals were estimated from the corresponding vectors at 500 m above ground level. In some circumstances, especially where terrain conditions were ideal, the model predicted winds close to the observed values. The agreement

	PREDICTED		OBSERVED		$\dfrac{PREDICTED}{OBSERVED}$	
	V_O (m/s)	σ_O (m/s)	V_O (m/s)	σ_O (m/s)	V_O	σ_O
Moosonee ($\overline{K} = .4$, $\sigma_G = 9.29$ m/s)	4.79	2.82	4.14	2.37	1.16	1.19
Sable Island ($\overline{K} = .7$, $\sigma_G = 11.16$ m/s)	10.07	5.94	6.93	3.54	1.45	1.68
The Pas ($\overline{K} = .5$, $L_i = .2$ $\sigma_G = 8.35$ m/s)	5.39	3.66	5.31	3.01	1.02	1.22

TABLE 3.7 PREDICTED AND OBSERVED MEANS AND STANDARD
DEVIATIONS OF SURFACE WINDS AT THREE CANADIAN LOCATIONS

was generally closer for a certain range of geostrophic drag coefficients.

c) An empirical relationship between the means and standard deviations of both the surface and gradient winds was investigated, again using Canadian upper air data. The resulting simple expressions can be applied in conjunction with the deterministic predictions of mean velocities.

d) Existing probabilistic approaches were discussed. A more general form was proposed which incorporated random functions to describe deviations from the average surface/gradient wind ratios and angles of veering. The function parameter $\sigma_{ln\epsilon}$ can be regarded as a universal constant.

e) From this were derived the distribution moments of surface wind speeds as functions solely of the terrain roughness and the standard vector deviation of gradient winds. In the absence of strong local winds, these are considered particularly useful indicators of surface wind climate.

CHAPTER 4.

ESTABLISHING THE CLIMATE OF MEAN WINDS

4.1   Some Common Difficulties

To establish an appropriate statistical description of the mean wind climate at a specific site is often a complex problem involving sparse data of diverse origins; seldom are suitable direct measurements available. Ideally, the recording anemometer should be situated away from the isolated flow regimes around individual obstacles, and sufficiently close to the chosen site to detect the unique contributions of local terrain and topography. Some good examples of the variation of surface wind climate over quite short distances have been given by Davenport (1968). From an original study by Graham and Hudson it was shown that the mean hourly winds transverse to the deck of a suspension bridge in Chesapeake Bay were 1.6 times the readings taken at Baltimore Friendship Airport in "more or less uniform rolling terrain", some 32 km (20 miles) to the northwest. The geography of the area is shown in Figure 4.1.

There is also a general discrepency between winds in cities and at nearby airports, due to a marked change of terrain roughness. This is well illustrated by the 50-year return winds quoted by Davenport for several locations in the United States (see Table 4.1). It will be noted that, although the anemometer in each city centre is at a higher elevation than its counterpart at the airport, the wind speed in the urban surroundings is always significantly lower.

The effects of terrain roughness on the vertical wind profile, and thus on the measurements, say, at the standard surface anemometer height of 10 m, have been
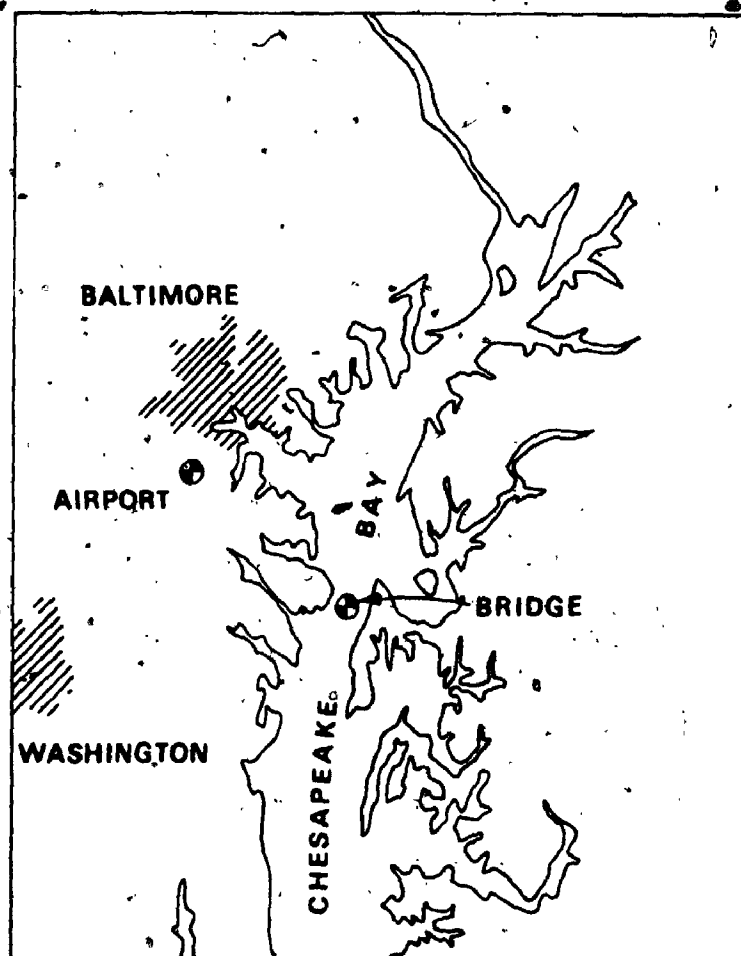
FIG 4.1   LOCATIONS, OF CHESAPEAKE
           BAY BRIDGE AND BALTIMORE
           FRIENDSHIP AIRPORT

CITY	CITY OFFICE		AIRPORT	
	Anem. Ht. (ft)	Wind Speed (mph)	Anem. Ht. (ft)	Wind Speed (mph)
Boston	188	72	63	103
New Haven	155	60	42	74
Chicago	—	57	38	70
S.S. Marie	52	63	33	85
Kansas City	181	63	76	95
Omaha	121	65	68	91
Knoxville	111	57	71	89
Nashville	191	73	42	86
Spokane	110	51	29	78

TABLE 4.1 50-YEAR RETURN WIND SPEEDS AT SOME U.S.
CITIES (after DAVENPORT, 1968)

examined in Chapter 3. The topographic effects will not be discussed in detail here, but can be briefly identified. These include accelerated flow on the windward faces and tops of hills, and the funnelling of winds along valleys. Local winds of a convective nature must also be considered in the overall wind climate, particularly near ground level. For example, sea breezes extend inland some 16 to 40 km (20 to 30 miles) and may reach 4 to 5 m/s. In hilly or mountainous regions differential heating and cooling give rise to valley and slope winds on a diurnal cycle, but perhaps of more importance to the climate of strong winds are the so-called compensating winds which blow between extensive mountain ranges and level country. These are again diurnal and convective in character and can produce strong nocturnal down-slope flows, especially if channelled through a valley or pass and perhaps accentuated by glacier cooling. On a larger scale, drainage of cool air from a mountain region can occur along the valleys towards a relatively warm body of water. Celebrated examples of this are the Mistral of the Rhone valley in France and the winds of the Santa Ana canyon of southern California. More detailed accounts of these and other related phenomena can be found in Humphreys (1964) and Geiger (1965).

In a typical situation the available data may consist of surface wind records at the closest meteorological stations (these will often pertain to various periods of years, elevations and averaging times), radiosonde data collected at the nearest upper air station, and perhaps a limited number of readings taken at or very near the site in question. This information must be statistically analysed and reconciled, bearing in mind the possible local influences suggested above, in order to synthesize a satisfactory description of wind climate. Many of the specific aspects of this process have been covered in previous chapters, but the overall approach will be reviewed in the following section.

4.2 Approaches to a Synthesized Description of Wind Climate

A number of meteorological studies, particularly relating to urban environments, have been undertaken by Davenport and associates in the course of assessing wind loads

on proposed tall buildings (for example, Davenport et al, 1969, 1971, 1972, 1973). These have generally followed certain logical steps from the available wind data to a synthesized wind climate description for the required site and elevation. A flow chart representing this process has been constructed (Figure 4.2), showing the individual steps and the roles of the three groups of input information, the meteorological data, horizontal and vertical velocity relationships, and design considerations specific to the study. Typical input items, which may or may not be considered in a given case, are suggested in the flow chart. Up to four distinct stages in the process can usually be identified as follows:

a) Statistical analysis of each set of wind data. This can be done on a monthly, seasonal or annual basis. Upper level data, representing the gradient wind climate, may be analysed according to a bivariate normal model or, as with surface winds, the frequency distributions may be fitted to a more flexible form, such as those given in Section 2.5 of this thesis. Distributions of wind speed regardless of direction and extreme value statistics may also be found by methods consistent with the available data.

b) Standardization, if necessary, of surface wind statistics relating to different averaging times, for example, mean hourlies and 2-second gusts (see Chapter 2).

c) Transformation of the various distributions and statistics to apply at the required site and elevation. This involves the observed or assumed spatial wind relationships, including velocity profiles appropriate to the terrain and probabilistic models linking surface and gradient wind climate (see Chapter 3). In the absence of direct experimental evidence, the horizontal variations near ground level can be treated by using the gradient climate as a reference common to the entire area.

d) Synthesis, involving an assessment of the suitability of the transformed distributions; such factors as the reliability of the original data and significant topographic effects may be considered. A particular distribution may be preferred or weighted averages of certain relevant statistics may be obtained. For example, in an investigation

METEOROLOGICAL DATA
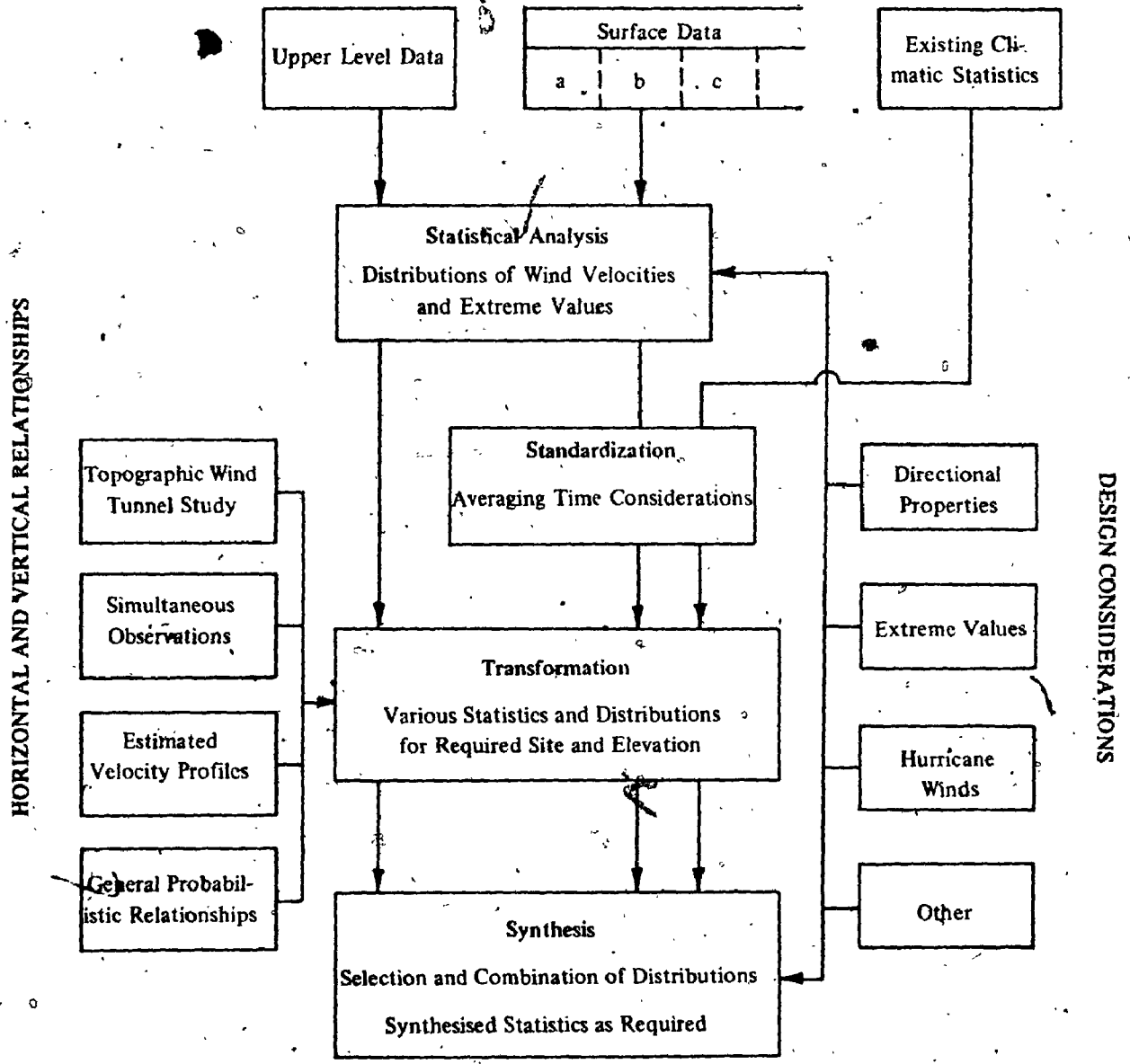
FIG. 4.2 FLOW CHART FOR ESTABLISHING THE CLIMATE OF MEAN WINDS AT A SPECIFIC LOCATION

of winds over Chicago, Davenport et al (1971) estimated from a number of data sources the wind vectors exceeded with a probability of 10^{-6}. The bivariate distribution for Midway Airport was then adjusted so that the 10^{-6} quantiles matched the averaged values.

4.3 Upper Wind Climate

It has been suggested that the statistics of upper winds, conveniently at gradient height, can be used as a common reference at various points in an area of study. Because the gradient winds are usually independent of terrain and topography, being just above the frictional influence of the earth and most convective circulations, the climatic parameters can be applied across broad geographic areas. Furthermore, they are generally amenable to analysis based on the circular bivariate normal distribution, defined simply by the vector mean, $\bar{V}_r$, and standard vector deviation, σ. As noted in Chapter 2, this is especially true where only one distinct flow regime predominates in the overall wind climate. The analysis is therefore best performed on a monthly or seasonal basis. Crutcher and Halligan (1967) indicate that the less convenient elliptical distributions are likely to be found where different regimes occur together, such as in regions affected by both westerlies and easterly trades, over mountain ranges and above coastlines.

The parameters $\bar{V}_r$ and σ have been mapped for most parts of the world and at the higher altitudes, utilizing data collected by rawinsonde or pilot balloon (Brooks et al, 1950, Henry, 1957 and Crutcher and Halligan, 1967). Recently an attempt has been made to map the gradient winds over Canada and neighbouring regions of the United States, based on 10 years of rawinsonde observations at 300 m and 500 m above ground level (Baynes, 1971). Contours of $\bar{V}_r$ and σ at 500 m are reproduced in Figures 4.3 and 4.4 for four months of the year, showing the pattern of seasonal changes. It can be seen that relatively strong mean circulations, that is high vector means, prevail along the eastern seaboard and, in the winter and autumn, to the west of the Great Lakes. Such information can be a useful first indicator of the wind environment for a proposed engineering project or activity.
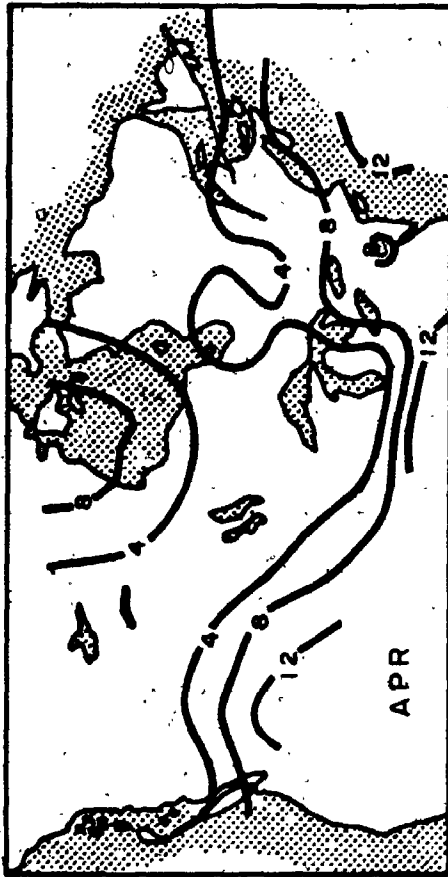
FIG. 4.3   SMOOTHED VECTOR MEAN WINDS AT 500 M (CONTOURS IN MPH;
1 MPH = 0.447 M/S) (FROM BAYNES, 1971)
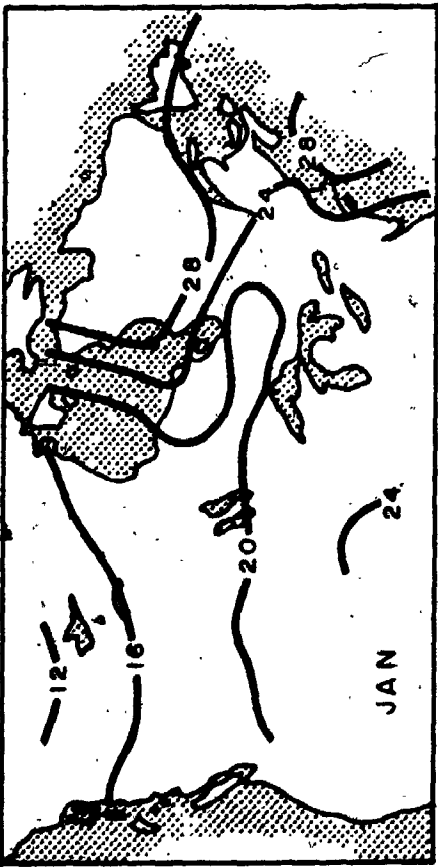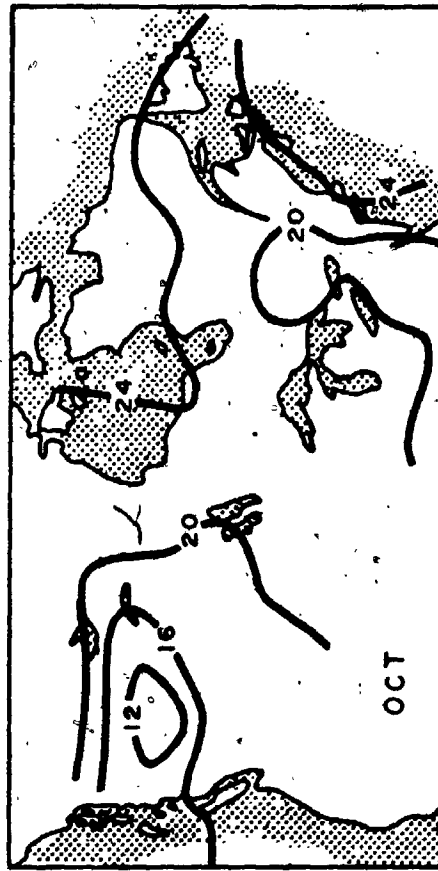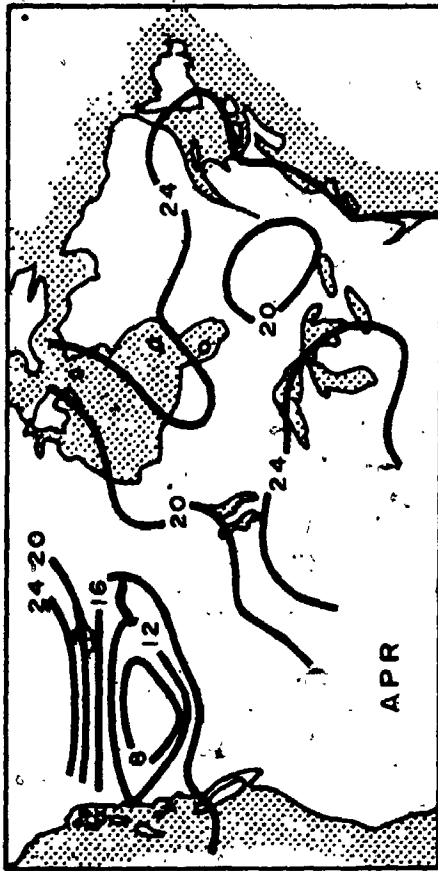
FIG. 4.4 SMOOTHED STANDARD VECTOR DEVIATIONS OF WINDS AT 500 M
(CONTOURS IN MPH; 1 MPH = 0.447 M/S) (FROM BAYNES, 1971)

The use of upper wind data, especially at the lower levels, should be tempered by a realization of the limitations of the radiosonde and the data handling system. The ascending radiosonde, or more specifically the sensor suspended below the balloon, is tracked by radar and its position is normally recorded every minute. The horizontal component of the vector differences between alternate fixes determines the mean wind velocity associated with the interjacent position. In this way, the velocities are essentially overlapping two-minute means. Elevations can be determined from the pressure recorder in the radiosonde and the hydrostatic equation.

The Canadian rawinsonde system now uses the concept of "significant wind levels", by which wind data is selected so that "the plotted wind speed profile can be reproduced to within 10 knots (5.14 m/s) of linearity at all levels, and the wind direction profile to within 30 degrees of linearity when wind speeds are 10 knots or less" (Titus, 1970). The winds at the standard isobaric surfaces (1000, 950, 900, 850, 800 mb, etc.) are then computed by linear interpolation of the zonal and meridional wind components at adjacent "significant wind" levels. Conditions at the required elevations above ground level can, in turn, be found from these by a similar process of interpolation.

An important feature of rawinsonde observations is the frequency of balloon releases, normally twice daily at 00 and 12 hours GMT. Thus, only atmospheric processes with frequency components below one cycle per day will be detectable, that is, well into the mesometeorological range (see Figure 1.6). The infrequency of these observations implies that the sampling of short duration local storms such as thunderstorms may be inadequate. Because of the regularity of the observations, the data may also be slightly biased by the diurnal cycle whereby winds at gradient height are generally reduced in the daytime, particularly in unstable atmospheres (Riehl, 1965).

The aspect of rawinsonde accuracy to be investigated in some detail below is the contribution of errors due to instrument characteristics and data reduction procedures to the total variance of wind velocities at gradient height. Corrections to the climatic statistics obtained from rawinsonde data can then be estimated and the impact on the variance of the surface/gradient wind speed ratio can be assessed.

4.4 An Analysis of Rawinsonde Errors

It is possible to distinguish three classes of error in measuring upper level winds. Firstly, lack of precision in the tracking techniques implies a discrepancy between the observed and actual positions of the sensor. Secondly, the behaviour of the balloon and sensor may be such as to produce extraneous motions which are of a time scale outside the range of interest, that is, outside the mesometeorological range. At lower elevations, the effects of atmospheric turbulence will be felt. Finally, the process of averaging the motion of the sensor over a given time period to obtain the mean velocity must be considered.

It has been suggested (Morrissey and Muller, 1968) that these various factors can be represented in the form of power spectra, combined to give the spectrum of recorded wind velocity errors, as follows:

$$S_s'(n) = R_a^2(n) (R_s^2(n) . S_i(n) + S_f(n)) + S_o(n) \qquad (4.1)$$

in which R_a^2 is an admittance function due to averaging the observed winds,

$\qquad\quad R_s^2$ is the response of the sensor to fluctuations in the wind field,

$\qquad\quad S_i$ is the spectrum of self-induced motions,

$\qquad\quad S_o$ is the spectrum of observational errors due to the tracking system,

and $\qquad S_f$ is the spectrum of wind fluctuations, particularly atmospheric turbulence.

When the observations are digitized the record is aliased such that the final spectrum becomes

$$S_s(n) = S_s'(n) + \sum_{q=1}^{\infty} S_s'(n + 2qn_N) + \sum_{q=1}^{\infty} S_s'(n - 2qn_N) \qquad (4.2)$$

where n_N is the folding or Nyquist frequency. A schematic diagram of the components of S_s is shown in Figure 4.5. Fortunately, most of these terms have been studied and it is possible to estimate S_s, and hence the error variance, for rawinsonde flights under representative atmospheric conditions.
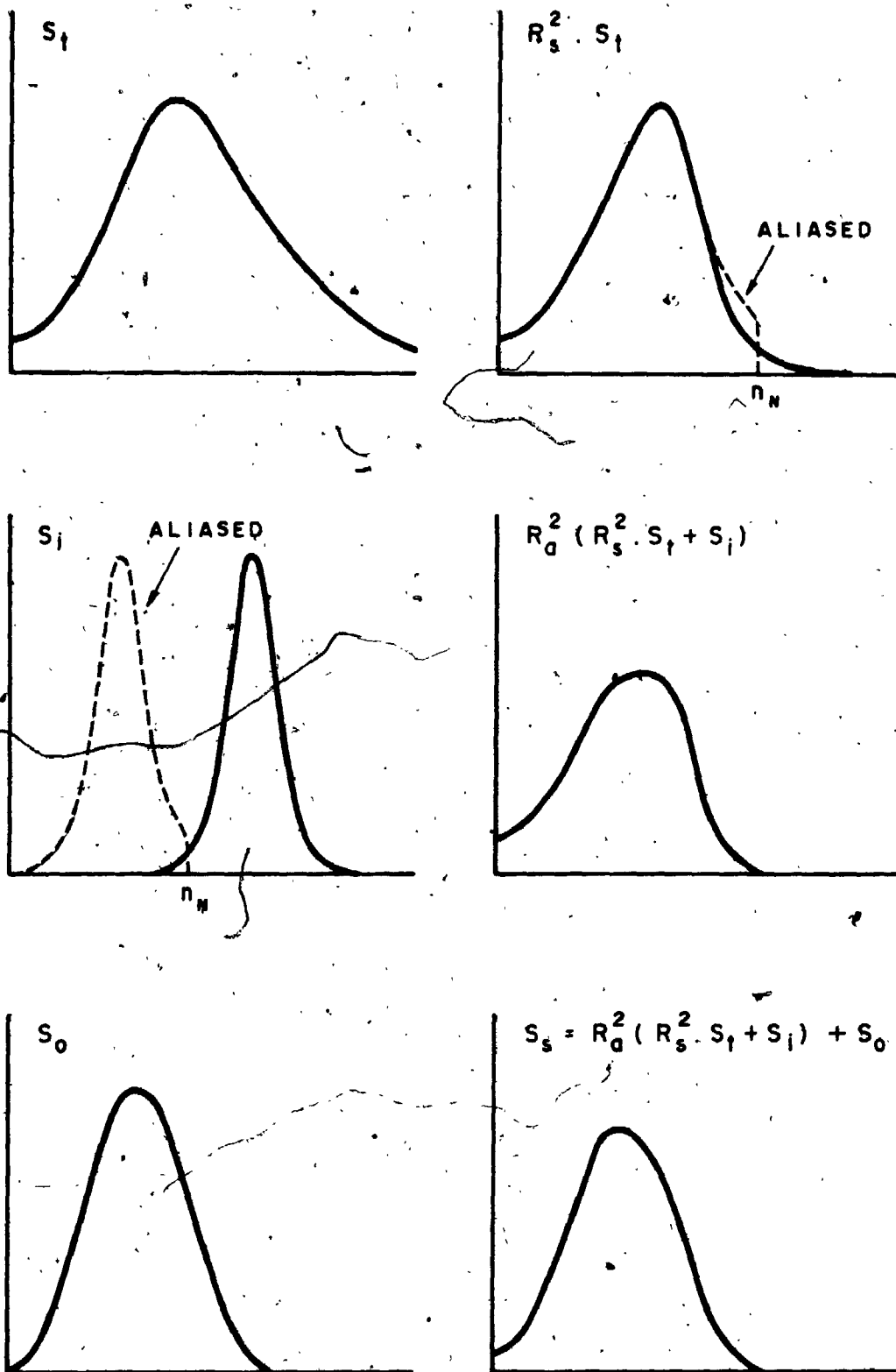
FIG. 4.5 SCHEMATIC OF THE COMPONENT POWER SPECTRA
OF RAWINSONDE VELOCITY ERRORS

The response of the sensor to the wind field can be derived from the basic equations of motion by representing the various components of the wind velocity and the sensor motion as sums of mean and small perturbation quantities. Such a theory has been proposed recently by Fichtl (1971) and is further described in Appendix VIII. It can be shown that the function $R_s^2(n)$ can be written

$$R_s^2(n) = \frac{1 + (2\pi Tan)^2}{1 + (2\pi Tn)^2} \tag{4.3}$$

where T and a are two parameters, being functions of balloon mass, m, its apparent mass, m_a, the mass of the air displaced, m_0, the mean ascent rate, $\bar{w}$, and the acceleration due to gravity, g. They are given by

$$T = \frac{(m + m_a)\bar{w}}{|m_0 - m|g} \quad ; \quad a = \frac{m_a}{m + m_a} \tag{4.4}$$

and, in order to be defined for a given situation, require a relationship between the balloon diameter, D, and its mean rate of ascent. It can be argued, for flights through the atmospheric boundary layer to around gradient height and idealizing the balloon as a sphere with a constant drag coefficient, that D and $\bar{w}$ are linked by an expression of the general form

$$a D^3 - b \bar{w}^2 D^2 - 1 = 0 \tag{4.5}$$

The values adopted for a and b will depend on the surface atmospheric density at the time, the mass of the balloon and gas, the specific gravity of the gas, and the assumed drag coefficient for the sphere.

In this application, the spectrum of wind velocity fluctuations, S_f, can be described by one of a number of formulae pertaining to turbulence in the atmospheric boundary layer (see Teunissen, 1970, for a summary of these). Davenport (1961) suggests a normalized spectrum of the form

$$\frac{n.S_t(n)}{\kappa\,V_0^2} = 4.0\,\frac{x^2}{(1+x^2)^{4/3}} \tag{4.6}$$

to represent horizontal gustiness in strong wind conditions up to about 150 m above ground level and, reasonably adequately, at higher altitudes in the boundary layer. Here κ is the surface drag coefficient, depending on the terrain roughness, V_0 is the mean wind speed referred to the standard anemometer height of 10 m, and x is defined by

$$x = \frac{1200\,n}{V_0} \tag{4.7}$$

An objection to Davenport's spectrum can be raised on the grounds that S_t should approach a constant value at very low frequencies. In fact, this constant will be proportional to the integral scale of turbulence. However, (4.6) suggests instead that $S_t \propto n$ as $n \to 0$. An alternative form proposed by von Karman and later by Harris (1971) is

$$\frac{n.S_t(n)}{\kappa\,V_0^2} \simeq 4.0\,\frac{x}{(2+x^2)^{5/6}} \tag{4.8}$$

where

$$x = \frac{1800\,n}{V_0} \tag{4.9}$$

It not only meets the theoretical requirements at low frequencies, but also incorporates the results of more recent measurements which suggest an increase in the length scale from 1200 to 1800 m. In consideration of the fact that the sensor response admits energy more strongly towards the left-hand end of the turbulence spectrum, (4.8) has been used here, although it must be noted that neither form will be particulary precise below about 1 cy/min.

When the response function, R_s^2, is applied to the spectrum of turbulence it is implicitly assumed that the resulting motion is associated with the sensor package as well as the balloon. The response of the pendulum constituted by the sensor suspended beneath the balloon is neglected. This can reasonably be supported by the fact that

the natural frequency of a typical instrument train is about 0.1 Hz, in a range where the power of the turbulent fluctuations is relatively small. This is especially valid towards the top of the boundary layer, where the inertial subrange portion of the spectrum in this frequency range is further suppressed.

The spectrum of observational errors, S_O, can be derived straightforwardly from the spectrum of displacement errors, S_d. The displacement, d, is the downwind horizontal distance to the sensor. A first assumption is that S_d is "white" up to the folding frequency, n_N. It can then be demonstrated that, for the Canadian rawinsonde system in which upper winds are calculated from overlapping observations taken every minute, S_d is related to the variance of the displacement errors, σ_d^2, and the folding frequency by

$$S_o(n) = 4 n_N \sigma_d^2 \sin^2 \pi \frac{n}{n_N} ; \quad n < n_N \tag{4.10}$$

(see Appendix VIII). In this case $n_N = 1/120 \ Hz$.

Some estimates of the magnitude of σ_d can be found in the work of de Jong (1966). In the "height-elevation" mode of operation, which is standard for the Canadian rawinsonde network, it has been shown that

$$\sigma_d^2 = \frac{h^2}{\sin^4 \delta} \sigma_\delta^2 + \cot^2 \delta \cdot \sigma_h^2 \tag{4.11}$$

where h is the height and δ is the angle of elevation. According to de Jong, typical values of the standard deviations σ_h and σ_δ in the height range of interest in this study are given by

$$\sigma_h = 0.02 \ h ; \sigma_\delta = 0.1^o \tag{4.12}$$

Perhaps the least well-defined element of Equation 4.1 is the spectrum of self-induced motions, S_i. As a first estimate, it is possible to idealize the balloon as a rigid sphere.

This approach has been followed in Appendix VIII, from the theory of Fichtl, deMandel and Krivo (1972). Unfortunately, the self-induced motions of the balloon are observed as motions of the sensor package suspended some distance below. An added complication is the flexible skin of the balloon. Thus, the detected motion actually results from that of a pear-shaped object and a simple pendulum.

The theory for the rigid sphere is again derived from a first-order approximation to the equations of motion, as used earlier by Fichtl (1971) to determine the sensor response. Fluctuating lift and drag terms are introduced; the components of the lift coefficient are treated as perturbation quantities and the drag coefficient is represented by a mean and perturbation quantity. This leads to expressions relating the spectra of the induced motions to the spectra of the aerodynamic coefficients. For a particular type of balloon with a roughened surface, the so-called JIMSPHERE, Fichtl et al rationalized that the induced motions are narrow-banded about n_o, and then obtained a normalized spectrum of the form

$$\frac{n_o S_i(n)}{\sigma_i^2} = \frac{1}{\beta\sqrt{2\pi}} exp\left(-\frac{(1 - n/n_o)^2}{2\beta^2}\right) \cdot \tag{4.13}$$

in which β is assumed to be a universal constant. However, it was noted, based on measurements by Rogers and Camnitz (1965), that the bandwidth for a smooth balloon is considerably larger. In fact, from experiments with a ROSE balloon comparable to the normal rawinsonde balloon, representative values of the defining parameters are given as $\beta = 0.2$, $\sigma_i = 2.6\ m/s$ and $n_o = 0.15\ Hz$. These apply up to an altitude of 7 Km and for supercritical Reynolds numbers $(Re > 2.5 \times 10^5)$.

Some other pertinent evidence of the behaviour of ascending balloons in the atmosphere is reviewed in Appendix VIII (McVehil, Pilie and Zigrossi, 1965, Murrow and Henry, 1965, and Morrissey and Muller, 1968). From this it can be concluded that (4.13) provides a reasonable description of self-induced motions for the rawinsonde sensor, taking $\beta = 0.2$, n_o as the natural frequency of the suspended pendulum ($\sim 0.1\ Hz$) and σ_i as approximately half the mean rate of ascent ($\sim 2.5\ m/s$).

Finally, the admittance function due to averaging, R_a^2, must be considered. In the rawinsonde system the sensor effectively integrates the winds over an interval of time, τ. This is equivalent to averaging a continuous record of velocity using a "boxcar" weighting function as follows:

$$W(t) = \frac{1}{\tau} \; ; \; t < \frac{\tau}{2}$$

$$W(t) = \frac{1}{2\tau} \; ; \; t = \frac{\tau}{2} \tag{4.14}$$

$$W(t) = 0 \; ; \; t > \frac{\tau}{2}$$

The corresponding spectral window is given by the Fourier transform of the function, that is (Blackman and Tukey, 1958),

$$R_a^2(n) = \left(\frac{\sin \pi n \tau}{\pi n \tau}\right)^2 \tag{4.15}$$

This is shown in Figure 4.6. It can easily be appreciated that the "side lobes", which exist above $n = 1/\tau$, are increasingly small so that, although some power is allowed to pass in this range, it can be neglected for the purposes of this study.

4.5 Estimates of Gradient Wind Variance due to Rawinsonde Errors

From the above considerations the overall spectrum of wind velocity errors can be synthesized for typical rawinsonde flights. The area enclosed by the spectrum $S_s(n)$ represents the contribution to the recorded variance. Three conditions of gradient wind speed $(V_G = 10, 15$ and $20 \; m/s)$ and three surface drag coefficients $(\kappa = 0.5, .015$ and $.005)$ have been considered, with gradient height taken as 500 m above ground level in each case. The power spectral models and other assumptions employed are now summarized:
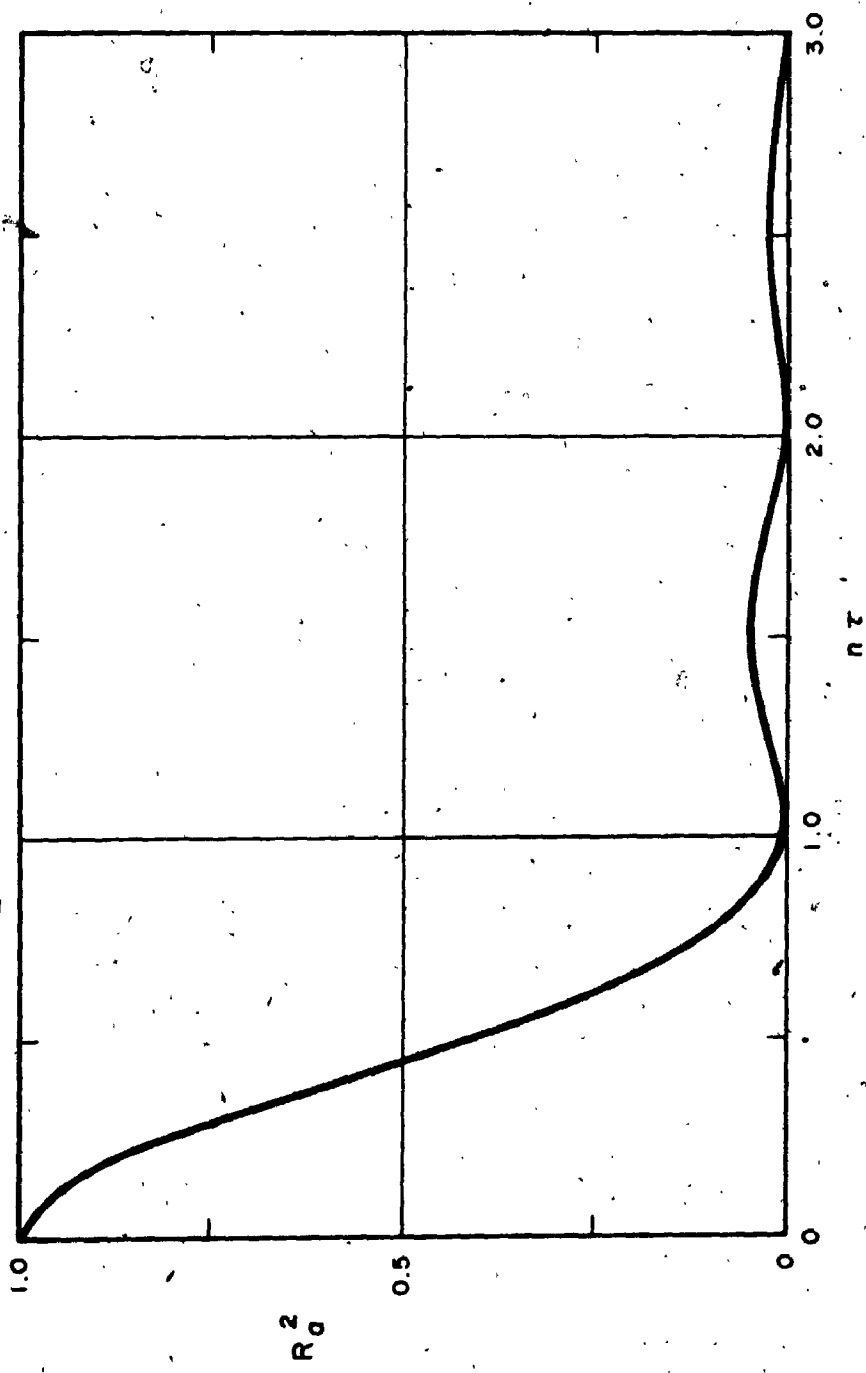
FIG. 4.6   SPECTRAL WINDOW DUE TO "BOX-CAR" AVERAGING OF WIND VELOCITY
OVER PERIOD τ

a) Atmospheric turbulence (S_t) was represented by von Karman's equation (4.8). The surface mean wind speed, V_0, was determined by the terrain roughness selected for each run (from Figures 3.2 and 3.13).

b) Sensor response (R_s) was defined by Fichtl's expression (Equation 4.3). As mentioned earlier, the parameters T and a depend on the balloon diameter and this, in turn, is a function of the mean ascent rate. In this synthesis it was assumed that the balloon has a drag coefficient of 0.3, the sensor package mass is 1 kg, the density of the ambient air is a constant 1.2 kg/m^3 and the balloon gas is hydrogen. Referring to Appendix VIII, it can then be shown that the required function reduces to

$$.585D^3 - .0144 \bar{w}^2D^2 - 1 = 0 \qquad (4.16)$$

and, with the balloon inflated to ascent initially at about 5 m/s, the diameter is 1.45 m.

c) Self-induced motions (S_i) were represented by Equation 4.13, in which the constant β is assigned a value of 0.2 and n_0 is the natural frequency of the pendulum, i.e.,

$$n_0 = \frac{1}{2\pi} \sqrt{\frac{g}{l}} \qquad (4.17)$$

l is 20 m, the length of the instrument train. It was assumed, from the evidence presented by Murrow and Henry, that the remaining parameter, σ_i, takes a value of 2.5 m/s.

d) The spectra S_i and $R_s^2.S_t$ were aliased with a folding frequency of 1/120 Hz before the averaging function R_a^2 was applied. The latter was given by Equation 4.15 with $\tau = 120$ sec.

e) Observational errors (ϑ_0) were treated following de Jong's theory. At a height of 500 m and with the typical values of σ_h and σ_δ suggested by de Jong,

(4.11) becomes

$$\sigma_d^2 = 500^2 (\frac{.001745^2}{\sin^4 \delta} + .02^2 \cot^2 \delta) \tag{4.18}$$

At the relatively low altitudes with which this synthesis is concerned, the angle of elevation can be approximated by

$$\tan \delta = \frac{2\bar{w}}{|V_G - V_o|} \tag{4.19}$$

Furthermore, the variance of the observational velocity errors can be calculated directly from the variance of displacement errors (see Appendix VIII) as

$$\sigma_o^2 = \frac{2 \sigma_d^2}{\tau^2} \tag{4.20}$$

where, as before, τ is 120 secs. This eliminates the need for the power spectrum.

To obtain the variances due to self-induced motions, σ_i^2, and the response of the sensor to atmospheric turbulence, σ_t^2, the aliased and averaged spectra were integrated using Simpson's rule with $\log_{10}$ increments of .05 over a range of $\log_{10} n$ from $-.3$ to 0. This contained almost all the energy associated with these motions. The results, together with the variances of observational errors and the combined totals, are listed in Table 4.2. In Figure 4.7 these are shown as percentages of the variance of the gradient wind climate suggested by the empirical formula derived in Chapter 3; i.e.,

$$\sigma_G^2 = (.3 V_G + 2.7)^2 \tag{4.21}$$

in which V_G is the mean gradient wind speed.

It is clear that the contribution of observational errors is always small. Generally, the effect of higher gradient winds is to decrease the percentage of the variance due

V_G (m/s)		OPEN SEA $\kappa = .0005$	OPEN COUNTRY $\kappa = .005$	FOREST $\kappa = .015$
10	σ_o^2	0.043	0.037	0.026
	σ_t^2	0.057	0.399	0.443
	σ_i^2	2.082	2.082	2.082
	σ_s^2	2.182	2.518	2.551
15	σ_o^2	0.100	0.085	0.060
	σ_t^2	0.119	0.833	0.940
	σ_i^2	2.082	2.082	2.082
	σ_s^2	2.301	3.000	3.082
20	σ_o^2	0.184	0.156	0.109
	σ_t^2	0.203	1.413	1.583
	σ_i^2	2.082	2.082	2.082
	σ_s^2	2.469	3.651	3.774

σ_o^2 = variance due to observational errors

σ_t^2 = variance due to balloon response to turbulence

σ_i^2 = variance due to self-induced motions

σ_s^2 = total variance

Units: $(m/s)^2$

TABLE 4.2. GRADIENT WIND VARIANCES DUE TO RAWINSONDE ERRORS
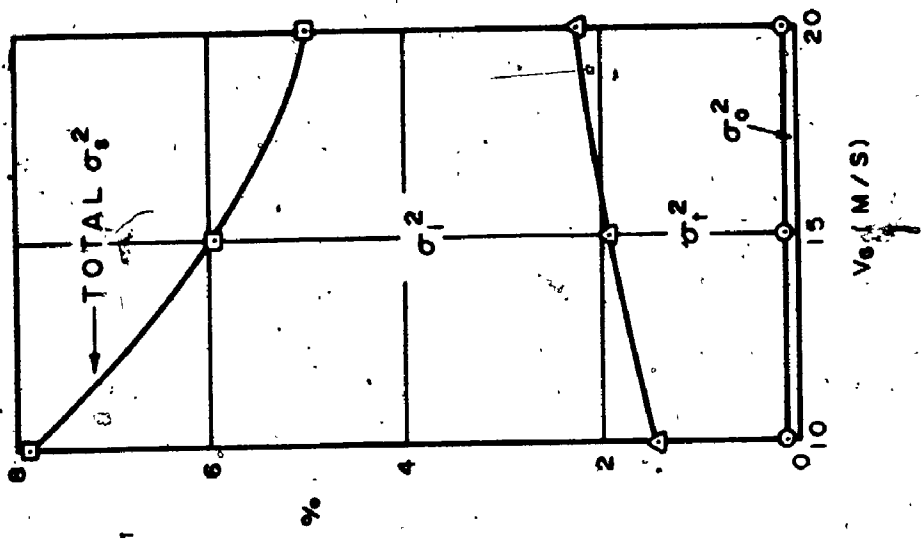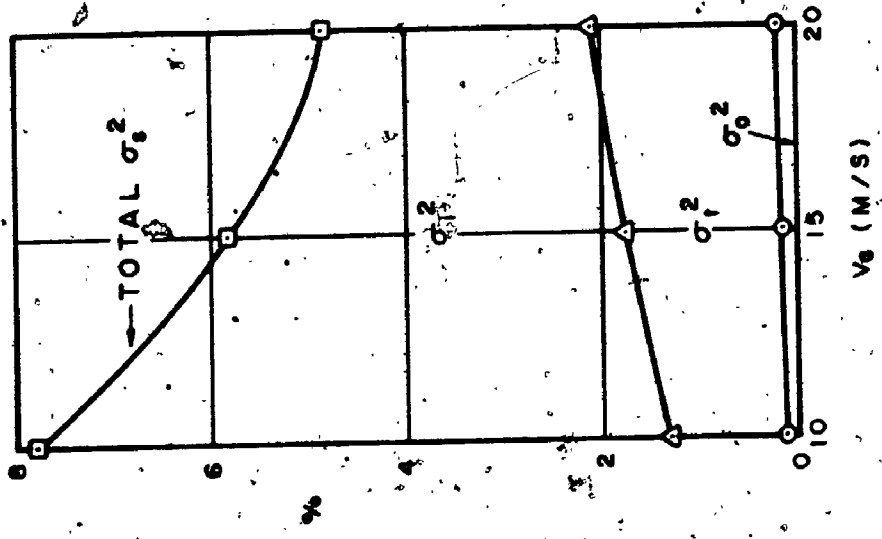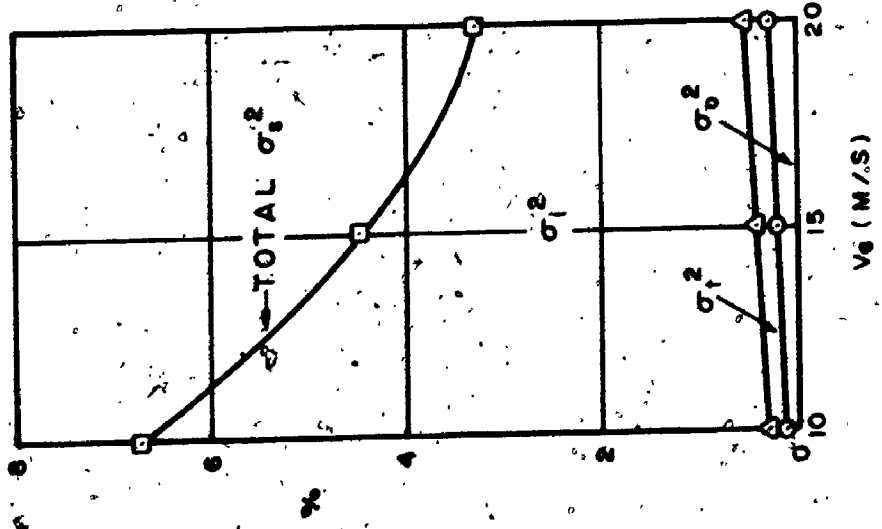
FIG. 4.7 ACCUMULATED RAWINSONDE VARIANCES FROM a) OBSERVATIONAL ERRORS, σ_o^2 b) SENSOR RESPONSE TO ATMOSPHERIC TURBULENCE, σ_t^2 c) SELF-INDUCED MOTION, σ_i^2 EXPRESSED AS PERCENTAGE OF GRADIENT WIND SPEED VARIANCE

to self-induced motions. Over rougher terrains the total percentage is increased, mainly because of the sensor's response to a greater degree of turbulence in the atmospheric boundary layer. Overall, the estimated values found here are reassuringly low, even for relatively low mean wind speeds.

4.6 Estimates of Surface/Gradient Error Variance

In the statistical analysis of the surface to gradient wind speed ratio (Chapter 3) a random function ϵ was introduced defined by

$$\ln \epsilon = \ln V_O - \ln V_G - \ln K \tag{4.22}$$

where K is the average ratio appropriate to the upwind terrain for a given wind direction. The variance of the important parameter $\ln \epsilon$ due to errors in measurements can therefore be represented by

$$\sigma^2_{e(\ln \epsilon)} = \sigma^2_{e(\ln V_O)} + \sigma^2_{e(\ln V_G)} \tag{.423}$$

Assuming that the errors in surface anemometer readings are negligible compared with those associated with the rawinsonde, it can then be shown that

$$\sigma^2_{e(\ln \epsilon)} \sim \frac{\sigma^2_{e(V_G)}}{V_G^2} = \frac{\sigma^2_s}{V_G^2} \tag{4.24}$$

in which V_G is the mean gradient wind velocity and $\sigma_{e(V_G)} (= \sigma^2_s)$ is the variance of errors in V_G. This standard result derives from a logarithmic series representative of $\sigma^2_{e(\ln V_G)}$ with $\sigma_{e(V_G)}$ small compared with V_G (see, for example, Benjamin and Cornell, 1970). Thus, the contribution of rawinsonde error to the total variance of $\ln \epsilon$, regarded earlier as a universal constant with a value of approximately 0.25^2, can be estimated directly from σ^2_s for various mean gradient wind speeds and terrain roughnesses. Some values of σ^2_s are listed in Table 4.2 and these have been used in the preparation of Figure 4.8, which shows the error variance in $\ln \epsilon$ as a percentage of the assumed universal constant.
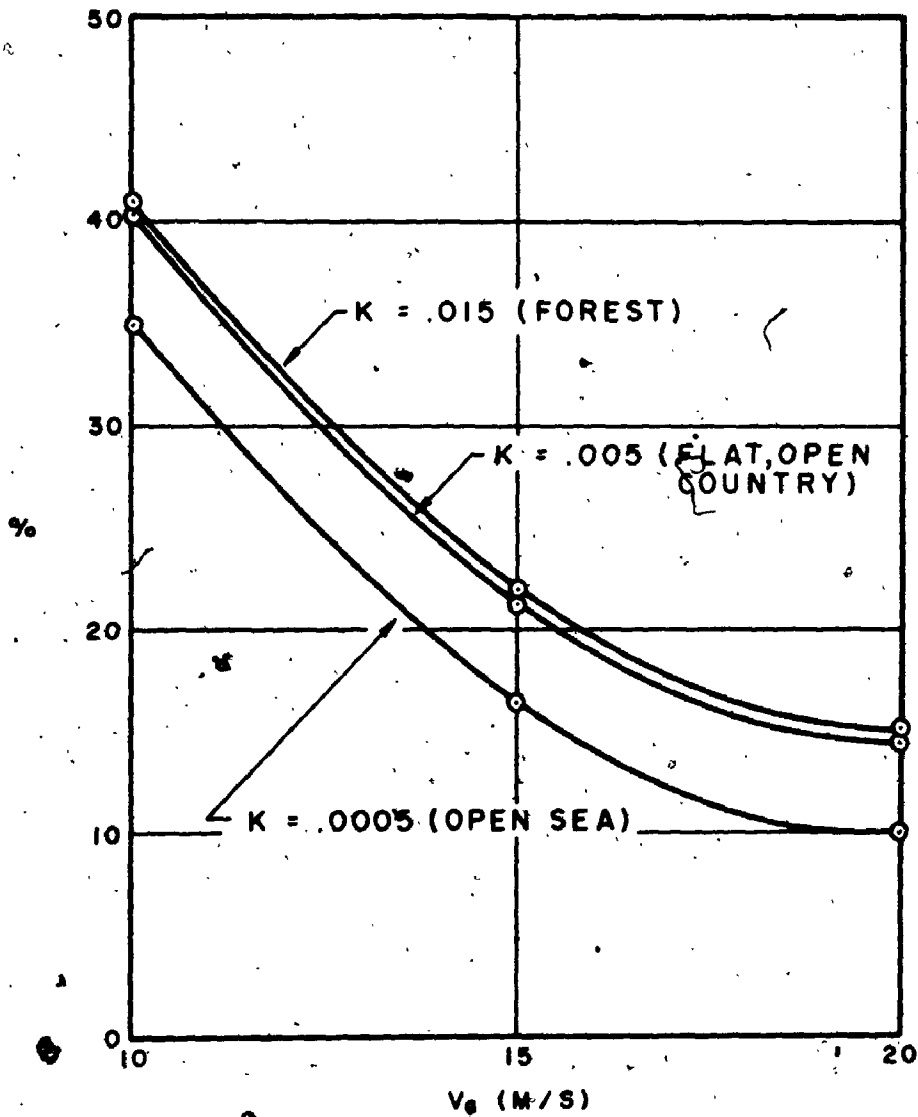
FIG. 4.8 ESTIMATED ERROR VARIANCE IN LN ϵ AS A PERCENTAGE OF AN ASSUMED CONSTANT, $\sigma^2_{Ln\epsilon} = .0625$

Apparently the variance of $ln\epsilon$ varies, over the range of conditions considered here, from about 60% to 90% of the value suggested by the earlier analysis. Based on $\sigma_{ln\epsilon} = 0.25$, this corresponds to new r.m.s. values from 0.19 to 0.24, still close to the figures suggested by the other sources discussed in Chapter 3. In the light of these findings, a suitable choice of $\sigma_{ln\epsilon}$, for use with gradient wind data obtained from other than rawinsondes (e.g., tower-mounted anemometers), would be 0.22.

4.7 Geostrophic, Gradient and Thermal Winds

A number of references have already been made to gradient and geostrophic winds, and so far these have been taken to mean the free stream flow at the top of the atmospheric boundary layer. It has been seen how the climatic properties of these winds, as measured directly by radiosonde balloons, can be mapped and provide a useful reference for extrapolating to lower elevations. An alternative source of potential upper wind information exists by virtue of the fact that the gradient and geostrophic winds are, in their strict meteorological definitions, functions of the horizontal gradient of atmospheric pressure. Before investigating this as a practical possibility it is first necessary to define more closely the terms involved.

Considering horizontal, frictionless flow, the motion of unit volume of atmosphere is governed by the balance of the pressure, centrifugal and Coriolis forces and, in the absence of any tangential accelerations, the flow must be along the isobars. The equation of motion can be written

$$-\frac{dp}{dN} = \rho_a\left(\frac{V_G^2}{R} + f V_G\right) \tag{4.25}$$

where $\frac{dp}{dN}$ is the pressure gradient, normal to the isobars and positive towards high pressure,

ρ_a is the air density,

V_G is the wind velocity satisfying the equation and known as the gradient wind,

R is the radius of curvature of motion, taken as the radius of the isobars

and f is the Coriolis coefficient, defined by

$$f = 2\omega \sin\lambda \tag{4.26}$$

in which ω is the earth's rotational speed $(\sim 7.29 \times 10^{-5}\ rad/sec)$ and λ is the angle of latitude. Circulation around a centre of low pressure in the northern hemisphere is illustrated in Figure 4.9.

It should be appreciated, however, that R is strictly the radius of the trajectory and, over an extended period of time, this is generally not the same as the isobaric radius even though the trajectory may be instantaneously along the isobars. There may be a considerable difference between the two in a rapidly moving weather system. Blaton's equation (Haltiner and Martin, 1957) gives the precise relationship which, in the context of this discussion, can be written

$$\frac{R_{isobar}}{R_{trajectory}} = (1 - \frac{c}{V_G}\ cos\ \psi) \tag{4.27}$$

where c is the velocity of the system and ψ is the angle subtended by the vectors of c and V_G, measured clockwise from the latter. In the case of a depression migrating from west to east, this means that R is reduced on the north side and correspondingly increased on the south side of the centre. Therefore, on average, the effect on the overall wind climate can be neglected, provided the systems do not follow a markedly preferred track around a given location. Moreover, for most practical purposes the systems can be regarded as relatively stationary.

A special case of gradient flow occurs where the isobaric curvature is zero, for which Equation 4.25 reduces to

$$-\frac{dp}{dN} = \rho_a f\ V_g \tag{4.28}$$

where V_g is called the geostrophic wind, again in a direction parallel to the isobars.
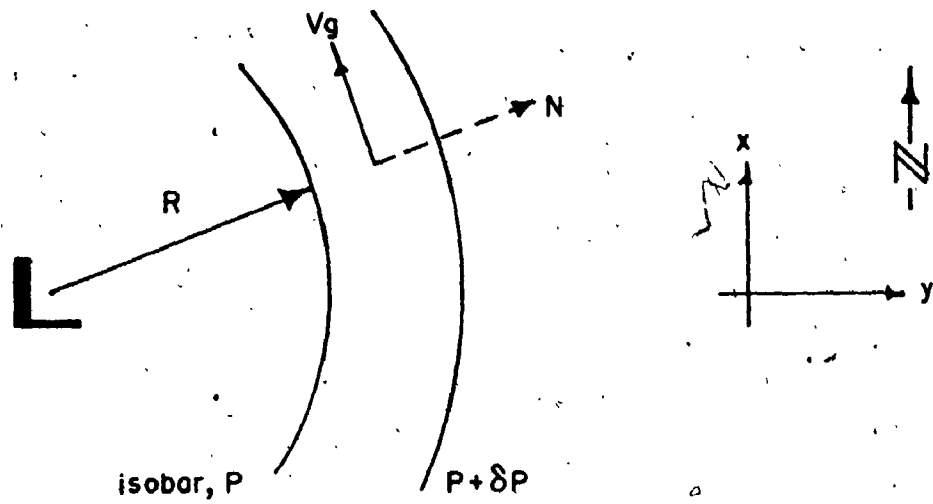
FIG. 4.9   GRADIENT FLOW AROUND A CENTRE OF LOW PRESSURE   (NORTHERN HEMISPHERE)
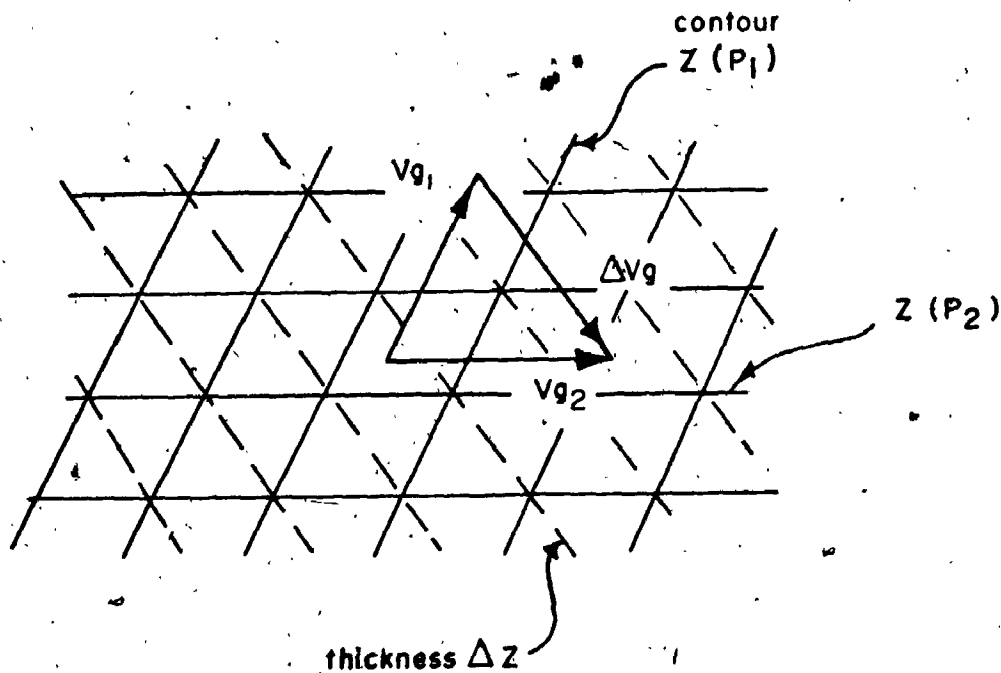
FIG. 4.10   THE THERMAL WIND VECTOR, ΔV_g, BETWEEN ISOBARIC SURFACES P_1 AND P_2

Substituting for the pressure gradient in (4.25),

$$\frac{V_G^2}{R} + f\,V_G - f\,V_g = 0 \qquad\qquad (4.29)$$

and, to a first approximation, it can be easily shown that the gradient and geostrophic wind speeds are related by

$$V_G = V_g \pm \frac{V_g^2}{f\,R} \qquad\qquad (4.30)$$

In the northern hemisphere, the positive sign is operative for circulation around a centre of high pressure and the negative sign around low pressure, although the corrective term is usually small.

The third wind to be defined in this brief review is the thermal wind, describing the vertical variation of geostrophic flow. Figure 4.10 illustrates the geostrophic vectors, V_{g1} and V_{g2}, on two constant pressure surfaces p_1 and p_2 (the height contours, z, for the isobaric surfaces are shown here, rather than the isobars at two elevations; the contour spacing determines the geostrophic velocity in a similar way since the equation of motion can be rearranged to the form $-\,dz/dN = f\,V_g/g$, or, in vector notation,

$$\vec{V}_g = -\frac{g}{f}\,\nabla z \times \vec{k} \qquad\qquad (4.31)$$

The vector difference ΔV_g is referred to as the thermal wind, given by

$$\vec{\Delta V}_g = -\frac{g}{f}\,\nabla\,(\Delta z) \times \vec{k} \qquad\qquad (4.32)$$

in which Δz is the vertical displacement or thickness between the pressure surfaces p_1 and p_2 at a given location. Thus, the thermal wind is parallel to the lines of constant thickness (the broken lines in Figure 4.10) with low values on the left in the northern hemisphere, and is defined in terms analagous to the geostrophic wind in (4.31). Now, by invoking the hydrostatic equation and the gas law for dry air, Equation 4.32 can be recast in the form

$$\vec{\Delta V}_g = - \frac{g}{f} \frac{R}{g} \ln \frac{p_1}{p_2} \nabla \overline{T} \times \vec{k} \qquad (4.33)$$

where R is the gas constant for air and $\overline{T}$ is the mean temperature of the thickness layer. Alternatively,

$$\vec{\Delta V}_g = - \frac{g}{f\overline{T}} \Delta z \nabla \overline{T} \times \vec{k} \qquad (4.34)$$

In scalar terms the thermal wind can be found from

$$\Delta V_g = - \frac{g}{f\overline{T}} \Delta z \frac{d\overline{T}}{dN} \qquad (4.35)$$

where $d\overline{T}/dN$ is the temperature gradient (strictly, on an isobaric surface) normal to the isotherms and positive towards high temperature. The wind direction is along the isotherms, counter-clockwise around areas of low temperature and clockwise around high temperature.

4.8 Gradient and Geostrophic Winds from Synoptic Data

Recently, it has become possible to determine with relative ease the climate of computed gradient and geostrophic winds over Canada. This has been facilitated by the magnetic tape archiving of hourly mean sea level (m.s.l.) pressures and other surface data in synoptic, rather than station, order[*].

The process of computing the winds at a particular time and location depends essentially on a valid objective analysis of the pattern of atmospheric pressure in the vicinity. Some preliminary work on this problem has been reported by Muller (1973). He studied the surface geostrophic winds at Montreal from simultaneous observations of surface pressure at 16 stations within a 400 km radius. The computed wind speeds and directions, obtained by four different methods, were compared with the winds estimated from manual isobaric analyses. Although this basis of comparison may be

---

[*]Data commencing May 1972 available at the Atmospheric Environment Service, Toronto, Canada

open to question; Muller's results give some indication of the suitability of the various computational techniques.

The pressure pattern at any given time was represented by either a plane or quadratic surface, as

$$p_i = a_1 x_i + a_2 y_i + \bar{p} \tag{4.36}$$

or $$p_i = a_1 x_i + a_2 y_i + a_3 x_i^2 + a_4 y_i^2 + a_5 x_i y_i + \bar{p} \tag{4.37}$$

where p_i is the computed pressure at station i,

x_i, y_i are the coordinates of station i

and $\bar{p}$ is the mean pressure taken over all the observing stations. The errors between the p_i's and observed pressures were minimized by the method of least squares and the appropriate coefficients in (4.36) or (4.37) were obtained as a result. In some cases a weighting function was applied to the errors, according to the distance, d, of the station from the mean position of all stations. Muller concluded that there was little to distinguish the following three models, all of which gave quite satisfactory results:

a) A quadratic pressure surface, weighted as a roughly sinusoidal and decreasing function of d.

b) A plane surface, weighted as a linearly decreasing function of d.

c) An unweighted plane surface.

In the present study m.s.l. pressures are also represented, in general, by Equation 4.37 with cartesian coordinates x, y positive towards the east and north (see Figure 4.9) and the origin at the mean position of those observing stations contributing to the analysis. The pressure gradient at the point x_i, y_i, and hence the geostrophic and gradient winds, is then given by.

$$\frac{dp}{dN} = \left(\frac{dp^2}{dx} + \frac{dp^2}{dy}\right)^{1/2} = (A_1^2 + A_2^2)^{1/2} \qquad (4.38)$$

in which the component gradients are

$$A_1 = a_1 + 2a_3 x_i + a_5 y_i$$

$$(4.39)$$

$$A_2 = a_2 + 2a_4 y_i + a_5 x_i$$

In the estimation of gradient winds, the radius of curvature of the isobars, R, must be found from the standard relationship

$$R = \frac{(1 + y'^2)^{3/2}}{y''} \qquad (4.40)$$

in which $y = fn(x)$ is the equation of the isobar through the required point. It can be shown that, in terms of the coefficients and location coordinates,

$$R = \frac{(A_1^2 + A_2^2)^{3/2}}{2a_5 A_1 A_2 - 2a_3 A_2^2 - 2a_4 A_1^2} \qquad (4.41)$$

A mathematical test must also be devised to determine whether the circulation is cyclonic or anticyclonic, and hence the appropriate sign in Equation 4.30. It turns out that flow around a low pressure system can be identified if both of the following conditions are met:

$$\frac{A_1}{|A_1|} = \frac{x_i - x_o}{|x_i - x_o|} \quad \text{and} \quad \frac{A_2}{|A_2|} = \frac{y_i - y_o}{|y_i - y_o|} \qquad (4.42)$$

x_o, y_o is the centre of curvature of the isobars and can be found from

$$x_a = x - \frac{y'(1 + y'^2)}{y''} \qquad (4.43)$$

and $y_o = y + \frac{(1 + y'^2)}{y''} \qquad (4.44)$

Again, in terms of the coefficients and location coordinates,

$$x_O = x_i + \frac{A_1 A_2^2(1 + A_1^2/A_2^2)}{2a_5 A_1 A_2 - 2a_3 A_2^2 - 2a_4 A_1^2}$$

(4.45)

$$y_O = y_i + \frac{A_2^3(1 + A_1^2/A_2^2)}{2a_5 A_1 A_2 - 2a_3 A_2^2 - 2a_4 A_1^2}$$

(4.46)

It must be emphasised that the winds computed in this way are based on atmospheric pressures corrected to m.s.l. and as such represent a hypothetical frictionless flow, at that level. Although they may closely correspond to the real flow regime existing at the top of the boundary layer (gradient height), there may be significant differences in the horizontal pressure pattern between the two levels. Under these conditions, known as a baroclinic atmosphere, the thermal wind must be introduced in order to obtain the geostrophic wind at the higher elevation.

The required thermal wind cannot be determined exactly from the synoptic data alone, but it can be approximated by considering a constant thickness layer (Δz) from m.s.l. to 500 m, representing gradient height, and taking $\overline{T}$ in (4.35) as the observed surface temperature. The fitting of an appropriate two-dimensional temperature surface, and hence the gradient $d\overline{T}/dN$, can then proceed as for the atmospheric pressures. There are, however, potential difficulties in applying this, such as the effects of strictly local temperature variations.

In this investigation, as in Muller's, the method of least squares is utilized to fit weighted and unweighted quadratic and plane surfaces to m.s.l. pressures and surface temperatures. The coefficients defining the surfaces can be computed for successive synopses using a single transformation matrix for each specified location and fitting procedure, thus effecting a considerable saving in computational effort. Taking the general quadratic surface to represent the horizontal variation of m.s.l. pressure, the method requires that the total squared error be minimized with respect to a_1, a_2, a_3 etc. With a weighting function included the quantity to be minimized is

$$\sum_{i=1}^{n} W_i E_i^2 = \sum_{i=1}^{n} W_i(p_i' - (a_1 x_i + a_2 y_i + a_3 x_i^2 + a_4 y_i^2 + a_5 x_i y_i))^2$$

(4.47)

where p_i' is the observed pressure departure from the mean (over n stations) and W_i is the weighting factor for station i. It can then be shown that the vector of coefficients is given by

$$A = \zeta \quad P$$
$$(5\times1) \quad (5\times n) \quad (n\times1)$$

(4.48)

P is the vector of pressure departures and ζ is the important transformation matrix, defined as

$$\zeta = (\chi \eta)^{-1} \chi$$

(4.49)

in which

$$\chi = \begin{vmatrix} x_1 W_1 & x_2 W_2 & \cdots & x_n W_n \\ y_1 W_1 & y_2 W_2 & \cdots & y_n W_n \\ x_1^2 W_1 & x_2^2 W_2 & \cdots & x_n^2 W_n \\ y_1^2 W_1 & y_2^2 W_2 & \cdots & y_n^2 W_n \\ x_1 y_1 W_1 & x_2 y_2 W_2 & \cdots & x_n y_n W_n \end{vmatrix}$$

(4.50)

and $$\eta = \begin{vmatrix} x_1 & y_1 & x_1^2 & y_1^2 & x_1 y_1 \\ x_2 & y_2 & x_2^2 & y_2^2 & x_2 y_2 \\ \vdots & & & & \\ x_n & y_n & x_n^2 & y_n^2 & x_n y_n \end{vmatrix}$$

(4.51)

4.9 Some Computed Wind Climates

Geostrophic and gradient winds were calculated for five Canadian locations at three-hourly intervals during the one year period from May 1972 to April 1973 (details of the data and analysis are contained in Appendix IX). Initially, three models of horizontal m.s.l. pressure and surface temperature variations were used; a weighted quadratic surface, a weighted plane and an unweighted plane. These were applied to

three data samples covering a six week period in May and June, 1972 at both Maniwaki and The Pas, and about three weeks in December 1972 at The Pas. The sample means and standard deviations of wind speeds are given in Table 4.3 and can be compared with similar statistics obtained from rawinsonde observations at 300 m and 500 m above ground level. An analysis was also carried out to find the correlation coefficients of the computed wind speeds with respect to those observed simultaneously at the 500 m level.

Generally the weighted quadratic and weighted plane models produce the closest agreement with upper wind observations, and this is supported by Muller's findings for Montreal. There is some evidence that the weighted quadratic form offers the best overall performance, and since it provides greater flexibility with the capacity to predict gradient winds, it has been retained in further computations.

It is apparent that values of the correlation coefficient are often disappointingly low. As might be expected, when the computed wind speeds are assessed against the surface anemometer readings the coefficients are even smaller, due to the interference of local winds. However, many of such irregularities can be effectively removed by averaging the surface observations over a number of hours and reworking the correlation analysis. This has been done here by taking the mean of j $(= 1, 3, 5, 9$ and $13)$ three-hourly readings, centred on the hours for which the gradient and geostrophic winds were available. The results given in Figures 4.11 — 4.13 illustrate the improvement usually achieved as j is increased to 5 or 9, corresponding to an averaging time of between 12 and 24 hours. It is also notable that the coefficients are highest for those data samples from which all but the strongest wind conditions have been excluded; values reach 0.8 for the December-January period at Stephenville. Evidence derived from a similar analysis based on observed 500 m winds also suggests an optimum averaging time of about 24 hours.

The quadratic description of atmospheric pressure as applied in this study attempts to model the circulation over a relatively large area 1600 km in diameter. Given the scope of the synoptic data, this is necessary in order to retain a reasonable

	MANIWAKI MAY-JUNE 1972			THE PAS MAY-JUNE 1972			THE PAS DECEMBER 1972		
	$\bar{V}$ (m/s)	σ (m/s)	r	$\bar{V}$ (m/s)	σ (m/s)	r	$\bar{V}$ (m/s)	σ (m/s)	r
OBSERVED									
300 m	5.70	3.29		7.63	3.54		5.49	3.05	
500 m	6.48	3.58		8.01	3.96		6.03	3.31	
COMPUTED									
a) Weighted Quadratic									
msl geostr	7.19	4.65	.66	7.37	4.17	.41	8.04	4.12	.23
msl grad	7.12	4.35	.66	7.39	3.51	.51	8.04	4.19	.23
500 m geostr	6.82	4.47	.70	7.04	4.32	.49	6.18	2.91	.49
b) Weighted Plane									
msl geostr	6.90	4.63	.64	5.92	2.96	.48	7.22	3.65	.15
500 m geostr	6.68	4.57	.68	5.74	2.75	.56	5.54	2.35	.44
c) Unweighted Plane									
msl geostr	7.96	5.58	.67	7.92	4.33	.41	8.64	4.46	.10
500 m geostr	8.02	6.09	.68	7.73	4.69	.50	7.12	3.11	.34

$\bar{V}$ = sample mean wind speed r = correlation coefficient with
σ = sample standard deviation (best estimate)   respect to observed 500 m wind

TABLE 4.3 STATISTICS OF OBSERVED AND COMPUTED WIND SPEEDS FOR SELECTED DATA SAMPLES
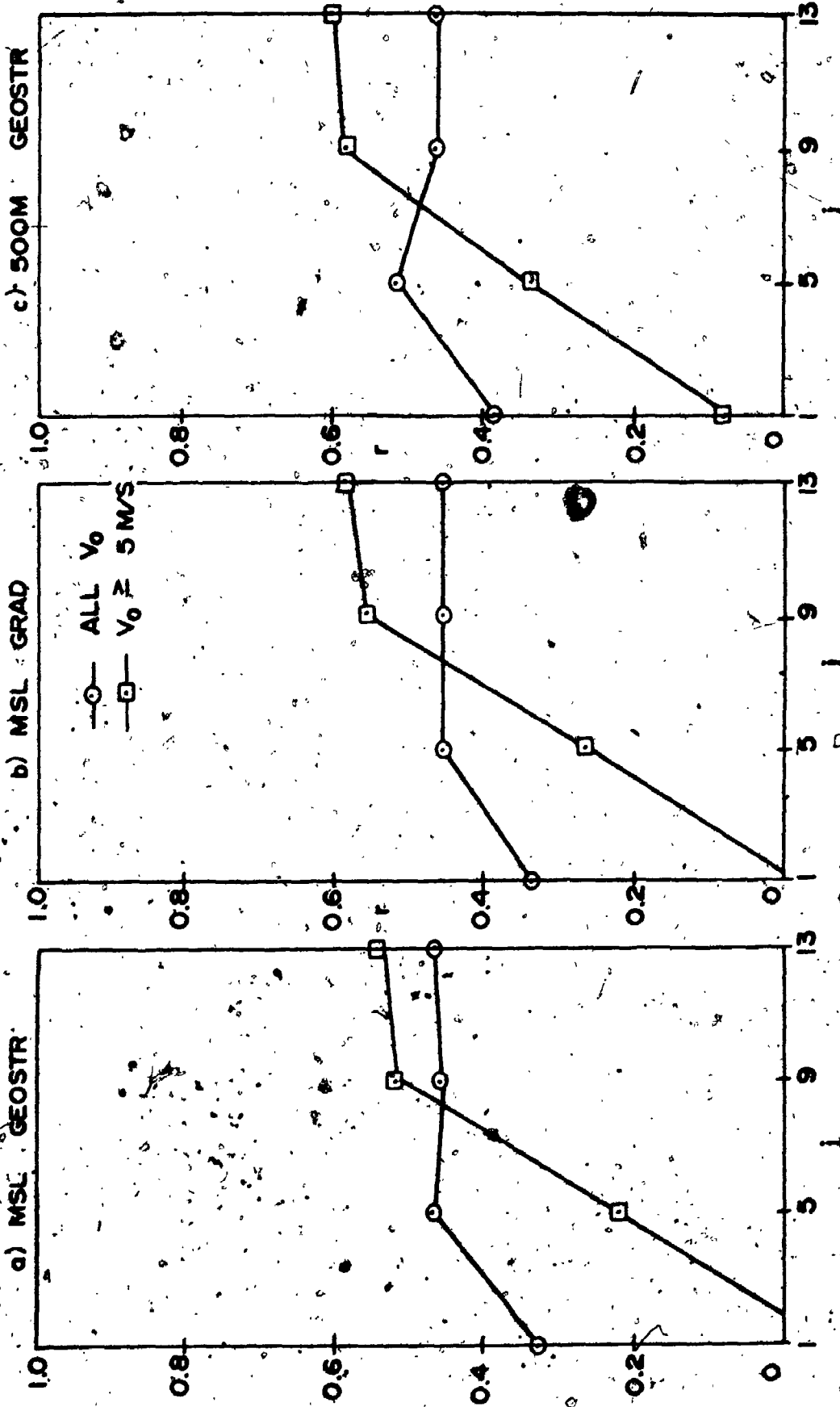
FIG. 4.11 CORRELATION COEFFICIENTS, r, WITH RESPECT TO OBSERVED SURFACE WIND SPEEDS AVERAGED OVER 3-HOURLY OBSERVATIONS (MANIWAKI, QUE., MAY–JUNE 1972)
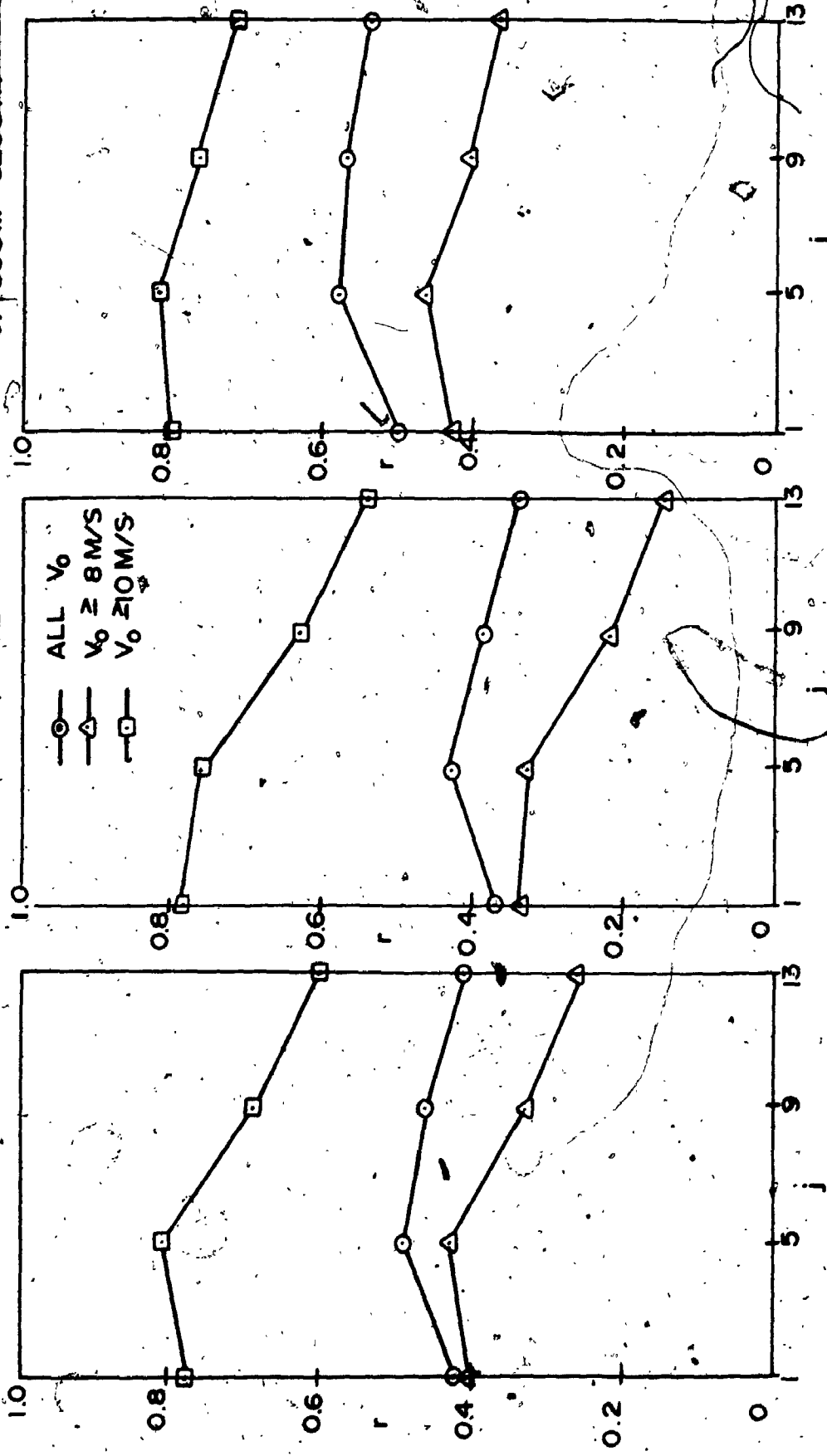
FIG. 4.12 CORRELATION COEFFICIENTS, r, WITH RESPECT TO OBSERVED SURFACE WIND SPEEDS AVERAGED OVER j 3-HOURLY OBSERVATIONS (STEPHENVILLE, NFLD., DEC 1972–JAN 1973)
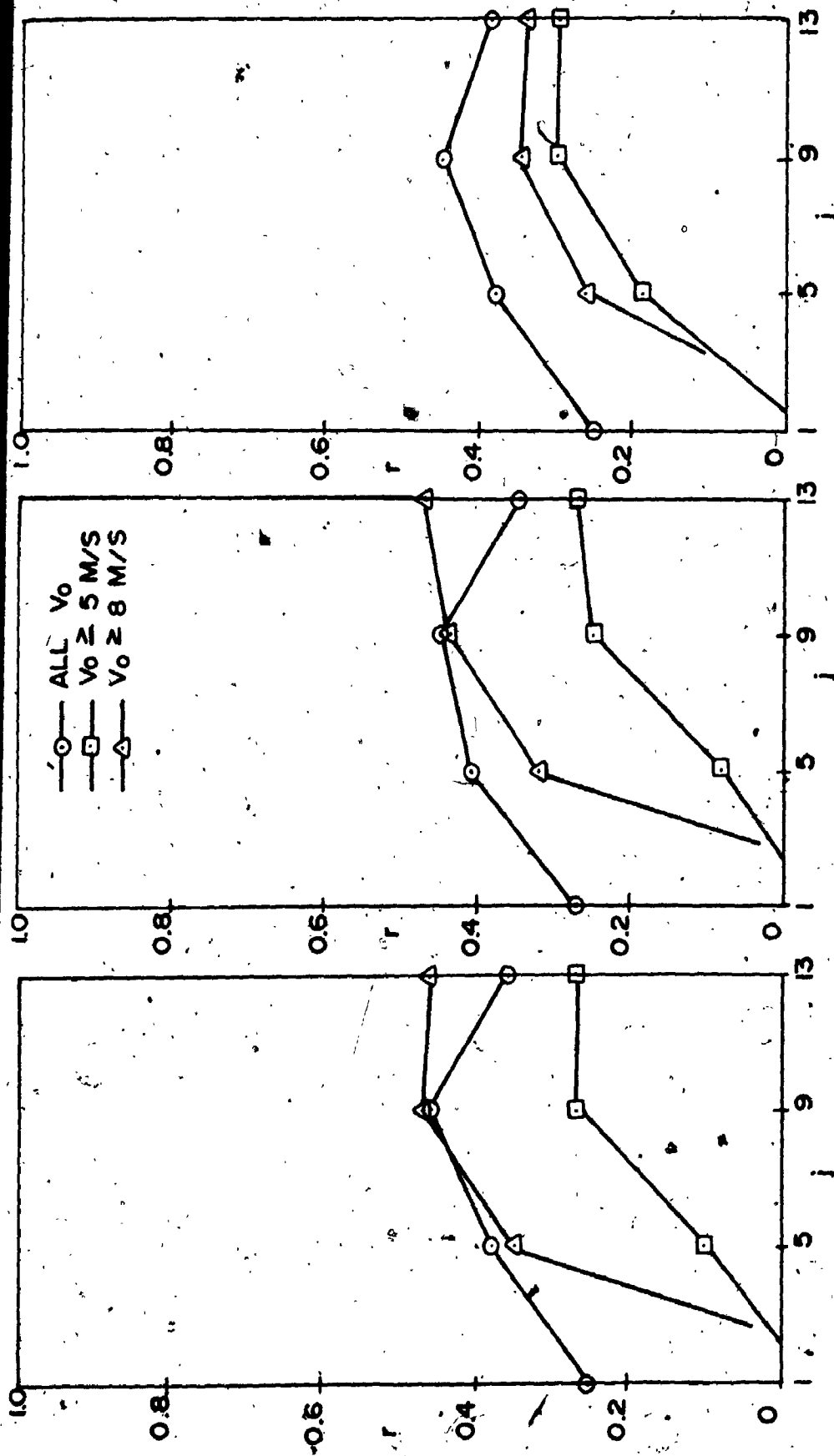
FIG. 4.13 CORRELATION COEFFICIENTS, r, WITH RESPECT TO OBSERVED SURFACE
WIND SPEEDS AVERAGED OVER j 3-HOURLY OBSERVATIONS
(THE PAS, MAN., MAY-JUNE 1972)

number of contributing stations. Clearly, some intermediate flow situations associated
with small weather disturbances are likely to be distorted, although the very strong
winds of deeper depressions should be well represented. This is reflected in the con-
sistently higher correlation coefficients shown, for example, in Figure 4.12 for
$V_o \geqslant 10\ m/s$, as compared with the subsample for which $V_o \geqslant 8\ m/s$.

The month-by-month and annual climates of geostrophic and gradient winds have
been obtained for the five selected locations. Since these were developed from a
single year of data the statistics are of little practical importance. Nevertheless, some
idea of their suitability, particularly regarding the climate of strong winds, can be
gained by comparing annual distributions of extreme wind speeds derived from
objective isobar analyses and upper air soundings. Recalling Equations 2.39 and 2.40
the Fisher-Tippett Type I parameters, U and $1/a$, were derived directly from the
annual Weibull parameters, c and k, as

$$U = c\ (ln\ N)^{1/k}\ ;\ \frac{1}{a} = \frac{c}{k}\ (ln\ N)^{1/k\ -\ 1} \qquad\qquad (4.52)$$

with $N = 876$. The resulting distributions are shown in Figure 4.14. Where
significant discrepencies occur between the curves for the computed and observed winds
(as at Moosonee, Stephenville and, to a lesser extent, at Maniwaki) this corresponds to
low estimates of the computed parameter, k, possibly due to the above-mentioned
effects of horizontal scale.

Although the climates of upper winds estimated from synoptic pressure data can
be reasonable representative, a high density of observing stations is preferable. A serious
attempt to establish a useful wind climatology for a country as extensive as Canada
would require large quantities of data for considerably more than the 96 stations used
here and, when available, spanning perhaps a period of ten years. Under present circum-
stances this would multiply many times the considerable computational effort which
was needed in this pilot investigation.
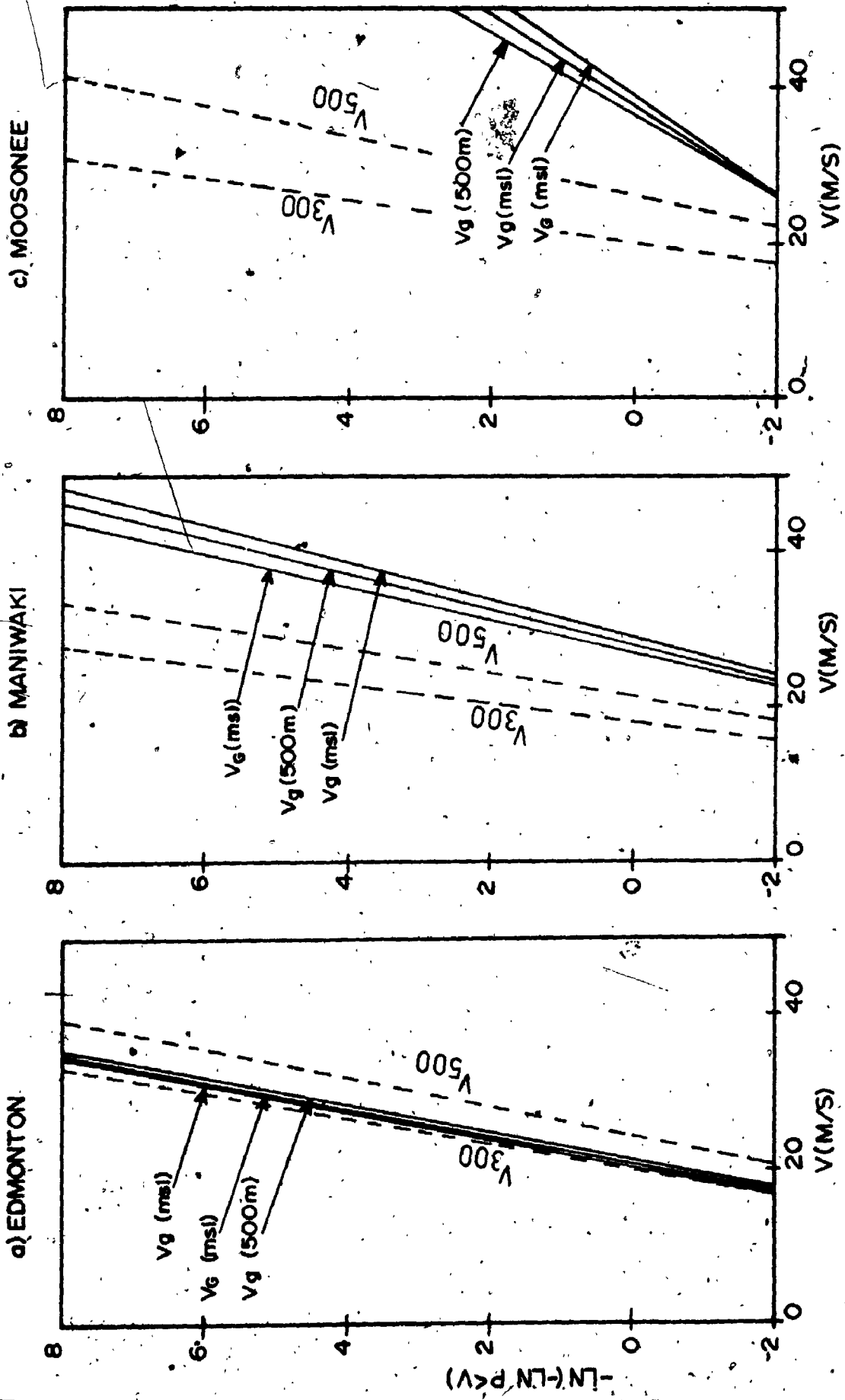
FIG. 4.1.4 TYPE I EXTREME DISTRIBUTIONS OF GEOSTROPHIC, GRADIENT AND OBSERVED UPPER WIND SPEEDS

e) THE PAS

Vg (msl)

Vg (msl)

Vg (500 m)

V 500

V 300

V(M/S)

d) STEPHENVILLE

V 500

V 300

Vg (500 m)

V G (msl)

V g (msl)

V(M/S)

-LN(-LN P<V)
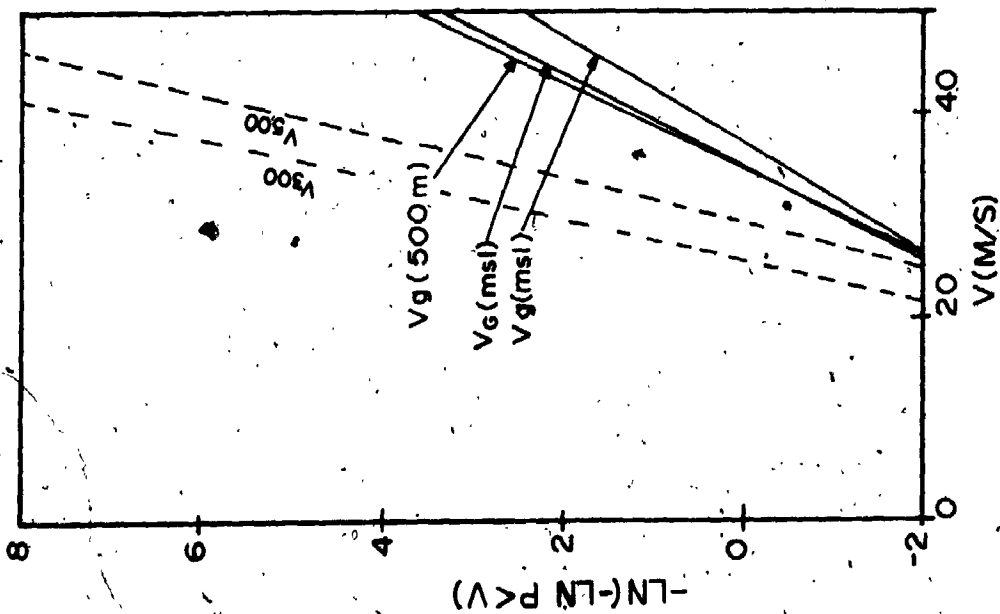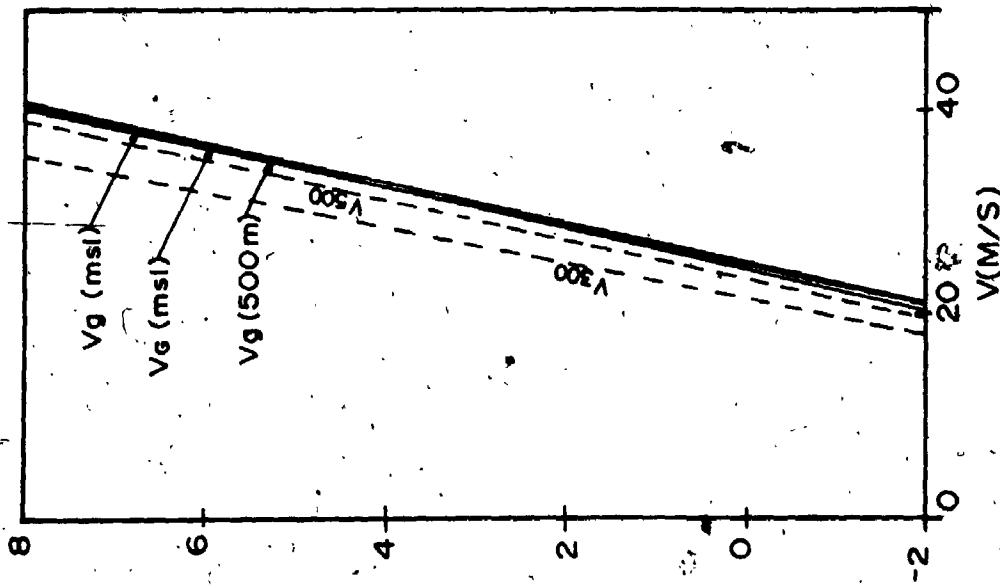
FIG. 4.14 (continued)

4.10 Conclusions

Problems relating to the establishment of the climate of mean winds have been discussed, beginning with an outline of topographic effects which might locally modify the regional wind climate prevailing at around gradient height. A flow chart has been constructed summarizing the methodology involved in the synthesis of wind climate at a given site from various data sources. Two further points concerning upper wind records were then investigated in some detail:

a) Sensor motions and measurement techniques contributing to errors in the rawinsonde system were studied by power spectral methods. A numerical synthesis was performed to assess the impact of such errors on observed climatic variances of gradient wind speeds under representative conditions of wind strength and terrain roughness. The error variances were estimated as less than 8% of the total. The effect on the ratio of surface to gradient wind speeds was also assessed; it was suggested that the random function parameter $\sigma_{ln\epsilon}$ introduced in Chapter 3 be slightly reduced where rawinsonde data is not involved.

b) Methods of objective isobar analysis using synoptic data were investigated with a view to obtaining gradient and geostrophic wind climates. A quadratic representation of the horizontal pattern of atmospheric pressures yielded reasonable results as measured against simultaneous upper air data, despite the relative sparseness of the available observing stations. Under present circumstances, this is not recommended as a practical approach in large scale climatic wind studies.

CHAPTER 5

SOME APPLICATIONS AND GENERAL CONCLUSIONS

5.1 The Runway Orientation Problem

A critical factor in airport usability is the orientation of the runways relative to strong cross winds. In an account of the effects of weather on present-day air transportation, Beckwith (1971) has identified this as an area of considerable importance in airline economics. It is noted that modern jet aircraft are allowed to land on dry runways in a cross wind of up to 15.43 m/s (30 knots), but water, slush, ice or packed snow on runways may reduce this to 2.57 m/s (5 knots); other maxima for particular aircraft types may be determined by the operators, 10.29 m/s (20 knots) being a commonly quoted figure.

In general the optimum runway layout will be that which, on the basis of the surface mean wind distribution, will be usable for the greatest proportion of the time. In some circumstances the selection may be restricted by other non-meteorological constraints, such as the proximity of natural obstacles or heavily populated areas. Nevertheless, a rigorous analysis of the wind climate can also be made to indicate the best layout within any such constraints.

One approach to the optimization problem has been described by Jacobs (1961) and, more recently, an assessment of runway alignments was included in a study of four sites for the proposed third London airport (Dawson, 1972). With a view to the construction of a landing strip for space shuttle vehicles at Cape Kennedy, Falls and Brown (1972) have presented two methods for finding the optimum alignment, one

a manual method making use of the standard summary of wind speed and direction frequencies, and the other based on a bivariate normal distribution model. The latter is particularly useful since, for any proposed alignment, it permits easy computation of the cross wind probability distribution from only a few defining parameters which are usually included in the wind summary. The form of the bivariate normal density function was given earlier as Equation 2.1, in terms of the zonal and meridional axes, x and y. For any rotation of the x axis, ϕ, corresponding to a proposed runway orientation, it can be shown that the distribution can be rewritten in the same form, but with transformed parameters referred to the new system of coordinates $x';y'$. These are:

$$\bar{V}_{x'} = \bar{V}_x cos\,\phi + \bar{V}_y sin\,\phi$$

$$\bar{V}_{y'} = \bar{V}_y cos\,\phi + \bar{V}_x sin\,\phi$$

$$\sigma_{x'}^2 = \sigma_x^2 cos^2\phi + \sigma_y^2 sin^2\phi + 2r_{xy}\sigma_x\sigma_y cos\,\phi\,sin\,\phi$$

$$\sigma_{y'}^2 = \sigma_y^2 cos^2\phi + \sigma_x^2 sin^2\phi - 2r_{xy}\sigma_x\sigma_y cos\,\phi\,sin\,\phi$$

(5.1)

in which $\bar{V}_{x'}$, $\bar{V}_{y'}$, are the transformed component means and $\sigma_{x'}$, $\sigma_{y'}$ are the component standard deviations. r_{xy} is the correlation coefficient of the original components. From this it follows that the distribution of cross winds is univariate normal, that is

$$p(V_{y'}) = \frac{1}{\sigma_{y'}\sqrt{2\pi}} exp(-\frac{(V_{y'} - \bar{V}_{y'})^2}{2\sigma_{y'}^2})$$

(5.2)

The probability of exceeding a prescribed crosswind can then be found from normal probability tables.

Although this approach offers relative speed and convenience, a distribution model more flexible than the bivariate normal may be preferred; such may be the case where very strong winds are associated with a particular direction. In urban centres the local

wind climate is also much less likely to follow a regular form, and this will be a consideration in the planning of downtown terminals for short take-off and landing (STOL) aircraft. The synthesis of a suitable statistical description of the winds in these situations was discussed in Chapter 4 and, specifically in the context of STOL operations, in a recent report by Ramsdell and Powell (1973).

Approaching the problem in general terms, it is required that the modulus of the wind vector subtending an angle ϕ with a given runway not exceed $|V_c cosec\, \phi|$ for that runway to be operational, where V_c is the allowable cross wind component. Thus, in the case of two (or more) runways as shown in Figure 5.1, the maximum permissible wind speed of azimuth ϕ is the greater of $|V_c cosec\, \phi_1|$ and $|V_c cosec\, \phi_2|$. The event of total airport unusability is then represented by the shaded area outside the locus of maximum wind speeds and its probability can be conveniently estimated by taking small increments of ϕ. This has been done in the following example.

A surface mean wind summary was obtained for the decade 1960-69 at Moosonee, Ontario, including the frequency distribution between ten speed classes and sixteen sectors of wind direction. This was fitted by the method of least squares to the bivariate model based on a distinct Weibull distribution within each sector. Recalling the earlier discussion of Chapter 2, this can be written

$$P(V,\theta) = a(\theta)(1 - exp[-(\frac{V}{c(\theta)})^{k(\theta)}]) \qquad (5.3)$$

and the functions $a(\theta)$, $c(\theta)$ and $k(\theta)$ represented as finite term Fourier series. In this study four harmonics were employed for each, such that

$$k(\theta) = k_0 + \sum_{i=1}^{4} k_{1_i} \cos i\theta + \sum_{i=1}^{4} k_{2_i} \sin i\theta$$

$$c(\theta) = c_0 + \sum_{i=1}^{4} c_{1_i} \cos i\theta + \sum_{i=1}^{4} c_{2_i} \sin i\theta \qquad (5.4)$$

$$a(\theta) = a_0 + \sum_{i=1}^{4} a_{1_i} \cos i\theta + \sum_{i=1}^{4} a_{2_i} \sin i\theta$$
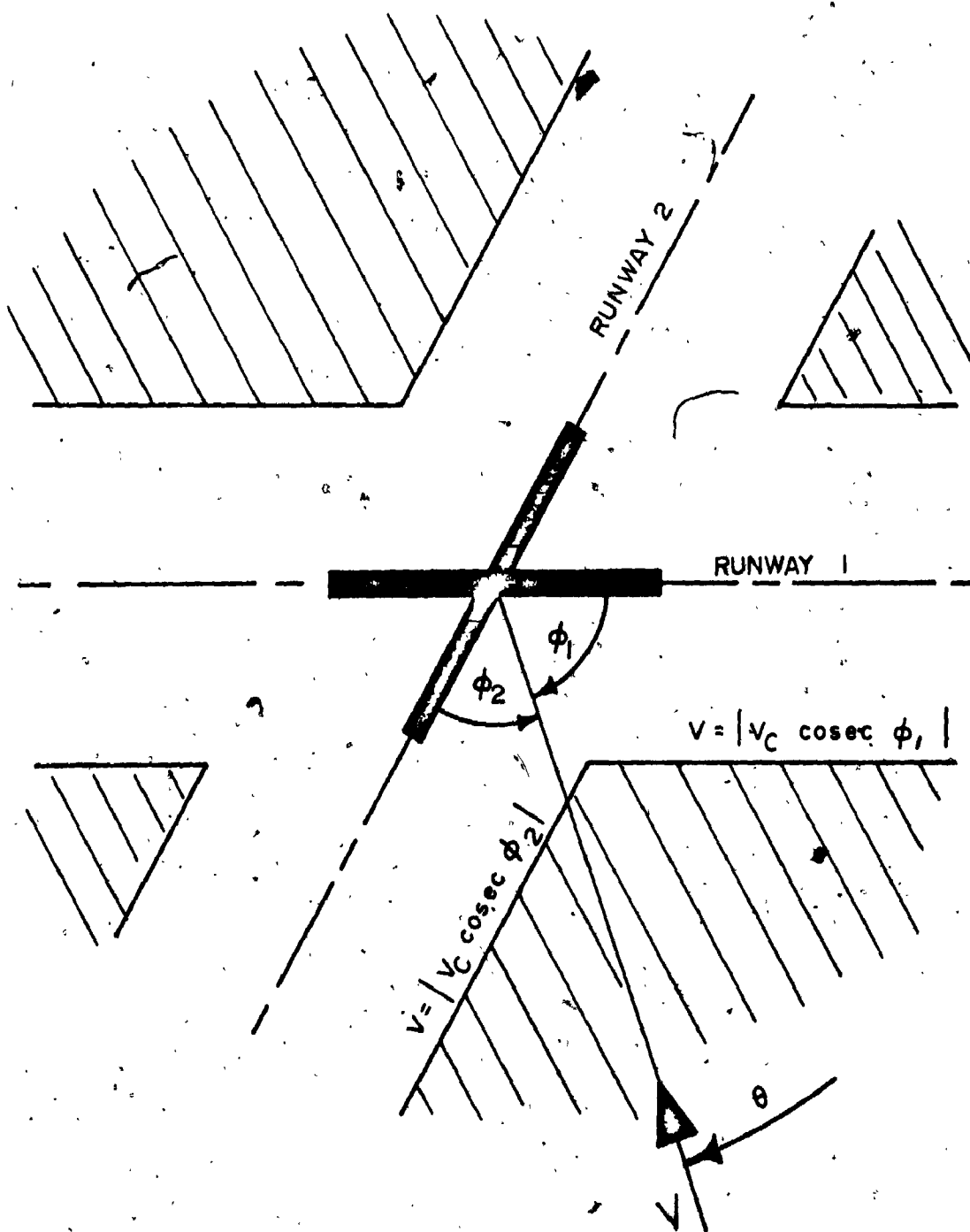
FIG. 5.1 SHOWING PERMISSIBLE WIND SPEED
V FROM DIRECTION θ, FOR GIVEN
MAXIMUM CROSS-WIND, V_C

with the necessary condition that

$$\int_0^{2\pi} a(\theta)d\theta = 1 \qquad (5.5)$$

The resulting fitted distribution is shown in Figure 5.2, and from this was computed the probabilities of airport unusability given one or two runways with all possible alignments at intervals of 10° from north (Tables 5.1 and 5.2). The optimum layouts consistent with maximum cross wind components of 10.29 and 15.43 m/s (20 and 30 knots) are illustrated in Figure 5.2. It will be noted that the single runway configuration does not correspond with either the prevailing wind direction (315°) or the direction of the vector mean wind (299°). As a further point of practical interest, it is clear that tables of probabilities similar to those given here can be used straightforwardly to select a second runway where one already exists. This is achieved by entering the table at the existing alignment and searching for the smallest value within the column and right to left diagonal below.

5.2 Power Generation from the Wind

With the increasing cost and sometimes curtailed supply of fossil fuels, attention has turned of late to alternative sources of energy, including the natural wind. This is hardly a novel idea; there is some evidence of the existance of windmills in the ancient civilizations of the eastern Mediterranean, and certainly they have been used in western Europe since the 12th century. Although employed primarily to grind corn and pump water, in the 1920's and 1930's the windmill was commonly adapted as a small domestic electrical power generator, notably in rural areas away from the commercial supply lines. With the exception of some isolated attempts to extract energy from the wind on a larger scale, there were no further developments in this field until quite recently. The lure of a "free", if somewhat capricious, power source has reawakened mankind's interest in the wind as a constructive force. The following section will be concerned with the influence of wind climate on power capacity and the identifisation of suitable statistical parameters.

ANNUAL
PROBABILITY DISTRIBUTION
OF SURFACE WINDS
[P(>v) PER 22.5° SECTOR]

10°
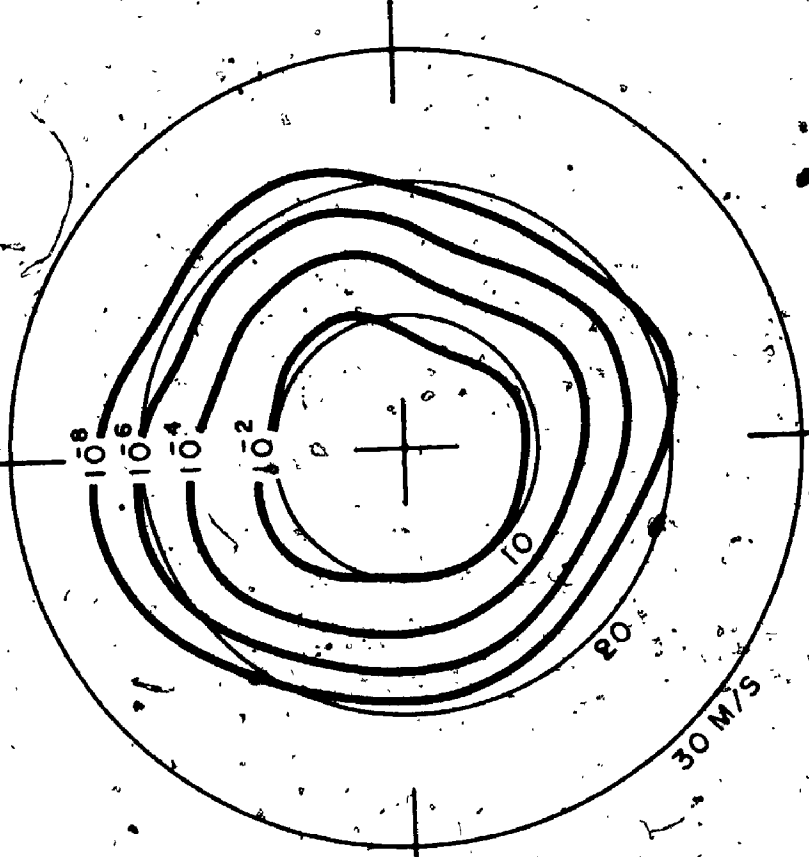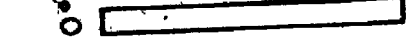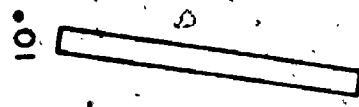
MAXIMUM CROSSWIND
15.43 M/S. (30 KNOTS)

50°

150°

MAXIMUM CROSSWIND
10.29 M/S (20 KNOTS)

0°

60°

150°

30 M/S

FIG. 5.2 OPTIMUM RUNWAY ORIENTATIONS AT MOOSONEE, ONT.

1.0
1.1
1.25
1.4
1.6
1.8
2.0
2.2
2.5
2.8
3.2
3.5
4.0

RESOLUTION TEST CHART
BUREAU OF STANDARDS 1963 A

ABC 274

RUNWAY 2 (DEG CLOCKWISE FROM 1)

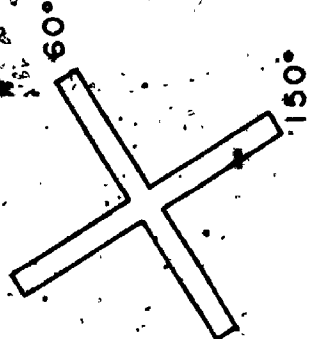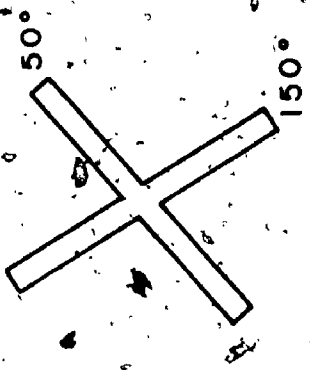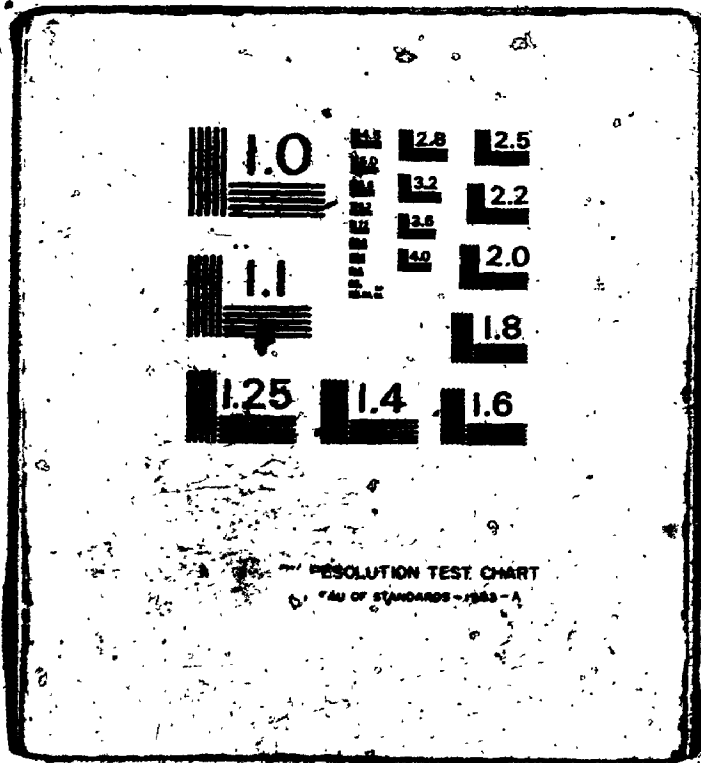|	0	10	20	30	40	50	60	70	80	90	100	110	120	130	140	150	160	170
0	.252 -2	.259 -2	.330 -2	.448 -2	.572 -2	.658 -2	.679 -2	.635 -2	.548 -2	.451 -2	.377 -2	.348 -2	.359 -2	.390 -2	.409 -2	.398 -2	.354 -2	.294 -2
10	.172 -2	.199 -2	.284 -2	.401 -2	.509 -2	.564 -2	.552 -2	.483 -2	.390 -2	.308 -2	.262 -2	.259 -2	.288 -2	.321 -2	.331 -2	.304 -2	.251 -2	
20	.115 -2	.157 -2	.242 -2	.346 -2	.425 -2	.447 -2	.408 -2	.331 -2	.252 -2	.197 -2	.178 -2	.193 -2	.225 -2	.250 -2	.245 -2	.208 -2		
30	.783 -3	.124 -2	.199 -2	.279 -2	.327 -2	.321 -2	.269 -2	.203 -2	.148 -2	.119 -2	.119 -2	.140 -2	.167 -2	.177 -2	.160 -2			
40	.538 -3	.940 -3	.153 -2	.206 -2	.226 -2	.203 -2	.156 -2	.109 -2	.790 -3	.689 -3	.769 -3	.959 -3	.112 -2	.111 -2				
50	.357 -3	.663 -3	.106 -2	.135 -2	.136 -2	.111 -2	.774 -3	.517 -3	.388 -3	.381 -3	.469 -3	.594 -3	.654 -3					
60	.216 -3	.415 -3	.642 -3	.756 -3	.685 -3	.500 -3	.321 -3	.212 -3	.174 -3	.195 -3	.256 -3	.315 -3						
70	.113 -3	.219 -3	.321 -3	.344 -3	.276 -3	.180 -3	.108 -3	.737 -4	.691 -4	.866 -4	.116 -3							
80	.474 -4	.913 -4	.124 -3	.118 -3	.830 -4	.479 -4	.278 -4	.208 -4	.226 -4	.312 -4								
90	.210 -4	.350 -4	.401 -4	.313 -4	.180 -4	.928 -5	.579 -5	.594 -5	.103 -4									
100	.421 -4	.447 -4	.334 -4	.179 -4	.848 -5	.598 -5	.863 -5	.197 -4										
110	.133 -3	.115 -3	.730 -4	.379 -4	.235 -4	.267 -4	.508 -4											
120	.314 -3	.240 -3	.145 -3	.850 -4	.724 -4	.109 -3												
130	.580 -3	.409 -3	.253 -3	.179 -3	.206 -3													
140	.896 -3	.613 -3	.413 -3	.374 -3														
150	.123 -2	.859 -3	.675 -3															
160	.157 -2	.119 -2																
170	.197 -2																	

NOTE: $.252 = .252 \times 10^{-2}$

TABLE 5.1 PROBABILITIES OF AIRPORT UNUSABILITY AT MOOSONEE, ONT. —
MAXIMUM CROSS WIND COMPONENT 10.29 M/S (20 KNOTS)

RUNWAY 1 (DEG FROM NORTH)

RUNWAY 2 (DEG CLOCKWISE FROM 1)	0	10	20	30	40	50	60	70	80	90	100	110	120	130	140	150	160	170
0	.376	.258	.466	.121	.266	.444	.5?3	.583	.482	.333	.208	.139	.124	.140	.159	.153	.119	.726
	-5	-5	-5	-4	-4	-4	-4	-4	-4	-4	-4	-4	-4	-4	-4	-4	-4	-5
10	.154	.160	.406	.112	.241	.383	.451	.406	.291	.177	.105	.796	.862	.107	.117	.100	.647	
	-5	-5	-5	-4	-4	-4	-4	-4	-4	-4	-4	-5	-5	-4	-4	-4	-5	
20	.631	.112	.343	.959	.198	.287	.299	.232	.143	.793	.500	.462	.580	.722	.717	.5?7		
	-6	-5	-5	-5	-4	-4	-4	-4	-4	-5	-5	-5	-5	-5	-5	-5		
30	.294	.781	.265	.730	.139	.179	.160	.105	.570	.309	.228	.259	.349	.408	.345			
	-6	-6	-5	-5	-4	-4	-4	-4	-5	-5	-5	-5	-5	-5	-5			
40	.143	.495	.178	.470	.805	.890	.667	.372	.184	.107	.976	.129	.174	.179				
	-6	-6	-5	-5	-5	-5	-5	-5	-5	-5	-6	-5	-5	-5				
50	.629	.264	.982	.241	.360	.333	.205	.984	.474	.323	.364	.523	.654					
	-7	-6	-6	-5	-5	-5	-5	-6	-6	-6	-6	-6	-6					
60	.222	.110	.411	.914	.115	.868	.438	.186	.942	.789	.106	.154						
	-7	-6	-6	-6	-5	-6	-6	-6	-7	-7	-6	-6						
70	.558	.321	.118	.231	.239	.142	.583	.229	.131	.136	.205							
	-8	-7	-6	-6	-6	-6	-7	-7	-7	-7	-7							
80	.836	.558	.199	.334	.272	.123	.406	.154	.105	.134								
	-9	-8	-7	-7	-7	-7	-8	-8	-8	-8								
90	.111	.534	.162	.216	.129	.414	.108	.415	.389									
	-9	-9	-8	-8	-8	-9	-9	-10	-10									
100	.214	.254	.161	.482	.777	.147	.179	.984										
	-8	-8	-8	-9	-10	-10	-10	-10										
110	.281	.241	.108	.247	.451	.305	.953											
	-7	-7	-7	-8	-9	-9	-9											
120	.166	.106	.374	.849	.319	.544												
	-6	-6	-7	-8	-8	-8												
130	.551	.278	.866	.236	.226													
	-6	-6	-7	-7	-7													
140	.121	.518	.165	.825														
	-5	-6	-6	-7														
150	.197	.786	.306															
	-5	-6	-6															
160	.265	.109																
	-5	-5																
170	.320																	
	-5																	

NOTE: $.376 = .376 \times 10^{-5}$
$\quad\;\; -5$

TABLE 5.2 PROBABILITY OF AIRPORT UNUSABILITY AT MOOSONEE, ONT. – MAXIMUM CROSS WIND COMPONENT 15.43 M/S (30 KNOTS)

The theory of windmills and fans has been given in Durand (1963). The energy of the air passing through the fan disc of radius R in unit time is proportional to the cube of the wind speed, V, as

$$E = \frac{1}{2} \pi R^2 \rho V^3 \qquad (5.6)$$

where ρ is the air density. However, it can be shown that the theoretical maximum power extracted is only 59.3% (16/27) of this, and the proportion is further reduced by the profile and induced drag of the rotor, depending on the particular design. In this respect a fast running windmill with only a few blades may be preferred (it also requires less mechanical gearing to drive a generator) over a slow running machine with a large number of blades. The latter will deliver a smaller percentage of the available power at its best operating speed, but a significant advantage is it's higher starting torque, thus enabling a more rapid cut-in after a lull in the wind. Durand has shown that the optimum operating condition is determined by the ratio of the blade tip velocity to the incident wind velocity; for fast running windmills this ratio may be 3 or higher and, for the slow machines, closer to unity. In practice, the desirability of maintaining this ratio throughout the operating range of wind speeds must be offset against the need for a fairly constant rotational velocity at the generator. It has been common to accept some loss of performance up to the design or rated wind speed for the rotor, and then to control the output above this speed by variable pitch blades, ailerons or some other form of governor. An additional decrease in the extracted power can be expected due to mechanical and generator losses, and there is now some indication that atmospheric turbulence contributes significantly to the overall reduction (Base, 1974).

The final ratio of power generated to power available in the incident flow is termed the overall power coefficient. Even for a two bladed rotor this seldom exceeds a value of 0.4.

To determine the effect of wind climate on windmill performance, it is necessary to define three design wind speeds; firstly, the cut-in velocity, V_i, at which electrical power generation begins (when the power developed just overcomes the no-load losses);

secondly, the rated wind speed, V_p, and finally the furling speed, V_f, at which it is necessary to close down the plant to avoid wind damage. It is assumed that the output is governed such that a constant rated power is developed at and above V_p, and that the overall power coefficient is effectively constant over the operating range. The annual distributions of wind speed and power can then be represented by the velocity- and power-duration curves, in which the power ordinate is simply the cube of the velocity ordinate at the same probability level (see Golding, 1957, and Figure 5.3). The annual output of energy can be measured by the unshaded area under the power-duration curve, expressed as a fraction of the rated power (or, strictly, the rectangular area indicated in the figure). The resulting parameter, called the specific output, T_s, can be interpreted as an equivalent proportion of the year during which a wind plant, in the given annual wind climate and with the particular design velocities, would deliver its full rated power.

Specific outputs have been computed for Weibull wind speed distributions regardless of direction (Equation 5.3, independent of θ) having values of the parameter c between 5 and 20 m/s and $k = 1.5, 2.0$ (the Rayleigh distribution) or 2.5. Windmills with rated velocities of 10, 15 and 20 m/s were considered and it was assumed in all cases that the no-load loss is 15% of the rated power, implying that

$$V_i = 0.531 \, V_p \qquad\qquad (5.7)$$

A furling speed of 27 m/s was also assumed. The results, which pertain to typical operating conditions, are shown in Figure 5.4. It is clear that windmills with lower rated velocities will generally yield higher specific outputs, although a larger rotor diameter would be required to produce as much power as a faster machine. It also appears that wind climates characterized by low values of k offer some advantage. However, it has been noted (Hogan, 1971) that this is usually accompanied by smaller c values, and hence a reduced specific output. Furthermore, Figure 5.4 shows that, in the range of c usually applicable to surface wind climate, the Rayleigh distribution is an adequate model for these purposes. It follows that T_s can be regarded as a
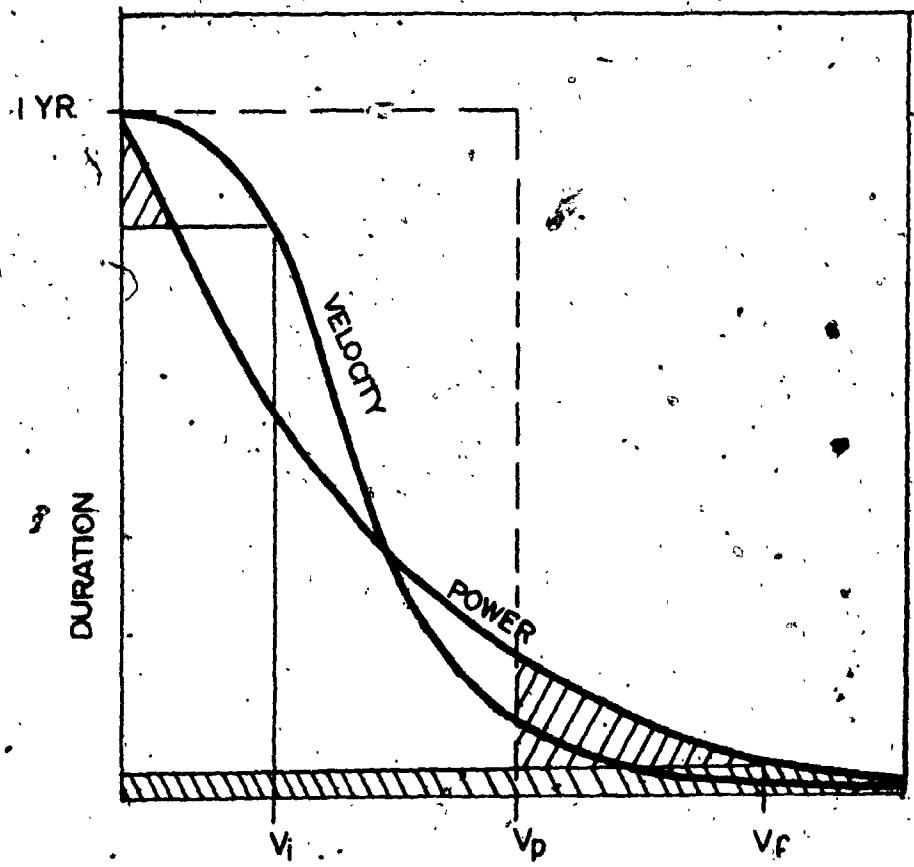
FIG. 5.3 VELOCITY AND POWER-DURATION CURVES
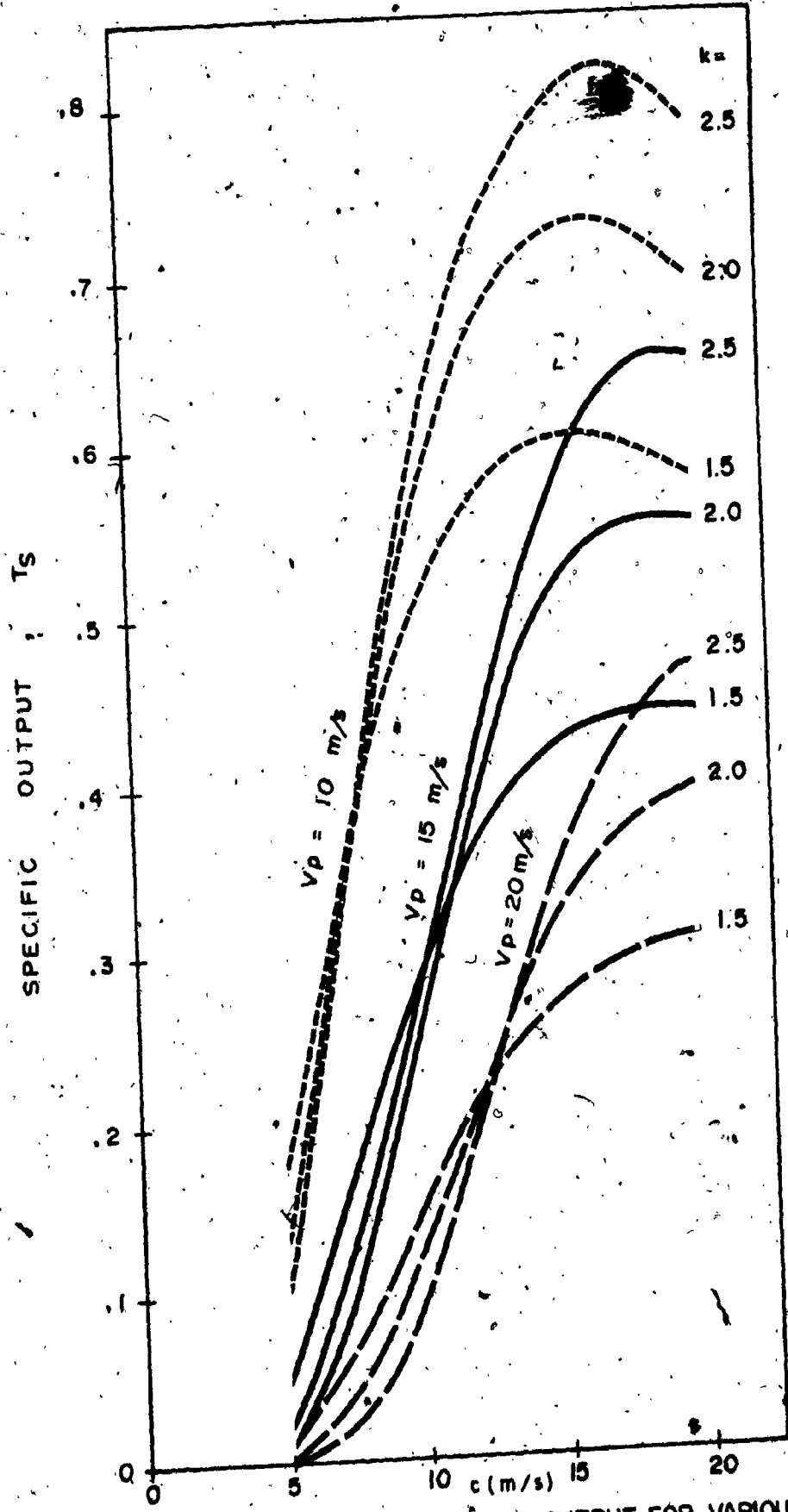
FIG. 5·4 CURVES OF SPECIFIC POWER OUTPUT FOR VARIOUS
WEIBULL WIND SPEED DISTRIBUTIONS AND RATED
VELOCITIES

function of the mean annual wind speed, and this is given in Figure 5.5. The new curves are similar to those obtained empirically by Tagg (1957) from observations at a number of potential wind power generating sites in the British Isles.

It has been seen that the sole statistic usually required to judge the suitability of the location of a proposed wind plant is the mean annual wind speed. Fortunately, this is commonly quoted in, climatic publications, for example, in "The Climate of Canada" (DOT, 1962). Table 5.3, which has been prepared from data contained in this source, lists 45 observing stations in all parts of Canada according to mean wind speed. Although the values in individual cases may be unduly influenced by local factors, the most advantageous sites in Canada appear to be along the Atlantic seaboard and in some areas of Manitoba and Saskatchewan. Perhaps a better idea of the regional variations in wind climate can be had by considering the standard vector deviation of gradient winds, σ_G (see Figure 5.6). As suggested in Chapter 3, the expected surface wind speed can be estimated from (Equation 3.60):

$$\bar{V} = 1.29 \, \bar{K} \, \sigma_G \qquad (5.8)$$

depending on terrain and topography; this is represented in $\bar{K}$, the average ratio of surface to gradient winds taken over all directions. Of course, wherever possible it would be desirable to place the windmill in open ground, on top of a hill, or on a tower, although the latter course might impose unjustifiable capital and maintenance costs as well as additional wind loading problems.

Finally, a note can be added on the expected duration of any interval when a windmill would be inoperative due to insufficient wind. This is of interest in the design of energy storage devices which could ensure a continued power supply on such occasions. Now, by considering the wind speed as a continuous random process with a Rayleigh probability density function, it has been suggested (see Rice, 1954, and Davenport, 1968) that the expected number of crossings of a level V in unit time is
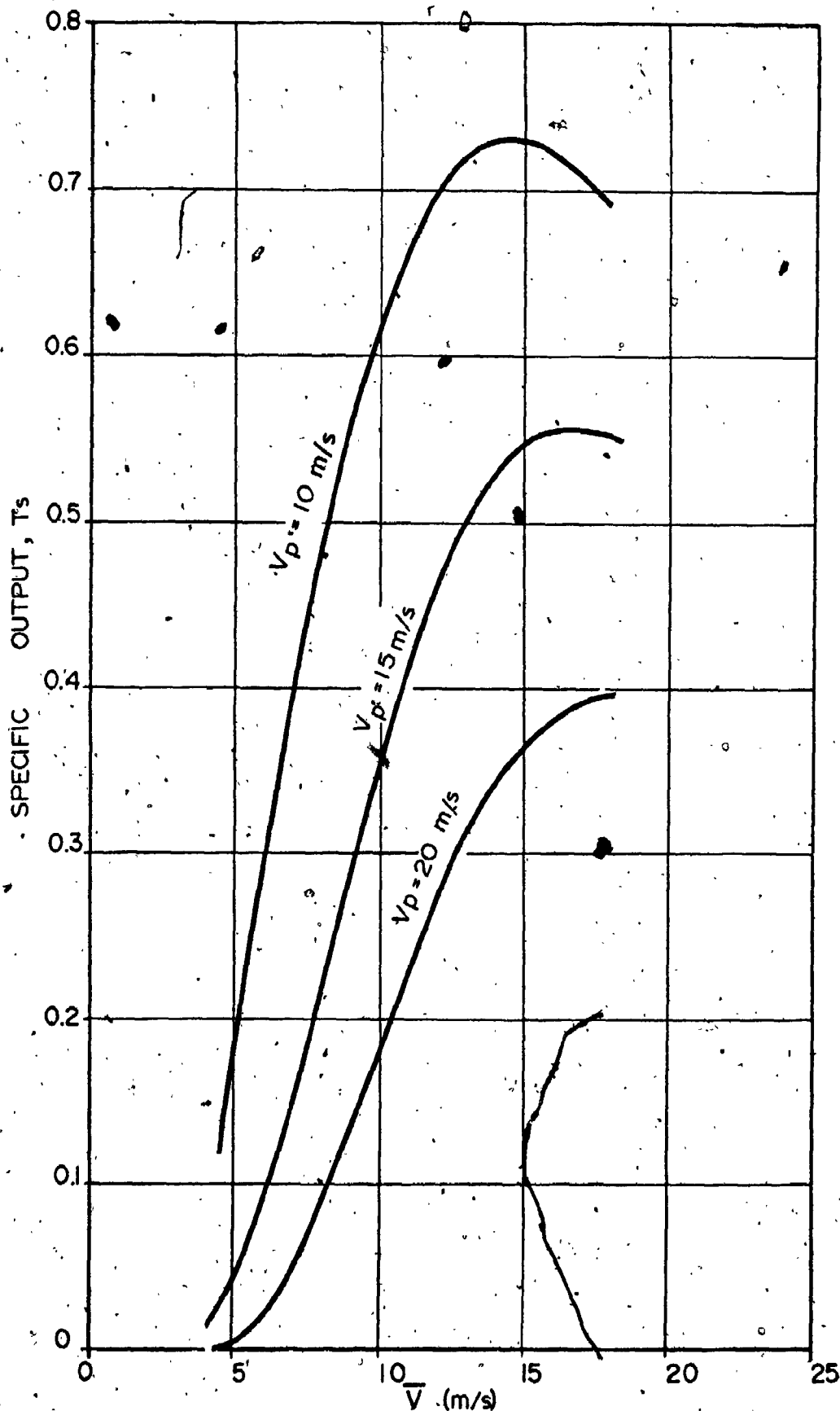
FIG. 5.5   CURVES OF SPECIFIC   POWER OUTPUT VERSUS
MEAN WIND SPEED (RAYLEIGH DISTRIBUTED)
FOR VARIOUS   RATED VELOCITIES

STATION		$\bar{V}$ (m/s)	
St. John's	Nfld	7.02	7.0
Swift Current	Sask	6.66	6.5
Gander	Nfld	6.26	
Churchill	Man	6.25	6.0
Moncton	N.B.	5.77	
Regina	Sask	5.77	
Coral Harbour	NWT	5.72	
Winnipeg	Man.	5.72	
Sydney	N.S.	5.68	5.5
Charlottetown	PEI	5.32	
Cambridge Bay	NWT	5.27	
Yarmouth	N.S.	5.23	
Toronto	Ont	5.19	
Saskatoon	Sask	5.05	5.0
Montreal	Que	4.96	
Victoria	B.C.	4.96	
Resolute	NWT	4.83	
Sept Illes	Que	4.83	
Bagotville	Que	4.78	
St. John	N.B.	4.78	
North Bay	Ont	4.74	
The Pas	Man	4.74	
Frobisher Bay	NWT	4.65	
Ottawa	Ont	4.60	
Halifax	N.S.	4.60	
Knob Lake	Que	4.56	
London	Ont	4.51	
Yellowknife	NWT	4.51	4.5
Calgary	Alta	4.43	
Kapuskasing	Ont	4.34	
Goose Bay	Nfld.	4.25	
Grande Prairie	Alta	4.11	
Thunder Bay	Ont	4.11	
Quebec City	Que	4.07	4.0
Chatham	N.B.	3.98	
Edmonton	Alta	3.93	
Whitehorse	Yuk	3.89	
Vancouver	B.C.	3.62	3.5
Penticton	B.C.	3.44	
Ft. Simpson	NWT	3.35	
Prince George	B.C.	3.31	3.0
Aklavik	NWT	2.91	
Prince Rupert	B.C.	2.86	2.5
Alert	NWT	2.41	
Ft. Nelson	B.C.	2.28	

TABLE 5.3 MEAN ANNUAL WIND SPEEDS IN CANADA
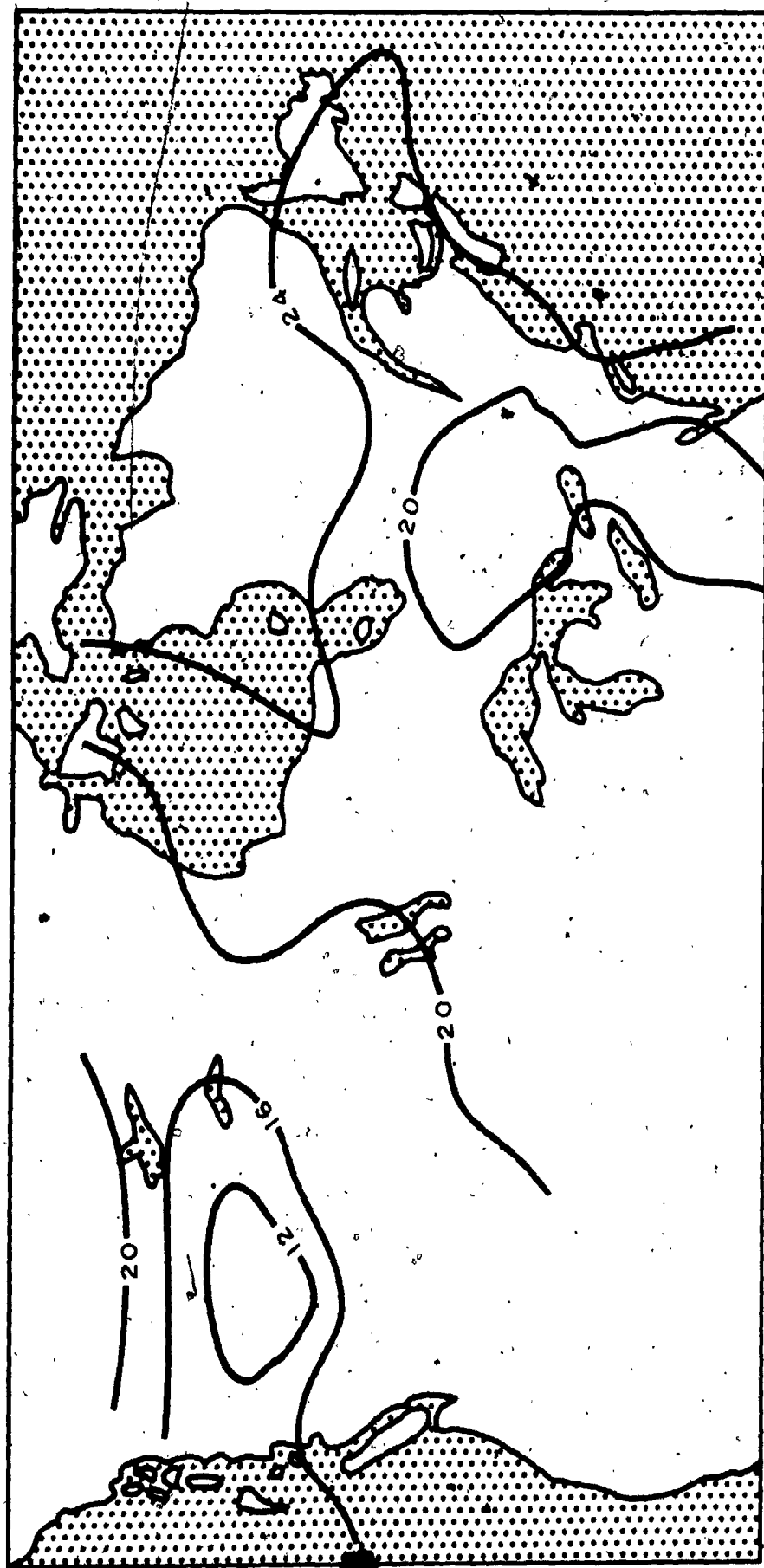
FIG. 5.6 ANNUAL STANDARD VECTOR DEVIATIONS OF WINDS AT 500 M.
(CONTOURS IN MPH; 1 MPH = 0.447 M/S) (FROM BAYNES, 1971)

$$N_V = \sqrt{2\pi}\ \nu\ \frac{V}{\sigma}\ exp(-\frac{V^2}{2\sigma^2})$$

<div align="right">(5.9)</div>

where ν is the effective cycling rate of the process, defined earlier in Equation 2.36, and σ is a measure of the statistical deviation related to the parameter c by $c = \sqrt{2}\sigma$. It is assumed that the distribution of the rate of change of velocity, V', is Gaussian and that V and V' are independent. The average length of the interval during which the process dips below a value V can therefore be given by

$$\bar{\tau} = \frac{P(<V)}{N_V} = \frac{1 - exp(-V^2/c^2)}{N_V}$$

$$= \frac{c}{2\sqrt{\pi}\nu V}(exp(-\frac{V^2}{c^2}) - 1)$$

<div align="right">(5.10)</div>

For this application, V is taken as the cut-in velocity, and since the mean wind speed is a constant proportion of c, $\bar{\tau}$ can be expressed as a function of $\bar{V}/V_i$. This has been done in Figure 5.7, with ν given a representative value of 0.1 cy/hr.

5.3 Extreme Winds and Wave Heights over Oceans

Since the generation of ocean waves is linked with the occurence of strong winds, it is reasonable to expect that the extreme value distributions of both will be in some way related. This notion is of some practical importance because wind climate, particularly at upper levels, is generally better defined than the distribution of wave heights. Drawing on the statistical theory of waves as a random process, combined with the empirical results reported in some recent publications, a simple approach to the prediction of extreme waves over the open ocean is discussed below.

The statistical distribution of waves has been considered by Cartwright and Longuet-Higgins (1956), beginning with the model of a continous, random and stationary function, $f(t)$. The probability density of the normalized crest height is then given by
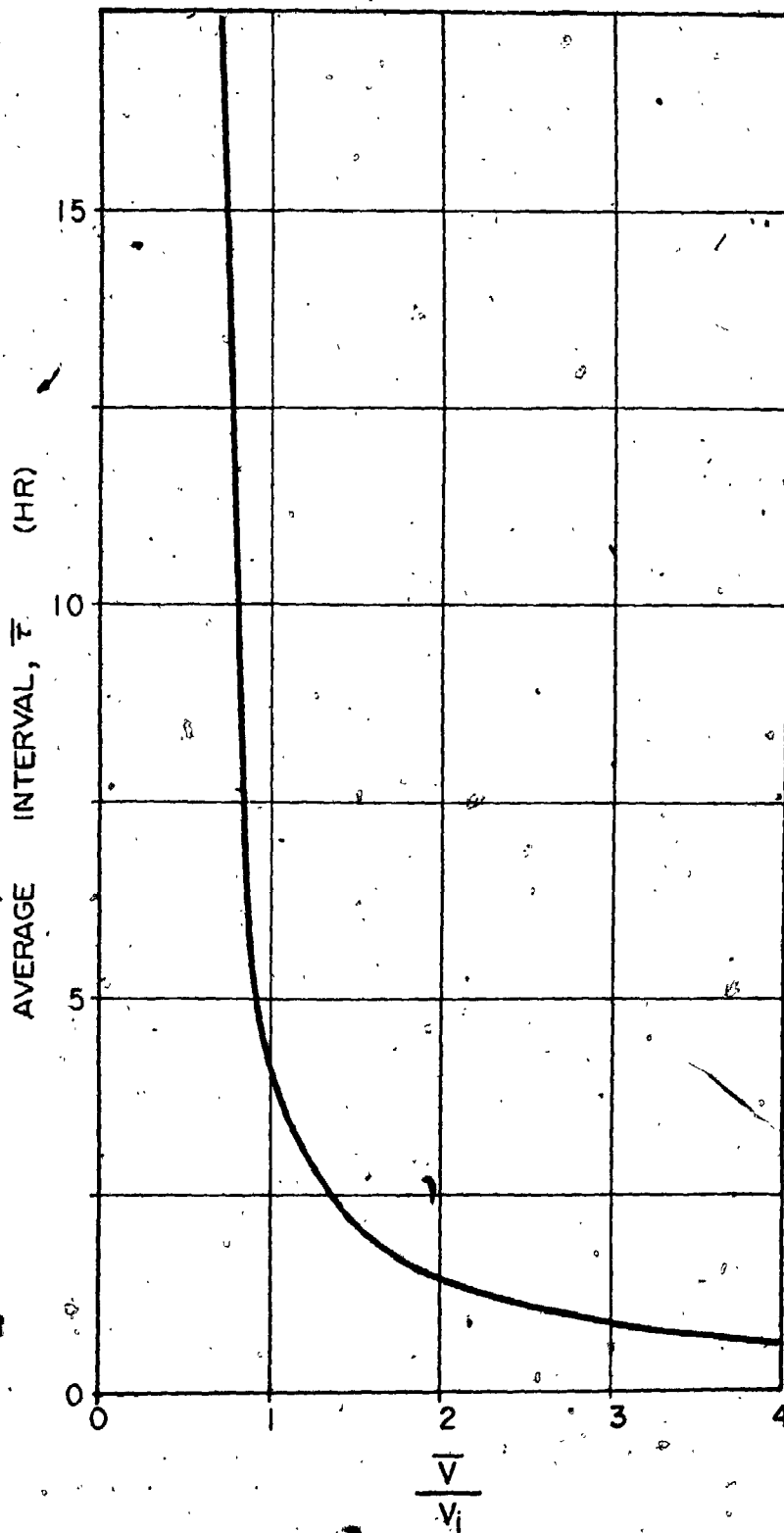
FIG.5.7 AVERAGE LENGTH OF INTERVAL DURING WHICH
WIND SPEED REMAINS BELOW THE CUT-IN
SPEED, Vi (FOR VARIOUS RAYLEIGH
WIND SPEED DISTRIBUTIONS WITH
MEAN VALUE $\overline{V}$)

$$q(\eta) = \frac{1}{\sqrt{2\pi}} \left(\epsilon \exp\left(-\frac{\eta^2}{2\epsilon^2}\right) + (1 - \epsilon^2)^{1/2} \eta \exp\left(-\frac{\eta^2}{2}\right) \right.$$

$$\left. \cdot \int_{-\infty}^{\eta(1-\epsilon^2)^{1/2}/\epsilon} \exp\left(-\frac{\eta^2}{2}\right) d\eta \right)$$

in which ϵ is determined by the various moments, λ_j,

$$\epsilon = \left(1 - \frac{\lambda_2^2}{\lambda_0 \lambda_4}\right)^{1/2}$$

η is measured with respect to the mean level of the fu
by $\lambda_0^{1/2}$. ϵ takes a value between 0 and 1; the two lim
to an infinitely narrow-banded process with a Rayleigh
widely distributed energy spectrum with a normal pro
can be physically realised where high-frequency ripples
on lower-frequency motion, or "swell". When swell a
the waves which persist away from the area of genera
more closely Rayleigh.

The extreme value distribution can be obtained
Davenport, 1964) with the restrictions of $\epsilon \neq 1$, a l
values of η. It can be written

$$P(>\eta) = 1 - \exp\left(-\nu_w \tau_w \exp\left(-\frac{\eta^2}{2}\right)\right)$$

giving the probability of exceeding η in a period
distribution of peak gust factors employed in Chapt
estimated cycling rate of the wave process has been
the sampling rate, N_w, has been shown by Rice (
so it follows from the definition of ϵ in (5.12) th

$$\nu_w = N_w (1 - \epsilon^2)^{1/2}$$

Clearly, as ϵ approaches zero, the cycling rate ap

properties of the distribution can be studied through such statistics as the mean value, the mode and the standard deviation, given by Davenport for $\nu_w \tau_w$ large. Under these circumstances the distribution of extreme crest heights can be represented by the familiar Type I form:

$$P(\eta) = exp[-exp(-a(\eta - U))]$$ (5.15)

in which the mode, U, is given by

$$U = (2ln\,\nu_w \tau_w)^{1/2}$$ (5.16)

and the dispersion

$$\frac{1}{a} = (2ln\,\nu_w \tau_w)^{-1/2}$$ (5.17)

The customary measure of wave height, H, is defined as the difference in level between a crest and the preceding trough. Its theoretical distribution is, in general, more difficult to obtain but, if η is Rayleigh, it is to be expected that H is distributed in like manner. Furthermore, for the purposes of extreme wave prediction, processes exhibiting a value of ϵ much greater than zero but less than 1 might be similarly treated with an equivalent number of maxima per unit time, ν_w, and a mean value given by (Weigel, 1964)

$$\bar{H} = \sqrt{\frac{\pi}{2}}\,\sigma_H \frac{\nu_w}{N_w} = \sqrt{\frac{\pi}{2}}\,\sigma_H (1 - \epsilon^2)^{1/2}$$ (5.18)

where σ_H is the r.m.s. value of H. The cumulative probability of H can be written

$$Q(H) = 1 - exp(-\frac{H^2}{2\sigma_H^2})$$ (5.19)

It is useful to obtain from this the annual extreme distribution of wave heights in terms of the extreme wind climate. To do this, it is first necessary to invoke some

relationship between the mean wave height and mean wind. Wiegel (1964) has collected together some relevant data which suggest the following as a reasonable approximation:

$$\bar{H} = 0.27 \, V \qquad (5.20)$$

in which the constant has units of m/m/sec. This is a considerable simplification, and in particular situations $\bar{H}$ will depend on the wind duration and fetch, but overall it appears to be representative of extreme conditions in the open ocean. Assuming the wind speed, V, closely follows the Rayleigh distribution, Equations 5.18 and 5.20 can now be used to give the cumulative probability of σ_H:

$$Q(\sigma_H) = 1 - exp(-\frac{K \, \sigma_H^2}{c^2}) \qquad (5.21)$$

where c is the Rayleigh parameter of wind speed and K is a constant formed from the coefficients in the equations.

Following the approach used in the previous section to estimate the number of crossings at a certain level of a random function, the expected crossing rate at H for the Rayleigh distributed function is (Rice, 1954, and Davenport, 1968)

$$N_H = \sqrt{\frac{\pi}{2}} \, \nu_e \, \frac{H}{\sigma_H} \, exp(-\frac{H^2}{2\sigma_H^2}) \qquad (5.22)$$

where ν_e is the effective cycling rate of the wave heights or envelope of η. The formulation must take account of the non-stationarity implied by the variation of σ_H over a one year period. This can be done by integrating (5.22) over all σ_H as

$$N_H = \int_0^\infty \sqrt{\frac{\pi}{2}} \, \nu_e \, \frac{H}{\sigma_H} \, exp(-\frac{H^2}{2\sigma_H^2}) \, q(\sigma_H) d\sigma_H \qquad (5.23)$$

which becomes

$$N_H = \frac{\pi}{\sqrt{2}} \, \nu_e \, \frac{KH}{c} \, exp(-\frac{\sqrt{2} \, KH}{c}) \qquad (5.24)$$

The probability distribution of extreme values is then obtained by considering crossings at high levels of H as rare events described by the Poisson distribution. This results in a function of the Fisher-Tippett Type I. The expression can be simplified by assuming that the distribution is narrow about its mode in the manner previously adopted by Davenport (1968). After some manipulation it is found that the Type I parameters are given by

$$a_H = \sqrt{2} \frac{K}{c} \left(1 - \frac{1}{\ln \frac{\pi}{\sqrt{2}} \nu_e \tau}\right) \qquad (5.25)$$

and

$$a_H U_H = \ln \frac{\pi}{\sqrt{2}} \nu_e \tau + \ln\left(\frac{1}{\sqrt{2}} \ln \frac{\pi}{\sqrt{2}} \nu_e \tau\right) - 1 \qquad (5.26)$$

in which U_H and $1/a_H$ are the mode and dispersion and τ is the relevant period (one year). The grouping $a_H U_H$ is apparently independent of the wind climate but a difficulty arises in its evaluation due to the uncertain cycling rate of the envelope process. Empirically, Thom (1973) has fitted several records of extreme waves to the Type II distribution and suggests a universal value for the shape parameter of about 6. When this is transformed to the Type I by fitting the two curves at a common mode (see Chapter 2), the corresponding value of $a_H U_H$ is identical. In the absence of more direct evidence this will be used in the forthcoming examples. Also, the dispersion can be approximated in terms of the mode of the annual extreme distribution of mean wind speeds, U_V. Provided that the parent distribution can be regarded as Rayleigh, this is

$$U_V = c(\ln \nu \tau)^{1/2} \qquad (5.27)$$

where ν is the average cycling rate of the wind process (about 0.1 cy/hr.). In summary, the distribution function of maximum wave heights can be estimated from

$$U_H = 0.44 \ U_V; \quad a_H U_H = 6 \qquad (5.28)$$

where the term $(1 - \epsilon^2)^{1/2}$ in K has been assigned the representative value of 0.8.

Table 5.4 shows calculated maximum wave heights at 4 Ocean Station Vessels (OSV's) in the northwest Atlantic. Since surface wind data for ocean regions is usually limited, it is often necessary, as has been done here, to resort to the available charts of upper air circulation, such as those compiled by Brooks et al (1950). This source gives the standard vector deviations of winds at the 700 mb pressure surface, but these must be reduced by about 10% to provide estimates of the same statistic at gradient height, σ_G. The expected surface wind speed then follows from Equation 5.8, given a suitable value for the average ratio of surface to gradient winds (taken here as 0.8). This in turn leads directly to the required parameters, given in the table together with the 10 and 50-year return period wave heights. The figures in parentheses are those projected by Thom (1971) from actual measurements using the Type II model. The comparison is further illustrated in Figure 5.8 which shows complete distributions for OSVs A and D.

It appears that the simplified procedure proposed above is both convenient and reasonably representative of actual conditions. There is reason to believe, however, that the approach should be modified for areas susceptible to hurricanes since the wind speeds recorded in storms of tropical origin appear to follow separate distributions. Thom has proposed a mixed extreme distribution of wind speeds of the general form

$$P(V) = (1 - p_t) P(V_e) + p_t P(V_t) \qquad\qquad (5.29)$$

where subscripts e and t refer respectively to extratropical and tropical winds and p_t is the probability of a tropical storm occuring at a given location. Referring to Appendix III of this thesis (Table III.2), this influence is manifested in some unusually high values of the Type I parameter grouping $I/\alpha U$, notably at stations in India, Hong Kong and along the Atlantic seaboard of the United States.

5.4 General conclusions

Several aspects of the statistical properties of strong winds have been studied. The principal features of the work and the conclusions arising from it have been given

POSITION		OSV			
	A	B	C	D	E
	60°00'N	56°30'N	52°45'N	44°00'N	35°00'N
	33°00'W	51°00'W	35°30'W	41°00'W	48°00'W
σ_G (m/s)	12.96	12.51	12.96	11.52	9.72
$\dot{U}_V$ (m/s)	39.3	37.9	39.3	35.0	29.5
a_V (s/m)	.341	.353	.341	.384	.455
U_H (m)	17.3	16.7	17.3	15.4	13.0
a_H (/m)	.347	.359	.347	.390	.462
H_{10} (m)	23.9 (25.6)	23.1 (23.5)	23.9 (22.3)	21.3 (22.3)	18.0 (19.8)
H_{50} (m)	28.6 (33.2)	27.6 (29.0)	28.6 (25.9)	25.4 (25.9)	21.5 (23.8)

TABLE 5.4 CALCULATED ANNUAL EXTREME WIND AND WAVE HEIGHT
PARAMETERS AT OCEAN STATION VESSELS (OSV'S)
IN THE NORTHWEST ATLANTIC
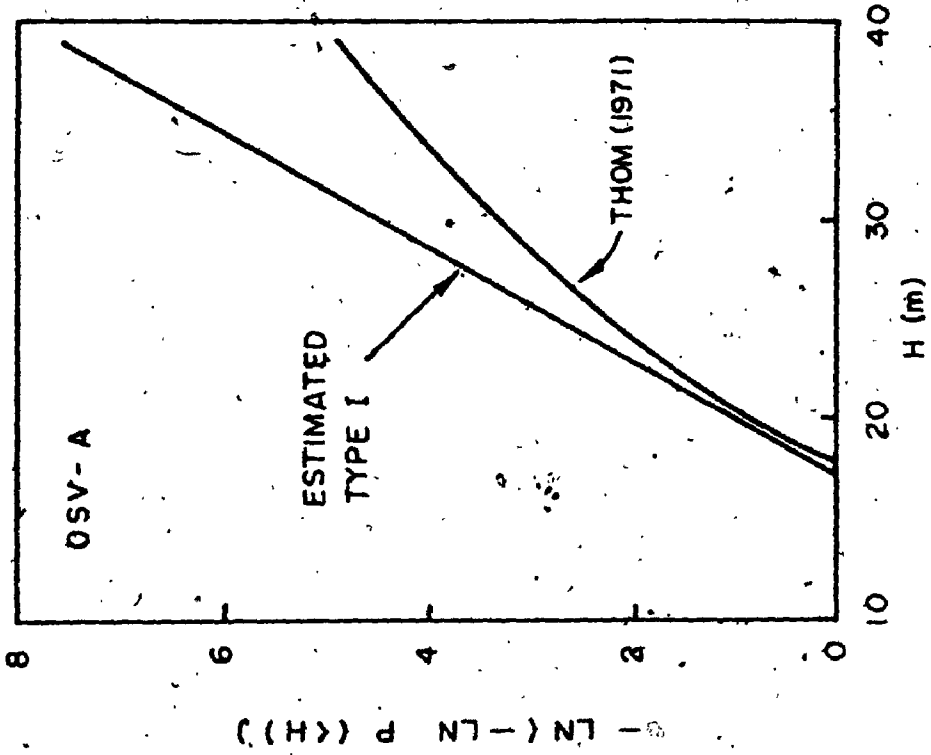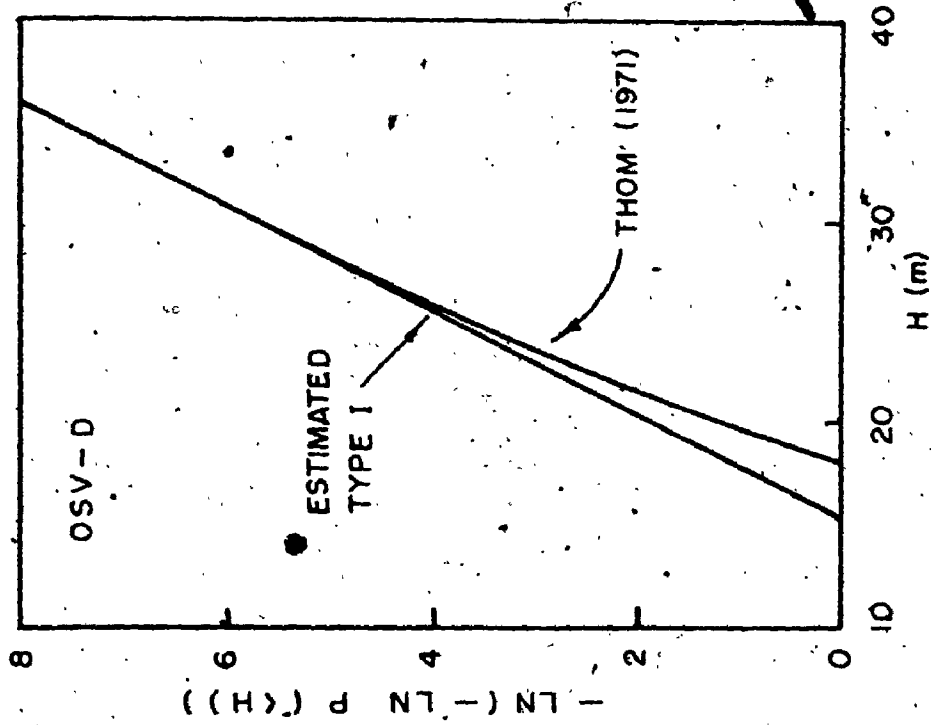
FIG. 5.8   EXTREME WAVE HEIGHT DISTRIBUTIONS AT OCEAN STATION VESSELS (OSV'S) A AND D

at the end of each chapter, but they will be summarised as follows:

a)   The Rayleigh distribution model of wind speeds was re-examined and its suitability, particularly at the upper levels, was generally confirmed.

b)   Theoretical relationships between the extreme value distributions of peak gust speeds and mean hourlies were developed and compared with some observational data. The evident scatter about the predicted functions was attributed, in part, to non-uniform terrain roughness around the observing stations.

c)   Considerations of such data properties and the inter-relation of various extreme value distributions then enabled the compilation of a set of consistent wind statistics for a number of locations around the world.

d)   A boundary layer similarity model was used to predict the mean surface wind from the mean gradient wind in neutrally stratified atmospheres. However, it appears that this can only be applied successfully under ideal fetch conditions.

e)   A general probabilistic approach to the prediction of surface wind climate was formulated, leading to a simple expression for the surface mean and standard deviation as a function of the gradient standard vector deviation. On the basis of a study of three Canadian sites this model was judged to provide a particularly useful description of surface wind speeds.

f)   The methodology for synthesising wind climate at a given site was reviewed and defined.

g)   Errors in the normal rawinsonde system for measuring gradient winds were analysed and the effects on the recorded variance of wind speeds was assessed for representative conditions. The error contribution was found to be less than 8%.

h)   Gradient and geostrophic wind climates at a number of Canadian locations were computed for a one year period using objective isobar analysis. In some cases the results compared very favourably with statistics derived from simultaneous upper air observations, but this was not recommended as a practical approach because of the extensive computational effort required.

By way of illustration, three applications of wind statistics have been discussed, utilizing some of the results of this work. A method for computing optimum runway alignments from general bivariate distributions of wind velocity was developed. It was then shown that the critical statistic in determining the best position for a wind power generating plant is the mean annual wind speed and hence, disregarding local influences, the standard vector deviation of gradient winds. Finally, a new and apparently successful method was proposed for the prediction of extreme wave heights in relation to extreme wind speeds over the open ocean.

5.5 Recommendations for Future Research

Many of the limitations of the present study, which are individually identified in the preceding chapters, will themselves suggest further work on specific points. However, broader avenues of investigation can be identified as follows:

a)   The practical suitability of the Weibull and Rayleigh distribution functions to describe surface and upper level winds should be re-examined. A useful course might be to consider a variety of wind records, classified according to the terrain and topography around the observing station, as well as the climate type of the region.

b)   There exists a continuing requirement for a general and easily applied description of the mean wind spiral in the atmospheric boundary layer. In the meantime, the probabilistic model introduced in Chapter 3 should be examined to include the effects of wind veering; thus providing a bivariate surface distribution directly from the gradient wind climate. A further statistical study of wind veering might be a fruitful first step.

c) More investigation of the rawinsonde system for measuring gradient winds is
required. This would include a closer definition of gradient height and the bias arising
from the regular 12-hour spacing of balloon flights. As more upper level data becomes
available, a new study of gradient wind climate over Canada might be undertaken.

7

APPENDIX I

EXTREME DISTRIBUTIONS OF MEAN WIND SPEEDS AND GUSTS

I.1 General

A general relationship between the parameters of the Fisher-Tippett Type I distributions of extreme mean hourly wind speeds and peak gusts will be developed below. This will, of course, depend on the nature of the upwind terrain and the accepted definition of the term "gust", these factors being reflected in a mean gust factor appropriate to the situation. In a simple approach it might be expected that the relationship consists only of a proportionality between the respective modes and dispersions, the connecting constant being the mean gust factor. However, this would imply that the maximum peak gust always occurs in the same record interval as the maximum mean hourly, and this is not necessarily true.

In approaching the problem a model will be required of the annual probability of mean winds. This could be the Weibull distribution, thus providing a straight-forward connection between its parameters and the various parameters of the distributions of the maxima, or the more complex model derived from a consideration of wind as a continuous stochastic process. Although the second model perhaps offers a truer picture, the multitude of defining parameters would render the end result of this analysis somewhat impractical. Instead, a slightly less rigorous variation will be employed in which the annual record of wind speed will be taken as one continuous process with a Weibull probability distribution, rather than a number of separate monthly or seasonal processes. In this way the defining parameters of the parent distribution can be reduced to two.

The second essential ingredient is a probabilistic description of the peak gust factor. For this, reference will be made to some earlier work by Davenport (1964), in

195

which a general theoretical distribution was obtained and compared quite favourably with some observations. The exact form will be determined by the frequency response curve of the gust anemometer combined with a typical power spectrum of atmospheric turbulence and a given mean wind speed. A mean gust factor, incorporating these effects and consistent with the terrain roughness, fixes the position of the distribution. Davenport himself points out that the theoretical model may not be completely satisfactory because of variations in terrain roughness around the anemometer site, deviation from the assumption of independence of gust factor and mean wind speed, and other factors arising from the choice of turbulence spectrum. The most significant of these, the question of inhomogeneous roughnesss, is considered in Chapter 2. Meanwhile it will be assumed that the mean gust factor will include such effects.

I.2 Mean Wind Speeds

From the continuous model (see Section 2.6 and Davenport and Baynes, 1972) with a single Weibull distribution of mean wind speeds, V_M, for the entire year, it can be shown that the distribution of the maxima becomes:

$$P(V) = exp[-B_M \, (\frac{V_M}{c})^{k-1} \, exp(-(\frac{V_M}{c})^{k})]$$ (I.1)

where

$$B_M = \sqrt{2\pi} \, \nu_M T \cdot \frac{k}{c} \, \sigma_M.$$ (I.2)

and ν_M is the average cycling rate of the process (usually about 0.1 cycles per hour),

T   is the appropriate time period (one year),

σ_M is the standard deviation of the variate,

k,c are the Weibull parameters.

σ_M for the Weibull distribution is given by the standard result:

$$\sigma_M^2 = c^2[\Gamma(1 + \frac{2}{k}) - \Gamma^2 (1 + \frac{1}{k})]$$ (I.3)

The extreme distribution can be matched to a curve of the Fisher-Tippett Type I at the

modal value, U_M, such that

$$\left(\frac{U_M}{c}\right)^{k-1} \exp\left(-\left(\frac{U_M}{c}\right)^k\right) = \frac{1}{B_M} \tag{I.4}$$

and

$$a_M = -\left.\frac{d\left[\ln\left(\frac{V_M}{c}\right)^{k-1} \exp\left(-\left(\frac{V_M}{c}\right)^k\right)\right]}{dV_M}\right|_{V_M = U_M} \tag{I.5}$$

or

$$\frac{1}{a_M} = \left[\frac{(1-k)}{U_M} + \frac{k}{c}\left(\frac{U_M}{c}\right)^{k-1}\right]^{-1} \tag{I.6}$$

I.3   Gust Speeds

The distribution of peak gust factors can be described by the following density function (Davenport, 1964):

$$p(\eta) = \eta\xi \exp(-\xi) \tag{I.7}$$

where ξ is defined by

$$\xi = \nu_a \tau \exp\left(-\frac{\eta^2}{2}\right) \tag{I.8}$$

ν_a is the average cycling rate of the atmospheric turbulence as seen by the gust anemometer and τ is the averaging time of the mean hourly wind speed (usually either 10 minutes or one hour).

If the mean wind and the gust factor are regarded as independent, then the density function of the peak gusts can be written as:

$$p(V_G) = p(\eta) \cdot p(V_M) \tag{I.9}$$

The probability distribution of exceeding V_G is given by:

$$P(> V_G) = \int_{\eta=-\infty}^{\infty} \int_{V_M = V_G/\eta}^{\infty} p(V_M) p(\eta) \eta \, dV_M d\eta \qquad (I.10)$$

or $\quad P(> V_G) = \int_0^{\infty} exp(-(\frac{V_G}{\eta c})^k) p(\eta) \eta \, d\eta \qquad (I.11)$

Now, from (I.8)

$$\eta exp(-(\frac{V_G}{\eta c})^k) = \eta exp[-(\frac{V_G}{c})^k \cdot \frac{1}{(2lnv_a\tau - 2ln\xi)^{k/2}}]$$

$$= \eta exp(-(\frac{V_G}{c})^k [\frac{1}{(2lnv_a\tau)^{k/2}} \cdot (1 + \frac{kln\xi}{2lnv_a} + \dots)])$$

$$= [(2lnv_a\tau)^{1/2} - \frac{ln\xi}{(2lnv_a\tau)^{1/2}} + \dots]$$

$$exp(-(\frac{V_G}{c})^k \cdot [\frac{1}{(2lnv_a\tau)^{k/2}} \cdot (1 + \frac{kln\xi}{2lnv_a\tau} + \dots)]) \qquad (I.12)$$

Assuming that $k>1$ and neglecting terms of order $(2lnv_a\tau)^{-3/2}$, this becomes

$$[(2lnv_a\tau)^{1/2} - \frac{ln\xi}{(2lnv_a\tau)^{1/2}}] \, exp(-(\frac{V_G}{c})^k \cdot \frac{1}{(2lnv_a\tau)^{k/2}}) \qquad (I.13)$$

Therefore, with (I.7) and the derivative of (I.8) in (I.11), and representing the quantity $(2lnv_a\tau)^{1/2}$ by A,

$$P(> V_G) = A \, exp[-(\frac{V_G}{c})^k \cdot \frac{1}{A^k}] \int_0^{\infty} exp(-\xi) d\xi$$

$$- \frac{1}{A} exp[-(\frac{V_G}{c})^k \cdot \frac{1}{A^k}] \int_0^{\infty} ln\xi \, exp(-\xi) d\xi \qquad (I.14)$$

The second integral is well known, being equal to -0.5772 (Euler's constant), so that

$$P(> V_G) = A(1 + \frac{0.5772}{A^2}) \, exp(-(\frac{V_G}{cA})^k) \qquad (I.15)$$

and the corresponding density function is:

$$p(V_G) = \frac{k}{c}(1 + \frac{0.5772}{A^2})(\frac{V_G}{cA})^{k-1} \exp(-(\frac{V_G}{cA})^k$$

This is in fact a modified Weibull distribution, f

be found by the same procedure followed for the m

$$P(V_G) = \exp[-B_G(\frac{V_G}{cA})^{k-1} \exp(-(\frac{V_G}{cA})^k)]$$

where

$$B_G = \sqrt{2\pi}\, \nu_G T \cdot \frac{k}{c}(1 + \frac{0.5772}{A^2})\, \sigma_G$$

and σ_G is the standard deviation of the peak gust

ν_G is the average cycling rate of the peak gu

Fitting this distribution to the Type I, as for

$$(\frac{U_G}{cA})^{k-1} \exp(-(\frac{U_G}{cA})^k) = \frac{1}{B_G}$$

and

$$\frac{1}{a_G} = [\frac{(1-k)}{U_G} + \frac{k}{cA}(\frac{U_G}{cA})^{k-1}]^{-1}$$

In order to evaluate the parameters of the extre

of the peak gusts in Equation I.18 must be fou

parameters, k and c. From the first and seco

(I.16), it can be shown that

$$\sigma_G^2 = c^2 A^3(1 + \frac{0.5772}{A^2}) [\Gamma(1 + \frac{2}{k}) +$$

$$A^2(1 + \frac{0.5772}{A^2}) \cdot (1 + \frac{0.5772}{A^2}$$

It is assumed that the average cycling rate of the record of peak gusts is the same as the cycling rate of the mean winds. Since an accurate figure is not required in the context of this formulation, it is reasonable to adopt the typical value of 0.1 cycles per hour in both cases.

Finally, it is required to determine A. This will be a function of terrain roughness and the anemometer's response to atmospheric turbulence. From Davenport's theory for the distribution of η, it is related to the mean gust factor, $\bar{\eta}$, by

$$\bar{\eta} = A + \frac{0.5772}{A} \qquad (I.22)$$

A is in fact the mode of the distribution. However, it must be noted that in the theory η is a normalized quantity defined by

$$\eta = \frac{x - \bar{x}}{\sigma_x} \qquad (I.23)$$

where x represents the original variate, the instantaneous gust velocity as a ratio of the mean wind, and $\bar{x}$ is unity. Therefore, before using the results of the above argument, A must be transformed to give the mode of the distribution of peak gust factors, x. Since σ_x is often unknown, this can be done by assigning a mean value for the maxima of x, hence giving the new mode as a function of this and the mode of the normalized peaks, A.

A COMPARISON OF THEORETICAL AND OBSERVED DISTRIBUTIONS OF EXTREME GUSTS AND MEAN WIND SPEEDS

II.1 Data

The wind observations used here are contained in a compilation of "Wind in Western Europe" recently prepared by the Laboratório Nacional de Engenharia Civil, Lisbon (1973). The information came originally from the various national meteorological agencies and includes listings of annual maximum mean hourlies and, where available, peak gusts. Accompanying each listing is an indication of the surrounding terrain roughness and the type and siting of the anemometers used at the observing station. For the purposes of this study, stations have been selected as follows:

a) Relatively smooth terrain in roughness categories A and B[*].

b) Records of maximum mean hourlies (one-hour averaging period) and gusts for a minimum period of 10 years.

c) Anemometer height between 10 and 20 metres above ground level.

Some 25 locations in Czechoslovakia, Spain and the United Kingdom were found to meet these requirements.

---

[*]Cat. A — open country with few trees; short or no vegetation
Cat. B — terrain with fairly numerous hedges and scattered trees, wind breaks, buildings etc.

Sample means and standard deviations of maxima are given in the source reference and these have been used to calculate the modes and dispersions of the distributions of extremes by Gumbel's method (see Section 2.6 and Gumbel, 1954). This is equivalent to a least squares fit of a Fisher-Tippett Type I distribution to the observed wind frequencies. Table II.1 gives the observing stations, separated according to terrain roughness, together with the calculated ratios of dispersions and modes, that is $1/a_M U_M$, U_G/U_M and a_M/a_G ($1/a$ denotes dispersion and U the mode; subscripts M and G refer to mean hourlies and peak gusts respectively).

II.2 Comparison

In Figure II.1 values obtained for each station in category A have been plotted over the theoretical mode and dispersion relationships derived in Section 2.11 for mean gust factors, $\bar{\eta}$, of 1.5 and 1.6. A similar comparison is shown in Figure II.2 for category B and $\bar{\eta}$ values of 1.6 and 1.7.

The observational data is widely scattered, although it exhibits a discernible trend towards higher ratios of the modes and dispersions as the characteristic variable $1/a_M U_M$ increases. If localities in the U.K. are considered alone, the amount of scatter is noticeably less, perhaps reflecting the climatic character of that part of Europe where strong mean winds and gusts are usually associated with large storm systems. The prevailing conditions are therefore more likely to accord with the underlying assumptions of the theoretical curves. The Spanish records, on the other hand, will be influenced to a greater degree by thermally induced winds and gusts. Any local effects of terrain or general topography have not been determined.

STATION	$\dfrac{I}{U_M a_M}$	$\dfrac{U_G}{U_M}$	$\dfrac{a_M}{a_G}$
Roughness Cat. A			
Popard, Czechoslovakia	.186	1.54	1.32
De Leon, Spain	.228	1.50	1.02
Pollensa	.180	3.24	3.94
Villafria	.068	1.63	2.09
Villanubla	.097	1.44	1.66
Fleetwood, U.K.	.123	1.57	1.18
Lerwick	.113	1.46	1.34
Lizard	.091	1.47	1.36
Point of Ayre	.102	1.56	1.25
Scilly	.109	1.51	1.38
Stornoway	.115	1.47	1.61
Tiree	.144	1.53	1.55
Roughness Cat. B			
Karlovy Vary, Czech.	.088	2.18	3.91
Armilla, Spain	.189	1.83	1.88
Cuatro Vientos	.114	1.97	2.98
Ebro	.225	1.97	0.73
Malaga	.197	2.18	2.10
Monflorite	.084	1.30	1.90
San Javier	.143	1.41	1.63
Santiago	.082	1.82	2.05
Aberporth, U.K.	.110	1.56	1.44
Eskdalemuir	.110	1.75	1.68
Manchester	.095	1.68	1.78
Prestwick	.117	1.70	1.63
South Shields	.130	1.54	1.37

**TABLE II.1 OBSERVED RATIOS OF DISPERSIONS AND MODES
AT SOME EUROPEAN STATIONS**
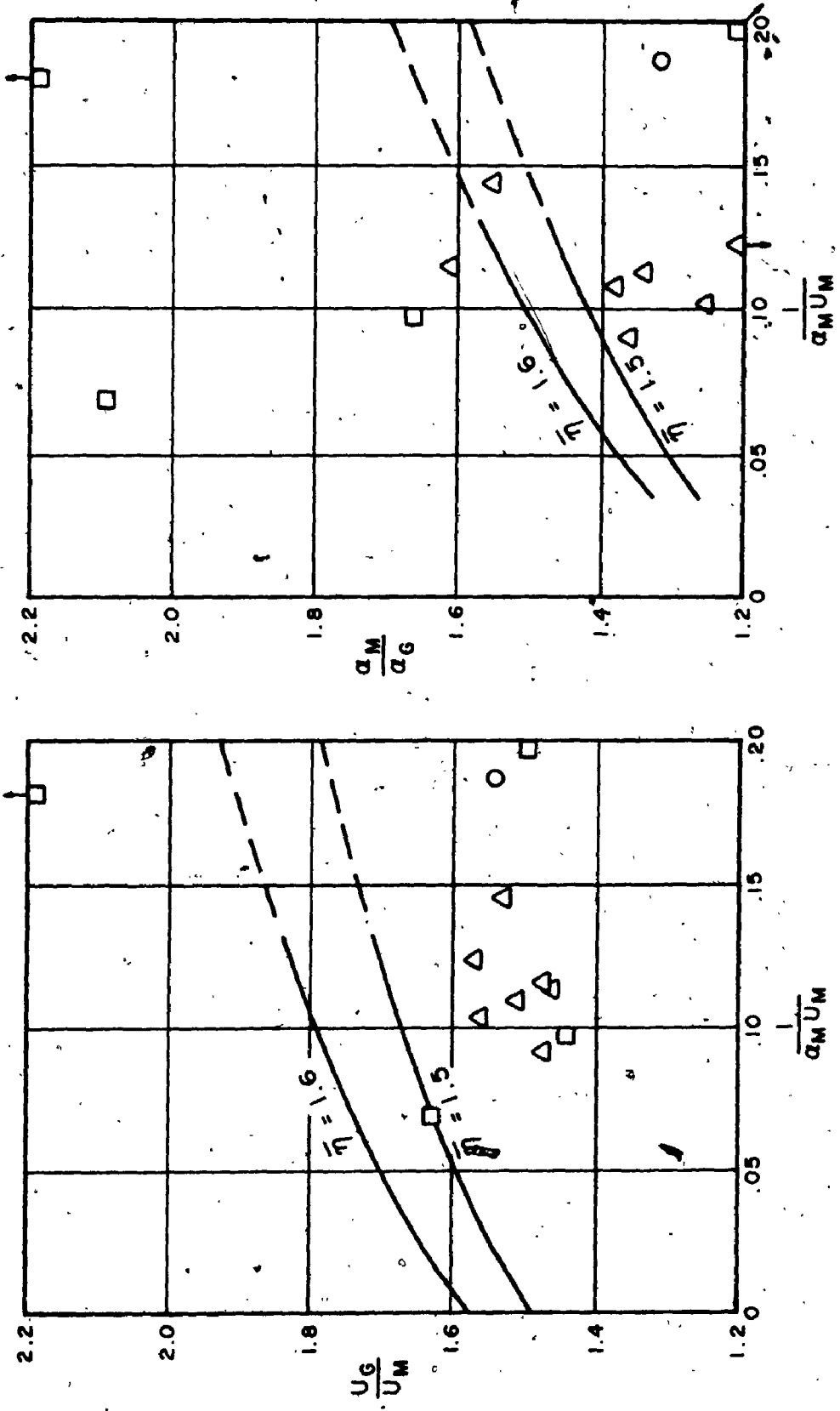
FIG. II.1. OBSERVED AND THEORETICAL RELATIONSHIPS OF MEAN WIND AND GUST MODES AND DISPERSIONS FOR TERRAIN ROUGHNESS CAT. A (AVERAGING PERIOD OF MEAN HOURLIES - 1 HOUR)

KEY: OBSERVING STATIONS IN
O CZECHOSLOVAKIA
□ SPAIN
△ U.K.
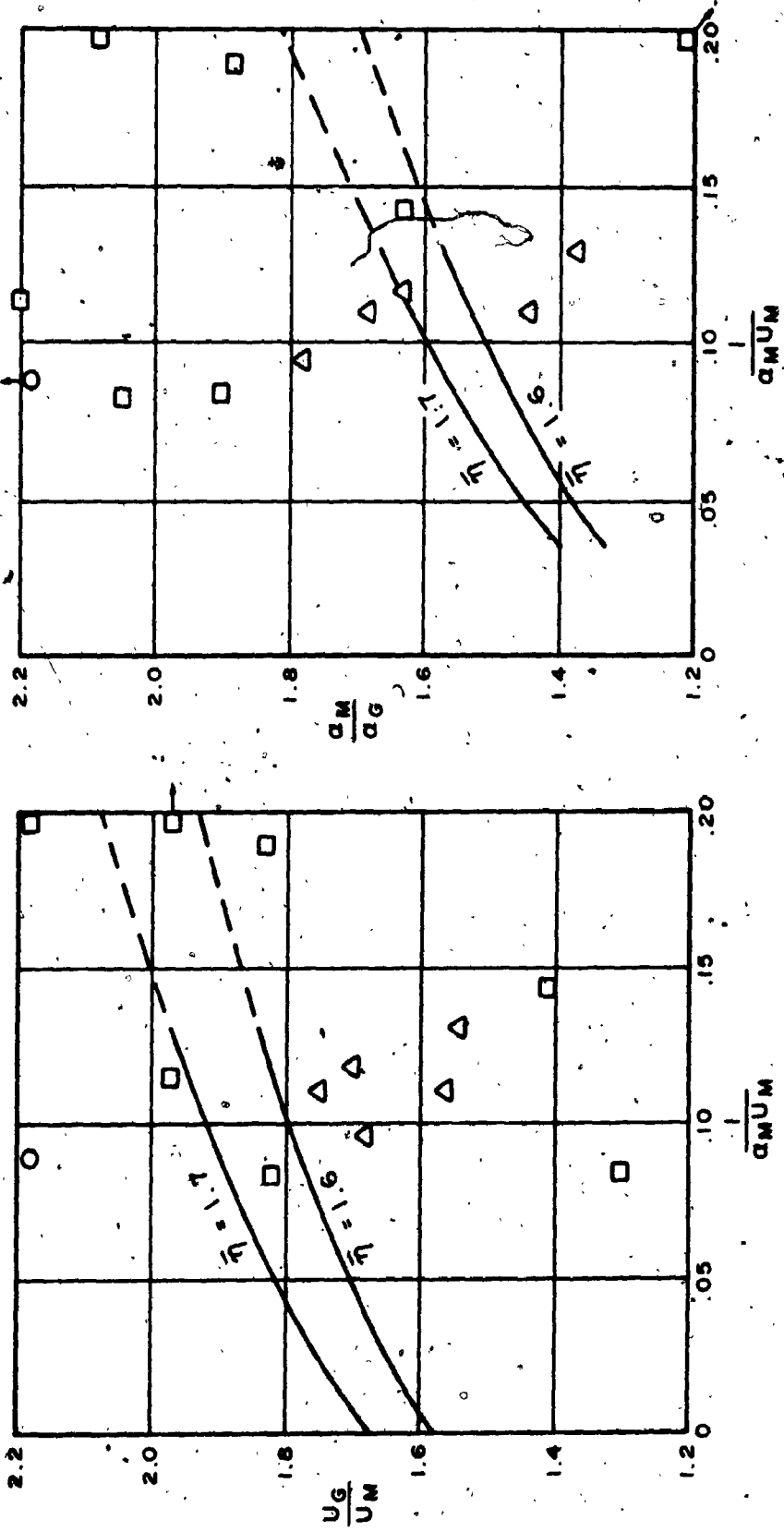
FIG. II.2 OBSERVED AND THEORETICAL RELATIONSHIPS OF MEAN WIND AND GUST MODES AND DISPERSIONS FOR TERRAIN ROUGHNESS CAT. B (AVERAGING PERIOD OF MEAN HOURLIES – 1 HOUR)

KEY: OBSERVING STATIONS IN –
O CZECHOSLOVAKIA
□ SPAIN
△ U.K.

APPENDIX III

A SURVEY OF SOME EXTREME WIND STATISTICS

III.1 Information Sources

This survey brings together some fifteen published accounts, of surface extreme wind climate in various parts of the world. It is not exhaustive, but concentrates on those studies employing the modern statistical approaches described in Chapter 2, and likely to provide useful and reasonably consistent information to the engineer.

The sources are listed in Table III.1, together with a summary of the type of data employed in each case (observing stations, period, instrumentation) and the subsequent statistical analysis (probability model, statistical parameters found, presentation of results).

III.2 Comparative Statistics

To provide an indication of extreme wind climate in the regions covered by the survey, the parameters of the Fisher-Tippett Type I distribution of maximum mean hourlies have been estimated for a number of centres in each country. Where these parameters are given in the original reference they have been quoted directly. Insofar as the information available to the writer specified, the statistics were selected for their applicability to relatively smooth terrain, with no more than scattered buildings and trees, and heights above ground level of around 10 metres.

To maintain a common basis of comparison it was necessary in some cases to transform peak gust statistics to mean hourlies using the relationships developed in Section 2.11. Where the Type II or some other extreme distribution was followed in the data source, it was first necessary to estimate the corresponding Type I distribution, again using the procedures described in the main body of this thesis (Section 2.7).

Table III.2 gives the resulting statistics, tabulated alphabetically by country. Details of any transformations are also given. Since the ratio of the dispersion to the mode of the extremes is often indicative of the strong wind climate, this has been included. A high value of this ratio may be connected with the occasional incidence of cyclones or strong local winds.

	REGION	REFERENCE	STATIONS	PERIOD	DATA ANEMOMETER	SITING	STATISTICS	MODEL	PARAMETERS	
1	Argentina	Riera & Reimundin (1970)	65 stations	1960-67			Maxm. annual 3-sec. gusts	F-T Type II	β	Max using gust
2	Australia	Whittingham (1964)	89 stations incl. Tasmania, N. Guinea, Cocos, Lord Howe, Norfolk Willis and Solomon Is.	Various between 1910 and 1962	Mostly Dines anemograph	Mostly at or near 10 m. above ground	Maxm. annual	F-T Type I	U and 1/a 10, 20, 50, 100 yr. return gusts	Gu me via ma
3	Canada	NRC (1970)	Direct obs. at over 100 stations Extreme gusts at additional 500	10 to 22 yrs.	Cup. anemom. Gust records with Dines		Maxm. annual	F-T Type I	30-yr. return mean winds	Gu
4	Denmark	Jensen & Franck (1970)	Torsminde, Gedser and Tune	Gedser 8 years Others 7 years	Dines	At top of 25 m. masts	Maxm. dynamic head, q for each storm passage	Exponential in q $q = A - B \ln P(q)$ where $P(q)$ is probab. of exceeding q in a given storm	A and B	L d
5	France	Duchene-Marullaz (1972)	114 stations incl. Corsica	23 yrs. maxm.	4-cup Papillon 3-cup at some stations from 1968	10 to 13 m. above ground at 80% of stations	Maxm. annual 1-sec. gusts	F-T Type I (Type II and normal distrib. also studied)	Mean and std. devn. of annual maxima Overall U and 1/a for 3 zones	L
6	Hong Kong	Mackay (1972)	Royal Obs., Kowloon Waglan Cheung Chau	1884-1969 at Royal Obs. 1953-1969 at Waglan and Cheung Chau	4-cup anemograph to 1938 Dines anemograph from 1935	10 to 20 m. above ground	Maxm. annual mean hourlies and gusts	F-T Types I, II and III		
7	India	Harihara & Goyal (1972)	25 stations	6 to 21 yrs.		10 to 30 m above ground	Maxm. annual	F-T Type I	U and 1/a	
8	Japan	Hanai (1963)	33 stations	17 to 18 yrs.		Mostly 10 to 20 m above ground	Maxm. daily	Exponential $P(V) = 1 - a\,e^{-bV}$	a and b	

TABLE III.1 SUMMARY OF EXTREME WIND INFORMATION

...ISTICS	ANALYSIS				
	MODEL	PARAMETERS	METHODS	PRESENTATION	FURTHER DETAILS
...annual gusts	F-T Type II	β	Maxm. likelihood fit using logs of observed gust speeds	Contour map of β Additional map of annual frequencies of thunderstorms	Uniform value of γ suggested for entire country (0.82) Results apply to 10 m above ground
...m. annual	F-T Type I	U and 1/a 10, 20, 50, 100 yr. return gusts	Gumbel's method using means and standard deviations of annual maxima	Contour maps of all parameters Additional maps – wind roses of maxm. annual gusts preferred time of yr. for maxm. gust, average annual thunderday	No adjustments of data to a standard height
...m. annual	F-T Type I	30-yr. return mean winds	Gumbel's method	Contour map of 30-yr. return winds 10, 30, 100 yr. return wind pressures tabulated for all stations	Empirical conversion of gust data to mean hourlies for the additional 500 stations
...xm. dynamic head, q ...each storm ...sage	Exponential in q $q = A - B \ln P(q)$ where P(q) is probab. of exceeding q in a given storm	A and B	Least squares fit to data		
...xm. annual sec. gusts	F-T Type I (Type II and normal distrib. also studied)	Mean and std. devn. of annual maxima Overall U and 1/a for 3 zones	Least squres fit to data	Map of 3 zones according to means and std. devns. of annual maxima (light, moderate and strong winds) Type I distrib. for each zone	No adjustments of data to a standard height Mean, std. devn. and Type I parameters of maxima listed for each station
Maxm. annual mean hourlies and gusts	F-T Types I, II and III		Types I and II fitted to data by least squares and maxm. likelihood. General form of the 3 types fitted by curvilinear regression	Distributions shown graphically	Empirical conversion of cup anemograph readings to Dines standard No adjustments of data to a standard height
Maxm. annual	F-T Type I	U and 1/a	Least squares fit to data	Contour maps of 2, 5, 10 25, 50, 100 yr. return gusts	
Maxm. daily	Exponential $P(V) = 1 - a\,e^{-bV}$	a and b	Least squares fit to data	Distributions shown graphically for all stations For 11 stations, tabulation of freq. of storms with mean winds greater than 10, 15 20, 25, 30 m/s in period 1949-58	Coefficients applied to allow for anemometer height and proximity to seashore

...ARY OF EXTREME WIND INFORMATION

9	Netherlands	Rijkoort (1964)	8 stations	Up to 60 yrs.		Mostly near 10 m above ground	Maxm. annual mean hourlies	F-T Type I	For 10, 2... and 500 y... periods, ...ceeded on... ...and with ...
10	South Africa	May (1972)	Johannesburg Kimberley, Durban Bloemfontein E. London, P. Elizabeth, Capetown	14 to 21 yrs		11 to 15 m above ground	Maxm. annual mean hourlies and gusts	F-T Type I	50-yr. re... 10 m. an... ht.
11	South Korea	Lee & Huh (1972)	14 stations incl. off-shore islands	1945-1969	3-cup Robinson	10 m. above ground	Maxm. annual mean hourlies	F-T Type I	50 and ... return w...
12	Sweden	Johnson (1953)	13 stations	Various between 1875 and 1950	Dines and cup anemom.		Maxm. annual gusts Maxm. annual mean hourlies at Uppsala	F-T Type I and normal distrib.	Means a... devns. o... maxima
13	United Kingdom	Shellard (1962)	56 stations	Various between 1913 and 1959	Dines anemograph	Mostly near 10 m. above ground	Maxm. annual mean hourlies and gusts	F-T Type I	U and ... hourlie...
14	United States	Thom (1968)	150 stations incl. Alaska, Hawaii, Puerto Rico	Average record length 21 yrs.			Maxm. annual fastest miles	F-T Type II	β and ... 100 y...
15	Western Europe	LNEC (1973)	158 stations in Belgium Czechoslovakia Denmark, Finland, France, Germany, Iceland, Ireland, Netherlands, Portugal, Spain, Sweden Switzerland and U.K.	Various	Various	Nominally at surface (10 m)	Maxm. annual mean hourlies and gusts	F-T Type I	Means ... (coef... of me... gusts ...

TABLE III.1 continued

104

Maxm. annual mean hourlies	F-T Type I	For 10, 25, 50, 100 and 500 yr. return periods, winds exceeded on average and with 95% probab.	Method of moments using mean and std. devns of annual maxima		No adjustments of data to a standard height Generally results apply to 10 m. above ground
Maxm. annual mean hourlies and gusts	F-T Type I	50-yr. return winds at 10 m. and gradient ht.	Extreme distribs. of mean hourlies and gusts plotted	Maps giving 50-yr. return winds	50-yr. gradient winds estimated from 50-yr. surface winds using power law with index and gradient ht. according to terrain roughness
Maxm. annual mean hourlies	F-T Type I	50 and 100 yr. return winds	Extreme distribs. plotted	Maps giving observing stations and 50, 100 yr. return winds	
Maxm. annual gusts Maxm. annual mean hourlies at Uppsala	F-T Type I and normal distrib.	Means and std. devns. of annual maxima		Distributions shown graphically	
Maxm. annual mean hourlies and gusts	F-T Type I	U and 1/a for mean hourlies and gusts	Gumbel's method using means and standard deviations of annual maxima	Contours maps of 50-yr. return mean hourlies and gusts. Tabulations of U, 1/a and 10, 20, 50, 100 yr. return winds at all stations	All winds reduced to 10 m. level by power law with index of 0.17 for mean hourlies and 0.085 for gusts
Maxm. annual fastest miles	F-T Type II	β and γ, 2, 10, 25, 50, 100 yr. return winds	Maxm. likelihood fit using logs of observed extreme winds	Contour maps of return winds. Results for Hawaii and Puerto Rico tabulated separately	Winds reduced to 30 ft. level by power law with index of 1/7
Maxm. annual mean hourlies and gusts	F-T Type I	Means and std. devns. (coeffs. of variation) of mean hourlies and gusts	Extreme distribs. plotted for each station	Distributions shown graphically Tables of other statistics	Data drawn from records of the national meteorological agencies

LOCATION	REF	ESTIMATED PARAMETERS			TRANSFORMATIONS
		U_M (m/s)	$1/a_M$ (m/s)	$1/U_M a_M$	
ARGENTINA	1				U_G, $1/a_G$ from β_G, γ_G (eqns. 2.71 and 2.72)
Buenos Aires		14.2	2.02	.142	U_M, $1/a_M$ from U_G, $1/a_G$ (Fig. 2.16)
Cordoba		14.9	2.13	.143	with mean peak gust factor 1.6
AUSTRALIA	2				U_M, $1/a_M$ from U_G, $1/a_G$ (Fig. 2.16)
Adelaide		16.3	2.04	.125	with mean peak gust factor 1.6
Melbourne		16.3	2.06	.127	
Perth		14.9	1.56	.104	
Sydney		14.5	2.73	.188	
CANADA	3				
Edmonton		16.5	2.54	.154	
Halifax		17.9	3.08	.172	
Montreal		17.9	1.70	.095	
Toronto		18.8	2.54	.135	
Vancouver		16.4	2.54	.155	
Winnipeg		19.1	1.88	.098	
CZECHOSLOVAKIA	15				Gumbel's method using mean and
Karlovy Vary		12.0	1.05	.088	and standard deviation of annual maxima
Poprad		19.1	3.55	.186	
EIRE	15				Gumbel's method using mean and
Dublin		21.1	2.14	.114	standard deviation of annual maxima
Shannon		22.3	2.77	.137	(10-min. mean hourlies)
FRANCE	5				U_G, $1/a_G$ from Gumbel's method
Brest		14.6	1.93	.133	U_M, $1/a_M$ from U_G, $1/a_G$ (Fig. 2.16)
Lyon		13.7	2.68	.195	with mean peak gust factor 1.6
Marseilles		15.0	2.67	.177	
Paris		14.0	1.52	.108	
GERMANY	15				Gumbel's method using mean and
Bremerhaven		19.9	2.70	.136	standard deviation of annual maxima
Dusseldorf		14.1	1.45	.103	
Kiel		15.6	2.18	.140	
Nurnberg		13.0	2.00	.154	
HONG KONG	6				U_M, $1/a_M$ estimated from Type I curve as
Waglan		23.7	7.16	.302	$U_M = 2V_{10} - V_{100}$, $1/a_M = V_{100} - V_{10}/2.3$ where V_{10}, V_{100} are 10 and 100 year return mean winds

TABLE III.2 ESTIMATED PARAMETERS OF EXTREME MEAN WIND DISTRIBUTIONS

INDIA	7			
Bangalore		12.0	1.54	.128
Bombay		12.3	2.18	.177
Calcutta		16.0	2.52	.158
Nagpur		14.2	2.58	.181
New Delhi		15.3	2.86	.186
JAPAN	8			
Fukuoka		29.2	3.87	.132
Nagoya		23.4	2.94	.126
Osaka		22.8	4.15	.182
Sapporo		19.8	1.38	.070
Tokyo		21.6	1.82	.08
NETHERLANDS	9			
Den Helder		22.7	1.70	.07
Grogingen		18.7	2.39	.12
Maastricht		13.6	1.26	.09
PORTUGAL	15			
Lisbon		18.3	1.69	.0
Porto		20.2	2.61	.1
SOUTH AFRICA	10			
Capetown		14.0	1.74	
Durban		15.0	2.61	
Kimberly		13.0	1.74	
Johannesburg		13.0	1.74	
SPAIN	15			
Ebro		15.92	3.58	
Madrid		11.22	1.28	
Malaga		9.52	1.88	
Pollensa (Majorca)		8.63	1.55	

TABLE III.2 continued

SWEDEN	12				
Gotska Sandön		12.2	1.77	.145	U_G, $1/a_G$ from Gumbel's method
Halsingborg		12.7	1.32	.104	U_M, $1/a_M$ from U_G, $1/a_G$ (Fig. 2.16)
Skanor		12.8	1.11	.086	with mean peak gust factor 1.6
UNITED KINGDOM	13				
Aberdeen		14.7	2.10	.143	
Belfast		17.6	1.88	.107	
Durham		17.71	1.65	.093	
Liverpool		20.5	1.48	.072	
London (Croydon)		16.7	1.77	.106	
Plymouth		21.8	2.11	.097	
Prestwick		18.8	1.94	.103	
UNITED STATES	14				10, 100 yr. fastest mile return winds to
Anchorage		16.3	3.00	.184	mean hourlies (Eqn. 2.81)
Atlanta		13.1	2.92	.222	U_M, $1/a_M$ from β_M, γ_M of corres-
Chicago		15.9	2.12	.133	ponding Type II curves (Eqns. 2.71 and
Denver		19.3	1.97	.102	2.72)
Fort Worth		17.9	1.26	.070	
Los Angeles		12.2	2.00	.163	
Miami		18.6	3.56	.191	
New York		14.6	2.58	.177	
Seattle		17.4	2.30	.132	

TABLE III.2 continued

APPENDIX IV

UPPER AIR STATION DESCRIPTIONS

The following information was obtained, in part, from the station history files maintained at the Atmospheric Environment Service, Toronto. Maps of the country surrounding the stations were extracted from the 1:50,000 series published by the Department of Energy, Mines and Resources, Ottawa.

Moosonee, Ontario

Position: 51° 16'N, 80° 39'W   Elevation: 10 m

Local times of observations: 0700, 1900 EST

Situation and local topography (see map, Figure IV.1):

Station is 1 mile south of the O.N.R. station on the northwest bank of the Moose River, 300 ft. from the river bank. Surrounding country is very flat muskeg, quite densely wooded, mostly with coniferous trees; numerous creeks drain into the river. The station area was cleared of trees, and ditches provide drainage. The instrument area was built up and levelled.

The river runs southwest to northeast past the station, emptying into James Bay about 10 miles to the northeast. The wind tower is located towards the centre of the clearing, 300 ft. west of the Operations Building. Trees of 20 to 30 ft. surround the tower at 500 ft. to the south and 1000 ft. to the west through northeast.

FIG. IV.1
MOOSONEE, ONT.

Sable Island, Nova Scotia

Position: 43° 56'N, 60° 01'W   Elevation: 4 m

Local times of observations: 0800, 2000 EST

Situation and local topography (see map, Figure IV.2):

Station is 1 mile east of the Main Station and about 4 miles east of the westerly tip of Sable Island, close to the north shore. The island, situated in the Atlantic Ocean off the coast of Nova Scotia, consists of rolling sand dunes. The dunes range in height up to about 75 ft., generally sloping away towards the south shore. From the station, visibility is restricted by dunes, except for the southeast to southwest quadrant where the ocean provides the horizon.

The Pas, Manitoba

Position: 54° 58'N, 101° 06'W   Elevation: 273 m

Local times of observations: 0600, 1800 CST

Situation and local topography (see map, Figure IV.3):

Located at The Pas airport, 12 miles northeast of The Pas direct. Exposure is fairly level. Dense bush surrounds the airport with Clearwater Lake immediately northwest to northeast. Instruments are sited about 500 ft. southeast of the Transair hangar. Treeline is about 0.6 miles to the east and 0.2 miles to the south.

216
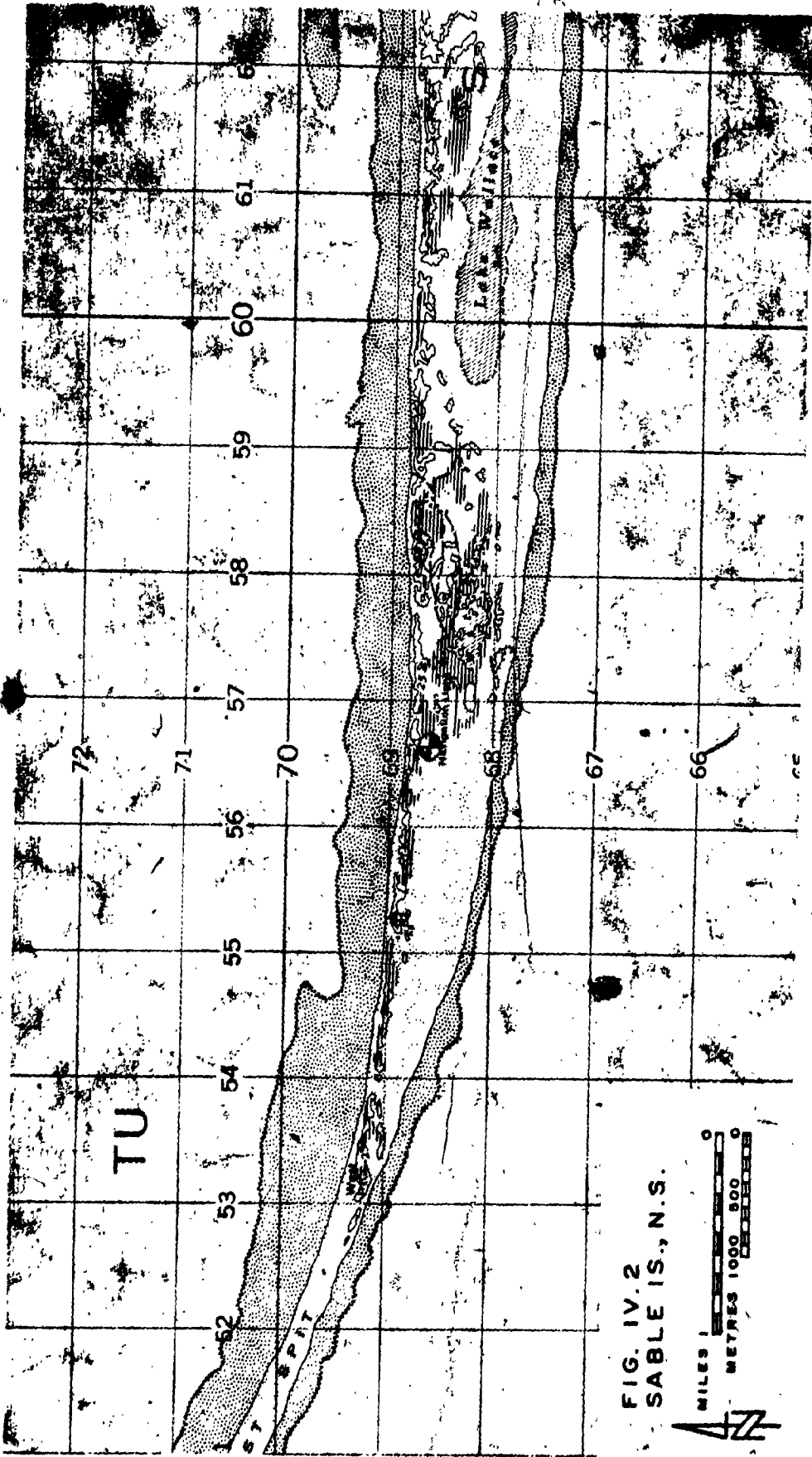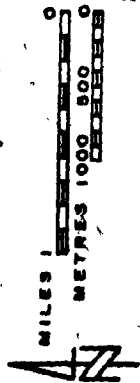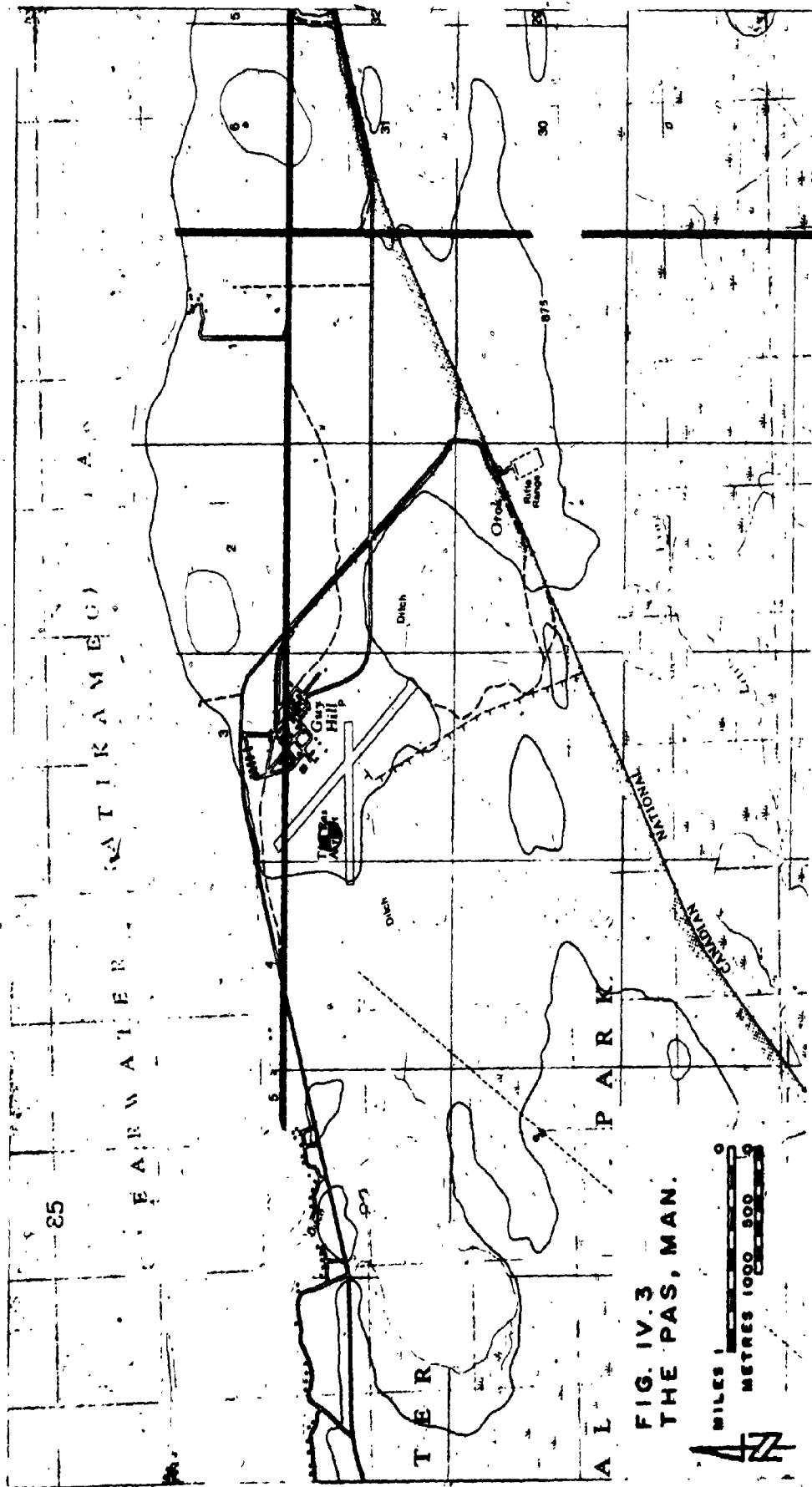
FIG. IV.2
SABLE IS., N.S.

FIG. IV.3
THE PAS, MAN.
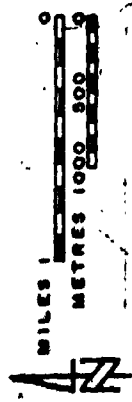
APPENDIX V

SELECTION OF NEUTRAL WIND PROFILES FROM UPPER AIR DATA

V.1 Data

The data consisted of the twice-daily radiosonde observations recorded over the period 1960-69 at three Canadian upper air stations. These were Moosonee, Ontario, Sable Island, N.S. and The Pas, Man., slected for their situtions in relatively uniform and level terrain (see Appendix IV).

The radiosonde ascents were generally made at 0000 hrs. and 1200 hrs. GMT daily. The following observations were recorded for the surface and standard pressure surfaces at 1000, 950, 900, 850, 800, 750 and 700 millibars:

a) Elevation above sea level (or atmospheric pressure, in the case of the surface observation).

b) Temperature.

c) Relative humidity.

d) Wind speed and direction.

V.2 Data Reduction

Since the investigation was to apply to neutrally stratified atmospheres only (Chapter 3), it was necessary to specify the criteria for the selection of useful observations. In establishing the definition of neutral conditions, the simple concept of static stability of a dry atmosphere was applied. The temperature distribution for neutral stability is then given by

218

$$T' = T\left(\frac{p_0}{p}\right)^{\gamma-1/\gamma} \qquad\qquad (V.1)$$

where T is the absolute temperature at pressure p,

p_0 is the surface pressure,

γ is the ratio of specific heats for dry air (~ 1.41)

and T' is the potential temperature.

It is required that T' be unchanged with height and equal to the surface absolute temperature.

The record of each radiosonde ascent was examined in turn. Firstly, all elevations were adjusted to give heights above ground level, then the data was tested against three acceptance criteria, in the following order:

a) Observations at all pressure surfaces, up to that immediately above or at 500 m, must be complete.

b) The potential temperature up to 500 m must be within $2^{\circ}C$ of the surface absolute temperature.

c) The surface wind speed must be $\geqslant 5$ m/s.

Table V.1 shows, for each of the three upper air stations, the number of ascents rejected by these criteria and the total number of records selected.

Finally, wind velocities at the standard pressure surfaces were translated into winds at 300 m and 500 m above ground level. In view of the accuracy of the data, it was felt adequate to employ simple linear interpolation between measurements immediately above and below the desired elevations. The zonal and meridional velocity components were separately interpolated.

STATION	TOTAL RECORDS	RECORDS EXCLUDED BY CRITERIA			TOTAL RECORDS CHOSEN
		a	b	c	
Moosonee	7300	316	5647	654	683
Sable Island	7291	1000	4146	391	1754
The Pas	7297	164	4835	671	1627

TABLE V.1 NUMBERS OF SELECTED RADIOSONDE RECORDS

APPENDIX VI

A MODIFICATION OF SWINBANK'S WIND SPIRAL

The following is an adaptation of the theory proposed by Swinbank (1970) and discussed further by Plate (1971). The spiral model rests on the assumption that, everywhere in the Ekman layer, the shearing stress, τ, is parallel to the direction of the mean wind. The equations of motion then become

$$\frac{d\tau}{dz} = -f V_G \sin(a - a_0) \qquad (VI.1)$$

where a is defined as the angle between the wind vectors at height z and the surface, a_0 is the corresponding angle at the height of geostrophic balance, f is the Coriolis parameter and V_G is the geostrophic wind (see Chapter 3, Figure 3.1).

The general influence of geostrophic veering or local topographic effects on Swinbank's spiral can be studied by introducing a superimposed shear flow, also parallel to the wind vector for all z. Thus

$$\frac{d\tau}{dz} = -f V_G \sin(a - a_0) + E(z) \qquad (VI.2)$$

Expanding τ in a Taylor series about $z = h$, where h is the scaling height of the Ekman layer,

$$\tau = \frac{1}{2} \frac{d^2\tau}{dz^2}\bigg|_h (z - h)^2 \qquad (VI.3)$$

Therefore

$$\tau \doteq (\frac{-fV_G}{2} \frac{da}{dz}\Big|_h + \frac{E'(h)}{2})(h-z)^2 \qquad (VI.4)$$

and

$$sin(a - a_0) \doteq (-\frac{da}{dz}\Big|_h + \frac{E'(h)}{fV_G})(h-z) + \frac{E(z)}{fV_G} \qquad (VI.5)$$

It will be noted that, in Swinbank's theory, the asymptotic solution as z approaches h is assumed to hold for all z. Hence, at $z = 0$

$$sin\ a_0 = (\frac{da}{dz}\Big|_h - \frac{E'(h)}{fV_G})h - \frac{E(0)}{fV_G} \qquad (VI.6)$$

The corresponding expression for the original model of Equation (VI.1) is

$$sin\ a_0 = \frac{da}{dz}\Big|_h \cdot h \qquad (VI.7)$$

Furthermore, from the similarity theory of Csanady (1967) and Blackadar and Tennekes (1968), and since Swinbank's spiral applies also to the "matched region" between the inner and outer sublayers,

$$sin\ a_0 = \frac{da}{dz}\Big|_h\ h = -\frac{B}{k}\frac{u_*}{V_G} \qquad (VI.8)$$

where u_* is the surface friction velocity. Similarly, retaining the same scaling parameters, h and V_G, (VI.6) can be rewritten in equivalent terms:

$$sin\ a_0 = (\frac{da}{dz}\Big|_h)_e\ h = -\frac{B_e}{k}\frac{u_*}{V_G} \qquad (VI.9)$$

Therefore, from (VI.5),

$$sin(a - a_0) = (\frac{B_e}{k}\frac{u_*}{V_G} - \frac{E(0)}{fV_G})\frac{(h-z)}{h} + \frac{E(z)}{fV_G} \qquad (VI.10)$$

and, from (VI.4),

$$\frac{\tau}{u_*^2} = \left(\frac{fV_G}{2u_*^2}\left(\frac{B_e}{k}\frac{u_*}{V_G} - \frac{E(0)}{fV_G}\right)\frac{(h-z)^2}{h}\right. \qquad (VI.11)$$

Since $\dfrac{\tau}{u_*^2} = 1$, at $z = 0$

$$h = 2\left(\frac{B_e}{k}\frac{f}{u_*} - \frac{E(0)}{u_*^2}\right)^{-1} \qquad (VI.12)$$

Substituting for h in (VI.9) and rearranging

$$\left(\frac{da}{dz}\bigg|_h\right)_e \frac{2V_G}{f} + \frac{B_e^2}{k^2} - \frac{B_e}{k}\frac{E(0)}{u_*f} = 0 \qquad (VI.13)$$

and

$$\frac{B_e}{k} = \frac{E(0)}{2u_*f} \pm \left[\frac{E(0)^2}{4u_*^2f^2} - \frac{2V_G}{f}\left(\frac{da}{dz}\bigg|_h\right)_e\right]^{1/2} \qquad (VI.14)$$

Consider now the case when the wind veering associated with the superimposed shear flow is negligible near $z = h$. This implies that

$$E'(h)h + E(0) \sim 0 \qquad (VI.15)$$

Also, for the original model, it can be shown that

$$\frac{B}{k} = \left(-\frac{2V_G}{f}\frac{da}{dz}\bigg|_h\right)^{1/2} \qquad (VI.16)$$

Equation VI.14 then becomes.

$$\frac{B_e}{k} = \frac{E(0)}{2u_*f} + \left[\left(\frac{E(0)}{2u_*f}\right)^2 + \left(\frac{B}{k}\right)^2\right]^{1/2} \qquad (VI.17)$$

This solution has two asymptotes:

$$\frac{B_e}{k} = 0, \frac{E(0)}{u_*f} \to -\infty \qquad (VI.18)$$

and $\dfrac{B_e}{k} = \dfrac{E(0)}{u_* f}$, $\dfrac{E(0)}{u_* f} \to \infty$ $\hspace{3cm}$ (VI.19)

yielding only positive values of B_e and permitting veering of the wind between the surface and the top of the Ekman layer. The alternative root gives negative values but can only apply for small angles, since the original spiral allows just veering and, in this formulation, it has been assumed that

$$\left(\dfrac{da}{dz}\Big|_h\right)_e \sim \left(\dfrac{da}{dz}\Big|_h\right) \hspace{3cm} (VI.20)$$

In conclusion, this modification of Swinbank's theory suggests that, for certain superimposed shear flows, wind veering and small angles of wind backing in the atmospheric boundary layer can be predicted using an expression of the form of (VI.9) with a variable coefficient B_e.

MOMENTS OF THE DISTRIBUTION OF SURFACE WIND
STATISTICAL SURFACE/GRADIENT WIND

VII.1 First Moment

Let the surface wind speed be represented thus:

$$V_O = \epsilon K V_G$$

in which ϵ is a random variable independent of the gradient V_G and θ_G, and K is some function of θ_G. It is assumed independent, so that the mean or expected value of V_O is g

$$E(V_O) = \int V_O \, p(V_O) dV_O$$

$$= \iiint \epsilon K V_G \, p(\epsilon) \, p(K) \, p(V_G) \, d\epsilon \, dK \, dV_G$$

Now,

$$p(K) \, dK = p(\theta_G) d\theta_G$$

so that

$$E(V_O) = \iiint \epsilon K V_G \, p(\epsilon) \, p(\theta_G) \, p(V_G) \, d\epsilon \, d\theta_G \, dV_G$$

If V_G follows the Rayleigh distribution

$$p(V_G) = \frac{V_G}{\sigma_G^2} \exp(-(\frac{V_G^2}{2\sigma_G^2})) \qquad (VII.6)$$

where σ_G is the standard vector deviation of the bivariate normal distribution of velocities from which the Rayleigh form is derived. This implies that θ_G is uniformly distributed and (VII.5) reduces to

$$E(V_0) = \iiint \frac{\epsilon K V_G^2}{2\pi\sigma_G^2} \exp(-(\frac{V_G^2}{2\sigma_G^2})) p(\epsilon) \, d\epsilon \, d\theta_G \, dV_G \qquad (VII.7)$$

The integral

$$\int V_G^2 \exp(-(\frac{V_G^2}{2\sigma_G^2})) dV_G$$

can be evaluated for all V_G between 0 and ∞ as $\sigma_G^3 \sqrt{\pi/2}$ and $E(V_0)$ rewritten as

$$E(V_0) = \frac{\sigma_G}{2\sqrt{2\pi}} \int_0^\infty \epsilon \, p(\epsilon) \int_0^{2\pi} K \, d\theta_G \, d\epsilon \qquad (VII.8)$$

The limits of integration have been specified to cover all possible values of ϵ and θ_G.

If K can be represented by a harmonic series of the form

$$K = \bar{K} + \sum_{i=1}^\infty L_i \cos i\theta_G + \sum_{i=1}^\infty M_i \sin i\theta_G \qquad (VII.9)$$

the inner integral of (VII.8) becomes simply $2\pi\bar{K}$ and $E(V_0)$ is further reduced to

$$E(V_0) = \sqrt{\frac{\pi}{2}} \, \bar{K} \, \sigma_G \int_0^\infty \epsilon \, p(\epsilon) d\epsilon \qquad (VII.10)$$

On the basis of some observational evidence it will be assumed that ϵ is log-normally distributed, that is

$$p(\epsilon) = \frac{1}{\epsilon\sqrt{2\pi}\sigma_{ln\epsilon}} \exp(-\frac{1}{2}(\frac{1}{\sigma_{ln\epsilon}} ln \frac{\epsilon}{m_\epsilon})^2) \qquad (VII.11)$$

where the standard deviation of $ln\epsilon$ is written $\sigma_{ln\epsilon}$ and m_ϵ is the median value of ϵ. Therefore, the remaining integral becomes

$$\int_0^\infty \epsilon\, p(\epsilon)\, d\epsilon = m_\epsilon\, exp\left(\frac{1}{2}\sigma_{ln\epsilon}^2\right) \qquad (VII.12)$$

and

$$E(V_0) = \sqrt{\frac{\pi}{2}}\,\bar{K}\,\sigma_G\,m_\epsilon\, exp\left(\frac{1}{2}\sigma_{ln\epsilon}^2\right) \qquad (VII.13)$$

VII.2 Second Moment

The second moment of V_0 is defined as

$$E(V_0^2) = \int V_0^2\, p(V_0)\, dV_0 \qquad (VII.14)$$

$$= \iiint \epsilon^2\, K^2\, V_G^2\, p(\epsilon)\, p(K)\, p(V_G)\, d\epsilon\, dK\, dV_G \qquad (VII.15)$$

Under the same set of assumptions and following the same steps as above, it can be shown that

$$E(V_0^2) = 2\left(\bar{K}^2 + \frac{1}{2}\sum_{i=1}^\infty (L_i^2 + M_i^2)\right)\sigma_G^2\, m_\epsilon^2\, exp\left(2\sigma_{ln\epsilon}^2\right) \qquad (VII.16)$$

APPENDIX VIII

SOME ASPECTS OF THE SPECTRAL ANALYSIS OF RAWINSONDE ERRORS

VIII.1 Response to Wind Fluctuations

The following discussion will be concerned with the response of the rawinsonde balloon to fluctuations in the environmental wind field. In the main, it describes the principal stages and assumptions of the theory proposed recently by Fichtl (1971).

The basic equations of motion for the balloon can be written (neglecting the Bassett memory terms)

$$m \frac{du}{dt} = \frac{1}{2} \rho_a C_D A |\vec{V}_e - \vec{V}| (u_e - u) + m_a \frac{d}{dt} (u_e - u)$$

$$m \frac{dv}{dt} = \frac{1}{2} \rho_a C_D A |\vec{V}_e - \vec{V}| (v_e - v) + m_a \frac{d}{dt} (v_e - v)$$

$$m \frac{dw}{dt} = \frac{1}{2} \rho_a C_D A |\vec{V}_e - \vec{V}| (w_e - w) + m_a \frac{d}{dt} (w_e - w)$$

$$- (m - m_0)g \qquad\qquad (VIII.1)$$

where A is the balloon cross-sectional area,

C_D is the drag coefficient

g is the acceleration due to gravity

m is the balloon mass,

m_a is its apparent mass,

m_0 is the mass of air displaced,

t is time,

u, v are horizontal velocity components,

w is the vertical component of velocity,

ρ_a is the density of the atmosphere

and subscript e denotes the environmental wind components. $\vec{V}_e - \vec{V}$ is the wind vector relative to the sensor and the drag force is assumed always to act in a direction opposed to this vector. The effect of the apparent mass, m_a, has been explained by Milne-Thomson (1960) and will be examined further towards the end of this discussion. Aerodynamically induced forces have been neglected.

Now, representing the motion and the various wind components as the sums of mean and perturbation quantities (e.g., $u = \bar{u} + u'(t)$, $v_e = \bar{v}_e + v'_e(t)$, $w_e = w'_e(t)$), then to satisfy the equations of motion

$$\bar{u} = \bar{u}_e, \quad \bar{v} = \bar{v}_e$$

and $\frac{1}{2} A \rho_a C_D |\bar{w}|\bar{w} = (m_0 - m)g$ (VIII.2)

Therefore, rewritting the equations of motion and neglecting products of the perturbation quantities,

$$m \frac{du'}{dt} = \frac{1}{2} \rho_a C_D A |\bar{w}| (u'_e - u') + m_a \frac{d}{dt}(u'_e - u')$$

$$m \frac{dv'}{dt} = \frac{1}{2} \rho_a C_D A |\bar{w}| (v'_e - v') + m_a \frac{d}{dt}(v'_e - v')$$

$$m \frac{dw'}{dt} = \rho_a C_D A |\bar{w}| (w'_e - w') + m_a \frac{d}{dt}(w'_e - w') \qquad (VIII.3)$$

where the term $\frac{1}{2} \rho_a C_D A |\bar{w}|\bar{w}$ has been substituted for $(m_0-m)g$.

It is assumed that the motion of the balloon is rapid enough that temporal fluctuations of the wind field can be neglected and the perturbations are functions of height, z, alone. It will be noted, in explanation, that

$$z = \bar{w} t + \int_0^t w'(t)dt \qquad (VIII.4)$$

and the integral will tend to vary in sign whilst remaining small. Now,

$$u'_e(z) = u'_e[(1 + \frac{I'}{\overline{w}t})\overline{w}t]$$ (VIII.5)

where I' denotes the integral. Expanding u'_e as a Maclaurin series about $I'/\overline{w}t = 0$,

$$u'_e(z) = u'_e(\overline{w}t) + (\frac{du'_e}{dz})_{z=\overline{w}t} I' + \ldots$$ (VIII.6)

Therefore, to first order significance,

$$u'_e(z) = u'_e(\overline{w}t)$$ (VIII.7)

It must also be noted that the reduced equations of motion (VIII.3) are valid only for sufficiently small perturbation velocity differences compared to the mean ascent rate of the sensor. Fichtl has concluded that this is certainly the case in the troposphere and lower stratosphere for spherical sensors with rise rates of about 5 m/s. A further implied assumption is that fluctuations in aerodynamic coefficients can be ignored. This is in some way supportable because the time for dominant velocity fluctuations to be traversed by the balloon is usually much larger than the time for a wake to become established as a result of accelerations in the relative flow.

The derivation now proceeds by means of a Fourier representation suggested in Lumley and Panofsky (1964). This consists of writing the random functions u', v', w', u'_e, etc. in terms of other random processes $Z_u(n)$, $Z_v(n)$, $Z_w(n)$, $Z_{u_e}(n)$, etc. for example

$$u'(t) = \int_{-\infty}^{\infty} exp\ (2\pi int)\ dZ_u$$

and

$$dZ_u(n) = \lim_{T \to \infty} \int_{-T}^{T} exp\,(-2\pi int).\left(\frac{1 - exp\,(-2\pi itdn)}{i\,t}\right) \cdot u'\,dt \qquad (VIII.8)$$

By substituting the Fourier integrals for the perturbation quantities in (VIII.3) it can be shown that

$$(1 + 2\pi inT)\,dZ_u = (1 + 2\pi ianT)\,dZ_{u_e}$$

$$(1 + 2\pi inT)\,dZ_v = (1 + 2\pi ianT)\,dZ_{v_e} \qquad (VIII.9)$$

$$(2 + 2\pi inT)\,dZ_w = (2 + 2\pi ianT)\,dZ_{w_e}$$

where

$$T = \frac{(m + m_a)|\overline{w}|}{|m_0 - m|g} \quad ; \quad a = \frac{m_a}{m + m_a} \qquad (VIII.10)$$

So, the Fourier amplitudes of the sensor motions are given by

$$dZ_u = \frac{1 + 2\pi ianT}{1 + 2\pi inT}\,dZ_{u_e}, \quad etc. \qquad (VIII.11)$$

By the Wiener-Khintchine theorem, the processes $Z_u(n)$, etc., have orthogonal increments, that is, the following ensemble averages are defined by

$$\overline{dZ_u(n_1)\,dZ_u^*(n_2)} = 0, \quad n_1 \neq n_2$$

$$\overline{dZ_u(n)\,dZ_u^*(n)} = S_u(n)\,dn \qquad (VIII.12)$$

where $dZ_u^*(n)$ is the complex conjugate of $dZ_u(n)$ and $S_u(n)$ is the power spectral density of u'. It follows that

$$\frac{S_u(n)}{S_{u_e}(n)} = \frac{S_v(n)}{S_{v_e}(n)} = \frac{1 + (2\pi n a T)^2}{1 + (2\pi n T)^2}$$

$$\frac{S_w(n)}{S_{w_e}(n)} = \frac{4 + (2\pi n a T)^2}{4 + (2\pi n T)^2} \qquad\qquad (VIII.13)$$

These are the response functions of the sensor to changes in the environmental wind.

In order to evaluate the parameters T and a it is necessary to determine the apparent mass term, m_a. Now, it can be shown that, for a sphere moving with velocity V in a fluid at rest at infinity, the velocity potential and stream function expressed in polar coordinates (r,θ) are (Milne-Thomson, 1960):

$$\phi = \frac{1}{8} V D^2 \frac{\cos\theta}{r^2}; \; \psi = -\frac{1}{16} V D^3 \frac{\sin^2\theta}{r} \qquad\qquad (VIII.14)$$

in which D is the sphere diameter. The kinetic energy of the fluid if then given by

$$E = -\pi \rho_a \int \phi \, d\psi \qquad\qquad (VIII.15)$$

where ρ_a is the density of the ambient fluid. In terms of the mass of fluid displaced, m_0,

$$E = \frac{m_0}{4} V^2 \qquad\qquad (VIII.16)$$

Therefore, the rate of doing work by the balloon is

$$\frac{dE}{dt} = \frac{1}{2} m_0 V \frac{dV}{dt} \qquad\qquad (VIII.17)$$

and the resistance of the fluid is given by

$$\frac{m_0}{2} \frac{dV}{dt} = m_a \frac{dV}{dt} \qquad\qquad (VIII.18)$$

Thus, for a spherical balloon,

$$m_o = \rho_a \frac{\pi D^3}{6} \; ; \; m_a = \rho_a \frac{\pi D^3}{12} \qquad\qquad (VIII.19)$$

The various mass terms, the ascent rate and the balloon diameter will depend on the inflation of the balloon and ambient conditions. In the context of a study of sensor behaviour in the first few hundred metres of the atmosphere, ρ_a can be considered constant and the drag coefficient for the idealized sphere taken as 0.3 (see Goldstein, 1965). With these simplifications it is possible to find a simple relationship between balloon diameter and mean rate of ascent.

The equation of mean motion is

$$m g + F_D = m_o g$$

$$\text{or} \quad m_s + m_g - m_o = -\frac{F_D}{g} \qquad\qquad (VIII.20)$$

where F_D is the mean drag force,

$\quad m$ is the sensor mass, consisting of the mass of the contained gas, m_g, and the mass of the sonde, m_s

The left-hand side of (VIII.20) is called the free lift. Therefore

$$\frac{\pi \rho_a}{6} \left(\frac{\rho_g}{\rho_a} - 1 \right) D^3 + \frac{\pi \rho_a}{8g} C_D D^2 \bar{w}^2 + m_s = 0 \qquad\qquad (VIII.21)$$

in which ρ_g is the density of the balloon gas, assumed to be at the same temperature and pressure as the ambient fluid.

VIII.2 Spectrum of Observational Errors

It can be shown that the spectrum of velocity errors due to imprecision in the tracking equipment can be derived straightforwardly from the spectrum of displacement errors. The displacement, d, is defined as the downwind horizontal distance to the sensor (see Figure VIII.1). It will be assumed that the displacement error spectrum is "white" up to the folding frequency, n_N, so that
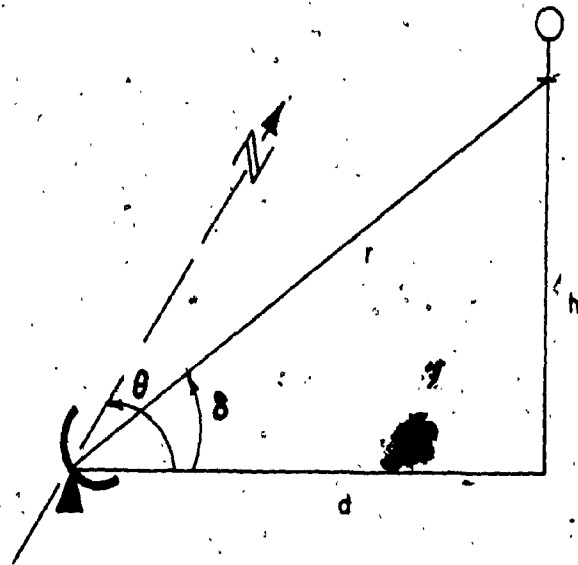
FIG. VIII. I   RAWINSONDE   GEOMETRY
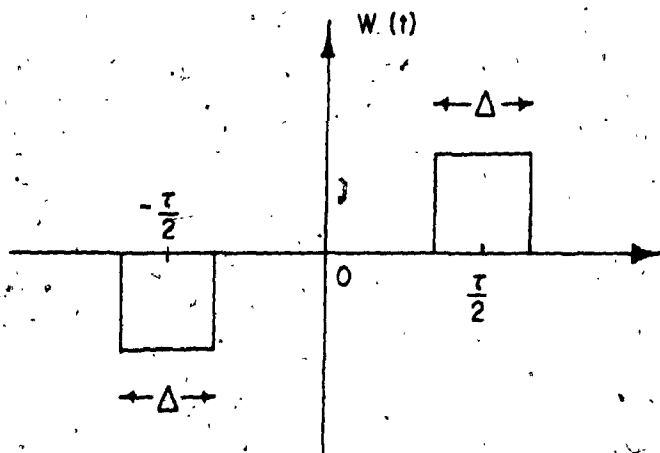
FIG. VIII. 2   WEIGHTING FUNCTION FOR DISPLACEMENT
OBSERVATIONS

$$S_d(n) = \frac{\sigma_d^2}{n_N} \qquad\qquad (VIII.22)$$

where S_d is the power spectral density and σ_d^2 the variance of errors in d. Now, in the rawinsonde system, upper winds are obtained by "finite difference" differentiation of the displacement observations. This is equivalent to applying a weighting function of the form shown in Figure VIII.2 with $\Delta = 0$. The corresponding response function in the frequency domain is then given by the Fourier transform

$$R_w^2(n) = (\int_{-\tau/2}^{\tau/2} W(t)\, exp(-2\pi int)dt)^2 \qquad\qquad (VIII.23)$$

in which $W(t)$ is the weighting function and τ is the time between fixes on the sensor position.

In the specific application of this theory considered in Chapter 4, the rawinsonde's position is in fact recorded every minute and velocities computed from alternate observations $(\tau = 120\ sec.)$, thus yielding overlapping two-minute mean winds at one minute intervals. Under these circumstances $n_N = 1/\tau = 1/120\ Hz$ and (VIII.23) becomes

$$R_w^2(n) = 4\pi^2 n^2 \left(\frac{\sin \pi \frac{n}{n_N}}{\pi \frac{n}{n_N}}\right)^2 \qquad\qquad (VIII.24)$$

Therefore, the spectrum of velocity errors is given by

$$S_0(n) = R_w^2(n) \cdot S_d(n)$$

$$= 4\, n_N\, \sigma_d^2\, \sin^2\pi \frac{n}{n_N}\ ;\ n < n_N \qquad\qquad (VIII.25)$$

Following de Jong (1966), estimates of the magnitude of σ_d can be found by considering first the basic geometry of rawinsonde tracking (shown in Figure VIII.1). The wind speed is obtained from the horizontal displacements and azimuths at the beginning and end of the period τ, as

$$V = \frac{(d_1^2 + d_2^2 - 2d_1 d_2 \cos(\theta_1 - \theta_2))^{1/2}}{\tau} \qquad (VIII.26)$$

(in the foregoing analysis of S_0 the term $\cos(\theta_1 - \theta_2)$ was considered as unity). Clearly, d can be determined by one of several modes of operation. These are:

- "height-elevation" mode (h, δ)
- "range-elevation" mode (r, δ)
- "height-range" mode (h, r)

or a method utilizing all three elements, h, r and δ. The precise form of the latter can be found from an optimization procedure which has been carried out by de Jong. It has been shown that the minimum displacement error variance is then given by

$$\sigma_d^2 = \frac{r^2 \sigma_\delta^2 \sigma_r^2 + r^2 \sigma_\delta^2 \sigma_h^2 \sin^2\delta + \sigma_r^2 \sigma_h^2 \cos^2\delta}{\sigma_r^2 \sin^2\delta + r^2 \sigma_\delta^2 \cos^2\delta + \sigma_h^2} \qquad (VIII.27)$$

Putting each of the components variances equal to ∞ in turn yields the corresponding error variances in the other three modes; of particular interest here

$$\sigma_d^2 = \frac{h^2 \sigma_\delta^2}{\sin^4\delta} + \cot^2\delta \cdot \sigma_h^2 \; ; \; (h, \delta) \text{ mode} \qquad (VIII.28)$$

For the simplified case of $(\theta_1 - \theta_2) \sim 0$ in Equation VIII.26 above, it follows that the variance of velocity errors is

$$\sigma_v^2 = \frac{2 \sigma_d^2}{\tau} \qquad (VIII.29)$$

which simply states that the variance of the difference of two quantities equals the sum of the separate variances. For practical purposes, therefore, there appears to be an avenue for estimating σ_v directly from σ_d without involving the spectrum S_0.

VIII.3 Spectrum of Self-induced Motions

Fichtl, deMandel and Krivo (1972) have developed a first-order theory of fluctuating lift and drag coefficients for the aerodynamically induced motions of spherical sensors. The equations of motion are written as before (Equation VIII.4) but with the addition of the induced lift-forces due to vortex shedding and wake instability of the form

$$\frac{1}{2} \rho_a A \vec{C}_L |\vec{V}_e - \vec{V}|^2 \tag{VIII.30}$$

The lift coefficient vector, $\vec{C}_L$, with components C_{L_x}, C_{L_y} and C_{L_z}, is treated as a time dependent perturbation quantity.

The lift vector acts in a plane perpendicular to the relative wind vector which, considering only first-order perturbations, is tilted only slightly from the horizontal. From this it follows that C_{L_z} is of second order and can be omitted from further consideration. Also, the lift forces in the horizontal x and y directions reduce to

$$\frac{1}{2} \rho_a A \bar{w}^2 C_{L_x} \text{ and } \frac{1}{2} \rho_a A \bar{w}^2 C_{L_y} \tag{VIII.31}$$

Now, representing the drag coefficient as

$$C_D = \overline{C_D} + C_D' \tag{VIII.32}$$

and eliminating second order terms from the drag forces, the equations of motion become

$$m \frac{du'}{dt} = \frac{1}{2} \rho_a \overline{C_D} A |\bar{w}| (u_e' - u') + m_a \frac{d}{dt}(u_e' - u') + \frac{1}{2} \rho_a C_{L_x} A \bar{w}^2$$

$$m \frac{dv'}{dt} = \frac{1}{2} \rho_a \overline{C_D} A |\bar{w}| (v_e' - v') + m_a \frac{d}{dt}(v_e' - v') + \frac{1}{2} \rho_a C_{L_y} A \bar{w}^2$$

$$m \frac{dw'}{dt} = \rho_a \overline{C_D} A |\bar{w}| (w_e' - w') + m_a \frac{d}{dt}(w_e' - w') - \frac{1}{2} \rho_a C_D' A \bar{w}|\bar{w}|$$

$$\tag{VIII.33}$$

Again, following the theory for the response of the sensor to wind fluctuations, the time dependent quantities are transformed to random functions in the frequency domain by the Fourier-Stieltjes integrals. Substituting these in the equations of motion,

$$(1 + 2\pi i n T) \, dZ_u = (1 + 2\pi i a n T) \, dZ_{u_e} + \frac{|\overline{w}| dZ_x}{C_D}$$

$$(1 + 2\pi i n T) \, dZ_v = (1 + 2\pi i a n T) \, dZ_{v_e} + \frac{|\overline{w}| dZ_y}{C_D}$$

$$(2 + 2\pi i n T) \, dZ_w = (2 + 2\pi i a n T) \, dZ_{w_e} - \frac{|\overline{w}| dZ_z}{C_D} \qquad (VIII.34)$$

where $dZ_x(n)$, $dZ_y(n)$ and $dZ_z(n)$ are the Fourier amplitudes of C_{L_x}, C_{L_y} and C_D' respectively. The parameters T and a are defined as before.

If the Fourier amplitudes of the aerodynamic coefficients can be assumed independent of those of the environmental wind components, then the fluctuating aerodynamic terms can be analysed separately. Multiplying each of the Fourier amplitudes by its complex conjugate and taking an ensemble average, the spectra of the induced motions are obtained in terms of the spectra of aerodynamic coefficients, as follows:

$$\widetilde{S}_{i_u}(n) = \frac{\overline{w}^2}{C_D^2} \frac{\widetilde{S}_x(n)}{(1 + (2\pi n T)^2)}$$

$$\widetilde{S}_{i_v}(n) = \frac{\overline{w}^2}{C_D^2} \frac{\widetilde{S}_y(n)}{(1 + (2\pi n T)^2)} \qquad (VIII.35)$$

$$\widetilde{S}_{i_w}(n) = \frac{\overline{w}^2}{C_D^2} \frac{\widetilde{S}_z(n)}{(4 + (2\pi n T)^2)}$$

$\widetilde{S}_{i_u}$, $\widetilde{S}_{i_v}$, $\widetilde{S}_{i_w}$ are the two-sided power spectral density functions of the induced motion components $(\widetilde{S}_i = S_i/2)$.

Fichtl et al estimated the r.m.s. lift and drag coefficients for the JIMSPHERE based on a narrow-band description of the spectra of induced motions. However, it was noted that measurements with a smooth ROSE balloon by Rogers and Camnitz (1965) indicate that the bandwidth of motions of a smooth balloon is considerably greater than

that of the JIMSPHERE. In fact, for a 2 m ROSE balloon at
and for supercritical Reynolds numbers $(Re > 2.5 \times 10^5)$,
suggest that the spectrum of velocity fluctuations be given

$$\frac{n_0 \, S_i(n)}{\sigma_i^2} = \frac{1}{\beta \sqrt{2\pi}} \, exp(-\frac{(1 - \frac{n}{n_0})^2}{2\beta^2})$$

with the universal constant $\beta = 0.2$; the velocity variance
$n_0 = .15 \, Hz.$ The above normalized spectrum was also used by
JIMSPHERE, the value of β being approximately .009.

Some other evidence of the nature of self-induced balloon
summarized as follows:

a) **McVehil, Pilié and Zigrossi (1965)**
Pulse Doppler radar was used to track 1 m and 2 m
Between 2 and 8 Km above ground level the 2 m ball
standard deviation of radial velocities of 2.52 m/s.
energy in the range 0.1 to 0.25 Hz; much of the obs
due to self-induced motions.

b) **Morrissey and Muller (1968)**
Spectra were obtained from two rawinsonde flights
tracked at 6-second intervals. Several spectral peak
greater than 1 cy/min (0.167 Hz), and particularly
cy/min. (.05 to .0833 Hz). With a folding frequency
attributed to aliased self-induced and pendulum m
When the estimated instrument errors were remov
more pronounced. It was pointed out that this could
before aliasing at around 0.7 cy / min. (0.11 Hz)
of the 20 m instrument train. It was also noted
was of the same magnitude as that of the induce
without an instrument package rising at the same
1965).

c) Murrow and Henry (1965)

A variety of balloons were released in a large hangar. Of particular relevance here is the behaviour of the rubber balloons carrying dummy radiosonde packages; two flights by this type of sensor showed r.m.s. horizontal velocities of about 10.6 ft./s (3.23 m/s). The balloons weighed 5.65 lb (2.56 kg), including train, with a free lift of 4 lb (1.81 kg) and a terminal ascent velocity of approximately 19 ft/s (5.8 m/s). For the 2 m ROSE, r.m.s. velocities appeared to increase directly with terminal velocity, such that $\sigma_i \sim \dot{w}/2$.

APPENDIX IX

DATA AND ANALYSIS FOR COMPUTED
GRADIENT AND GEOSTROPHIC WINDS

IX.1   Data

Two distinct sets of data, both extending over a period of one year from May 1972 to April 1973, were used in the investigation:

a)   Hourly synoptic data for 96 selected observing stations in Canada and the United States. These are given in Table IX.1 and their distribution across the continent is shown in Figure IX.1. Each hourly record contains the mean sea level (m.s.l.) pressure, surface temperature, mean surface wind speed and direction, and the peak gust speed, listed by station and in a consistent order for easy identification.

b)   Upper air data for 5 Canadian stations:; Edmonton, Alta., Maniwaki, Que., Moosonee, Ont., Stephenville, Nfld., and the Pas, Man. (also identified in Figure IX.1). These twice-daily records are of the standard form previously described in Appendix V.

IX.2   Analysis

Various estimates of the geostrophic and gradient winds were obtained for the selected upper air stations listed above (following the theory described in Chapter 4). All analyses were carried out for the set times of 00 hrs. GMT and every three hours thereafter. In order to determine those stations contributing to the fitting of pressure

241

BC	Baie Comeau	Que	QY	Sydney	NS
BF	Battle Harbour	Nfld	RJ	Roberval	Que
CJ	Cape St. James	BC	RL	Red Lake	Ont
DL	Dease Lake	BC	RV	Revelstoke	BC
DN	Dauphin	Man	SA	Sable Is.	NS
EC	Border	Que	SB	Sudbury	Ont
EG	Edmonton Int. A.	Alta	TH	Thompson	Man
EI	Ennadai Lake	NWT	TL	Trout Lake	Ont
EN	Esteven	Sask	TS	Timmins	Ont
EO	Lake Eon	Que	TW	Twillingate	Nfld
ET	Edson	Alta	UL	Monteal Int. A	Que
FL	Fort Reliance	NWT	VC	La Ronge	Sask
FS	Fort Simpson	NWT	VO	Val d'Or	Que
GP	Gaspé	Que	WG	Winnipeg	Man
GR	Grindstone Is	Que	WK	Wabush Lake	Nfld
GW	Poste de la Baleine	Que	WL	Williams Lake	BC
HE	Hope	BC	WR	White River	Ont
HY	Hay River	NWT	XH	Medicine Hat	Alta
HZ	Halifax Int. A	NS	XI	Killaloe	Ont
JT	Stephenville	Nfld	XJ	Fort St. John	BC
LB	Lac la Biche	Alta	XS	Prince George	BC
MQ	Moosonee	Ont	XT	Terrace	BC
NW	Maniwaki	Que	YC	Calgary Int. A	Alta
NA	Natashquan	Que	YE	Fort Nelson	BC
NI	Nitchequon	Que	YJ	Victoria Int. A	BC
PE	Pease River	Alta	YL	Lynn Lake	Man
PY	Fort Chipewyan	Alta	YN	Swift Current	Sask
QB	Quebec City	Que	YO	Wynyard	Sask
QD	The Pas	Man	YQ	Churchill	Man
QG	Windsor	Ont	YR	Goose	Nfld
QI	Yarmouth	NS	YW	Armstrong	Ont
QM	Moncton	NB	YZ	Toronto Int. A	Ont
QT	Thunder Bay	Ont	ZT	Port Hardy	BC
QW	North Battleford	Sask	ZW	Teslin	Yuk

TABLE IX.1a SYNOPTIC OBSERVING STATIONS (CANADA)

ACK	Nantucket	Mass	FCA	Kalispell	Mont
APN	Arpena	Mich	GEG	Spokane	Wash
AST	Astoria	Ore	GGW	Glasgow	Mont
AUW	Wausau	Wis	GTF	Great Falls	Mont
BGR	Bangor	Me	INL	International Falls	Minn
BIL	Billings	Mont	IPT	Williamsport	Pa
BIS	Bismarck	N Dak	JFK	New York Kennedy A	NY
CAR	Caribou	Me	MKG	Muskegon	Mich
CGA		Alask	MQT	Marquette	Mich
CON	Concord	NH	MSP	Minneapolis	Minn
CSP		Alask	RFD	Rockford	Ill
DAY	Dayton	Ohio	SYR	Syracuse	NY
DLH	Duluth	Minn	YKM	Yakima	Wash
FAR	Fargo	N Dak	YNG	Youngstown	Ohio

TABLE IX.1b SYNOPTIC OBSERVING STATIONS (U.S.A.)
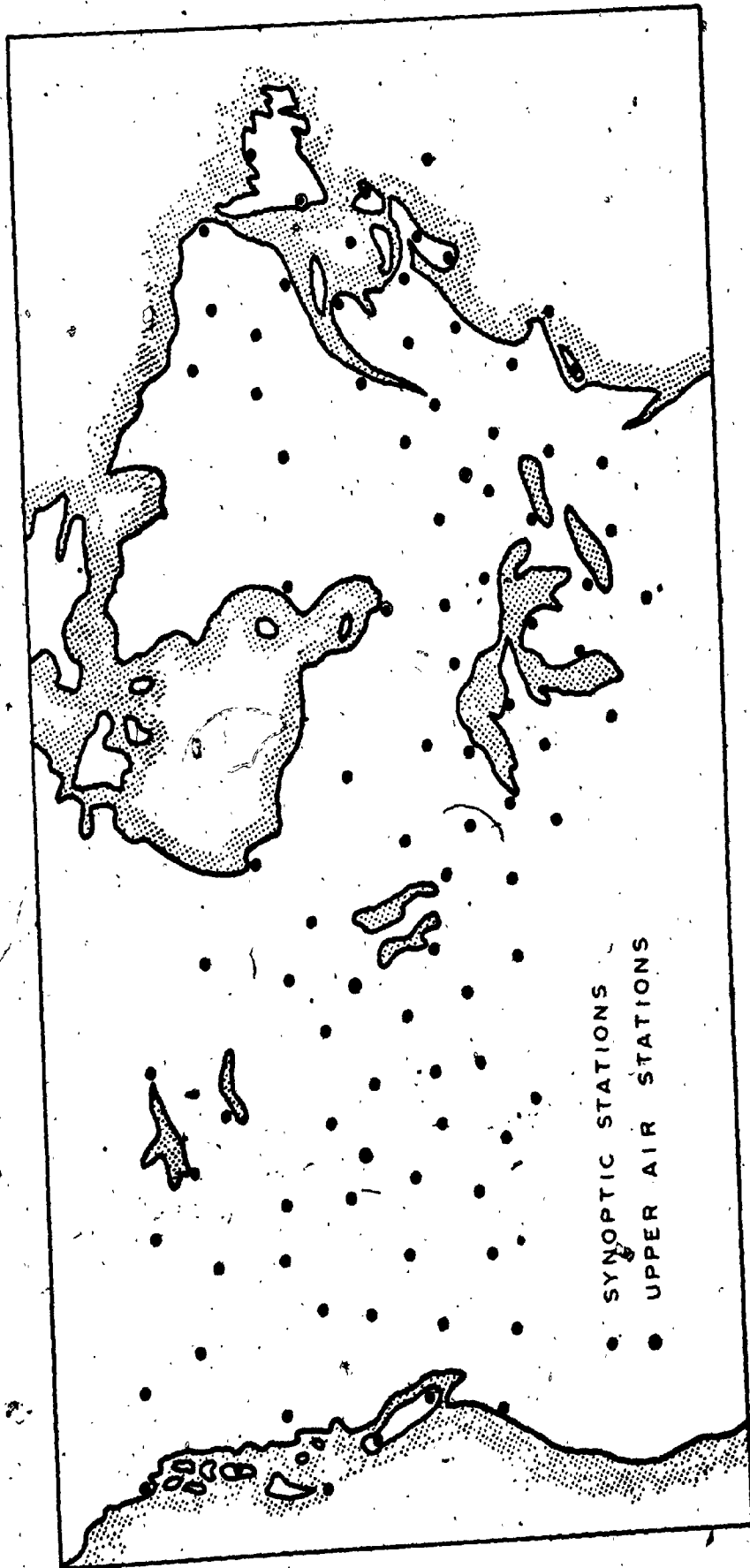
FIG. IX.I DISTRIBUTION OF OBSERVING STATIONS

SYNOPTIC STATIONS
UPPER AIR STATIONS

and temperature surfaces, a maximum distance of 800 km from the upper air stations was prescribed. In the event of missing pressure or temperature data at any observation point, the mean of the readings one hour before and after the analysis time was taken. If both of these were missing the mean over all stations for that hour was adopted, provided that no more than three pressure or temperature values were determined in this way; otherwise, that analysis was omitted. (An alternative treatment of the problem of missing data is to assign a weight of zero to the observing station involved, but this approach was rejected here because of the necessity of repeatedly forming a new transformation matrix.)

In the initial stages of this study three models were used to describe both the m.s.l. pressures and surface temperatures (only the weighted quadratic form was retained throughout). These were:

a)   A quadratic surface, weighted as

$$W = \frac{1}{2}(1 + \cos \frac{\pi d}{800\ km}); \quad d \leqslant 800\ km \qquad\qquad (IX.1)$$

where d is the distance of the observing station from the mean position of all stations considered in that analysis.

b)   A plane surface, weighted as

$$W = (1 - \frac{d}{800\ km}); \quad d \leqslant 800\ km \qquad\qquad (IX.2)$$

c)   An unweighted plane, for $d \leqslant 400\ km$.

These methods led to separate estimates of the following:

a)   The m.s.l. geostrophic wind vector.

b)   The m.s.l. gradient wind speed (by the quadratic surface model only).

c)   The thermal wind vector for the thickness layer between m.s.l. and 500 m

above ground level.

d) The resulting 500 m geostrophic wind vector.

IX.3 Observed Gradient Winds

For purposes of comparison, the observed winds at elevations of 300 m and 500 m were extracted from the upper air data in the manner adopted earlier (see Chapter 3 and Appendix V). Briefly, this consisted of simple linear interpolation with respect to height of the zonal and meridional wind components recorded, at the adjacent standard pressure surfaces.

REFERENCES

CHAPTER 1

BOWNE, N.E., 1969: A simulation model of air pollution over Connecticut. Jnl. A.P.C.A., 19, No. 8, 570-574.

BRITISH STANDARDS INSTITUTION, 1972: British Standard Code of Practice CP3: Chapter V, Part 2. British Standards Institution, London, 49 pp.

BROOKS, C.E.P., DURST, C.S. & CARRUTHERS, N., 1946: Upper winds over the world — Part I. Quart. Jnl. Roy. Met. Soc., 72, 55-73.

CARTWRIGHT, D.E. & LONGUET-HIGGINS, M.S., 1956: The statistical distribution of the maxima of a random function. Proc. Roy. Soc. London, Srs. A., 237, 212-232.

DAVENPORT, A.G., 1968: The dependence of wind loads on meteorological parameters. Proc. Intl. Res. Seminar on Wind Effects on Buildings and Structures, NRC, Ottawa, Sept. 1967, Univ. of Toronto Press, 19-82.

DAVENPORT, A.G., 1971: On the statistical prediction of structural performance in the wind environment. Proc. A.S.C.E. Natl. Struct. Engng. Mtg., Baltimore, Md., April 1971, Preprint 1420.

EIFFEL, G., 1900: Travaux scientifiques. L. Maretheux, Paris.

FALLS, L.W. & BROWN, S.C., 1972: Optimum runway orientation relative to crosswinds. NASA TN D-6930.

FISHER, R.A. & TIPPETT, L.H.C., 1928: Limiting forms of the frequency distribution of the largest or smallest member of a sample. Proc. Cambridge Phil. Soc., Pt. 2, 24,

180-190.

GARBETT, L.G., 1926: Admiral Sir Francis Beaufort and the Beaufort scales of wind and weather. Quart. Jnl. Roy. Met. Soc., 52, 161-168.

GUMBEL, E.J., 1954: Statistical theory of extreme values and some practical applications. Natl. Bur. of Standards, Appl. Math. Srs. No. 33, 51 pp.

HART, I.B., 1963: The mechanical investigations of Leonarda da Vinci. Univ. of California Press (first published 1925).

HORT, Sir A., 1916: Theophrastus – Enquiry into plants, Vol. II. Heinemann, London, 499 pp.

LUDLAM, F.H., 1966: The cyclone problem. Imperial Coll. of Sci. and Tech., London.

NATIONAL RESEARCH COUNCIL, 1970: Climatic information for building design in Canada. Suppl. No. 1 to the National Building Code of Canada, NRC, Ottawa, 48 pp.

PATTERSON, J., 1926: The cup anemometer. Trans. Roy. Soc. Canada, Srs. III, 20, 1-54.

RICE, S.O., 1954: Mathematical analysis of random noise. In "Selected Papers on Noise and Stochastic Processes" (N. Wax, ed.), Dover, New York, 133-294.

ROSS, W.D. (ed.), 1913: The works of Aristotle. Clarendon Press, Oxford.

SHELLARD, H.C., 1960: Extreme wind speeds over the United Kingdom for periods ending 1959. Met. Mag., 91, 39-47.

SMALLWOOD, C., 1857: On the meteorology of the vicinity of Montreal. Canadian Naturalist, 2, 328-335.

SMEATON, J., 1759: An experimental enquiry concerning the natural powers of water and wind to turn mills, and other machines, depending on a circular motion. Phil. Trans. Roy. Soc. London, 51, 100-174.

TAGG, J.R., 1957: Wind data related to the generation of electricity by wind power. Tech. Rep. C/T115, Elect. Res. Assocn., Leatherhead, Surrey, 52 pp.

THOM, H.C.S., 1968: New distributions of extreme winds in the United States. Jnl. Struct. Divn., Proc. A.S.C.E., 94, No. ST7, 1787-1801.

THOM, H.C.S., 1970: Engineering climatology of wind speed with special reference to the Pacific area. Proc. U.S. – Japan Res. Seminar on Windloads on Structures, Univ. of Hawaii, Oct. 1970.

THOM, H.C.S., 1973: Extreme wave height distributions over oceans. Jnl. Waterways, Harbors and Coastal Engng. Divn., Proc. A.S.C.E., 99, No. WW3, 355-374.

THOMAS, M.K., 1961: A bibliography of Canadian climate, 1763-1957. Queen's Printer, Ottawa, 114 pp.

WING, S.P., 1932: Discussion on wind-bracing in steel buildings. Proc. A.S.C.E., 58, No. 6, 1103-1119.

Historical background was also obtained from the following sources:

HUGHES, P., 1970: A century of weather service. Gordon & Breach, New York, 212 pp.

SHAW, Sir N., 1926: Manual of meteorology, Vol. 1 – Meteorology in history. Cambridge Univ. Press, 343 pp.

THOMAS, M.K., 1971: A brief history of meteorological services in Canada (in 3 parts). Atmosphere, 9, Nos. 1, 2, 3, 1-15, 37-47, 69-79.

WOLF, A., 1961: A history of science, technology and philosophy in the 18th century, Vol. I. Harper, New York, 409 pp. (first published 1938).

CHAPTER 2

ABRAMOWITZ, M. & STEGUN, I.A. (eds.), 1964: Handbook of mathematical functions. Natl. Bur. of Standards, 1046 pp.

BAYNES, C.J., 1971: An approach to the mapping of winds at gradient height over Canada. M.E.Sc. Thesis, Univ. of Western Ontario, London, Canada.

BENJAMIN, J.R. & CORNELL, C.A., 1970: Probability, statistics and decision for civil engineers. McGraw-Hill, New York.

BROOKS, C.E.P., DURST, C.S. & CARRUTHERS, N., 1946: Upper winds over the world – Part I. Quart. Jnl. Roy. Met. Soc., 72, 55-73.

BROOKS, C.E.P., DURST, C.S., CARRUTHERS, N., DEWAR, D. & SAWYER, J.S., 1950: Upper winds over the world. Geophys. Memoirs, No. 85, Met. Office, H.M.S.O.

CARTWRIGHT, D.E. & LONGUET-HIGGINS, M.S., 1956: The statistical distribution of the maxima of a random function. Proc. Roy. Soc. London, Srs. A., 237, 212-232.

CRUTCHER, H.L. & HALLIGAN, D.K., 1967: Upper wind statistics of the northern western hemisphere. Envir. Data Serv. EDS-1, ESSA, U.S. Dept. of Commerce, Silver Spring, Md.

DAVENPORT, A.G., 1964: Note on the distribution of the largest value of a random function with application to gust loading. Proc. Instn. Civil Engrs., 28, 187-196.

DAVENPORT, A.G., 1968: The dependence of wind loads on meteorological parameters. Proc. Intl. Res. Seminar on Wind Effects on Buildings and Structures, NRC, Ottawa, Sept. 1967, Univ. of Toronto Press.

DAVENPORT, A.G. & BAYNES, C.J., 1972: An approach to the mapping of the statistical properties of gradient winds (over Canada). Atmosphere, 10, No. 3, 80-92.

DAVENPORT, A.G., HOGAN, M. & ISYUMOV, N., 1969: A study of wind effects on the Commerce Court Tower — Part I. Engng. Sci. Res. Rep. BLWT-7-69, Univ. of Western Ontario, London, Canada.

DAVENPORT, A.G. & JANDALI, T., 1973: A study of the wind climate for Columbus, Ohio. Engng. Sci. Res. Rep. BLWT-SS3-73, Univ. of Western Ontario, London, Canada.

DEACON, E.L., 1965: Wind gust speed: averaging time relationship. Austral. Met. Mag., No. 51, 11-14.

DURST, C.S., 1960: Wind speeds over short periods of time. Met. Mag., 89, 181-186.

GOMES, L. & VICKERY, B.J., 1974: On the prediction of extreme wind speeds from the parent distribution: Res. Rep. R 241, School of Civil Engineering, Univ. of Sydney.

GRINGORTEN, I.I., 1963: A simplified method of estimating extreme values from data samples. Jnl. Appl. Met., 2, 82-89.

GUMBEL, E.J., 1954: Statistical theory of extreme values and some practical applications. Natl. Bur. of Standards, Appl. Math. Srs. No. 33, U.S. Dept. of Commerce.

HAMMING, R.W., 1962: Numerical methods for scientists and engineers. McGraw-Hill, New York, 411 pp.

HENRY, T.J.G., 1957: Maps of upper winds over Canada. Met. Branch, Dept. of Transport, Toronto.

HOLLISTER, S.C., 1969: The engineering interpretation of weather bureau records for wind loading on structures. Proc. Technical·Mtg. on Wind Loads on Buildings and Structures, Gaithersburg, Md., Jan. 1969, Natl. Bur. of Standards, Building Sci. Srs. No. 30, U.S. Dept. of Commerce, 151- 164.

JENKINSON, A.F., 1955: The frequency distribution of the annual maximum (or minimum) values of meteorological elements. Quart. Jnl. Roy. Met. Soc., 81, 158-171.

PARK, J.H., Jr., 1961: Moments of the generalized Rayleigh distribution. Quart. of Appl. Math., 19, No. 1, 45-49.

PATNAIK, P.B., 1949: The non-central chi^2 — and F — distributions and their applications. Biometrika, 36, 202-232.

RICE, S.O., 1954: Mathematical analysis of random noise. In "Selected Papers on Noise and Stochastic Processes" (N. Wax, ed.), Dover, New York, 133-294.

SHELLARD, H.C., 1958: Extreme wind speeds over Great Britain and Northern Ireland. Met. Mag., 87, 257-265.

SHELLARD, H.C., 1963: The estimation of design wind speeds. Proc. Intl. Conf. on Wind Effects on Buildings and Structures, NPL, Teddington, June 1963, H.M.S.O.

SMITH, O.E., 1971: An application of distributions derived from the bivariate normal density function. Proc. Intl. Symp. on Probability and Statistics in the Atmos. Sci., Honolulu, June 1971, Amer. Met. Soc.

WEIL, H., 1954: The distribution of radial error. Ann. of Math. Statistics, 25, 168-170.

YADAVALLI, S.V., 1967: On applications of some results related to bivariate Gaussian density distribution functions. Intl. Jnl. of Control, 5, No. 2, 191-194.

CHAPTER 3

BAYNES, C.J., 1971: An approach to the mapping of winds at
Canada. M.E.Sc. Thesis, Univ. of Western Ontario, London, Can

BLACKADAR, A.K., 1962: The vertical distribution of wind ar
in a neutral atmosphere. Jnl. Geophys. Res., 67, No. 8, 3095-3

BLACKADAR, A.K. & TENNEKES, H., 1968: Asymptotic sim
barotropic planetary boundary layers. Jnl. Atmos. Sci., 25, 101

CSANADY, G.T., 1967: On the "Resistance Law" of turbule
Atmos. Sci., 24, 467-471.

CSANADY, G.T., 1972: Turbulent diffusion in the environme
Dortrecht, 248 pp.

DAVENPORT, A.G., 1960: Rationale for determining design
Struct. Divn., Proc. A.S.C.E., 86, No. ST5, 39-68.

DAVENPORT, A.G, 1963: The relationship of wind structur
Symp. on Wind Effects on Buildings and Structures, N.P.L.
HM.S.O.

DAVENPORT, A.G., unpublished: World Trade Center wind
1964-65.

DAVENPORT, A.G., HOGAN, M. & ISYUMOV, N., 196
on the Commerce Court Tower — Part I. Engng. S
Western Ontario, London, Canada.

DAVENPORT, A.G. & JANDALI, T., 1973: A study of the wind climate for Columbus, Ohio, Engng. Sci. Res. Rep. BLWT-SS3-73, Univ. of Western Ontario, London, Canada.

DEACON, E.L., 1973: Geostrophic drag coefficients. Boundary Layer Met., 5, 321-340.

FINDLATER, J., HARROWER, T.N.S., HOWKINS, G.A. & WRIGHT, H.L., 1966: Surface and 900 mb wind relationships. Met. Office Scientific Paper No. 23, H.M.S.O. London, 41 pp.

HARRIS, R.I., 1971: The nature of the wind. Proc. Seminar on the Modern Design of Wind-Sensitive Structures. London, June 1970, Construction Industry Research and Information Assocn.

HELLIWELL, N.C., 1971: Wind over London. Proc. 3rd Intl. Conf. on Wind Effects on Buildings and Structures, Tokyo.

LETTAU, H.H, 1962: Theoretical wind spirals in the boundary layer of a barotropic atmosphere. Beit. Phys. Atmos., 35, 195-212.

LUMLEY, J.L. & PANOFSKY, H.A., 1964: The structure of atmospheric turbulence. Wiley Interscience, New York, 239 pp.

McNAMARA, K.F., 1974: Ph.D. Thesis, Univ. of Western Ontario, London, Canada (in preparation).

MENDENHALL, B.R., 1967: A statistical study of frictional wind veering in the planetary boundary layer. Atmos. Sci. Paper No. 116, Colorado State Univ., Fort Collins, Colo.

PERSHINA, R.A., 1968: Certain peculiarities of vertical variability of wind speed in the boundary layer of the atmosphere. Trans. Sci. Res. Inst. of Aeroclimatology, Moscow,

No. 52, 93-97 (Machine Transl. FTD-MT-24-249-69, USAF Systems Command).

PLATE, E.J., 1971: Aerodynamic characteristics of atmospheric boundary layers. U.S. Atomic Energy Comm., Oak Ridge, Tenn.

SIMIU, E., 1973: Logarithmic profiles and design wind speeds. Jnl. Engng. Mech. Divn., Proc. A.S.C.E., 99, No. EM5, 1073-1089.

SWINBANK, W.C., 1970: Structure of wind and the shearing stress in the planetary boundary layer. Arch. Met. Geoph. Biokl., Ser. A, 19, 1-12.

TAYLOR, R.J., 1962: Small-scale advection and the neutral wind profile. Jnl. Fluid. Mech., 13, 529-539.

TENNEKES, H., 1973a: The logarithmic wind profile. Jnl. Atmos. Sci., 30, 234-238.

TENNEKES, H., 1973b: Similarity laws and scale relations in planetary boundary layers. In "Workshop on Micrometeorology" (D.A. Haugen, ed.), Amer. Met. Soc., Boston, 177-216.

CHAPTER 4

BAYNES, C.J., 1971: An approach to the mapping of winds at gradient height over Canada. M.E.Sc. Thesis, Univ. of Western Ontario, London, Canada.

BENJAMIN, J.R. & CORNELL, C.A., 1970: Probability, statistics and decision for civil engineers. McGraw-Hill, New York.

BLACKMAN, R.B. & TUKEY, J.W., 1958: The measurement of power spectra. Dover, New York.

BROOKS, C.E.P., DURST, C.S., CARRUTHERS, N., DEWAR, D. & SAWYER, J.S., 1950: Upper winds over the world. Geophys. Memoirs, No. 85, Met. Office, H.M.S.O.

CRUTCHER, H.L. & HALLIGAN, D.K., 1967: Upper wind statistics of the northern. western hemisphere. Envir. Data Serv. EDS-1, ESSA, U.S. Dept. of Commerce, Silver Spring. Md.

DAVENPORT, A.G., 1961: The spectrum of horizontal gustiness near the ground in high winds. Quart. Jnl. Roy. Met. Soc., 87, 194-211.

DAVENPORT, A.G., 1968: The dependence of wind loads on meteorological parameters. Proc. Intl. Res. Seminar on Wind Effects on Buildings and Structures, NRC, Ottawa, Sept. 1967, Univ. of Toronto Press, 19-82.

DAVENPORT, A.G., HOGAN, M. & ISYUMOV, N., 1969: A study of wind effects on the Commerce Court Tower — Part I. Engng. Sci. Res. Rep. BLWT-7-69, Univ. of Western Ontario, London, Canada.

DAVENPORT, A.G., ISYUMOV, N. & JANDALI, T., 1971: A study of wind effects for the Sears project. Engng. Sci. Res. Rep. BLWT-5-71, Univ. of Western Ontario, London, Canada.

DAVENPORT, A.G., ISYUMOV, N. & JANDALI, T., 1972: A study of wind effects for the Federal Reserve Bank Building, New York, U.S.A., Engng. Sci. Res. Rep. BLWT-5-72, Univ. of Western Ontario, London, Canada.

DAVENPORT, A.G. & JANDALI, T., 1973: A study of the wind climate for Columbus, Ohio. Engng. Sci. Res. Rep. BLWT-SS3-73, Univ. of Western Ontario, London, Canada.

FICHTL, G.H., 1971: The responses of rising or falling spherical wind sensors to atmospheric wind perturbations. Jnl. Appl. Met., 10, 1275-1284.

FICHTL, G.H., deMANDEL, R.E. & KRIVO, S.J., 1972: Aerodynamic properties of spherical balloon wind sensors. Jnl. Appl. Met., 11, 472-481.

GEIGER, R , 1965: The climate near the ground. Harvard Univ. Press, Cambridge, Mass.

HALTINER, G.J. & MARTIN, F.L., 1957: Dynamical and physical meteorology. McGraw-Hill, New York.

HARRIS, R.I., 1971: The nature of the wind. Proc. Seminar on the Modern Design of Wind-Sensitive Structures, London, June 1970, Construction Industry Research and Information Assocn.

HENRY, T.J.G., 1957: Maps of upper winds over Canada. Met. Branch, Dept. of Transport, Toronto.

HUMPHREYS, W.J., 1964: Physics of the air. Dover, New York (first published 1940).

de JONG, H.M., 1966: A new process for the evaluation of upper winds. Jnl. Appl. Met., 5, 436-449.

McVEHIL, G.E., PILIÉ, R.J. & ZIGROSSI, G.A., 1965: Some measurements of balloon motions with Doppler radar. Jnl. Appl. Met., 4, 146-148.

MORRISSEY, E.G. & MULLER, F.B., 1968: Spectral aspects of upper wind measurement systems. Canadian Met. Memoirs No. 26, Met. Branch, Dept. of Transport, Toronto.

MULLER, F.B., 1973: Objective estimation of surface geostrophic winds. Proc. 3rd Conf. on Probability and Statistics in the Atmospheric Sciences, Boulder, Colo., June 1973.

MURROW, H.N. & HENRY, R.M., 1965: Self-induced balloon motions. Jnl. Appl. Met., 4, 131-138.

RIEHL, H., 1965: Introduction to the atmosphere. McGraw-Hill, New York.

ROGERS, R.R. & CAMNITZ, H.G., 1965: Project Baldy — an investigation of aero-dynamically-induced balloon motions. NAS8-11140, Cornell Aero. Lab. Inc.

TEUNISSEN, H.W., 1970: Characteristics of the mean wind and turbulence in the planetary boundary layer. UTIAS Review No. 32, Inst. for Aerospace Studies, Univ. of Toronto.

TITUS, R.L., 1970: Method used for processing Canadian upper air data for climatological purposes. CLI 1-70, Met. Branch, Dept. of Transport, Toronto.

CHAPTER 5

BASE, T.E., 1974: The effect of atmospheric turbulence on windmill performance. Proc. Conf. on the Hydrogen Economy, Miami, March 1974, Univ. of Miami.

BECKWITH, W.B., 1971: The effect of weather on the operations and economics of air transportation today. Bull. Am. Met. Soc., 52, No. 9, 863-868.

BROOKS, C.E.P., DURST, C.S., CARRUTHERS, N., DEWAR, D. & SAWYER, J.S., 1950: Upper winds over the world. Geophys. Memoirs No. 85, Met. Office, H.M.S.O.

CARTWRIGHT, D.E. & LONGUET-HIGGINS, M.S., 1956: The statistical distribution of the maxima of a random function. Proc. Roy. Soc. London, Srs. A, 237, 212-232.

DAVENPORT, A.G., 1964: Note on the distribution of the largest value of a random function with application to gust loading. Proc. Instn. Civil Engnrs., 28, 187-196.

DAVENPORT, A.G., 1968: The dependence of wind loads on meteorological parameters. Proc. Intl. Res. Seminar on Wind Effects on Buildings and Structures, N.R.C., Ottawa,

Sept. 1967, Univ. of Toronto Press, 19-82.

DAWSON, J.L., 1972: Engineering aspects of the selection of sites for the third London airport. Proc. Instn. Civil Engnrs., Part 2, 53, 337-367.

DOT (Department of Transport), 1962: The climate of Canada. Department of Transport, Meteorological Branch, Toronto.

DURAND, W.F. 1963: Aerodynamic theory — Vol. IV. Dover, New York (first published 1935).

FALLS, L.W. & BROWN, S.C., 1972: Optimum runway orientation relative to cross-winds. NASA TN D-6930, Washington, D.C.

GOLDING, E.W., 1957: Electrical energy from the wind. Engng. Jnl., 40, 809-819.

HOGAN, M., 1971: The influence of wind on tall building design. Ph.D. Thesis, Univ. of Western Ontario, London, Canada.

JACOBS, L., 1961: The planning of runway layouts as affected by weather. Jnl. Inst. of Navigation, 15, No. 3, 295-307.

RAMSDELL, J.V. & POWELL, D.C., 1973: Meteorological information for vertical and short take-off and landing (V/STOL) operations in built-up urban areas — an analysis. Rep. No. FAA-RD-72-135, Federal Aviation Agency, Washington, D.C.

RICE, S.O., 1954: Mathematical analysis of random noise. In "Selected Papers on Noise and Stochastic Processes" (N. Wax, ed.), Dover, New York, 133-294.

TAGG, J.R., 1957: Wind data related to the generation of electricity by wind power. Tech. Rep. C/T115, Elect. Res. Assocn., Leatherhead, Surrey.

THOM, H.C.S., 1971: Asymptotic extreme-value distributions of wave heights in the open ocean. Jnl. of Marine Res., 29, No. 1, 19-27.

THOM, H.C.S., 1973: Extreme wave height distributions over oceans. Jnl. Waterways, Harbors and Coastal Engng. Divn., Proc. A.S.C.E., 99, No. WW3, 355-374.

WIEGEL, R.L., 1964: Oceanographic engineering. Prentice-Hall, Englewood Cliffs, N.J.

APPENDIX I

DAVENPORT, A.G., 1964: Note on the distribution of the largest value of a random function with application to gust loading. Proc. Instn. Civil Engnrs., 28, 187-196.

DAVENPORT, A.G., & BAYNES, C.J., 1972: An approach to the mapping of the statistical properties of gradient winds (over Canada). Atmospher, 10, No. 3, 80-92.

APPENDIX II

GUMBEL, E.J., 1954: Statistical theory of extreme values and some practical applications. Natl. Bur. of Standards, Appl. Math. Srs. No. 33, U.S. Dept. of Commerce.

LNEC (Laboratorio Nacional de Engenharia Civil), 1973: Wind in Western Europe: Results of an enquiry. LNEC, Lisbon, 454 pp.

APPENDIX III

DUCHENE-MARULLAZ, P., 1972: Etude des vitesses maximales annuelles de vent. Cahiers du Centre Scientifique et Technique du Batiment, No. 131.

HANAI, M., 1963: Studies on decision of design wind load. Report of Inst. of Indust. Sci., Univ. of Tokyo, 12, No. 6.

HARIHARA, P.S. & GOYAL, S.C., 1972: Extreme wind speeds over India. Ind. Jnl. Met. and Geophys., 23, 67-70.

JENSEN, M. & FRANCK, N., 1970: The climate of strong winds in Denmark. Danish Technical Press, Copenhagen.

JOHNSON, A.I., 1953: Strength, safety and economical dimensions of structures. Staten Kommittee for Byggnadsforskning, Bull. No. 22, Stockholm.

LEE, K.S. & HUH, C.K., 1972: Design wind velocities in Korea. Proc. 3rd Intl. Conf. on Wind Effects on Buildings and Structures, Univ. of Tokyo Press.

LNEC (Laboratório Nacional de Engenharia Civil), 1973: Wind in Western Europe: Results of an enquiry. LNEC, Lisbon, 454 pp.

MACKAY, S., 1972: Extreme wind studies in Hong Kong. Proc. 3rd Intl. Conf. on Wind Effects on Buildings and Structures, Univ. of Tokyo press.

MAY, H.I., 1972: Some wind speed data for estimating wind loads on structures in South Africa. Trans. S. Afr. Instn. Civil Engnrs., 14, 175-180.

NRC (National Research Council), 1970: Climatic information for building design in Canada. Suppl. No. 1 to the National Building Code of Canada, NRC, Ottawa, 48 pp.

RIERA, J.D. & REIMUNDIN, J.C., 1970: Velocidad del viento para el diseño de estructuras en la República Argentina: Recomendaciones Preliminares. Informe I-70-4, Laboratorio de Ensaya Estructuras, Universidad Tucuman.

RIJKOORT, P.J., 1964: Enkele gegevens omtrent extreme windsnelheden voor een berekening van de maximale windbelasting op gebouwen. Koninklijk Nederlands Meteorologisch Instituut, De Bilt.

SHELLARD, H.C., 1962: Extreme wind speeds over the United Kingdom for periods ending 1959. Met. Mag., 91, 39-47.

THOM, H.C.S., 1968: New distributions of extreme winds in the United States. Jnl. Struct. Divn., Proc. ASCE, 94, No. ST7, 1787-1801.

WHITTINGHAM, H.E., 1964: Extreme wind gusts in Australia. Bull. No. 46, Bur. of Met., Melbourne.

APPENDIX VI

BLACKADAR, A.K. & TENNEKES, H., 1968: Asymptotic similarity in neutral barotropic planetary boundary layers. Jnl. Atmos. Sci., 25, 1015-1020.

CSANADY, G.T., 1967: On the "Resistance Law" of a turbulent Ekman layer. Jnl. Atmos. Sci., 24, 467-471.

PLATE, E.J., 1971: Aerodynamic characteristics of atmospheric boundary layers. U.S. Atomic Energy Comm., Oak Ridge, Tenn.

SWINBANK, W.C., 1970: Structure of wind and the shearing stress in the planetary boundary layer. Arch. Met. Geoph. Biokl., Ser. A, 19, 1–12.

APPENDIX VIII

FICHTL, G.H., 1971: The responses of rising or falling spherical wind sensors to atmospheric wind perturbations. Jnl. Appl. Met., 10, 1275-1284.

FICHTL, G.H., deMANDEL, R.E. & KRIVO, S.J., 1972: Aerodynamic properties of spherical balloon wind sensors. Jnl. Appl. Met., 11, 472-481.

GOLDSTEIN, S. (ed.), 1965: Modern developments in fluid dynamics – Vol. II. Dover, New York, (first published 1938).

de JONG, H.M., 1966: A new process for the evaluation of upper winds. Jnl. Appl. Met., 5, 436-449.

LUMLEY, J.L. & PANOFSKY, H.A., 1964: The structure of atmospheric turbulence. Wiley-Interscience, New York.

McVEHIL, G.E., PILIE, R.J. & ZIGROSSI, G.A., 1965: Some measurements of balloon motions with Doppler radar. Jnl. Appl. Met., 4, 146-148.

MILNE-THOMSON, L.M., 1960: Theoretical hydrodynamics. St. Martin's Press, New York.

MORRISSEY, E.G. & MULLER, F.B., 1968: Spectral aspects of upper wind measurement systems. Canadian Met. Memoirs No. 26, Met. Branch, Dept. of Transport, Toronto.

MURROW, H.N. & HENRY, R.M., 1965: Self-induced balloon motions. Jnl. Appl. Met. 4, 131-138.

ROGERS, R.R. & CAMNITZ, H.G., 1965: Project Baldy – an investigation of aerodynamically-induced balloon motions. NAS8-11140, Cornell Aero. Lab. Inc.